An investigation into the interacting partners of the ubiquitin ligase, SIAH1, and the tumour suppressor protein, ASPP1

Marie MacLennan

A thesis submitted for the degree of Doctor of Philosophy

Institute of Human Genetics and
Institute for Cellular and Molecular Biosciences

Newcastle University

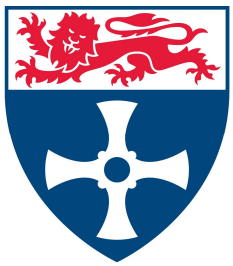

September 2010

Declaration

I, Marie MacLennan, declare that no portion of the work compiled in this thesis has been submitted in support of another degree or qualification at this or any other University or Institute of Learning. This thesis includes nothing which is the work of others, nor the outcomes of work done in collaboration, except where otherwise stated.

.....
Marie MacLennan

Acknowledgements

Firstly, I would like to thank my supervisor David Elliott for his guidance, encouragement and continual support. I have thoroughly enjoyed working in David's lab and I have learnt a lot from him. I will always be grateful for having such a brilliant mentor. Thanks also to my co-supervisor Keith Jones for his valuable advice and supervision during the early years of this project.

I would like to thank all members of the David Elliott laboratory group, both past and present. I would particularly like to thank Caroline Dalgliesh and Ingrid Ehrmann for showing me the ropes and sharing their valuable expertise. Thank you both for all of your support and continual advice. Thanks to Yilei Liu, Agata Rozanska, Sushma Grellscheid, Prabhakar Rajan, Vasileios Floros and Masha (good luck with the PhD!). You have all made my PhD so enjoyable and I feel very privileged to work with such a great group of people.

Special thanks to collaborators: Professor David Bowtell (Peter MacCallum Cancer Centre, Melbourne), Dr Steve Darby (National Institute for Cancer Research, Newcastle University), Dr Nicholas Watkins, Dr Andrew Knox (Institute for Cell and Molecular Biosciences, Newcastle University) and Dr Kaveh Emami (North East Proteome Analysis Facility, Newcastle upon Tyne). Thanks also to Dr Timothy Cheek and Professor Brian Morgan for their helpful advice and feedback during the course of my PhD. I also gratefully acknowledge the BBSRC (Biotechnology and Biological Sciences Research Council) for funding this project.

A big thank you to all of my family and friends. To Uncle Pete for 'tea on Tuesday', always the highlight of my week! Thank you to the Gooding gang for all of your invaluable advice(!) and happy times. Thanks to the girls for the laughs, the wine(!), and providing a welcome break from everything science-related. Big thanks to Steven for putting up with my occasional grumps, the western cowboy impressions and for never failing to make me laugh.

Lastly I would like to thank my parents, Ray and Joy. Thank you so much for everything. This thesis is for you.

Table of contents

List of figures and tables

Chapter 1

Chapter 2

Chapter 3

Chapter 4

Chapter 5

Chapter 6

Chapter 7

Abbreviations

APC	Adenomatous Polyposis Coli
ASPP	Apoptosis Stimulating Protein of p53
ATF3	Activating transcription factor 3
CDS	Coding Sequence
ChIP	Chromatin Immunoprecipitation
CLU	Clusterin
COPB1	Coatomer Protein Complex, Subunit beta 1
CRE	cAMP Responsive Element
CRUK	Cancer Research, United Kingdom
C-terminus	Carboxy-terminus
CtIP	C-terminal interacting protein
DAB	3,3'-Diaminobenzidine
DAPI	4’,6-diamidino-2-phenylindole
DCC	Deleted in Colorectal Cancer
dH_2O	Distilled water
DMEM	Dulbecco's Modified Eagle Medium
DNA	Deoxyribonucleic Acid
dNTP	Deoxynucleotide Triphosphate
DRB	5,6-Dichloro-1-β-D-ribofuranosylbenzimidazole
DSIF	DRB-sensitivity inducing factor
DTT	Dithiothreitol
DUB	Deubiquitinating enzyme
EDTA	Ethylenediaminetetraacetic acid
EMSA	Electrophoretic Mobility Shift Assay
FBS	Foetal Bovine Serum

FIH	Factor Inhibiting HIF1α
GAPDH	Glyceraldehyde 3-Phosphate Dehydrogenase
GEF	Guanine Nucleotide Exchange Factor
GFP	Green Fluorescent protein
GST	Glutathione S-Transferase
HCC	Hepatocellular Carcinoma
HIF1α	Hypoxia Inducible Factor α
HIPK2	Homeodomain Interacting Protein Kinase 2
HPRT	Hypoxanthine-guanine phosphoribosyltransferase
IEG	Immediate Early Gene
IGD	In-Gel Digest
IHG	Institute of Human Genetics
IP	Immunoprecipitation
IVT	*In vitro* translated
KCl	Potassium Chloride
Kid	Kinesin-like DNA binding protein
kV	Kilo Volts
LB	Luria Bertani
LCMS	Liquid Chromatography-Mass Spectronomy
LiAc	Lithium Acetate
mRNA	Messenger Ribonucleic Acid
MS	Mass Spectrometry
NCBI	National Centre for Biotechnology Information
N-CoR	Nuclear Receptor Co-Repressor
NELF	Negative Elongation Factor
NMR	Nuclear Magnetic Resonance
N-terminus	Amino-terminus

OD	Optical Density
PBS	Phosphate Buffered Saline
PCR	Polymerase Chain Reaction
PD	Parkinson's Disease
PEG	Polyethylene Glycol
PEG10	Paternally Expressed Gene 10
PFA	Paraformaldehyde
PHD	Prolyl-hydroxylase
Phyl	Phyllopod
PMSF	Phenylmethanesulphonylfluoride
PP1	Protein Phosphatase 1
Repp86	Restrictedly Expressed Proliferation-Associated Protein 86
RING	Really Interesting New Gene
RNA	Ribonucleic Acid
rpm	Revolutions Per Minute
RT-PCR	Reverse Transcriptase PCR
Saos	Sarcoma Osteogenic
SBD	Substrate Binding Domain
SCF	Skp1-Cullin-F-box Protein Complex
SDS	Sodium Dodecyl Sulphate
SDS-PAGE	Sodium Dodecyl Sulphate Polyacrylamide Gel Electrophoresis
SIAH	Seven in Absentia Homolog
SINA	Seven in Absentia
SIP	Siah Interacting Protein
Skp1	S-phase kinase-associated protein 1
Spry2	Sprouty 2
TAE	Tris-acetate-EDTA buffer

TE	Tris, pH 8.0 EDTA
TIEG1	Transforming Growth Factor β-Inducible Early Gene
TK	Thymidine Kinase
TRAF2	TNF Receptor-Associated Factor 2
Ttk	Tramtrack
Ubc	Ubiquitin Conjugating Enzyme
UBL	Ubiquitin-Like Protein
UV	Ultraviolet
WHSC2	Wolf-Hirschhorn syndrome candidate 2
X-Gal	5-bromo-4-chloro-3-indoyl-β-D-galactopyranoside
Y2H	Yeast 2-Hybrid
ZnF	Zinc Finger

Abstract

Selective protein degradation is a crucial control mechanism which impacts nearly every aspect of eukaryotic cell biology. It is achieved via the ubiquitin-proteasome pathway whereby multimers of ubiquitin are conjugated to substrate proteins and subsequently recognised and degraded by the proteasome. The specificity of substrate recognition is provided by E3 ubiquitin ligase enzymes. Seven in Absentia homologue-1 (SIAH1) is a highly conserved E3 ubiquitin ligase which recognises and binds to an array of substrate proteins facilitating their ubiquitination and degradation. The identification of various SIAH protein substrates has revealed that SIAH1 and its family members play a role in a number of cellular processes including cell-cycle regulation, cell differentiation, and apoptosis. Previous studies also revealed that SIAH1 has a novel role in the testes as removal of the equivalent gene in mice (*Siah1a*) results in male sterility. Despite the numerous studies which have led to the identification of various SIAH substrates, how these proteins and their stability relates to the observed *Siah1a* mutant phenotype of male sterility remains unclear. Therefore, to better understand SIAH1 function in the testes, a number of SIAH1 interacting proteins identified in a yeast 2-hybrid screen of a human testes cDNA library were investigated. Primarily, experiments focused on finding out whether or not any of these proteins were targets for SIAH1-mediated degradation. Two prime candidates were further investigated including NELF-A, a transcriptional regulator of developmental control genes, and ASPP1, a p53 interacting protein which promotes apoptosis. Further investigation into the SIAH1:NELF-A interaction confirmed that a genuine molecular interaction occurred *in vitro*. Transient transfection assays and analysis of NELF-A protein in *Siah1a*$^{-/-}$*Siah2*$^{-/-}$ fibroblasts revealed that SIAH proteins predominantly target ectopically expressed NELF-A protein for degradation and analysis of NELF-A regulation by the murine family of Siah proteins revealed that the closely related Siah1a protein, Siah1b, has diverged in function. Consistent with SIAH1's role in apoptotic regulation, SIAH1 was found to regulate the stability of ASPP1 and its homolog ASPP2. To better understand the downstream consequences of SIAH1-mediated degradation of ASPP1 and to shed light on ASPP1 function, protein interaction screens were carried out to identify major ASPP1-binding protein partners. A diverse set of interacting partners were identified implying ASPP1 is a multifunctional protein involved in a number of cellular pathways.

Chapter 1. Introduction

1.1 The importance of regulated protein degradation

In eukaryotes, intracellular protein degradation is a highly selective process, whereby proteins are broken down into their constituent amino acids at widely differing rates. Protein half lives can vary from several minutes for some regulatory enzymes, to several days or weeks. This selective process impacts a range of cellular functions and serves several important homeostatic purposes. For example, regulated turnover of cell cycle regulators and signal transducers is essential to control cell cycle progression, cell division and signal transduction . Similarly, gene expression patterns and developmental programs can be altered via coordinated destruction of transcriptional regulatory proteins, such as general initiation and elongation factors (Conaway et al., 2002). Additionally, turnover of proteins that are mutated, damaged, or mis-folded prevents the accumulation of aberrant proteins, which may pose a threat to cellular integrity. This is essential in protecting cells against environmental stress.

Not surprisingly, aberrations in the tightly controlled process of protein degradation have been implicated in the pathogenesis of many diseases including cancer, neurodegenerative disorders, immunological disorders and several others (Ciechanover et al., 2004). Understanding the mechanisms involved in this process are therefore of the upmost importance for understanding and treating human disease. Over the last 30 years, studies primarily carried out by Avram Hershko, Aaron Ciechanover, and Irwin Rose revealed that selective protein degradation is achieved largely via the ubiquitin-proteasome pathway. It soon became apparent that this pathway impacts nearly every aspect of eukaryotic cell biology and as a result, Hershko, Ciechanover, and Rose were awarded the Nobel prize in chemistry in 2004. Their experimental studies and findings are reviewed by Hershko (2005), Varshavsky (2005) and Kresge et al., (2006).

1.2 The ubiquitin-proteasome pathway

Eukaryotic proteins which are destined for degradation in the ubiquitin-proteasome pathway are firstly ‘tagged’ with multimers of an extremely well conserved protein known as ubiquitin (76 amino acids, 8.6kDa). This marcomolecular tag serves to mark

proteins for recognition and subsequent destruction by the 26S proteasome, a large multi-subunit protease (Figure 1).

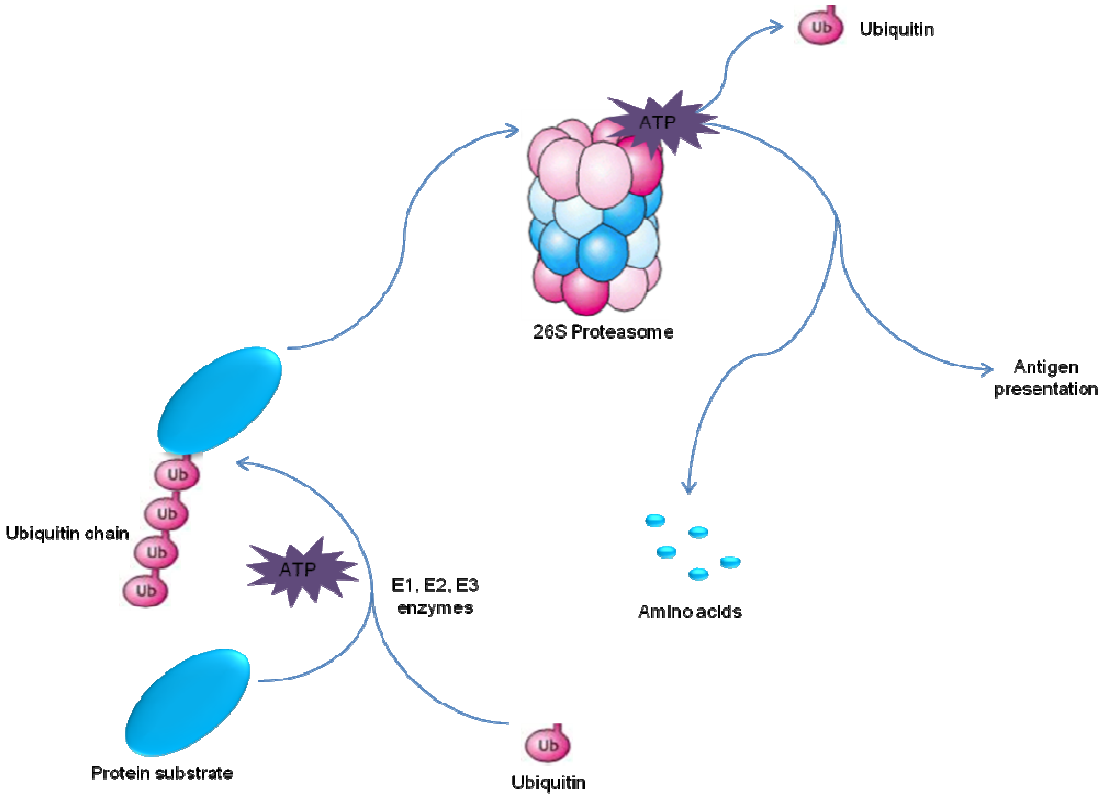

Figure 1. The ubiquitin-proteasome pathway. Proteins are marked for degradation by the covalent attachment of several ubiquitin molecules forming a polyubiquitin chain. This chain is recognised by the 26S proteasome, which cleaves the protein into numerous small peptide fragments. The ubiquitin tag is recycled and the small peptide fragments are then degraded to amino acids by peptidases in the cytoplasm or used for antigen presentation.

Tagging proteins with ubiquitin chains, known as ubiquitination or ubiquitylation, is an ATP-dependent process which requires three enzymatic components, an E1 (ubiquitin-activating enzyme), an E2 (ubiquitin-conjugating enzyme) and an E3 (ubiquitin ligase enzyme). Firstly, the process begins with a single E1 ubiquitin-activating enzyme which activates the C-terminus of ubiquitin via a two-step intra-molecular ATP-dependent reaction. Activated ubiquitin is then transferred to the active site cysteine of an E2 enzyme (Hershko et al., 1998). To date, 35 active E2 enzymes have been identified in humans (van Wijk et al., 2010). E2 enzymes then interact with a specific E3 partner to catalyze the attachment of ubiquitin to target proteins. This process culminates in the formation of a stable isopeptide linkage between the carboxyl-terminal glycine of ubiquitin and the ε-amino group of an acceptor lysine residue in the target protein (Figure

2). In some cases, an additional component referred to as an E4 aids the E3 in polyubiquitination of the target protein (Koegl et al., 1999; Hoppe 2005).

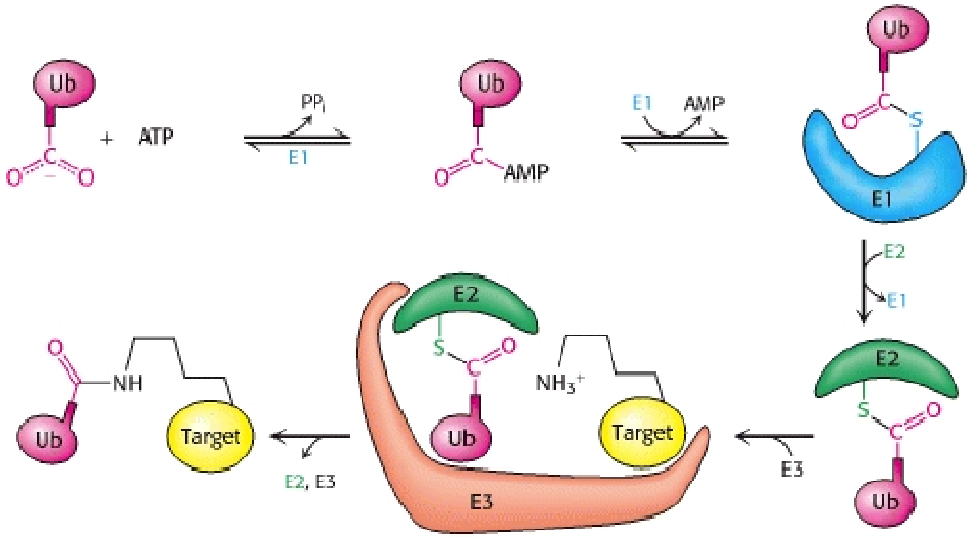

Figure 2. Ubiquitin conjugation. E1 adenylates ubiquitin and links the terminal carboxylate group of ubiquitin to a sulfhydryl group of E1 by a thioester bond. Activated ubiquitin is then shuttled to a cysteine residue in the active site of an E2 ubiquitin-conjugating enzyme. Finally, an E3 ligase catalyzes the transfer of ubiquitin from E2 to a ε-amino group on the target protein. Figure from Berg et al., (2002).

Since the initial description of the ubiquitin proteasome pathway as a protein tagging and breakdown system, knowledge in this area has rapidly advanced, with thousands of proteins being shown to be degraded by this mechanism.

Protein modification by ubiquitin also has non-conventional (non-degradative) functions. These non-traditional functions are dictated by the number of ubiquitin units attached to proteins (mono- versus polyubiquitination) and also by the type of ubiquitin linkage chain that is present. Monoubiquitination for example (i.e. the attachment of a single ubiquitin molecule to a single site on a protein) is implicated in many cellular functions including protein trafficking between various cellular compartments, DNA repair and transcriptional regulation. Protein regulation by monoubiquitination is reviewed by Hicke (2001). Ubiquitination can also be reversed by specific deubiquitinating enzymes (DUBs) which cleave covalent isopeptide linkages.

1.2.1 Types of ubiquitin chains

A single ubiquitin molecule contains seven lysine residues (K6, K11, K27, K29, K33, K48 or K63), and multi-ubiquitin chains are built by formation of an isopeptide bond

between Gly76 of one ubiquitin to the ε-amino group of one of the seven potential lysine residues. Each residue is capable of chain initiation and all seven chain types have been identified *in vivo* (Meierhofer et al., 2008). As well as homotypic ubiquitin chains whereby the same lysine residue is sequentially used for conjugation, matters are greatly complicated by reports of mixed lineage chains, utilising several distinct lysines to connect consecutive ubiquitins and heterologous chains, connecting ubiquitin with other ubiquitin-like proteins (Ikeda et al., 2008). It is the E2 enzymes and specific E2/E3 combinations which are the main determinants for lysine selection from which to construct ubiquitin chains (van Wijk et al., 2010).

The most common site of chain initiation and linkage is K48. It is the K48 chains that are the predominant signal for degradation by the proteasome and these are the most abundant ubiquitin chains in the cell. Chain linkage through K63 however is also quite common. K63 chains do not seem to play a role in protein turnover but have been implicated in a number of other processes such as signal transduction, endocytosis, and DNA damage repair (Sun et al., 2004; Mukhopadhyay et al., 2007). K63-ubiquitination has also been associated with protein inclusion bodies in neurodegenerative disease (Lim et al., 2010). Although various other types of chains exist, available information is not yet sufficient to fully understand their function.

1.2.2 Ubiquitin-like proteins

In addition to ubiquitin itself, many ubiquitin-like proteins (UBLs) have been identified (Hochstrasser 2009). These ubiquitin-like molecules are structurally similar to ubiquitin and are processed, activated, and conjugated to target proteins by enzymatic steps that are similar to the corresponding mechanisms for ubiquitin (Kerscher et al., 2006). These conjugates can also be removed by specific UBL-isopeptidases which function similarly to deubiquitinating enzymes.

To date, at least ten UBLs have been identified in mammalian cells. These include APG8, APG12, SUMO (small ubiquitin-related modifier), NEDD8, ISG15 (interferon stimulated gene), FAT10, UBL5, UFM1, URM1 and HUB1. Covalent attachment of these UBLs to target proteins does not generally signal for protein degradation. Instead, attachment of UBLs can adjust substrate conformation, affect affinity for ligands or other interacting molecules and alter substrate localisation. They influence a variety of

biological processes including DNA synthesis, DNA repair, cell-cycle control, transcription, translation, signal transduction, protein quality control and more (Welchman et al., 2005).

Cross regulation between the various conjugation pathways often occurs as some proteins can be modified by more than one UBL. For instance, SUMO modification often acts antagonistically to that of ubiquitination resulting in stabilisation of protein substrates (Denuc et al., 2010). Thus, the attachment of ubiquitin and UBLs to proteins is now a widely recognised form of protein modification, involved in all cellular regulatory activities.

1.2.3 E3 Ubiquitin Ligases

E3 ubiquitin ligases play a particularly important role in regulating protein breakdown as it is these which select specific protein substrates for ubiquitination (Hershko et al., 1986). They constitute a large and complex superfamily and many hundreds of genes encoding E3 ubiquitin ligases have been identified in the human genome (Li et al., 2008). Each E3 ligase can target a number of proteins for ubiquitin modification, however the detailed molecular mechanisms of protein selection are poorly understood and the exact protein substrates for each E3 are mostly unknown. E3 enzymes which are specific for targeting proteins for modification with UBLs such as SUMO and NEDD8 have also been identified, however herein ubiquitin-specific E3's are discussed.

The importance of E3 ubiquitin ligases is highlighted by the number of cellular processes they regulate and the number of human diseases associated with absence or inefficiency of E3 ligase function. For example, germline mutations in the gene encoding the BRCA1 E3 ubiquitin ligase result in defective E3 activity and are associated with an inherited predisposition for breast and ovarian cancer (Futreal et al., 1994; Miki et al., 1994). Also, mutations in the E3-ubiquitin ligase parkin cause a recessively transmitted early onset form of Parkinson's disease (Kitada et al., 1998), a degenerative disorder of the central nervous system. These mutations result in defective ligase activity so protein substrates accumulate in neurons and contribute to disease development (Dawson 2006). Abnormal protein ubiquitylation due to loss of an E3 ligase or inappropriate targeting is also associated with other neurodegenerative disorders such as Alzheimer's and Huntington's disease. For reviews on the role of ubiquitin-protein ligases in

neurodegenerative disease see Mayer (2003) and Ardley and Robinson (2004). For further examples of how dysregulated ubiquitin ligase activity contributes to the development and progression of various cancers see Newton and Vucic (2007), Sun (2006) and Confalonieri et al (2009). Not surprisingly, E3 ubiquitin ligases are attractive therapeutic targets for treatment of human disease.

Generally, E3 ubiquitin ligases can be classified into three main types based on their structure and mechanism of action. These include the HECT (homologous to E6-AP carboxy-terminus) domain family, the U-box family and the RING (really interesting new gene) finger family (Jackson et al., 2000). Each of these three classes of E3 ligases have distinct domains responsible for binding to E2 enzymes (RING-finger, HECT or U-box domain), and other domains which function to recruit substrates.

The HECT domain proteins are large monomeric E3's which contain a cysteine residue that forms a covalent bond with the activated ubiquitin before transferring it to the substrate (Scheffner et al., 1995). For reviews on HECT E3 ligase regulation, function and their roles in human disease see Kee and Huibregtse (2007); Scheffner and Staub (2007); Rotin and Kumar (2009). RING and U-box E3 ligases however do not possess an active-site cysteine residue and these E3's simply serve as a scaffold, bringing the E2-ubiquitin complex and substrate in close proximity to mediate the transfer of ubiquitin from the E2 enzyme directly to the substrate.

The vast majority of E3 ubiquitin ligases are members of the RING finger family and over 600 human genes encoding RING finger E3s have been identified (Freemont 2000; Deshaies et al., 2009), The RING finger constitutes a small zinc-binding domain that binds to specific E2 enzymes (Lorick et al., 1999; Joazeiro et al., 2000). The U-box E3s have a similar tertiary structure to that of the RING finger except that the U-box scaffold is stabilised by salt-bridges and hydrogen bonds rather than zinc ions (Aravind et al., 2000; Hatakeyama et al., 2003).

The RING-type and U-box ligases can be further subdivided into monomeric ligases, or multi-subunit E3's. Examples of monomeric RING-type ligases include the oncoprotein, Mdm2, which regulates the stability of the tumour suppressor, p53 (Fang et al., 2000); Parkin, which modulates the stability of the transcription factor SIM2 (Okui et al., 2005); and Cbl, which catalyzes the ubiquitination of tyrosine-kinase cell surface receptors

(Levkowitz et al., 1999). The best understood multisubunit E3's are the SCF (Skp1-Cul1-F-box) complexes. For a review on these ligases see Willems et al., (2004). A number of diverse substrates of SCF complexes have been identified, including key regulators of the cell cycle and key molecules that control inflammation, such as NF-κB (Karin et al., 2000) and β-catenin (Latres et al., 1999).

In addition to substrate ubiquitination, many E3 ligases can also self- or auto-ubiquitinate in the presence of an E2 enzyme, a property that may be used as an autoregulatory mechanism to control its own intracellular levels.

1.3 The Siah family

Drosophila SINA (Seven in Absentia) and its mammalian orthologs are evolutionarily conserved E3 ubiquitin ligases containing an N-terminal RING-finger domain required for interaction with E2 ubiquitin conjugating enzymes, and a C-terminal substrate binding domain which interacts with target proteins (Hu et al., 1997a). *Drosophila SINA* was first isolated in a screen for mutations which affect the morphology of the *Drosophila* eye and it was the first of the family to be defined (Carthew et al., 1990). SINA targets the transcriptional repressor, tramtrack for degradation and is essential for the correct development of R7 photoreceptor cells in the compound eye (Carthew et al., 1994; Tang et al., 1997). More recently, Cooper et al., (2008) identified a novel *Drosophila* protein which is homologous to Sina which they named Sina-Homologue, SinaH (46% identical to SINA). SinaH can also direct the degradation of the transcriptional repressor Tramtrack (Cooper et al., 2008).

Characterisation of murine *Sina* homologues by Della et al., (1993) revealed that the mouse genome contains a family of five *Siah* (*Seven in Absentia Homologue*) genes found at unlinked chromosomal positions (Holloway et al., 1997). Two of these genes, *Siah1-ps1* and *Siah1-ps2,* are pseudogenes as they contain a number of frame shifts and in-frame stop codons within the expected coding region. However, the remaining three genes, *Siah1a*, *Siah1b* and *Siah2* have open reading frames and are expressed. Comparison of *Siah1a* and *Siah1b* cDNA revealed that they were 97% identical at the nucleotide level, differing by only 25 nucleotides (Holloway et al., 1997). Comparison of their protein sequence revealed they were 97.8% identical at the amino acid level

differing by only six amino acids (Holloway et al., 1997). The *Siah2* cDNA sequence however, is more divergent showing 73% nucleotide and 78% amino acid homology with Siah1a/1b (Della et al., 1993; Holloway et al., 1997).

In contrast, only two SINA homologues have been identified in the human genome, *SIAH1* and *SIAH2* (Adams et al., 1992; Nemani et al., 1996; Holloway et al., 1997), both of which encode functional proteins. The SIAH1 and SIAH2 proteins are 76% and 68% identical to the *Drosophila* SINA protein and 44% and 40% identical to SinaH (Hu et al., 1997a; Cooper et al., 2008). The human SIAH1 and murine Siah1a proteins differ by only one amino acid and the ancestral *Siah1* gene of humans and mice is *Siah1a* (Hu et al., 1997a). Despite efforts by various groups, no human variant cDNAs corresponding to murine *Siah1b* have been identified (Hu et al., 1997a; Holloway et al., 1997). Therefore this suggests that *Siah1b* arose after the human and mouse lineages separated. Also, Wheeler et al., (2002) were unable to detect rat cDNAs corresponding to murine *Siah1b* suggesting that *Siah1b* is a mouse specific gene which does not exist in other species.

1.3.1 SIAH expression

The *Drosophila Sina* gene was reported to be widely expressed in embryonic, larval, pupal and adult tissues (Carthew and Rubin, 1990) and the murine *Siah1a*, *Siah1b* and *Siah2* genes were reported to be widely expressed at a low levels in the embryo and adult (Della et al., 1993). Similarly, Hu et al (1997a) reported that human *SIAH1* and *SIAH2* are expressed at low, but uniform levels in most adult tissues and it was later established that levels of Siah family proteins are maintained at low levels through ubiquitination-dependent protein turnover (Hu et al., 1999). Human SIAH1 and SIAH2 were found to auto-regulate their own stability through interactions of their RING-domains with E2 enzymes (Hu and Fearon, 1999).

More recently, splicing variants of human SIAH1 have also been identified. These are designated SIAH-1L, encoding a 298 amino acid protein, and SIAH-1S, encoding a 195 amino acid protein, and these appear to have differing expression patterns and functional activity compared to the 282 amino acid SIAH1 protein (Iwai et al., 2004; Mei et al., 2007; Wen et al., 2010a).

1.3.2 SIAH substrates

The SINA and SIAH proteins have been found to localise in both the nucleus and the cytoplasm whereby they facilitate the ubiquitination and degradation of several, seemingly unrelated proteins listed in Table 1 (Carthew et al., 1990; Roperch et al., 1999). They can achieve this either by binding directly to the substrate (Susini et al., 2001) or by functioning as a multi-subunit complex, binding to 'co-factor' proteins, which instead of becoming ubiquitinated, act as molecular links to other substrates. For example, SIAH1, APC (adenomatous polyposis coli), SIP (Siah interacting protein), Skp1 and Ebi form a multi-subunit complex and target β-catenin for degradation (Matsuzawa et al., 2001). Both SIP and APC have been shown to interact with the C-terminus of SIAH1, although no direct interaction with the substrate, β-catenin has been reported (Liu et al., 2001).

In a second example, formation of a complex including *Drosophila* SINA, Phyllopod (Phyl) and the F-box protein Ebi, results in the ubiquitination and degradation of the transcriptional repressor, tramtrack. In this complex it is the nuclear protein, Phyl, which functions as the adaptor to physically link tramtrack with SINA (Tang et al., 1997; Li et al., 2002; Cooper et al., 2008). Thus, not all SIAH-binding proteins are targets for SIAH mediated degradation. All of the SIAH interacting proteins identified to date which are not targets for SIAH-mediated degradation are listed in Table 2.

Substrate	Protein function	References
Transcriptional regulators		
BOB1/ OBF-1	Transcriptional co-activator which regulates transcriptional activity in B lymphocytes.	(Boehm et al., 2001; Tiedt et al., 2001)
c-myb	Oncogenic transcription factor involved in cellular proliferation and apoptosis.	(Tanikawa et al., 2001)
CtIP	Transcriptional co-repressor involved in cellular proliferation, DNA repair and cell cycle control.	(Germani et al., 2003)
HDAC3	Histone deacetylase which represses transcription.	(Zhao et al., 2010)
N-CoR	Transcriptional co-repressor which promotes chromatin condensation.	(Zhang et al., 1998; Frasor et al., 2005)
PML	Transcriptional co-regulator and key component of PML bodies. The PML gene is often involved in oncogenic chromosomal translocation with the retinoic acid receptor (RAR)α gene associated with acute myelocytic leukemia (AML).	(Fanelli et al., 2004)
TIEG1	Transcription factor which regulates cell proliferation, differentiation and apoptosis.	(Johnsen et al., 2002)
Enzymes		
FIH	A hydroxylase which regulates the hypoxia inducible factor (HIF1α) a central regulator of the hypoxic response.	(Fukuba et al., 2008)
PHD1 and PHD3	Catalyze the hydroxylation of HIF1α resulting in HIF1α ubiquitination and degradation.	(Nakayama et al., 2004a; Nakayama et al., 2004b)
OGHDC	Rate-limiting enzyme in the mitochondrial Krebs cycle.	(Habelhah et al., 2004)
Neuronal		
AF4	Transcription cofactor which is important in the normal function of the central nervous system. The *Af4* gene is also frequently disrupted in childhood leukaemia.	(Bursen et al., 2004; Oliver et al., 2004)
Synphilin-1	Synaptic vesicle protein of unknown function. Interacts with α-synuclein in neuronal tissue and is a major component of Lewy bodies, which characterise pathological conditions such as Parkinson's disease.	(Nagano et al., 2003; Liani et al., 2004; Avraham et al., 2005)
Synapto-physin	Synaptic vesicle membrane protein of unknown function.	(Wheeler et al., 2002)
Group 1 mGluRs	G protein-coupled receptors which perform a variety of functions in the central and peripheral nervous systems. Only the long splice forms of mGluR1 are down regulated by SIAH proteins.	(Moriyoshi et al., 2004)
Others		
AML1-ETO and PML-RARα	Chimeric fusion proteins which contribute to the pathogenesis of leukaemias.	(Kramer et al., 2008)
β-catenin	Functions as both a transcriptional activator and a cellular adhesion molecule. Mutated in multiple cancers.	(Liu et al., 2001; Matsuzawa et al., 2001)
BAG-1*	Inhibitor of apoptosis. A study by Matsuzawa et al., (1998) implied that BAG-1 negatively regulates Siah1a. In contrast, studies by Sourisseau et al., (2001) imply that Siah2 targets BAG-1 ubiquitination and degradation.	(Matsuzawa et al., 1998; Sourisseau et al., 2001)
DCC	Transmembrane receptor for netrin-1 required for axon guidance.	(Hu et al., 1997b)
EB3	Microtubule plus-end-binding protein involved in	(Ban et al., 2009)

	microtubule polymerisation. Facilitates cell cycle progression and may play a role in cell migration.	
HIPK2	Protein kinase which interacts with several transcription factors. Key regulator of apoptosis and the hypoxic response.	(Winter et al., 2008; Calzado et al., 2009; Kim et al., 2009)
Kid	A chromosome and microtubule binding-protein implicated in the normal progression of mitosis and meiosis.	(Germani et al., 2000)
KSHV ORF45	Protein encoded by the Kaposi's sarcoma-associated herpes virus (KSHV) genome which is essential for KSHV infection.	(Abada et al., 2008)
MYPT1	A subunit of the myosin phosphatase holoenzyme. Control of myosin phosphorylation plays an important role in many cellular functions including smooth muscle contraction.	(Twomey et al., 2010)
Numb	Membrane-associated protein which plays a role in the determination of cell fate during development.	(Susini et al., 2001)
PEG10*	Suppresses apoptosis in hepatocellular carcinoma although functional mechanism is unknown. Studies by Yoshibayashi et al., (2007) suggest that PEG10 is another target of SIAH1-mediated degradation however this was not confirmed.	(Yoshibayashi et al., 2007)
PLC_C	Hydrolyses phospholipids and plays an important role in various signal transduction processes.	(Yun et al., 2008)
Polycystin-1	Transmembrane protein involved in cell adhesion. May regulate intracellular calcium homoeostasis and other signal transduction pathways.	(Kim et al., 2004b)
repp86	Integral component of the mitotic spindle which plays an essential role in cell cycle progression.	(Szczepanowski et al., 2007)
Spry2	Regulates receptor tyrosine kinase signalling, cell growth and differentiation.	(Nadeau et al., 2007)
TRAF2	Associates with, and mediates signal transduction from members of the TNF receptor superfamily.	(Habelhah et al., 2002)
Tramtrack	Transcriptional repressor involved in eye development in *Drosophila*.	(Li et al., 1997; Tang et al., 1997; Cooper et al., 2008)
TRB3	Negative regulator of various signal transducers including AF4. Also involved in insulin signalling.	(Zhou et al., 2008)
T-STAR	Alternative splicing factor.	(Venables et al., 2004)
RINGO	A cyclin dependent kinase (CDK) activator involved in cell cycle regulation	(Gutierrez et al., 2006)

Table 1. SIAH substrate proteins identified to date that are targeted for proteasomal degradation. Abbreviations: AML, acute myeloid leukemia; BOB-1, B-cell Oct-binding protein; CtIP, C-terminal interacting protein; DCC, deleted in colorectal cancer; EB3, end-binding protein 3; FIH, factor inhibiting HIF1α; HIPK2, homeodomain interacting protein kinase 2; Kid, Kinesin like DNA binding protein; KSHV ORF45, Kaposi's sarcoma-associated herpes virus open reading frame 45; mGluRs, metabotropic glutamate receptors; MYPT1, myosin phosphatase target subunit 1; N-CoR, nuclear receptor co-repressor; OBF-1, Oct binding factor 1; OGHDC, 2-oxoglutarate dehydrogenase complex; PEG10, paternally expressed gene 10; PHD1 and PHD3, prolyl-hydroxylases 1 and 3; PLC_C, phospholipase Cγ; PML, promyelocytic leukemia protein; repp86, restrictedly expressed proliferation-associated protein; Spry2, sprouty 2; TIEG1, transforming growth factor β inducible early gene-1; TRAF2, TNF receptor-associated factor 2; TRB3, tribbles 3 homolog. *Although evidence suggests these proteins are substrates for SIAH mediated degradation, published studies are not conclusive.

Interacting protein	Protein function	References
E2 enzymes		
UbcH5	A canonical E2 enzyme which is active in a broad number of ubiquitin transfer reactions.	(Matsuzawa et al., 2001)
UbcH8	E2 enzyme enriched in the brain. Facilitates the ubiquitination of α-synuclein, AML1-ETO and PML-RARα in combination with Siah.	(Wheeler et al., 2002; Kramer et al., 2008; Lee et al., 2008b)
UbcH9	SINA interacts with *Drosophila* Ubc9, and both human SIAH1 and SIAH2 were found to interact with the human homolog, UbcH9 in a yeast 2-hybrid assay. UbcH9 however conjugates SUMO, not ubiquitin (Desterro et al., 1997).	(Hu et al., 1997b)
Neuronal		
α-synuclein	Protein of unknown function, primarily found in neural tissue. Monoubiquitination of α-synuclein by Siah proteins promotes its aggregation into insoluble fibrils found in Lewy bodies.	(Liani et al., 2004; Engelender 2008; Lee et al., 2008b; Rott et al., 2008)
Dab-1	Signal transducer which regulates neuronal positioning in the developing brain. Interaction with Siah results in inhibition of Siah activity.	(Park et al., 2003)
Synphilin-1A	Protein of unknown function. Ubiquitination by SIAH does not promote its degradation but instead increases the formation of synphilin-1A inclusions found in Lewy bodies. Synphilin-1A also appears to regulate SIAH activities.	(Szargel et al., 2009)
Others		
α-tubulin	Cytoskeletal protein.	(Germani et al., 2000)
APC	Plays a critical role in several cellular processes such as cell division, cell growth and cell migration. It is a member of the protein complex which targets β-catenin for degradation.	(Liu et al., 2001; Matsuzawa et al., 2001)
GAPDH	Glycolytic enzyme which plays a major role in apoptosis. Interaction with SIAH results in translocation to the nucleus, SIAH stabilisation and apoptosis.	(Hara et al., 2005; Hara et al., 2006)
PEG3	Induces apoptosis in cooperation with Siah1a.	(Relaix et al., 2000)
Phyllopod	*Drosophila* adaptor protein required for tramtrack degradation by SINA. A fragment of the phyllopod protein has been shown to inhibit mammalian Siah protein activity.	(Li et al., 2002; Cooper et al., 2008; Moller et al., 2009)
POSH	A scaffold component of the apoptotic JNK pathway	(Xu et al., 2006)
Ski	A transcriptional co-repressor. Interaction with Siah2 inhibits Siah2 activity.	(Zhao et al., 2010)
SIP	Adaptor protein required for SIAH-mediated degradation of β-catenin. Recently identified as a potential regulator of apoptosis.	(Matsuzawa et al., 2001; Santelli et al., 2005; Luo et al., 2010)
Vav	GDP/GTP exchanger protein which regulates cytoskeletal reorganisation and signalling pathways. SIAH2 inhibits its activity.	(Germani et al., 1999)

Table 2. SIAH-interacting proteins identified to date which are not targeted for proteasomal degradation. Abbreviations: APC, adenomatous polyposis coli; Dab-1, disabled-1; GAPDH, glyceraldehyde-3-phosphate dehydrogenase; PEG3, paternally-expressed gene 3; POSH, plenty of SH3s; SIP, Siah interacting protein; Ubc, ubiquitin conjugating enzyme.

Some of the SIAH substrates listed in Table 1 are targeted for proteolytic degradation by both human SIAH1 and SIAH2 proteins. For example, DCC is regulated by both SIAH1 in SIAH2 (Hu et al., 1997b). In some cases, substrates are targeted for degradation by solely one SIAH member, for example TRAF2 is targeted for proteasomal degradation by SIAH2 but not SIAH1 (Habelhah et al., 2002). In most publications however, only one SIAH family member is analysed and often it is not clear which SIAH family member is under scrutiny. Thus, further investigation is needed to determine whether or not the proteins in tables 1 and 2 are regulated by or are regulators of each of the murine and human Siah/SIAH proteins.

It is clear however that SIAH proteins operate in diverse signalling pathways as they interact with such a varied array of proteins. As a result SIAH proteins play a critical role in a range of biological processes including cell cycle control, apoptosis, tumour suppression (discussed further in sections 1.3.4 and 1.3.5), axon guidance (Hu et al., 1997b), and the hypoxic response (see section 1.3.7).

1.3.3 Siah1b and SIAH1 are direct transcriptional targets of p53

A number of studies have reported that overexpression of p53 induces expression of *Siah1* family genes. p53 is a homotetrameric transcription factor that can activate/repress the transcription of a number of genes controlling cell cycle progression, apoptosis, and DNA repair. It plays an extremely important role in regulating cell proliferation and is one of the most frequently mutated genes in human tumours (Bergamaschi et al., 2004). p53 is normally present at low levels in the cell but in response to various types of cellular stress, protein levels increase considerably and it accumulates in the nucleus where it binds to specific DNA sequences (El-Deiry et al., 1992). Activation of p53 results in either cell cycle arrest or the induction of apoptosis.

The murine *Siah1b* gene was found to be activated during p53-mediated apoptosis by Amson and colleagues in (1996). Later, analysis of the *Siah1b* promoter revealed that it contains a functional p53 responsive element which is bound by p53 *in vitro* and *in vivo* and activation of p53 leads to a significant increase in *Siah1b* transcription (Fiucci et al., 2004). Thus *Siah1b* is a direct transcriptional target of p53.

A number of reports have also shown that the human *SIAH1* gene is activated by p53. For instance, Matsuzawa et al., (1998) found that genotoxic stress or overexpression of p53 in 293 cells resulted in an increase in *SIAH1* mRNA levels. Liu et al., (2001) further confirmed this in 293T cells showing that *SIAH1* mRNA levels increased when p53 was overexpressed. They also showed that levels of the SIAH1 substrate, β-catenin were dramatically reduced when p53 was transiently overexpressed. Gene expression analysis by Yoon et al., (2002) also revealed that human *SIAH1* transcription significantly correlated with the dosage of p53.

Maeda et al., (2002) also found that *SIAH1* mRNA was increased by p53 overexpression in three different cell lines (Saos2, 293, K562). Surprisingly however, reporter plasmids containing the promoter region of *SIAH1* did not respond to p53 (Maeda et al., 2002). They therefore hypothesised that p53 may activate the *SIAH1* gene through another region of *SIAH1* or induction by p53 may not be due to transcription, but by mRNA stabilisation.

Later, a novel *SIAH1* transcript, *SIAH-1L* was characterised (Iwai et al., 2004). This transcript contains an extra 48bp and is transcribed from an alternative in-frame ATG start codon. A p53 responsive element was identified upstream of this alternative in-frame ATG start codon and it was revealed that *SIAH-1L* mRNA was strongly induced after p53 activation whereas the 849bp *SIAH1* mRNA remained unchanged (Iwai et al., 2004). Thus, this study implied that is was *SIAH-1L* which was the p53 inducible transcript.

It is important to note that, in the majority of publications, the effect of p53 on *Siah* gene expression is largely investigated through overexpression studies. In order to investigate whether *Siah* genes are activated by p53 physiologically, David Bowtell and colleagues analysed levels of *Siah1a*, *Siah1b*, and *Siah2* mRNA in tissues harvested from wild-type mice in which p53 activation was induced by whole body gamma-irradiation (Frew et al., 2002). In this study they found that established p53 target genes (including p21 and cyclin G) were strongly activated, but *Siah* gene expression was not (Frew et al., 2002). It is possible that regulation of *Siah* gene expression differs between human and murine cells or alternatively, p53 may not play a major role in regulating *Siah* expression *in vivo*. However, in stark contrast to other publications they also report that transfection of p53 in 293 or 293T cells had no affect on *SIAH1* expression (Frew et al., 2002).

Discrepancies between studies may be due to differing experimental conditions. However, in support of *SIAH1* being a direct p53 transcriptional target, several studies have shown that overexpression of SIAH1 mimics the effects of p53 activation, promoting either apoptosis or cell cycle arrest.

1.3.4 SIAH1, apoptosis and cell cycle control

A number of publications have revealed that SIAH1 plays an important role regulating cell proliferation and cell apoptosis. Overexpression of SIAH1 was reported to induce apoptosis in U937 cells, a human leukemic monocyte lymphoma cell line (Roperch et al., 1999), and SIAH1 overexpression in MCF-7 cells, a breast cancer cell line, was found to both inhibit cell growth and increase apoptosis (Bruzzoni-Giovanelli et al., 1999).

Consistent with a role in apoptosis, elevated expression of SIAH1 has been observed in dying cells. For example, Nemani et al., (1996) demonstrated that expression of SIAH1 is elevated in some leukemic cells and normal intestinal epithelial cells that have reached the terminal stage and are dying by apoptosis. It has also been shown that SIAH1 protein is stabilised upon activation of the apoptotic JNK pathway and contributes to JNK-mediated cell death (Xu et al., 2006; Wen et al., 2010b).

Matsuzawa et al., (1998) found that transient transfection of SIAH1 in 293 cells and GM107 fibroblast cells resulted in growth arrest without induction of apoptosis. Similarly, Reliax et al., (2000) reported that expression of Siah1a alone in murine fibroblasts induced growth arrest however, when they co-expressed PEG3 another p53-inducible gene, cells underwent apoptotic cell death. Thus, they demonstrated that PEG3 co-operates with Siah1a to promote apoptosis. PEG3 was found to be specifically activated during p53 mediated apoptosis but not during p53-dependent cell cycle-arrest and so it was proposed that PEG3 performed a pivotal role in determining the choice between cell death and survival.

It is possible that SIAH1 induces apoptosis or inhibits cell growth through ubiquitination and proteasomal degradation of some of its targets proteins. A number of functional studies have revealed that SIAH proteins can target various transcription factors (including c-myb, CtIP and TIEG1, see Table 1) for degradation which are important in controlling cell cycle progression and apoptosis. SIAH proteins also regulate β-catenin, a

multifunctional protein which activates expression of target genes to promote cell cycle progression and inhibit apoptosis, thus providing a link between SIAH proteins and cell cycle control. As well as transcription factors and β-catenin, SIAH proteins also target the protein kinase HIPK2 for degradation (Winter et al., 2008; Calzado et al., 2009). HIPK2 is a key a mediator of DNA damage-induced apoptosis thus implicating SIAH in the DNA damage response. The exact way in which SIAH1 contributes to the decision between promotion of apoptosis or cell-cycle arrest, however is not clearly defined.

1.3.5 SIAH1 and tumour suppression

Given that SIAH1 can promote apoptosis and inhibit cell growth, SIAH1 is often referred to as a tumour suppressor. In support of SIAH1 functioning as a tumour suppressor, studies by Robert Amson and Adam Telerman whose research focuses on tumour reversion, the process by which some cancer cells lose their malignant phenotype, have revealed that up-regulation of SIAH1 expression is crucial to tumour reversion (Nemani et al., 1996; Roperch et al., 1999; Tuynder et al., 2002). The molecular programme of tumour reversion is reviewed by Telerman and Amson (2009). It is perhaps therefore not surprising that there is accumulating evidence in the literature suggesting that *SIAH* genes, particularly *SIAH1* are down regulated or inactivated in human cancer and so SIAH1 may be an effective therapeutic molecule in treating the disease.

1.3.6 SIAH1 and disease

Mutational analysis of the *SIAH1* gene in gastric tumours identified two somatic missense mutations in two out of the nine gastric cancers examined (Kim et al., 2004a). Functional analysis revealed that these mutants were unable to down-regulate β-catenin in HEK293T cells and they were unable to induce apoptosis (Kim et al., 2004a). Thus, mutation of the *SIAH1* gene appears to contribute to the development and/or progression of a subset of gastric cancers via β-catenin stabilisation and inhibition of apoptosis. Also, down regulation of *SIAH1* expression has been observed in advanced stages of hepatocellular carcinoma (HCC) suggesting that inactivation of SIAH1 plays an important role in HCC progression (Matsuo et al., 2003; Yoshibayashi et al., 2007). Introduction of SIAH1 into hepatoma cells has been shown to efficiently induce apoptosis and inhibit cell growth thus demonstrating that SIAH1 may be an effective therapeutic molecule for HCC

(Yoshibayashi et al., 2007). Downregulation of both SIAH1 and SIAH2 in breast tumours has also been reported (Confalonieri et al., 2009) and analysis of *SIAH1* and *SIAH-1L* mRNA expression in breast cancer cell lines revealed that *SIAH1* and *SIAH-1L* mRNAs were absent in four of five breast cells lines (He et al., 2010). Thus, SIAH genes, and SIAH1 in particular, are believed to be a key genes in halting cancer progression.

As well as playing a role in tumorigenesis, SIAH activity plays an important role in Parkinson's disease (PD), the second most common neurodegenerative disorder in humans. PD is characterised by progressive loss of dopaminergic neurons due to accumulation of ubiquitinated protein aggregates called Lewy bodies. These deposits have been found to contain both SIAH1 and SIAH2, and the SIAH substrates α-synuclein and synphilin-1. SIAH proteins have been shown to interact with and mono-ubiquitinate α-synuclein which is the primary protein component of Lewy bodies (Liani et al., 2004; Lee et al., 2008b; Rott et al., 2008). Monoubiquitination of α-synuclein does not result in protein degradation but instead appears to promote protein aggregation both *in vitro* and *in vivo* which is toxic to cells (Lee et al., 2008b; Rott et al., 2008; Engelender 2008). SIAH proteins have been also shown to promote polyubiquitination and proteasomal degradation of synphilin-1 (Nagano et al., 2003; Liani et al., 2004). However, inability of the proteasome to degrade polyubiquitinated synphilin-1 again leads to the formation of ubiquitinated inclusions. Thus, SIAH proteins play a key role in promoting inclusion formation.

Mutation screening of the SIAH1 gene in 209 PD patients failed to identify any disease causing mutation suggesting that genetic alterations of SIAH1 do not contribute to the pathogenesis of PD (Franck et al., 2006). It is possible however that too few patients were used in this study or, alternatively, PD pathogenesis may result from defects in other components of the ubiquitin proteasome pathway.

1.3.7 SIAH2, the hypoxic response and tumorigenesis

In contrast to SIAH1, SIAH2 plays an important role in regulating the cellular response to hypoxia which is triggered when cells are deprived of adequate oxygen. Cells exposed to decreased oxygen alter various cellular activities in order to maintain homeostasis.

Essentially SIAH2 controls the stability of prolyl hydroxylases, PHD3 and PHD1 (see Table 1), which in turn regulate the stability of hypoxia inducible factor (HIF), a transcription factor which is considered to be a key regulator of the hypoxic response. HIF regulates the expression of many genes involved in the cell cycle, cell death, cellular metabolism, cell migration and angiogenesis (formation of blood vessels). For a more in depth summary on the role of SIAH2 in the hypoxic pathway see the review by Nakayama (2009).

Hypoxia often occurs in tumorigenic environments. As tumours grow, they rapidly outgrow their blood supply leaving regions with insufficient oxygen. In these hypoxic regions HIF triggers a response necessary to recruit new blood vessels thus playing an important role in promoting tumour cell survival. This pathway is reviewed by Semenza (2007). As SIAH2 indirectly controls HIF abundance, the potential role of SIAH2 in tumour development has been studied in various mouse models (Qi et al., 2008). Results showed that SIAH2 seems to promote vasculogenesis, cell growth and metastasis (Qi et al., 2008). Consistent with this, a number of studies have shown that inhibition of SIAH2 activity blocks formation of tumours (Schmidt et al., 2007; Ahmed et al., 2008; Qi et al., 2008; Moller et al., 2009).

1.3.8 Siah mutants

As noted earlier (section 1.3) the *Drosophila sina* mutant lacks R7 photoreceptor cells in the compound eye. However, the mutant phenotype is not restricted to the eye. Flies which are homozygous null for the *sina* allele have sensory bristle abnormalities, a reduced adult life-span, lethargic adult behaviour and they are sterile (Carthew et al., 1990). While SINA's role in R7 cell fate determination has been elucidated, it remains unknown as to why the *sina* mutant flies are subviable and infertile.

In order to gain a greater physiological understanding of the role of mammalian Siah proteins, *Siah1a* and *Siah2* mutant mice were generated by David Bowtell and colleagues (Dickins et al., 2002; Frew et al., 2003). *Siah1a* mutant mice were postnatally growth retarded (Figure 3) and few survived beyond 3 months (Dickins et al., 2002). Females were sub-fertile and males were sterile due to cell cycle arrest during the first meiotic division of spermatogenesis (Dickins et al., 2002). It was hypothesised that the previously identified Siah substrate Kid (see Table 1), which is a chromosome and

microtubule binding-protein, may be required for successful chromosome segregation and completion of meiosis. However researchers were unable to detect any difference in Kid abundance in *Siah1a* mutants and controls (Germani et al., 2000; Dickins et al., 2002). The abundance of other known Siah target proteins including β-catenin and Bag-1 were also measured in a various tissues, but again no differences were detected in the steady state levels of these proteins when comparing *Siah1a* mutants and controls. Further analysis revealed that *Siah1a* mutant mice also had a low bone volume phenotype and exhibited skeletal abnormalities, thus showing Siah1a is also essential for normal bone metabolism (Frew et al., 2004).

Due to *Siah1* genes being linked to negative regulation of the cell cycle, Dickins et al., (2002) compared the growth of murine embryonic fibroblasts (MEFs) derived from wild-type and *Siah1a*$^{-/-}$ embryos. They found that *Siah1a*$^{-/-}$ MEFs did not display cell cycle or proliferative defects (Dickins et al., 2002). Since Siah1a and Siah1b are almost identical, it was hypothesised that *Siah1b* expression may mask the full consequences of Siah1a absence. Interestingly, *Siah1b* resides on the X chromosome, which is transcriptionally silenced during meiosis in male germ cells. Therefore it is likely that it is only when this gene is silenced by X chromosome inactivation during spermatogenesis that a true *Siah* gene loss of function phenotype is observed. For that reason, this may explain why removal of Siah1a has dire consequences solely in the meiotic cells of the testes.

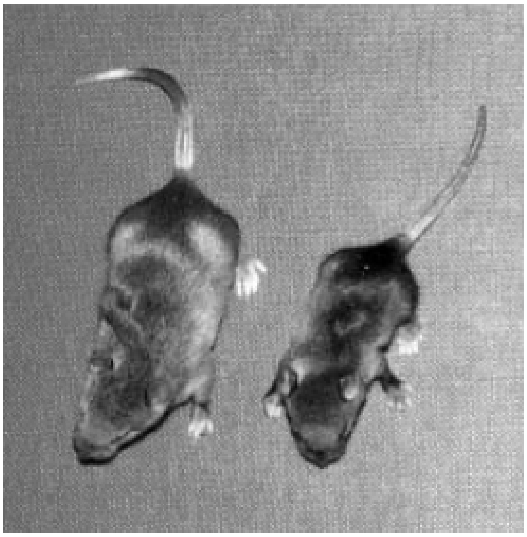

Figure 3. Siah1a deficiency causes growth retardation. A two week old *Siah1a*$^{-/-}$ mutant mouse (right) and a wild-type littermate of the same sex (left). Figure from Dickins et al, (2002).

In contrast to *Siah1a*$^{-/-}$ mice, *Siah2* mutant mice were largely phenotypically normal. Cellular responses that were regulated by previously identified Siah2 substrates (TRAF, OBF-1 and DCC) also appeared to be unaffected (Frew et al., 2003). Combined mutation of *Siah1a* and *Siah2*, however, resulted in neonatal lethality, proving that Siah1a and Siah2 do have overlapping functions which is perhaps not surprising considering their high degree of similarity (Frew et al., 2003).

Given the proposed tumour suppressor function of human SIAH1 and its murine homolog Siah1a, it is of interest to note that there was no apparent increase in tumour incidence in *Siah1a* or *Siah2* knockout mice. Therefore, this implies that Siah proteins do not play a significant role in tumour development. However, it is likely that multiple gene disruptions affecting various cellular pathways are required for tumour formation.

David Bowtell and colleagues also attempted to generate a *Siah1b* mutant mouse, however *Siah1b*$^{-/-}$ embryos exhibited either severe developmental abnormalities or were reabsorbed during pregnancy (Frew et al., 2002). Therefore, *Siah1b* appears to be essential for viability during embryonic development.

Despite the numerous biochemical studies which have led to the identification of various Siah substrates, how these proteins and their stability relates to the observed Siah mutant phenotypes, particularly male sterility, remains unclear. Therefore, ongoing experiments aiming to identify the full repertoire of Siah substrates and interacting proteins should further our understanding of the physiological functions of the Siah gene family.

1.4 SIAH1 yeast 2-hybrid screen

Prior to this study, a yeast 2-hybrid screen was performed to identify interacting partners of the human T-STAR protein, an alternative splicing factor which is predominantly expressed in the developing brain and testes (Venables et al., 1999; Stoss et al., 2001). Alternative splicing of precursor-mRNA (pre-RNA) is an important regulatory mechanism that increases the diversity of proteins transcribed from a single gene. The highest levels of alternative splicing events are observed in testes tissue and this is believed to be important during spermatogenesis which involves many cellular changes and regulatory steps (Venables 2002; Yeo et al., 2004; Grosso et al., 2008). The principal interactors identified in the T-STAR yeast 2-hybrid screen were SIAH1 and SIAH2.

Because the murine SIAH1 homlog, Siah1a, was known to be essential for male germ cell development (Dickins et al., 2002), it was hypothesised that the SIAH1:T-STAR interaction may be essential to successful germ cell production. Further investigation into this interaction however, found that although human T-STAR was targeted for degradation by SIAH1, mouse T-STAR was not (Venables et al., 2004). Therefore, modulation of T-STAR by SIAH1 could not help explain the *Siah1a* mutant phenotype.

In order to further characterise the role of SIAH1, a yeast 2-hybrid screen of a human testis cDNA library was carried out using SIAH1 as bait (Dr Julian Venables, unpublished data). A human testis cDNA library was used because high levels of *Siah* expression in mouse testes were previously reported which correlates with the defective spermatogenic phenotype in *Siah1a* mutant mice (Della et al., 1995).

Ten proteins were identified in this screen, two of which were previously identified SIAH binding proteins, T-STAR (Venables et al., 2004) and SIAH1BP1 (identified as an interacting partner of SIAH in the 2-hybrid system by Gang Hu, Andrew Holloway, and David Bowtell, unpublished data). The eight remaining proteins represented novel SIAH1 interactors some of which are involved in apoptosis, transcriptional regulation and splicing. A brief summary of the principal interactors is presented in Table 3.

Gene symbol	Protein name	Function
ATF3	Activating transcription factor 3 (ATF3)	Binds CRE elements and represses/activates transcription. ATF3 expression is induced by many physiological stresses and numerous studies have shown it plays an important role in host defence against invading pathogens and cancer (Thompson et al., 2009). An investigation into the interaction between SIAH1 and ATF3 was previously reported (MacLennan 2007).
PPP1R13B	Apoptosis-stimulating protein of p53 (ASPP1)	Binds to and regulates various proteins which play key roles in controlling apoptosis. Interacting proteins include the tumour suppressor protein p53 and its family members (Samuels-Lev et al., 2001; Bergamaschi et al., 2004). The biological function of the ASPP family proteins and their potential role in tumorigenesis is discussed by Sullivan and Lu (2007).
CCDC92	Coiled-coil domain containing protein 92 (CCDC92)	The CCDC92 gene was recently identified as one of 43 genetic loci involved in lipid metabolism (Chasman et al., 2009) however the function of the encoded protein is unknown.
PHC2	Polyhomeotic-like protein 2 (PHC2)	Component of the chromatin-associated polycomb repressive complex involved in homeotic gene regulation (Isono et al., 2005). It is also a component of an E3 ubiquitin ligase complex which ubiquitinates histone H2A (Wang et al., 2004). Thus, PHC2 plays an important role in regulating chromatin dynamics and transcription.
PUF60	SIAH binding protein 1 (SIAH1BP1)	A splicing factor homologous to U2AF65, a subunit of the U2 small nuclear ribonucleoprotein auxiliary factor (U2AF) which is an essential component of the splicing machinery (Page-McCaw et al., 1999; Hastings et al., 2007). This protein also regulates expression of the proto-oncogene, *c-myc* via interactions with transcription factor IIH and the far upstream element (FUSE) binding protein (Liu et al., 2006; Cukier et al., 2010).
KHDRBS3	RNA-binding protein T-STAR	Member of the SAM68 family of RNA-binding proteins involved in signal transduction and mRNA splicing. Previously shown to be specifically degraded by SIAH1 (Venables et al., 2004).
WHSC2	Negative elongation factor A (NELF-A)	Component of the negative elongation factor (NELF) complex which binds to elongating RNA polymerase II and stalls transcription (Yamaguchi et al., 2001).
VAPA	Vesicle-associated membrane protein A (VAPA)	Type IV integral membrane protein which associates with intracellular vesicles and the endoplasmic reticulum (Skehel et al., 2000). It is involved in the regulation of membrane trafficking, lipid transport and metabolism, and the unfolded protein response (Nishimura et al., 1999; Peretti et al., 2008)
ZC3H14	Zinc finger CCCH-type containing protein 14 (ZC3H14)	Binds to polyadenosine RNA (Kelly et al., 2007). Multiple ZC3H14 transcripts have been identified and alternate isoforms locate to different areas of the cell. Nuclear isoforms are implicated in mRNA processing and a cytoplasmic isoform may modulate gene expression in the cytoplasm (Leung et al., 2009).
ZC3H11A	Zinc finger CCCH-type domain containing protein 11A (ZC3H11A)	Reported to interact with U2AF65 (Prigge et al., 2009) and the TREX mRNA export complex (Dufu et al., 2010) however the functional outcome of these associations are undefined.

Table 3. SIAH1 interacting proteins identified in a yeast 2-hybrid screen of a human testis cDNA library. Positive clones were sequenced and a BLAST search was carried out to confirm which proteins were encoded by the positive hits.

1.5 Research objectives

Siah proteins are involved in an array of cellular functions due to their ability to target many different proteins for proteasomal degradation. Previous studies revealed that the *Siah1a* gene in mice is essential for germ cell production in the testes as *Siah1a* male mutant mice are sterile. Despite the wealth of knowledge on Siah proteins however, very little is known as to how SIAH proteins regulate germ cell development in the testes. Therefore the aim of this study was to further investigate SIAH1 interacting proteins identified in a human testes yeast 2-hybrid screen performed by Dr Julian Venables. The overall objective was to establish whether or not any of these proteins were targets for SIAH1-mediated ubiquitination and subsequent proteasomal degradation. Initially, we set out to determine whether or not these proteins contained a SIAH-binding motif, map the interacting domains, in both SIAH1 and its target proteins, and investigate the stability of the SIAH1 interactors in the presence and absence of SIAH1 in cell culture. Once likely SIAH1 targets were identified we sought to analyse endogenous protein regulation in *Siah* deficient cells in an attempt to further understand the consequences of the interaction *in vivo*.

One of the likely SIAH1 target proteins identified in the SIAH1 yeast 2-hybrid screen was a protein called ASPP1 (Apoptosis Stimulating Protein of p53) which has been shown to promote p53 mediated apoptosis, much like SIAH1. The mechanisms by which SIAH1 and ASPP1 proteins stimulate apoptosis however are not clearly defined, therefore in order to better understand ASPP1 protein function and the downstream effect of SIAH1 mediated degradation of this protein, we carried out protein interaction screens in order to identify its major protein binding partners. A more detailed introduction into ASPP1 and our interest in this protein is discussed in context in the introductions to chapters 5 and 6.

Chapter 2. Materials and Methods

2.1 Standard molecular biology techniques

2.1.1 PCR

The reagents used in a typical 50µl reaction mixture are listed in Table 4.

Reagent	Quantity for a 50µl reaction
dH_2O	39.3µl
10X PCR Buffer (contains 500mM KCl, 100mM Tris-HCl and 15mM $MgCl_2$)	5µl
2mM dNTPs	2.5µl
10µM Forward primer	1µl
10µM Reverse primer	1µl
Template DNA (~100ng)	1µl
Taq polymerase	0.2µl

Table 4. PCR recipe.

10X PCR buffer and Taq DNA polymerase were purchased from New England Biolabs. Deoxyribonucleotide triphosphates (dNTPs) were purchased from Promega. Primers used in this project are listed in appendix A.

Typical PCR conditions consisted of an initial denaturation step at 92ºC for 1 minute followed by 32 cycles of denaturation at 92ºC for 30 seconds, annealing at 60ºC for 30 seconds, extension at 72ºC for 1 minute with a final extension at 72ºC for 4 minutes. PCR amplification was carried out using a DNA Engine DYAD thermal cycler (MJ Research).

2.1.2 Restriction digests

Approximately 500ng of plasmid DNA or PCR product were digested using 5-10 units of the appropriate restriction enzyme with the suitable buffer (New England Biolabs or Promega) in a total volume of 50µl. Samples were incubated at 37ºC for 1-3 hours.

2.1.3 Purification of DNA after PCR or restriction digest

To remove residual enzymes, buffers and dNTPs, samples were purified using a QIAquick PCR purification kit (Qiagen) according to the manufacturer's instructions.

2.1.4 Ligations and re-cleavage

The appropriate vector and DNA insert were ligated in a 20µl reaction volume. Reactions consisted of 200 units of T4 DNA ligase and T4 DNA ligase buffer (New England Biolabs). Ligations were incubated at 16ºC overnight in a DNA Engine DYAD thermal cycler (MJ Research). Re-cleavage of the vector was carried out after ligation in a 50µl reaction volume, using an enzyme which would cut the re-ligated vector. This was to select against any vector which had re-circularised/re-ligated without the desired insert.

2.1.5 Dialysis

Dialysis of 50µl ligation/re-cleavage mixes was carried out on dialysis discs (Millipore) to remove residual salt from the ligation/digest buffers. Samples were dialyzed against dH_2O for 1 hour at room temperature.

2.1.6 Transformation of electrocompetent bacterial cells

Plasmids were transformed into *E. coli* DH5α by electroporation using a method derived from Dower et al., (1988). In brief, plasmid DNA was mixed with electro-competent cells on ice and then transferred to a pre-cooled 1mm electroporation cuvette (Molecular BioProducts). Electro-competent DH5α frozen stocks were prepared by Caroline Dalgliesh (IHG, Newcastle University, UK). Cells were electroporated at 1.5kV, 25µF capacitance, and 200Ω resistance using a Gene Pulser (Bio-Rad). Electroporated cells were immediately incubated in 1ml of LB broth (10g/l Sodium Chloride, 10g/l Tryptone, 5g/l Yeast extract) for 1 hour at 37ºC, allowing them to recover. Cells were plated out on LB agar plates containing the appropriate selective antibiotic (LB Broth + 15g/l Agar + 50µg/ml Ampicillin or 50µg/ml Kanamycin). Plates were incubated overnight at 37ºC.

2.1.7 Transformation of heat-shock competent bacterial cells

Plasmid DNA was mixed with a 30µl aliquot of JM109 *E. coli* cells and incubated on ice for 1 minute. Cells were heat-shocked at 42°C for 1 minute and immediately transferred to ice. After 1 minute on ice, 1ml of pre-warmed LB medium was added and transformants were allowed to recover for 1 hour at 37°C. Cells were pelleted by

centrifugation and excess medium was discarded. Cell pellets were re-suspended in the remaining LB and then plated out on LB-agar containing the selective antibiotic. Plates were incubated overnight at 37ºC.

2.1.8 Purification of plasmid DNA

Single colonies of transformed bacteria were used to inoculate 5ml of LB broth containing the selective antibiotic (50µg/ml) and were incubated in a 37ºC shaker overnight. Cultures were centrifuged at 2,500rpm at 15ºC for 10 minutes and plasmid DNA was prepared from the pelleted bacteria using a QIAprep Miniprep Kit (Qiagen) following the manufacturer's instructions. All plasmids used in this project are listed in appendix B.

2.1.9 Agarose gel electrophoresis

1-2% agarose gels were prepared containing 1X Tris-acetate-EDTA buffer (TAE) (0.04M Tris base, 0.04M Acetate and 0.001M EDTA) pH 8, and ethidium bromide (final concentration of 0.5µg/ml). DNA samples were prepared by adding an appropriate amount of 10X Orange G loading dye (20% ficoll, 1mM EDTA and 2µg/µl Orange G). Samples were run at 60-100 volts in 1X TAE until sufficient separation was achieved. DNA was visualised under UV light using a Gene Genius Bioimaging System (Syngene) and sizes were estimated using either 10Kb SmartLadder (Eurogentec) or 1Kb plus ladder (New England Biolabs).

2.1.10 DNA sequencing

Sequencing reactions were carried out by Geneservice (Cambridge, UK). Purified plasmid DNA at a minimum concentration of 100ng/µl was sent along with 32pmol of the appropriate primer.

2.1.11 Microscopy

GFP fluorescence in HEK293 cells was viewed using a Zeiss Axiovert200 Fluor Arc microscope. Immunofluorescence images were captured using a fluorescence Axioplan2 microscope.

2.1.12 Site-directed mutagenesis

Mutagenic oligonucleotide primers were designed to contain the desired point mutation in the middle of the primer with 10-15 bases of correct *Siah1b* sequence either side. They were designed to have a minimum GC content of 40%, a C/G base on either end and to have a minimum melting temperature of 74°C. For each mutation, two oligonucleotides were designed which anneal to the same sequence on opposite strands of the *Siah1b*-FLAG plasmid. Primers used for mutagenesis are listed in Table 5.

Primer name	Target	Sequence (5′-3′)	Mutation
Siah1b-a (pos13/5)F	Siah1b	GAGCCGTCAGACTGCTACAGCATTATCC	A5T
Siah1b-a (pos13/5)R		GGATAATGCTGTAGCAGTCTGACGGCTC	A5T
Siah1b-a (pos28/10)F	Siah1b	GCTACAGCATTACCCACTGGCACCTC	S10P
Siah1b-a (pos28/10)R		GAGGTGCCAGTGGGTAATGCTGTAGC	S10P
Siah1b-a (Pos80/27)F	Siah1b	CCTGCCTTGACTGGCACAACTGCATCC	D27G
Siah1b-a (Pos80/27)R		GGATGCAGTTGTGCCAGTCAAGGCAGG	D27G
Siah1b-a (Pos301/101)F	Siah1b	CCCCTGTAAATATGCCGCTTCTGGATGTG	S101A
Siah1b-a (Pos301/101)R		CACATCCAGAAGCGGCATATTTACAGGGG	S101A
Siah1b-a (Pos303/102)F	Siah1b	CTTCCCCTGTAAATATTCCTCTTCTGGATGTG	A102S
Siah1b-a (Pos303/102)R		CACATCCAGAAGAGGAATATTTACAGGGGAAG	A102S
Siah1b-a (Pos336/113)F	Siah1b	GCCACACACCGAAAAGGCAGAGCACG	K113E
Siah1b-a (Pos336/113)R		CGTGCTCTGCCTTTTCGGTGTGTGGC	K113E

Table 5. Primers used for site-directed mutagenesis. Primers were purchased from IDT.

Siah1b point mutants were generated following the Stratagene QuickChange mutagenesis protocol. Reactions were set up as indicated in Table 6.

Reagent	Quantity for a 50µl reaction
dH_2O	35µl
10x Pfu Buffer (Stratagene)	5µl
dNTPs (100mM total)	1µl
Primer mix (100ng/µl each)	3µl
Template (10ng/µl)	5µl
PfuTurbo DNA polymerase (Stratagene) 100U	1µl

Table 6. Site-directed mutagenesis PCR recipe (adapted from the Stratagene QuickChange mutagenesis protocol).

Mutants were generated by temperature cycling using a DNA Engine DYAD thermal cycler (MJ Research). The template plasmid was denatured by an initial denaturation step at 95ºC for 2 minutes followed by 18 cycles of denaturation at 95ºC for 30 seconds, annealing of oligonucleotide primers containing desired mutation at 65ºC for 1 minute, PfuTurbo DNA polymerase extension at 72ºC for 10 minutes followed by a final extension at 72ºC for 10 minutes.

1µl of the *Dpn*I restriction enzyme (10 U/µl) was added directly to each sample and reactions were incubated at 37°C for 3 hours to permit digestion of the parental (i.e., the non-mutated) DNA. The plasmid DNA was then cleaned up using the Qiagen PCR purification kit following manufacturer's instructions and transformed into heat-shock competent JM109 *E. coli* cells. Plasmid DNA was purified from JM109 colonies and mutations were verified by DNA sequencing.

2.2 RNA-based methods

2.2.1 RNA extraction

Total cellular RNA was extracted from cultured cells or tissue using Trizol Reagent (Invitrogen) following manufacturer's instructions. Briefly, samples were resuspended in 100µl of Trizol reagent and incubated at room temperature for 5 minutes. 20µl of chloroform was added and samples shaken to mix. After a further incubation for 10 minutes, the samples were centrifuged at maximum speed for 15 minutes at 4ºC. The top aqueous layer was transferred to a new tube and an equal volume of isopropanol was added. The samples were incubated at room temperature for 10 minutes and then centrifuged again at maximum speed for 10 minutes at 4ºC. The supernatant was removed and the RNA pellet was washed in 70% ethanol. The RNA pellet was then resuspended in nuclease free dH_2O and quantified using a NanoDrop Spectrophotometer (NanoDrop Technologies).

2.2.2 Reverse transcriptase PCR (RT-PCR)

cDNA was transcribed from total RNA and then amplified using the OneStep RT-PCR kit (Qiagen) following manufacturer's instructions. Briefly, 5µl reactions were set up as indicated in Table 7.

Reagent	Quantity for a 5µl reaction
5x OneStep RT PCR Buffer	1µl
dNTPs (10mM each)	0.2µl
10µM Forward primer	0.3µl
10µM Reverse primer	0.3µl
Q-Solution	1 µl
RNA (50ng/µl)	2µl
OneStep RT PCR Enzyme mix	0.2µl

Table 7. OneStep RT-PCR recipe (adapted from the Qiagen protocol).

Reactions were incubated at 50°C for 30 minutes, then 95°C for 15 minutes, followed by 34 cycles of denaturation at 94°C for 30 seconds, annealing at 56°C for 30 seconds, extension at 72°C for 1 minute with a final extension at 72°C for 10 minutes. Reactions were carried out using a DNA Engine DYAD thermal cycler (MJ Research). Primers used for RT-PCR are listed in Table 8.

Primer name	Sequence (5′-3′)	Purchased from
HPRT-F	CTGGTGAAAAGGACCTCTCG	Sigma
HPRT-R	TGGCAACATCAACAGGACTC	Sigma
Siah1a-F	ATTACCCACTGGCACCTCAA	IDT
Siah1a-R	TGGCCACTCTGACACTGAAG	IDT
Siah2-F	GGGCTGTTCCCTGACTCTAC	IDT
Siah2-R	CCCTGGCAGGTTAATGTCTG	IDT
Siah1b-F	TGACCAAGAATGTGGAACCTT	Sigma
Siah1b-B	TGGCAACACATAGTCAAAGCA	Sigma

Table 8. Primers used for RT-PCR.

2.3 Protein based methods

2.3.1 SDS-PAGE

Samples were sonicated in 2X SDS sample loading buffer (100mM Tris-HCl pH6.8, 200mM DTT, 4% SDS, 20% Glycerol, 0.2% Bromophenol Blue) to disrupt any intact DNA. Samples were incubated for 5 minutes at 95ºC and centrifuged at 10,000rpm for 2 minutes before loading onto a discontinuous gel. Gels were made with a 4% stacking gel (0.125mM Tris pH6.8, 0.1% SDS, 0.1% ammonium persulphate, 0.2% TEMED and 4% acrylamide) and a 10% acrylamide resolving gel (375mM Tris pH8.8, 0.1% SDS, 0.1% ammonium persulphate, 0.2% TEMED and 10% acrylamide). Samples were electrophoresed in 1X SDS-PAGE running buffer (30mM Tris, 188mM Glycine, 0.1% SDS) at 150V for 45 minutes.

Gels were used either for Western blotting (see below), or stained using either SimplyBlue Safe stain (Invitrogen) or PlusOne Coomassie Blue PhastGel (GE Healthcare). One tablet of PlusOne coomassie was dissolved in 400ml of staining solution (25% Methanol and 10% acetic acid). De-staining of coomassie stained gels was carried out in 7% acetic acid and 50% Methanol and SimplyBlue stained gels were de-stained with dH_2O. For both Western blotting and staining, protein sizes were estimated using Broad Range Pre-stained Protein Marker (New England Biolabs).

2.3.2 Western blot

PAGE gels were transferred in Western transfer buffer (39mM Glycine, 58mM Tris, 0.04% SDS, 20% Methanol) to Hybond-C Extra nitrocellulose membrane (Amersham Biosciences) using a Semi-Dry Trans-Blot apparatus (Bio-Rad) for 45 minutes at 15V. Filters were soaked with Ponceau stain (Sigma) to determine blotting efficiency then washed in TBS-T (8.75g/l NaCl, 6.5g/l Tris-HCl, 2ml/l Tween). Filters were incubated with block solution (10% non-fat dried milk in TBS-T) for 1 hour at room temperature on a rotating wheel to block non-specific binding sites. Block was then removed and the primary antibody added at the appropriate dilution in block (for dilutions see Table 9). This was incubated at room temperature for 1 hour on a rotating wheel. Filters were then washed three times in TBS-T to remove residual primary antibody (5 minutes per wash). Horseradish peroxidase (HRP) conjugated secondary antibody was added at the appropriate dilution in block and incubated at room temperature for 1 hour on a rotating wheel. Filters were then washed twice in TBS-T to remove residual secondary antibody. The resulting signals were visualised by enhanced chemiluminescence (ECL). For this, equal volumes of ECLI (1% Luminol, 0.44% Coumaric acid, and 100mM Tris pH 8.5) and ECLII (0.02% hydrogen peroxide in 100mM Tris pH 8.5) were added to the membrane and left for 1 minute. Excess ECL was then removed and filters were exposed on photographic film (Kodak). Films were developed in a Compact X4 developer (Xograph Imaging Systems).

Antibody name	Source	Mono/ Polyclonal	Species	Dilution for WB	Dilution for IF/TS
α-ASPP1	Thornton, 2005	Polyclonal	Sheep	1:500	1:100
α-β Actin	Sigma	Polyclonal	Rabbit	1:1000	-
α-Clusterin	Santa Cruz	Polyclonal	Goat	1:250	-
α-FLAG	Sigma	Monoclonal	Mouse	1:1000	-
α-GFP	Clontech	Monoclonal	Mouse	1:1000	-
α-HA	CRUK	Monoclonal	Mouse	1:500	-
α-Hsp70	Stressgen	Monoclonal	Mouse	1:500	-
α-NELF-A	Santa Cruz	Polyclonal	Rabbit	1:300	1:50
α-p53	CRUK	Polyclonal	Mouse	1:250	-
α-RNAPII	Upstate	Monoclonal	Mouse	1:500	-
α-Sec16A	Watson et al., 2006	Polyclonal	Sheep	1:1000	-
α-tubulin	Sigma	Monoclonal	Mouse	1:3000	-
α-Ubiquitin	Sigma	Polyclonal	Rabbit	1:100	-
α-V5	Invitrogen	Monoclonal	Mouse	1:5000	1:200
α-YBX1	Cohen et al., 2010	Polyclonal	Rabbit	1:1000	-
α-mouse IgG(HRP)	Amersham	Polyclonal	Sheep	1:1000	-
α-goat IgG(HRP)	DAKO	Polyclonal	Rabbit	1:1000	-
α-rabbit IgG(HRP)	Jackson Lab	Polyclonal	Goat	1:1000	-
α-sheep IgG(HRP)	DAKO	Polyclonal	Rabbit	1:1000	-
α-rabbit IgG(488)	Molecular Probes	Polyclonal	Donkey	-	1:400
α-sheep IgG(594)	Molecular Probes	Polyclonal	Donkey	-	1:400
α-mouse IgG(594)	Molecular Probes	Polyclonal	Donkey	-	1:400
α-rabbit IgG(Biotin)	DAKO	Polyclonal	Goat	-	1:300

Table 9. Antibodies used for Western blotting (WB), immunofluorescence (IF) and tissue staining (TS).

2.3.3 Stripping Western blots

When investigating more than one protein on the same Western blot, in some cases blots were stripped to remove primary and secondary antibodies from the membrane. To do this, stripping buffer (62.5mM Tris-HCl pH 6.8, 2% SDS) was warmed by microwaving at 900W for 20 seconds and then 2-beta mercaptoethanol was added to a final concentration of 0.1M. Blots were incubated in this solution with agitation for 40 minutes at room temperature. Stripping solution was disposed of and blots were washed with TBS-T (three 5 minute washes). Efficiency of stripping was checked by the enhanced chemiluminescence (ECL) reaction described previously (see 2.3.2).

2.3.4 In vitro transcription and translation

Plasmids encoding the appropriate proteins downstream of a T7 promoter (SIAH1pCDNA and Luciferase T7 TNT control plasmid) were transcribed and translated using the TNT-quick T7 coupled Transcription/Translation system (Promega). ^{35}S-

methionine was incorporated into the protein products, which were subsequently analysed by SDS-PAGE and autoradiography.

2.3.5 In vitro pull down

Pull-downs were performed as described previously (Venables et al., 2004). Briefly, *in vitro*-translated and ^{35}S-methionine-labelled proteins were added to GST-fusion proteins attached to glutathione agarose. They were then incubated for 1 hour with rotation at room temperature. The samples were washed four times in PBS, containing 1mM DTT to remove any unbound protein before analysis by SDS-PAGE and autoradiography.

2.3.6 Immunocytochemistry

Cells were grown on coverslips (in 12-well plates) in the appropriate growth medium until 60-75% confluent. Cells were washed in 1X PBS and fixed in 100% methanol for 1 minute at -20°C. The methanol was removed and cells were washed three times with 1X PBS.

Cells were permeabilised by incubating in 1% Triton X-100 for 10 minutes at room temperature. Permeabilised cells were then washed three times with PBS to remove Triton X-100. Cells were incubated in blocking solution (10% horse serum in 1X PBS) for 1 hour at room temperature and then incubated in the appropriate primary antibody diluted in blocking solution for 2 hours at room temperature (for antibodies and dilutions see Table 9). After three washes in 1X PBS, the cells were then incubated with the appropriate fluorescent conjugated secondary antibody diluted in blocking solution for 1 hour at room temperature and washed as before. The coverslips were then mounted in VectaShield Mounting Medium with 4',6-diamidino-2-phenylindole (DAPI) (Vector Laboratories) and images were captured using a fluorescence Axioplan2 microscope.

2.3.7 Immunohistochemistry

Slices of paraffin wax-embedded tissue sections (7-8μm) from wild-type mouse testes were prepared and mounted on slides by Dr Ingrid Ehrmann (IHG, Newcastle University). Sections were de-waxed by washing twice in HistoClear (National Diagnostics) for 12 minutes. Sections were then hydrated by washing in ethanol (2x 5

minute washes in 100% ethanol, followed by a 5 minute wash in 70% ethanol and finally a 5 minute wash in 50% ethanol). To block endogenous peroxidase activity sections were incubated in a methanol peroxide solution (3% H_2O_2 in Methanol) for 30 minutes and then rinsed in water. Antigens were revealed by microwaving the sections at 900W for 20 minutes in 0.01M sodium citrate buffer pH 6.0. Once cooled, the sections were incubated in blocking solution (10% horse serum in TBS) to block non-specific antibody binding sites for 20 minutes at room temperature. The sections were then incubated with the primary antibody diluted in TBS overnight at 4°C in a humidified chamber (for dilutions see Table 9). Sections were then washed 4X with TBS before addition of the appropriate biotinylated secondary antibody which was diluted in blocking solution (for dilutions see Table 9). Sections were incubated with the secondary antibody at room temperature for 30 minutes followed by another 3 washes in TBS. Biotinylated secondary antibody was visualised using the avidin-biotin-horseradish peroxidase system (ABC-HRP) and diaminobenzidine (Sigma) following manufacturer's instructions.

Sections were counter-stained with haematoxylin to stain nuclei, dehydrated through graded alcohols (2x 5 minute washes in 70% ethanol, followed by 2x 5 minute washes in 100% ethanol) and HistoClear (5 minute wash), before being mounted in Histomount (National Diagnostics). Images were captured/analysed using a Zeiss Axioplan 2 light microscope.

2.3.8 Bacterial expression and purification of fusion proteins

2.3.8.1 BL21 calcium chloride transformation

For expression of GST and histidine-tagged fusion proteins, *E. coli* BL21 cells were transformed with the appropriate plasmid (pGEX or pET32a) encoding the fusion protein. 1µl of standard mini-prepped plasmid DNA was added to 100µl of competent *E. coli* BL21 cells and incubated on ice for 20 minutes. The cells were then heat shocked at 42°C for 1 minute and immediately returned to ice for a further minute. The cells were allowed to recover in 1ml LB broth for 1 hour at 37°C. The cells were then plated out onto LB agar plates containing the selective antibiotic, ampicillin, and were incubated overnight at 37°C.

2.3.8.2 Large-scale protein expression

Large scale protein expression was carried out using Overnight Expression Instant TB Medium (Novagen) according to the manufacturer's instructions. Briefly, a single colony was taken from the transformed BL21 cell plate and used to inoculate 3mls of Overnight Express Instant TB Medium (Novagen) containing ampicillin to generate a 'starter culture'. This culture was incubated in a 37°C shaker until an optical density of 0.5 at A_{600nm} was reached. 100mls of pre-warmed Overnight Express Instant TB Medium (Novagen) (containing ampicillin) was then inoculated with the whole starter culture. At this point 0.5ml samples of the cultures were taken. The 100ml culture was then incubated at 37°C for a further 16 hours. After 16 hours, further 0.5ml samples were taken and the remaining cultures were centrifuged at 3,000rpm for 10 minutes and the supernatants removed.

2.3.8.3 Purification of GST-fusion proteins

Bacterial cell pellets containing GST fusion proteins were resuspended in 10ml 1X PBS. 2mg of Lysozyme (Sigma) were added to lyse the cells, and incubated for 20 minutes at room temperature. Lysates were then sonicated on ice to break up DNA. DTT was added to a final concentration of 1mM, 1X PMSF was added, triton X-100 was added to a final concentration of 2% along with 200 units of DNase I (Roche). Samples were incubated with shaking for 30 minutes, at room temperature. KCl was added to a final concentration of 500mM. The sample volume was then made up to 20ml with 1X PBS. The samples were re-sonicated and freeze-thawed between -80°C and room temperature to ensure there was no intact DNA. To test solubilisation, 10µl of cell lysate was saved. The remaining cell lysate was centrifuged at 14,000rpm for 10 minutes at 4°C. The supernatant containing the soluble material was retained, and the pelleted insoluble material was discarded. Total cell lysate and soluble supernatant were analysed via SDS-PAGE to ensure the GST-fusion protein was soluble.

To purify the GST-tagged peptide, 40mg of glutathione agarose (Sigma) was resuspended in 1ml dH_2O and rotated for 2 hours at room temperature. The agarose was then washed 4 times in 1X PBS. After the last wash a 50% slurry was created by resuspending the agarose in equal amount of 1X PBS. 500µl of the 50% slurry was added to 10ml of the soluble cell lysate (containing the GST-tagged protein). This was incubated with rotation

for 1 hour at room temperature. Following the 1 hour incubation, the agarose was pelleted by centrifugation at 3,000rpm for 1 minute. The supernatant was removed and saved for analysis of purification efficiency. The glutathione agarose with the attached GST-fusion protein was then washed 5 times in 10ml PBS, containing 0.5mM DTT and 0.25M KCl. Agarose was pelleted between washes by centrifugation at 3,000rpm for 1 minute. Finally, the GST-fusion-bound beads were re-suspended in an equal volume of the PBS wash buffer. To check purification, 10µl of the GST-fusion-bound beads were analysed by SDS-PAGE.

2.3.8.4 Purification of Histidine-fusion proteins

Bacterial cell pellets containing histidine fusion proteins were resuspended in 50ml equilibration buffer (50mM sodium phosphate pH 8.0, 0.3M sodium chloride and 10mM imidazole). The samples were then freeze-thawed between -80°C and room temperature and then sonicated on ice. The lysed cultures were centrifuged at 10,000rpm for 30 minutes at 4°C and the soluble supernatant material was retained.

For ASPP1(357-532)His, purification was carried out under native conditions using ProCatch His resin (Macs Molecular). The required amount of ProCatch His resin was transferred to a sterile tube and pelleted by centrifugation at 3,000rpm for 2 minutes. The supernatant was discarded and the resin was pre-equilibrated by adding 10 volumes of equilibration buffer. The resin was pelleted again and the pre-equilibration wash was repeated. The soluble cell lysate containing the histidine-fusion protein was then added to the resin and mixed on a rotating wheel for 1 hour at room temperature. The samples were centrifuged at 3,000rpm at 4°C for 5 minutes to pellet the resin and the supernatants discarded. The His-bound resin was then washed five times in wash buffer (50mM sodium phosphate pH 8.0, 0.3M sodium chloride and 20mM imidazole).

Bound protein was eluted by adding 1ml of elution buffer (50mM sodium phosphate pH 8.0, 0.3M sodium chloride and 250mM imidazole) and mixing on a rotating wheel for 10 minutes at room temperature. The samples were then centrifuged at 7,000rpm for 30 seconds and the supernatants retained. The elution process was repeated twice and eluted samples were assayed by SDS-PAGE.

2.3.9 Purification of α-ASPP1 polyclonal antibody

2.3.9.1 IgG isolation

Total IgG was separated from the sera by caprylic acid purification, a method derived from Mckinney and Parkinson (1987). Sera was diluted in four volumes of 60mM sodium acetate pH 4.0. To precipitate non-IgG proteins caprylic acid (25µl per ml of serum/acetic acid) was added in drop wise manner whilst stirring. The mixture was incubated at room temperature for 30 minutes, and centrifuged at 10,000rpm for 30 minutes at 4ºC. The supernatant was then filtered through Whatman paper to remove any protein precipitate. The resulting IgG was neutralised with one tenth volume of 10X PBS and cooled to 4°C. Ammonium sulphate (0.277 g per ml) was slowly added whilst stirring to precipitate the IgG. This was incubated for a further 30 minutes whilst stirring at 4°C. IgG was collected by centrifugation at 10,000rpm for 15 minutes at 4°C. The supernatant was discarded and the precipitated IgG was resuspended in 25ml of 1X PBS and dialysed overnight at 4°C in 1X PBS.

2.3.9.2 Affinity purification

The purified His-tagged ASPP1 epitope (see section 2.3.8.4) was coupled to a SulfoLink column (Pierce) following the manufacturer's instructions. The column was then washed sequentially with 10 gel-bed volumes of 10mM Tris pH 7.5, 100mM glycine pH 2.5, 10mM Tris pH 8.8, 100mM triethylamine pH 11.5 and 10mM Tris pH 7.5, respectively. Total IgG (see above, section 2.3.9.1) was run through the column three times to attach the antibody to the epitope. The columns were then washed with 20 gel-bed volumes of 10mM Tris pH 7.5 and then with 10mM Tris pH 7.5 containing 0.5M sodium chloride. To elute the antibody, first 10 gel-bed volumes of 100mM glycine pH 2.5 was added to the column and elutions were collected in 850µl fractions. Each collected fraction was neutralised by addition of 150µl 1M Tris pH 8.0. The pH of the column was then adjusted by washing with 10 gel-bed volumes of 10mM Tris pH 8.8. The basic elution was performed following the same procedure but this time 10 gel-bed volumes of 100mM triethylamine pH 11.5 was added. Each collected fraction was tested for protein content by Bradford assay (Bio-Rad, following manufacturer's instructions) and the positive fractions were dialysed overnight at 4°C against 1X PBS.

2.3.9.3 Pre-absorption assay

To test the specificity of the generated antisera, the His-tagged ASPP1 epitope attached to ProCatch His resin (see section 2.3.8.4) was first incubated with agitation in blocking solution (10% non-fat dried milk in TBS-T) for 30 minutes at room temperature. The antisera was then added at the optimum concentration (for dilutions see Table 9) and incubated for a further 30 minutes. The peptide and antiserum mixtures in blocking solution were then used as the primary antibody and the standard method for Western blotting was followed.

2.3.10 Immunoprecipitation with Protein A Dynabeads

To analyse proteins co-immunoprecipitating with ASPP1 in mouse testes the outer membrane of the mouse testes were removed, and testes were broken down in 1X PBS using a pipette. Tissue was transferred to an eppendorf and spun down at maximum speed for 5 minutes in a cooled centrifuge. The supernatant was discarded and tissue was lysed in IP lysis buffer (50mM Tris pH 7.4, 100mM KCl, 5mM $MgCl_2$, 0.1% NP-40, 5mM NaF, 175µg/ml PMSF and 1X Roche Complete Protease Inhibitor Cocktail) on ice for 20 minutes. To detect ASPP1 interacting proteins in Saos2 cells, cells were harvested as described in section 2.5.6 and the cell pellet was lysed in IP lysis buffer as above. In both experiments soluble material was separated by centrifugation at maximum speed for 15 minutes at 4ºC. Soluble cell lysate was then added to approximately 80µg of ASPP1 antibody or, as a control, 80µg of sheep IgG. Soluble cell lysate plus antibody was incubated overnight with rotation at 4ºC.

When immunoprecipitating GFP-tagged proteins, HEK293 cells were transfected and harvested as described in sections 2.5.1 and 2.5.6. Harvested cells were resuspended in IP lysis buffer and soluble cell lysate prepared as described above. Soluble cell lysate was then added to 10µg of GFP antibody and incubated overnight with rotation at 4ºC.

The next day, protein A Dynabeads (Invitrogen) were washed 3 times with 0.1M sodium phosphate pH 8.1 (100µl of Dynabeads per IP). Soluble cell lysate was then added to washed beads and incubated on a rotating wheel at room temperature for 1 hour. Samples were then washed three times with 1X PBS and subsequently resuspended in SDS sample loading buffer followed by analysis by Western blotting.

2.3.11 Immunoprecipitation using α-FLAG affinity resin

When immunoprecipitating FLAG-tagged proteins, transfected HEK293 cells or Flp-In HEK293 cells were harvested as described in section 2.5.6. The cell pellets were resuspended in 1ml IP lysis buffer (50mM Tris pH 7.4, 100mM KCl , 5mM $MgCl_2$, 0.1% NP-40, 5mM NaF and 1X Roche Complete Protease Inhibitor Cocktail) and incubated for 20 minutes on ice. Meanwhile FLAG resin (Sigma) was prepared by washing 3X in TBS pH 7.4 (20µl of 50% slurry per sample). Cell lysates were then centrifuged at maximum speed for 10 minutes at 4ºC to separate any insoluble material. Soluble supernatants were added to the prepared FLAG resin and incubated overnight at 4°C with rotation.

The next day the samples were centrifuged for 30 seconds at 9,000rpm and supernatants were saved to check IP efficiency. The resin was then washed three times (5 minutes with rotation per wash) in 1ml IP wash buffer (50mM Tris pH 7.4, 100mM KCl, 0.1% NP-40). To determine whether or not immunoprecipitations were successful, 5µl of FLAG slurry was removed and added to 5µl of SDS sample loading buffer. Samples were resolved by SDS-PAGE and analysed by Western blotting.

2.3.12 Mass spectrometry

Protein samples were separated on pre-cast SDS-PAGE gels (NuPAGE 4-12% Bis-Tris Gel, Invitrogen) and stained with SimplyBlue SafeStain (Invitrogen) following the manufacturer's instructions. Protein bands of interest from the ASPP1-FLAG immunoprecipitation (IP) were excised using a clean scalpel and digested using a Trypsin Profile In-gel digest (IGD) kit (Sigma). In brief, excised protein bands were placed in 1.5ml eppendorfs which were pre-washed with 100µl of peptide extraction solution. Gel pieces were then de-stained by incubating at 37°C for 30 minutes with 200µl de-staining solution. This de-staining process was repeated and the gel pieces were dried using a Speed Vac for approximately 30 minutes. Proteins in the dried gel were digested overnight at 37°C with trypsin. Following the overnight incubation, liquid (containing the extracted tryptic peptides) was removed from the re-hydrated gel piece and transferred to a new tube. ASPP1 IP and Sheep IgG IP protein samples were prepared by Karen Lowdon and sample peptides were analysed via mass spectrometry by the North East Proteome Analysis Facility (NEPAF) at Newcastle University.

2.4 Yeast 2-hybrid

2.4.1 Yeast culture

Yeast strain Y190 was streaked out from a frozen stock on YP agar plates (18g/l Agar, 20g/l Peptone, 10g/l Yeast extract, 2% Glucose and 20µg/ml Adenine). Freezer stocks were prepared by Dr Ingrid Ehrmann (IHG, Newcastle University). Plates were incubated at 30ºC for 72 hours. A single colony of Y190 was picked from a YP agar plate and used to inoculate 100ml of YP broth (20g/l Peptone, 10g/l Yeast extract, 2% Glucose and 20µg/ml Adenine). Inoculations were incubated over night in a 30ºC shaker (200rpm). Cultures were diluted to an optical density of approximately 0.2 at A_{600nm} and incubated further until the optical density reached 0.4-0.8 (i.e. when the cells are still in log phase).

2.4.2 Yeast transformation

Cultured cells were transformed using a lithium acetate-based transformation procedure. Briefly, log phase cultures were pelleted by centrifugation at 5,000rpm for 5 minutes and resuspended in dH_2O to wash away excess media. Cells were centrifuged again and were resuspended in 2ml of 0.1M LiAc. 100µl of competent yeast cells were added to each DNA mixture, including 5µl salmon sperm DNA (~10µg/µl, Sigma), and approximately 200ng of each plasmid (Gal4-DNA binding domain fusion protein in the pGBKT7 vector, and Gal4-activation domain fusion protein in the pGADT7 or pACTII vectors, all BD Biosciences). 600µl of 0.1M LiAc/40% PEG was added to each sample and vortexed. Transformation mixtures were then incubated at 30ºC for 30 minutes, followed by incubation at 42ºC for 15 minutes. The transformed yeast were plated onto SD agar plates (7g/l Difco Yeast Nitrogen Base, 28g/l Agar, 2% Glucose and 20µg/ml Adenine) and incubated at 30ºC for 72 hours.

2.4.3 Filter lift assay

Transformed colonies were transferred onto Hybond-C Extra nitrocellulose membrane (Amersham Biosciences) and snap frozen in liquid nitrogen. Membranes were then placed on filter-paper pre-soaked in filter lift solution (5ml Z Buffer (8.5g/l Na_2HPO_4, 5.5g/l NaH_2PO_4, 0.7g/l KCl, 0.24g/l $MgSO_4$, pH 7.0) 100mM β-mercaptoethanol and

50µl X-Gal at 100mg/ml) and incubated at 37ºC, noting the time taken for any colour changes.

2.5 Cell culture

2.5.1 HEK293 transfection

HEK293 cell lines were provided and maintained by Caroline Dalgliesh (IHG, Newcastle University). Cells were grown at 37ºC in 5% CO_2 in Dulbecco's MEM (DMEM) with glutamax-1 medium supplemented with 10% Foetal Bovine Serum (FBS) and 1% penicillin-streptomycin (all Invitrogen). Cells were seeded 24 hours before transfection to be approximately 65% confluent upon transfection. They were transfected using the GeneJammer transfection reagent (Stratagene) as per the manufacturer's instructions. Cells were incubated for a further 24 hours before harvesting.

2.5.2 HeLa transfection

HeLa cell lines were provided and maintained by Caroline Dalgliesh (IHG, Newcastle University). Cells were grown at 37ºC in 5% CO_2 in DMEM with glutamax-1 medium supplemented with 10% FBS. Cells were seeded into appropriate plates or dishes and cultured for 24 hours until they had reached 60% confluency. Cells were transfected using Lipofectamine2000 (Invitrogen) according to the manufacturer's instructions. Cells were incubated for 24 hours before harvesting.

2.5.3 Saos2 cells

Saos2 cell lines were provided and maintained by Caroline Dalgliesh (IHG, Newcastle University). Cells were grown at 37ºC in 5% CO_2 in DMEM with glutamax-1 medium supplemented with 10% FBS.

2.5.4 Murine embryonic fibroblasts (MEFs)

Murine embryonic fibroblasts derived from wild-type embryos and *Siah1a*$^{-/-}$*Siah2*$^{-/-}$ embryos were supplied by Professor David Bowtell (Peter MacCallum Cancer Centre, Australia). MEFs were grown at 37ºC in 5% CO_2 and cultured in DMEM supplemented

with 10% FBS, penicillin (500IU/ml), streptomycin (500µg/ml) (PenStrep from GIBCO) and 200µM β-mercaptoethanol.

2.5.5 Generation of ASPP1 HEK293 stable cell line

Flp-In HEK293 cells were supplied by Dr Nicholas Watkins and Dr Andrew Knox (Institute for Cell and Molecular Biosciences, Newcastle University). Cells were cultured at 37ºC in 5% CO_2 in DMEM with glutamax-1 supplemented with 10% FBS. These cells contain a flippase recognition target (FRT) site which is stably integrated along with a Blasticidin resistance gene in their genome. Therefore, Blasticidin (final concentration 10µg/ml) was routinely added every third feed to ensure the FRT site was maintained in these cells.

Cells were seeded 24 hours before transfection to be approximately 50% confluent upon transfection. The pOG44 plasmid encoding the FRT recombinase was combined with the relevant pCDNA5 plasmid in a 9:1 ratio (2µg of DNA in total). Cells were transfected using GeneJammer transfection reagent (Stratagene) according to the manufacturer's instructions.

In brief, for each transfection in a 6-well plate, 3µl of GeneJammer was added to 100µl of serum free DMEM and left to equilibrate at room temperature for 5 minutes. This was then combined with the 2µg of DNA and incubated for a further 10 minutes at room temperature. The complexes were then added to the cells in a dropwise manner. Levels of confluency were checked 24 hours later and if very high (>70%), cells were split to 50%. 48 hours after transfection, fresh medium was added and selection for transfectants began by adding 1µg/ml Hygromycin B (Sigma-Aldrich). Cells were monitored daily and when many cells died and detached they were removed by washing with 1X PBS and medium was changed. Hygromycin B selection was maintained and Blasticidin was routinely added every third feed. Once cells were sufficiently established *ASPP1-FLAG* expression was induced by adding 1µg/ml Tetracycline (Sigma-Aldrich).

2.5.6 Harvesting cells

The growth medium was removed and cells were washed in 1X PBS (Invitrogen) to remove residual serum. Cells were then treated with Trypsin-EDTA (Invitrogen) and

incubated at 37ºC for 2 minutes to allow for detachment of adherent cells. Following trypsinisation, an equal volume of growth medium was added to inactivate the trypsin and the cell suspension was collected and centrifuged at 8,000rpm for 2 minutes. Cell pellets were washed with 1X PBS, centrifuged again and resuspended in 2X SDS sample loading buffer for Western analysis or IP lysis buffer for immunoprecipitation.

2.5.7 Degradation assay

This was carried out as per Venables et al., 2004.

2.6 Computational analysis

2.6.1 Sequence alignments

Sequence alignments were carried out using the ClustalW program available online at http://www.ebi.ac.uk/clustalw/.

2.6.2 BLAST searches

Nucleotide similarity searches were carried out using the NCBI Basic Local Alignment Search Tool programme available online at http://www.ncbi.nlm.nih.gov/BLAST/.

2.6.3 Molecular weight prediction

The molecular weight of uncharacterised proteins or partial protein constructs was predicted using the scansite tool, available online at http://scansite.mit.edu/.

Chapter 3. An investigation into the interacting partners of SIAH1

3.1 Introduction

Previous studies have shown that Siah1a appears to play a crucial role in cell cycle control as *Siah1a*$^{-/-}$ mice are postnatally growth retarded and males are sterile due to meiotic arrest during spermatogenesis (Dickins et al., 2002). Despite numerous biochemical studies which have led to the identification of various Siah co-factors and substrates, none of these interactions seem to relate to the observed *Siah1a*$^{-/-}$ mutant phenotype of male sterility. A yeast 2-hybrid screen, carried out by Dr Julian Venables, using a human testes cDNA library identified a set of potentially interesting SIAH1 interacting proteins (see introduction, Table 3). In an attempt to better understand SIAH1 function in the testes, the SIAH1 interacting proteins identified in this screen were further investigated.

The primary objective was to establish whether or not any of these proteins were targets for SIAH1-mediated degradation. To achieve this, the SIAH1 interaction domain for each protein was mapped using a yeast 2-hybrid approach, proteins were analysed for the presence of a SIAH-binding motif and the effect of SIAH1 on the stability of each interactor was assayed by expressing GFP-fusion constructs in cell culture and monitoring GFP levels when SIAH1 was over-expressed.

By identifying likely SIAH1 targets for degradation we could then go on to study how these interactions affect cellular processes.

3.2 Confirmation of specificity of hits from the SIAH1 yeast 2-hybrid screen

Since the yeast 2-hybrid system is based on reconstitution of a functional transcription factor (in this case, the yeast Gal4 transcriptional activator), checking the auto-activation capacity of both the bait and target is crucial. The ability to initiate transcription, due to some underlying activating activity is present in approximately 5% of all proteins (Criekinge et al., 1999). These proteins which can activate transcription by themselves are classified as false positives.

In the yeast 2-hybrid screen carried out by Dr Julian Venables, full length *SIAH1* was cloned into the pGBKT7 vector so that it is expressed as a fusion protein with the DNA

binding domain of Gal4 (Figure 4). This construct was previously tested for auto-activation and proven not to auto-activate (Thornton 2005). Subsequently, this construct was used to screen a human testis cDNA-pACTII library and a number of hits were identified (Table 3).

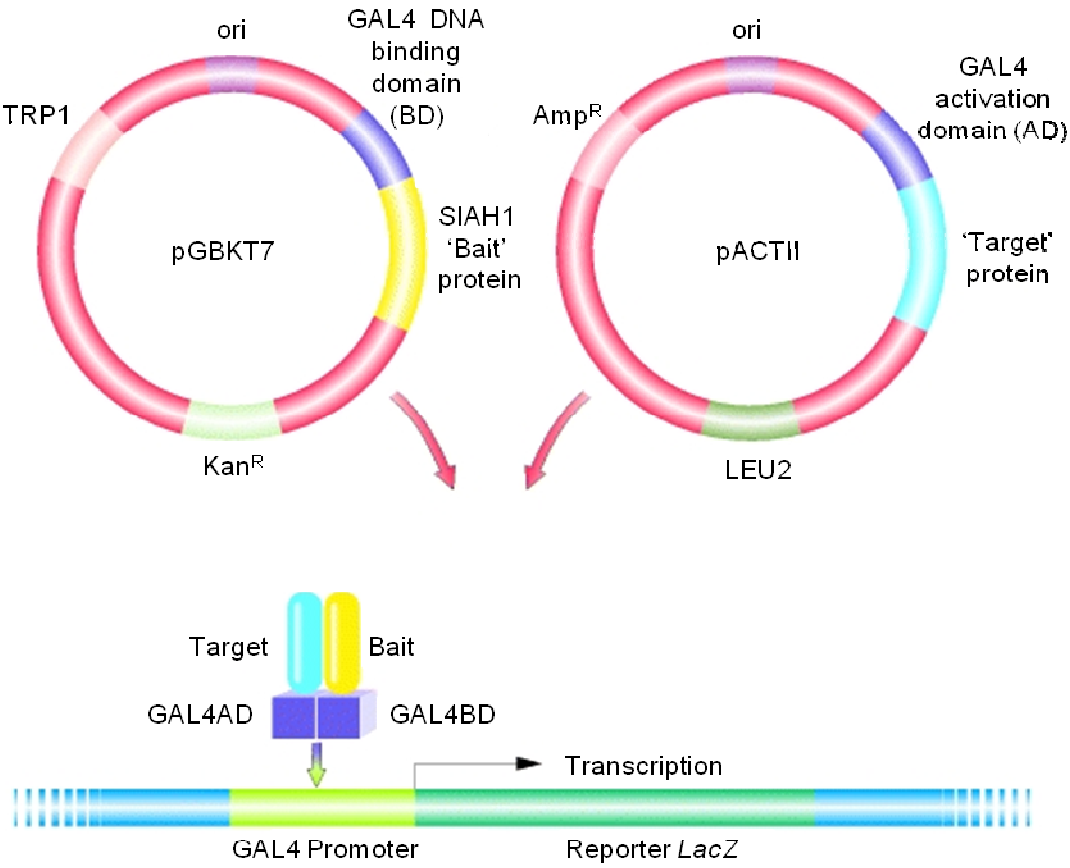

Figure 4. The SIAH1 yeast 2-hybrid screen. The yeast 2-hybrid system uses two types of yeast expression plasmid. One of the plasmids (pGBKT7) contains the Gal4 binding domain sequence fused to the coding sequence of the protein under investigation, in this case, SIAH1. This protein acts as the 'bait'. The second plasmid (pACTII) contains the Gal4 activation domain sequence fused to a protein coding sequence from a library of cDNAs (this is the 'prey'). The two plasmids are then co-transformed into the same cell. Gal4$^-$ cells are used so they do not have any endogenous Gal4 activity. As well as being Gal4$^-$, the target cells are engineered to carry a reporter gene downstream of a *Gal4* promoter. In this screen, the reporter gene *LacZ* from *E. coli* was used, which encodes β-galactosidase. Yeast colonies expressing this enzyme turn blue in the presence of a colourless substrate X-Gal. β-galactosidase is expressed only if the unknown protein of the activation domain fusion interacts with the DNA binding domain fusion protein, thereby bringing the Gal4 activation and binding domains close together to switch on expression. Figure modified from Griffiths (2000).

To identify whether each of the fused prey-Gal4 activation domain proteins could activate transcription of the *LacZ* reporter gene alone, yeast strain Y190 was co-transformed with each of the prey plasmids individually and empty pGBKT7 using a lithium acetate-based transformation procedure (see methods section 2.4.2). If the

expression of the reporter gene was due to the prey alone then the *LacZ* reporter gene would be activated in the absence of the SIAH1 bait. Resultant colonies were subjected to a filter-lift assay to determine the presence/absence of an interaction via X-Gal blue/white screening. There were no observable blue colonies in the samples which were co-transformed with empty pGBKT7 (Figure 5). Therefore none of the SIAH1 interacting proteins appeared to auto-activate. The Y190 strain of yeast used in this assay characteristically turns from white to red during growth due to an adenine$^-$ mutation. The red pigment exhibited by adenine$^-$ mutants is a putative precursor which accumulates if grown in medium with low adenine. Therefore, it is likely that the red SIAH1BP1 colonies (Figure 5) were grown on medium containing an insufficient amount of adenine.

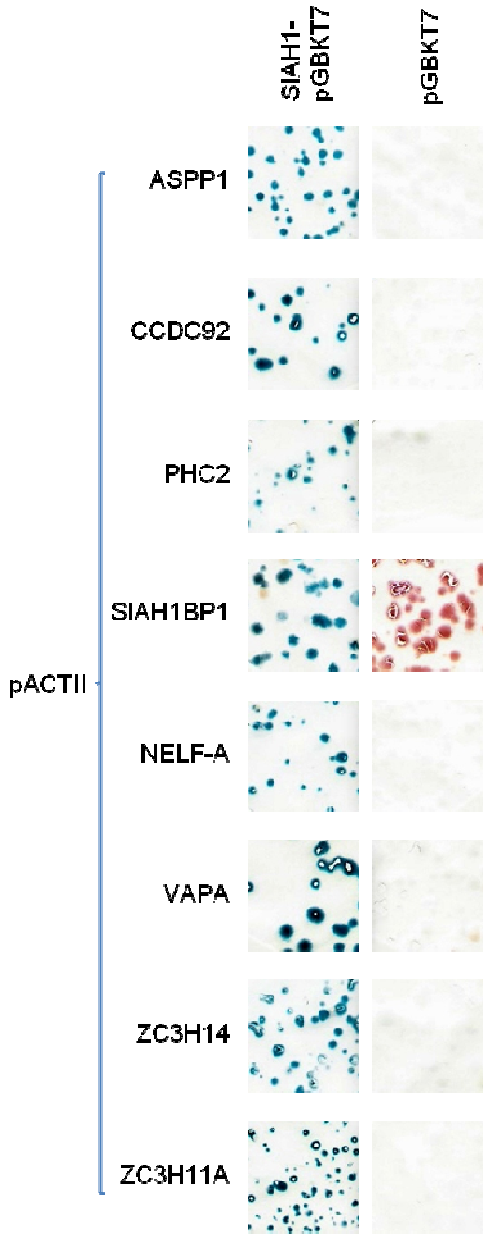

Figure 5. False positive analysis of hits from the SIAH1 yeast 2-hybrid screen. Filters stained with X-Gal are shown. When there is no interaction, colonies remain white or red whereas positive interactions manifest as blue colonies. SIAH1-pGBKT7 was tested against all positive hits from the two-hybrid screen as a positive control. Empty bait plasmid pGBKT7 was used to test for auto-activation of prey plasmids. None of the SIAH1 interactors appeared to auto-activate.

3.3 Mapping the SIAH1 interaction domains

SIAH1 is a dimeric protein which can be divided into three regions – an N-terminal RING finger domain (amino acids 1-99), a central zinc-finger region (amino acids 99-153) and a novel C-terminal substrate binding domain (amino acids 153-282) (Figure 6). The RING finger domain binds to specific E2 enzymes functioning as a platform to

position the charged E2 in close proximity to the target protein (Zheng et al., 2000). The substrate binding domain is the region implicated in binding various substrate proteins, including the degraded proteins, DCC, N-CoR and Kid (see Table 1), as well as various co-factor proteins such as APC and SIP (see introduction, section 1.3.2). In order to determine which region of SIAH1 interacts with each of the SIAH1 hits, deletion derivatives containing different regions of SIAH1 were tested in a yeast 2-hybrid screen against each of the interactors.

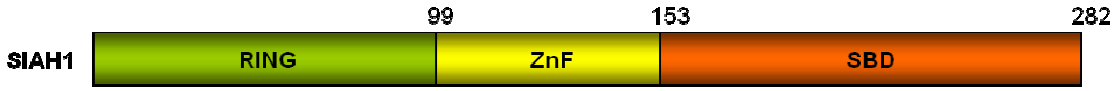

Figure 6. SIAH1 domain structure. SIAH1 consists of an N-terminal RING domain followed by two zinc finger motifs (ZnF) and a C-terminal substrate binding domain (SBD).

3.3.1 Generation of partial SIAH1 constructs

Full length SIAH1 and the SIAH ring finger domain (1-99) were previously cloned into the pGBKT7 Gal4 DNA binding domain vector (Thornton 2005). However, the zinc finger region (99-153) and the substrate binding domain (153-282) constructs were only available in the pGADT7 Gal4-activation domain vector. In order to test these constructs against the positive hits from the 2-hybrid screen (which were cloned into pACTII, a Gal4-activation plasmid), these partial SIAH1 sequences needed to be transferred to the pGBKT7 vector. This was achieved via PCR-based cloning.

PCR primers flanking the coding regions were used to amplify the partial SIAH1 sequences from the pGADT7 vector (SIAH95-F and SIAH155-B, SIAH153-F and SIAH1protein-B). PCR products were then digested with *Eco*RI/*Xho*I and ligated into complementary digested sites in pGBKT7. The ligations were then re-cleaved with *Sal*I, followed by dialysis (*Sal*I cuts the part of the polylinker which is removed by *Eco*RI/*Xho*I digestion). 1µl of each of the ligation mixes was then transformed into *E. coli* DH5α by electroporation. The resultant transformation mix was then plated out on LB plates containing the selective antibiotic kanamycin and incubated at 37ºC overnight. Colonies were then screened by PCR using a vector specific forward primer (T7-F) and an insert specific reverse primer (SIAH155-B or SIAH1protein-B). Insert positive colonies were further grown in LB-kanamycin overnight before plasmid purification.

3.3.2 Mapping interaction domains using the yeast 2-hybrid assay

To identify the region of SIAH1 that recognises each of the interacting proteins, the three separate domains of SIAH1 were tested for their ability to bind each interactor. Full length SIAH1 was also tested as a positive control. Results are presented in Table 10.

		SIAH1 construct in pGBKT7 (amino acids)			
		SIAH1 Full length	SIAH1(1-98) Ring finger domain	SIAH1(99-153) Zinc finger region	SIAH1(153-282) Substrate binding domain
pACTII	ASPP1	++++	-	-	-
	CCDC92	++++	-	-	+++
	PHC2	++++	+	+	+
	SIAH1BP1	++++	-	-	-
	NELF-A	++++	-	-	++
	VAPA	++++	++	+++	+++
	ZC3H14	+++	-	-	-
	ZC3H11A	++++	-	-	+++
	pACTII	-	-	-	-

Table 10. Mapping of SIAH1 interaction domains. Each interacting pACTII construct was tested against the partial SIAH1 constructs to elucidate the interacting region. The table summarises the filter lift assay results. Key, ++++ strong interaction, positive blue colour within 30 minutes, +++ positive blue colour observable within 2 h, ++ positive blue colour observable within 3 hours, + positive blue colour observable within 24 hours, - no noticeable interaction after 24 hours of exposure.

ASPP1, SIAH1BP1 and ZC3H14 only interact with the full length SIAH1 protein in this assay. VAPA and PHC2 interact with all three of the SIAH1 domains, whereas NELF-A, CCDC92 and ZC3H11A interact specifically with the substrate binding domain. Negative results for interaction between the empty pACTII activation domain plasmid and the various SIAH1 regions in pGBKT7 confirmed that the positive results were not due to auto-activation by the Gal4 DNA-binding domain SIAH1 fusions alone.

3.4 Analysis of SIAH1 hits for presence of a SIAH-binding motif

It has been reported that many SIAH binding proteins contain a common binding motif that may act as a degradation signal (House et al., 2003). This core sequence, PxAxVxP, often referred to as the 'degron motif', was found to be conserved and functional in a number of SIAH-interacting proteins, (such as SIP, OBF-1 and TEIG-1 with a more degenerate consensus sequence found in N-CoR). The crystal structure of SIAH

(residues 92-282) in a complex with a peptide containing this motif was later elucidated (Santelli et al., 2005; House et al., 2006).

To ascertain whether or not this peptide sequence was present in our identified SIAH1 interactors, we performed sequence analysis using ClustalW (Larkin et al., 2007). Because SIAH1 interacts with a diverse array of un-related proteins, only the fragments of four SIAH binding proteins which contain the acknowledged degron motif, were aligned with the full length protein sequences of each of our interactors (Figure 7).

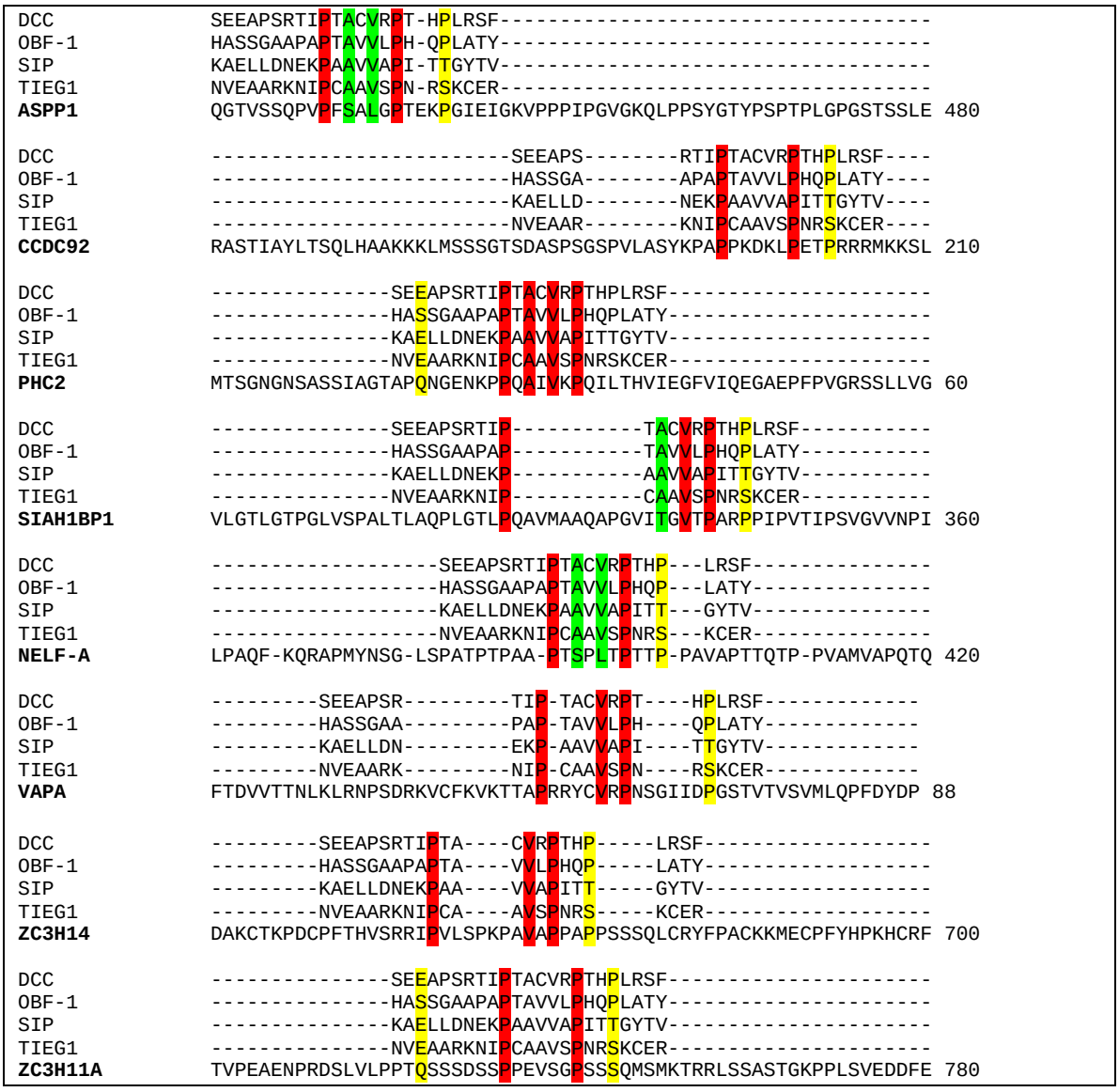

Figure 7. Sequence alignment of the SIAH binding motif in recognised SIAH interacting proteins and our identified SIAH1 interactors. Alignments were generated with ClustalW. Identical residues are highlighted in red columns. Conserved and semi-conservative residues are shown in green and yellow columns, respectively.

The ClustalW alignments revealed that the PHC2 protein contains the precise 'PxAxVxP' core degron motif. ASPP1 and NELF-A contain a conserved version of the motif, in which both the N- and C-terminal prolines are identical in both alignments and two conserved substitutions are present in the central part of the motif. CCDC92 and ZC3H11A contain a more degenerate motif, again with both the N- and C-terminal prolines identical in both alignments. SIAH1BP1, VAPA, and ZC3H14 however, contain gaps in the core PxAxVxP alignment. It is unlikely that these constitute SIAH binding motifs. The crystal structure of the SIAH substrate binding domain bound to a peptide containing this motif has shown that key residues in the degron facilitate the interaction (Santelli et al., 2005; House et al., 2006). Therefore insertions/deletions observed in the SIAH1BP1, VAPA, and ZC3H14 alignments are likely to affect the secondary structure of this region thus abrogating any possible interaction with the SIAH1 substrate binding domain.

3.5 Assay for SIAH1 mediated degradation in cultured cells

Several SIAH1-interacting proteins have been shown to act as substrates of SIAH1 mediated degradation (see Table 1). To determine whether or not the interaction with SIAH1 had direct consequences on the stability of our proteins of interest, each of the interactors were cloned into the pGFP3 vector to create in-frame GFP-fusion proteins (C-terminal GFP tag). These GFP-fusion proteins were then co-transfected into HEK293 cells along with the SIAH1pCDNA3 expression vector or the empty pCDNA3 plasmid. The GFP-expression vector (pGFP3) was also included to act as a transfection control. The relative levels of the GFP-fusion protein were then monitored in the presence/absence of SIAH1. The pGFP3 vector is a eukaryotic expression vector which has been shown to express well in cultured HEK293 cells (Venables et al., 2004).

3.5.1 Generation of GFP-fusion protein constructs

To create the GFP constructs, PCR primers were designed to amplify the clone sequence from the pACTII, yeast 2-hybrid vector (see appendix B). In most cases the full length gene sequence was amplified. A subset of the pACTII SIAH1 hits however were partial clones and therefore only partial sequences were amplified. PCR products were digested and ligated into complementary digested sites in pGFP3 followed by selection on ampicillin-LB plates. Colonies were screened by PCR using a target specific forward

primer and a pGFP3-specific reverse primer (pCDNArev). Insert positive colonies were further grown overnight before plasmid purification.

3.5.2 GFP-fusion protein expression in HEK293 cells

To check that the GFP fusion proteins were the correct/expected size, each pGFP3-fusion plasmid was transfected into HEK293 cells. Cells were incubated for 24 hours before checking for GFP fluorescence using fluorescence microscopy. Following confirmation of GFP fluorescence, cells were harvested and subject to SDS-PAGE and Western blot analysis. Blots were probed for GFP using the α-GFP antibody to ensure that the fusion proteins were of the correct size.

The known/predicted molecular weight of each of the SIAH1 interactors is presented in Figure 8. GFP is a 27kDa protein therefore addition of the GFP tag should cause a shift in migration of the resultant fusion proteins by approximately 27kDa. It is important to bear in mind however that a subset of these interactors are partial clones and therefore will have a smaller molecular weight than expected.

Protein	Molecular weight
CCDC92*	37kDa
PHC2	91kDa
SIAH1BP1	60kDa
VAPA	33kDa
NELF-A	66kDa
ZC3H11A*	89kDa
ZC3H14*	83kDa

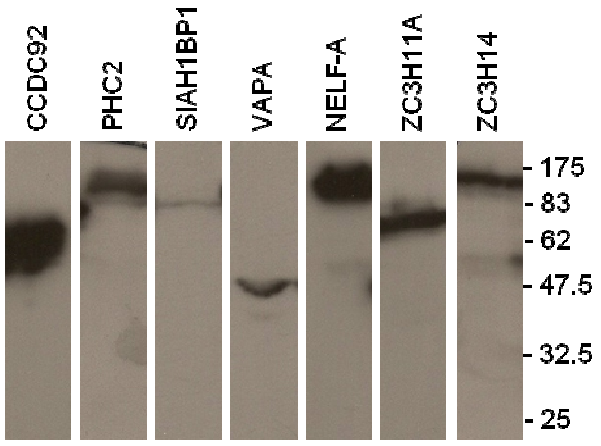

Figure 8. SIAH1 interacting GFP-fusion proteins. A Western blot of HEK293 cells transfected with the SIAH1 interacting GFP-fusion plasmid preparations. Blots were probed with α-GFP primary antibody and HRP-conjugated α-mouse secondary antibody. The migration of molecular weight markers is indicated on the right. The table shows the known/predicted molecular weight of each of the proteins minus the GFP tag. *Highlighted proteins represent partial clones.

As expected, all of the fusion proteins, except ZC3H11A, appear to migrate slower than their predicted full size molecular weight, as a result of the GFP moiety. The pGFP-ZC3H11A clone however is partial, missing the N-terminal 1638bp's (total CDS

2433bp's). The predicted molecular weight of the C-terminal half of the protein should be approximately half that of the full length protein (~44.5kDa). Therefore, addition of GFP should result in a molecular mass of approximately 71.5kDa, which is indeed the case.

The ASPPpGFP3 construct was previously created, sequenced and shown to run with the 175kDa marker (Thornton 2005).

3.5.3 In vivo degradation assay using HEK293 cells

In order to determine whether or not SIAH1 targets any of these interactors for degradation, the GFP-fusion proteins and SIAH1pCDNA3 were co-transfected into HEK293 cells with the GFP expression vector internal standard to show the relative amount of the GFP-fusion protein. Empty pCDNA3 plasmid was co-transfected in the minus SIAH1 controls. Cell extracts were analysed by Western blot and probed with GFP antisera in an attempt to determine if any of these proteins were being destabilised in response to SIAH1 expression. To ensure SIAH1 was being expressed and was functional, the same experiment was carried out using T-STAR protein, a known SIAH1 substrate. Previously Venables et al., (2004) had shown using a T-STAR-GFP fusion protein that SIAH1 bound T-STAR and targeted it for proteasome-dependent degradation. Results are presented in Figure 9.

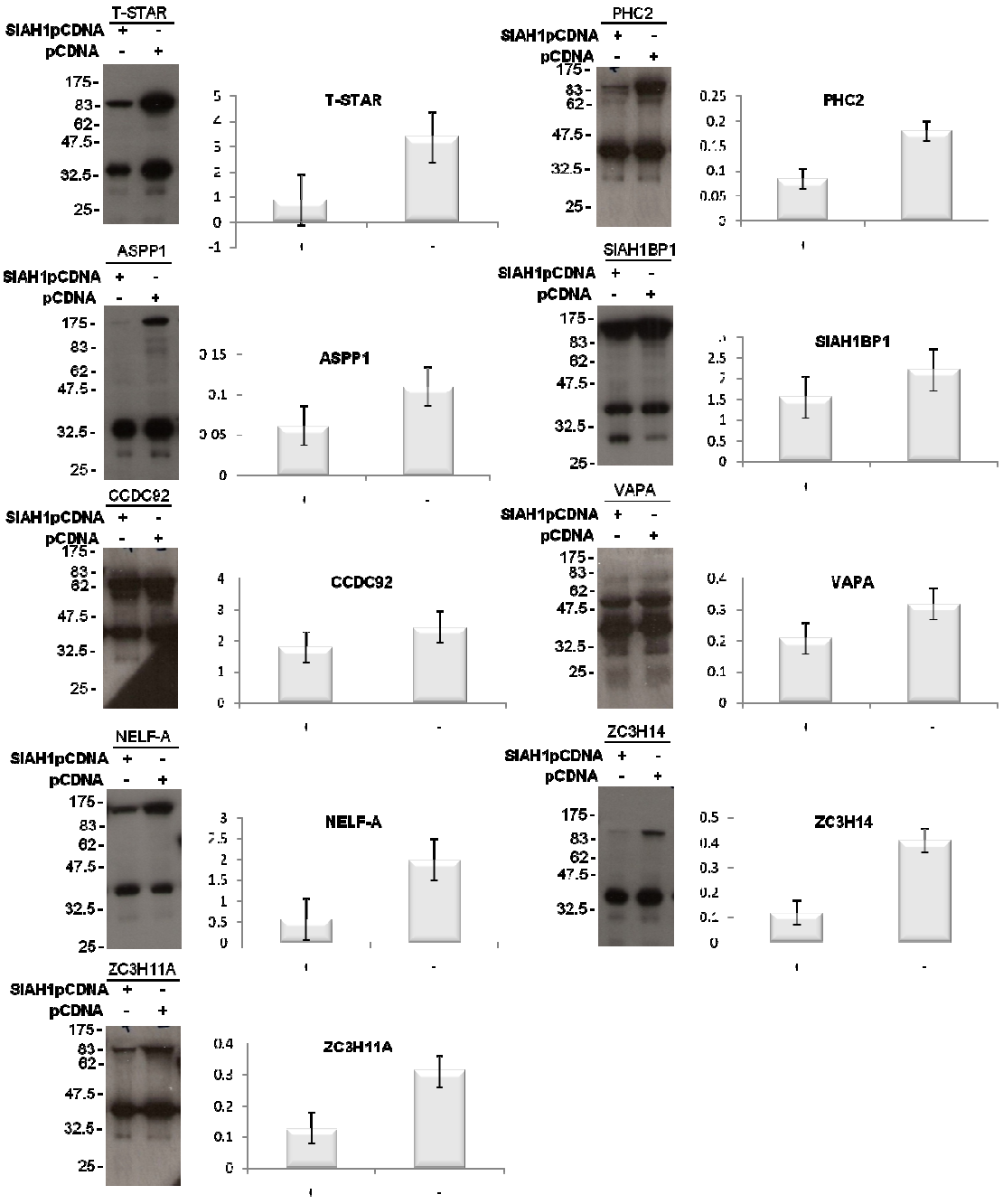

Figure 9. Representative Westerns of co-transfection assays to monitor SIAH1 interacting protein stability in the presence (+) and absence (-) of SIAH1. Cells were harvested 24 hours after transfection and analysed by Western blotting. Blots were probed with anti-GFP primary antibody and HRP-conjugated anti-mouse secondary antibody. The migration of molecular weight markers is indicated on the left of the Westerns. The GFP control band migrates just above the 32.5kDa marker. The graphs show the relative amount of the GFP-fusion proteins in each of the co-transfections. Data is presented as the mean ± SD and is representative of two experiments.

It is evident from the Westerns presented in Figure 9 that the levels of T-STAR, ASPP1, PHC2, NELF-A, ZC3H11A and ZC3H14 GFP-fusion proteins, relative to GFP, decrease when co-expressed with SIAH1. However, when comparing the SIAH1BP1, CCDC92

and VAPA bands in the presence and absence of SIAH1, there does not appear to be any obvious affect. To achieve a more quantitative result, Westerns were subjected to densitometry to determine the relative amount of each of the fusion proteins relative to GFP (see graphs in Figure 9). Such a relative measurement means the assay is independent of the total amount of DNA co-transfected in each transfection, and hence the amount of protein in each sample.

From the T-STAR data, we can see that the T-STAR-GFP protein levels were noticeably reduced in the presence of SIAH1. Therefore, this implied that SIAH1 was being expressed efficiently.

On the whole, all GFP-fusion protein levels were reduced when co-expressed with SIAH1. However this effect was most noticeable in the ASPP1, PHC2, NELF-A, ZC3H11A and ZC3H14 transfections.

3.6 Further mapping the SIAH1 binding site in ZC3H11A and ZC3H14

The *in vivo* degradation assay showed that ZC3H11A and ZC3H14 were de-stabilised when co-expressed with SIAH1. ZC3H11A contained a possible degenerate SIAH binding motif, however there was no recognisable motif found in ZC3H14. If these are genuine SIAH1 targets, then this implies that SIAH1 can bind to proteins via a non-canonical binding site.

In attempt to map the SIAH1 binding sites in ZC3H11A and ZC3H14, constructs containing different regions of these proteins were generated and tested for their ability to interact with SIAH1 in the yeast 2-hybrid system.

3.6.1 Generation of partial ZC3H11A and ZC3H14 constructs and mapping the SIAH1 interacting region via yeast 2-hybrid

ZC3H11A and ZC3H14 were first divided into two regions by PCR. The PCR templates used were the pACTII clones originally pulled out of the SIAH1 yeast 2-hybrid screen. Both clones contained only the C-terminal half of the coding sequence. ZC3H14 was divided in to amino acids 374-594 and 554-736. ZC3H11A was divided into amino acids 546-700 and 678-810 (see appendix for primer and cloning information). Each PCR

product was cloned into the pGADT7 vector and each construct was then tested for interaction with full length SIAH1 protein in a directed yeast 2-hybrid assay (Figure 10A).

SIAH1 interacted with amino acids 546-700 of ZC3H11A and amino acids 374-594 of ZC3H14. The SIAH1:ZC3H14 interaction however was slightly weaker in comparison to ZC3H11A. In order to narrow down the SIAH1 binding site further, these interacting regions were again divided into two by PCR.

ZC3H14 was divided in to amino acids 374-490 and 483-607. ZC3H11A was divided into amino acids 546-633 and 625-706 (see appendix for primer and cloning information). As before, PCR products were cloned into the pGADT7 vector and yeast 2-hybrid assay was repeated (Figure 10B).

A.

	ZC3H14 pACTII	ZC3H14 constructs in pGADT7 (amino acids)		ZC3H11A pACTII	ZC3H11A constructs in pGADT7 (amino acids)	
		ZC3H14 (374-594)	ZC3H14 (554-736)		ZC3H11A (546-700)	ZC3H11A (678-810)
SIAH1pGBKT7	++	+	-	+++	++	-
pGBKT7	-	-	-	-	-	-

B.

	ZC3H14 pACTII	ZC3H14 constructs in pGADT7 (amino acids)		ZC3H11A pACTII	ZC3H11A constructs in pGADT7 (amino acids)	
		ZC3H14 (374-490)	ZC3H14 (483-607)		ZC3H11A (546-633)	ZC3H11A (625-706)
SIAH1pGBKT7	+++	-	-	+++	-	++
pGBKT7	-	-	-	-	-	-

Figure 10. Mapping of the ZC3H11A and ZC3H14 interaction domains with SIAH1. Full length SIAH1-pGBKT7 was tested against partial ZC3H11A and ZC3H14 constructs to elucidate the interacting region. (A) The ZC3H pACTII clones were first divided into two, and each half tested for an interaction with SIAH1. (B) The positive SIAH1 interacting regions in turn were divided into two, and were tested in a second yeast 2-hybrid assay for their ability to interact with SIAH1. Empty bait plasmid, pGBKT7, was used to test for auto-activation of prey plasmids. Filters stained with X-Gal are shown. Positive

interactions manifest as blue colonies, while if no interaction is present, the colonies remain white or red. Key, +++ strong interaction, positive blue colour within 30 minutes, ++ positive blue colour observable within 1 hour, + positive blue colour observable within 2 hours, - no noticeable interaction after 24 hours of exposure.

The SIAH1:ZC3H11A region was mapped down to 81 amino acids (625-706). However, neither of the 374-490 (116 amino acids) or 483-607 (124 amino acids) ZC3H14 constructs interacted with SIAH1. This suggested that the SIAH1 binding site either lies in the region whereby this construct was divided, or there are secondary binding sites in the larger ZC3H14 fragment (374-594) that are required for a stable interaction. It is also possible that these protein fragments do not fold correctly hence altering their ability to bind to other proteins.

In order to determine whether or not there was a degenerate SIAH1 binding motif present in the ZC3H11A and ZC3H14 SIAH1-interacting fragments, sequence analysis was performed. Again, the fragments of four SIAH binding proteins containing the acknowledged degron motif, were aligned with the ZC3H11A(625-706), and ZC3H14(374-594) SIAH1-interacting fragments using ClustalW (see section 3.4 in this chapter). Alignment results are presented in Figure 11 and Figure 12.

```
DCC                 --------------SEEAPSRTIPTACVRP------THPLRSF-----------------
OBF-1               --------------HASSGAAPAPTAVVLP------HQPLATY-----------------
SIP                 --------------KAELLDNEKPAAVVAP------ITTGYTV-----------------
TIEG1               --------------NVEAARKNIPCAAVSP------NRSKCER-----------------
ZC3H11A(625-706)    GIGDSLLNVKCAAQTLEKRGKAKPKVNVKPSVVKVVSSPKLAPKRKAVEMHAAVIAAVKP


OBF-1               ----------------------
DCC                 ----------------------
TIEG1               ----------------------
SIP                 ----------------------
ZC3H11A(625-706)    LSSSSVLQEPPAKKAAVAVVP
```

Figure 11. Sequence alignment of the SIAH binding motif in recognised SIAH interacting proteins and the ZC3H11A(625-706) 81 amino acid SIAH1 interacting fragment. Alignments were generated with ClustalW. Identical residues and semi-conserved residues in the predicted SIAH binding site are highlighted in red and yellow columns, respectively.

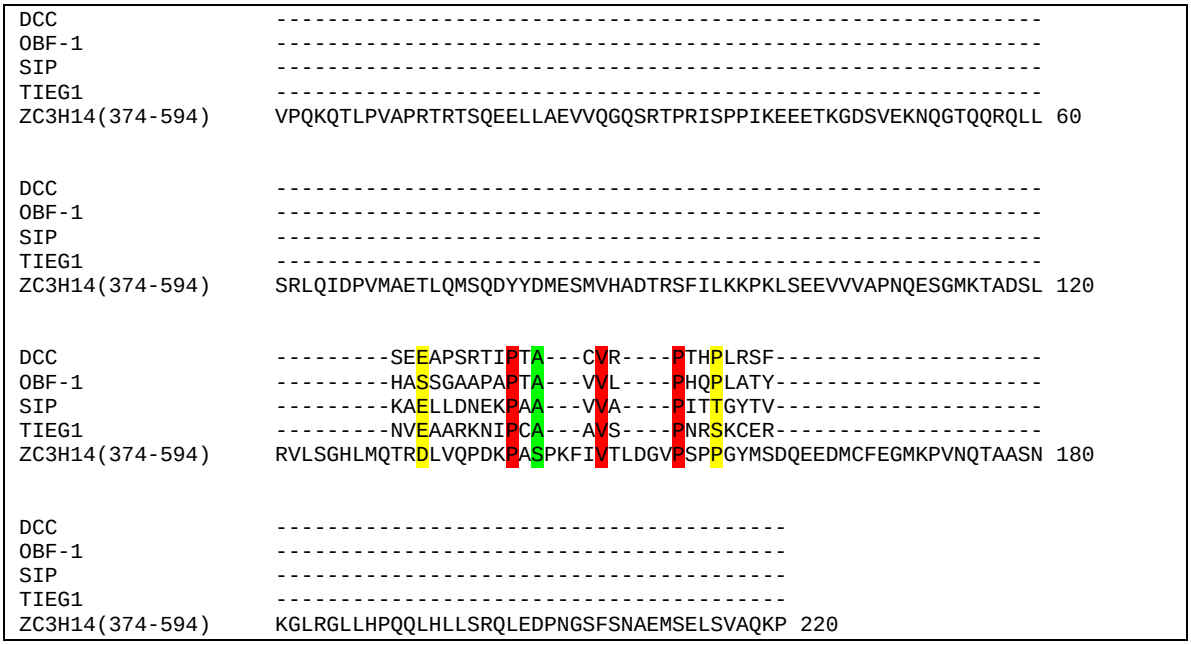

Figure 12. Sequence alignment of the SIAH binding motif in recognised SIAH interacting proteins and the ZC3H14(374-594) 220 amino acid SIAH1 interacting fragment. Alignments were generated with ClustalW. Identical residues are highlighted in red columns. Conserved and semi-conservative residues in the predicted SIAH binding site are shown in green and yellow columns, respectively.

A second potential SIAH1 binding motif, different to the one previously identified (section 3.4 of this chapter) was found in the 81 amino acid ZC3H11A SIAH1-interacting fragment. In contrast, no obvious SIAH1 binding motif was found in the 220 amino acid ZC3H14 SIAH1-interacting fragment as there were gaps in the core PxAxVxP alignment.

3.7 Summary and discussion

Several interesting SIAH1 interacting proteins were identified in the yeast 2-hybrid screen carried out by Dr Julian Venables. These included proteins involved in transcriptional regulation (NELF-A, PHC2, SIAH1BP1), vesicle trafficking (VAPA), apoptosis (ASPP1) and regulation of mRNA splicing and stability (T-STAR, ZC3H14).

A directed yeast 2-hybrid assay revealed that a number of these interactors (CCDC92, NELF-A and ZC3H11A) bound specifically to the substrate binding domain of SIAH1, the region implicated in binding its various target proteins. ASPP1, SIAH1BP1 and ZC3H14 interacted with full length SIAH1 protein only, however it is possible that these proteins primarily interact with the SIAH1 SBD *in vivo* and the RING-finger or central zinc finger regions are necessary for stabilising the interaction.

Protein sequence analysis revealed that some of these hits (PHC2, ASPP1 and NELF-A) contained a conserved SIAH binding motif, which is present in a number of known SIAH-interacting proteins (House et al., 2003). The presence of a putative binding motif in these SIAH1 interactors substantiates the likelihood that these proteins are genuine interactors *in vivo*. However, because this is such a small motif, it is possible that its presence may simply be a coincidence. Also, a poor alignment does not necessarily signify that a protein is not a genuine SIAH1 substrate because not all of the recognised SIAH1 substrates contain this motif (see later).

When analysing the stability of each of the hits when co-expressed with or without SIAH1, it was observed that protein levels on the whole, were reduced when co-expressed with SIAH1. This may be due to competition for transcription and translational machinery when both the SIAH1 and GFP-fusion plasmids are present in the cell. However, empty pCDNA plasmid was co-transfected in minus SIAH1 controls suggesting that the observed affect is more likely to be due to SIAH1 mediated breakdown. Quantitative analysis revealed that co-expression of SIAH1 had the most noticeable effect on levels of ASPP1, PHC2, NELF-A, ZC3H11A and ZC3H14.

As noted in the introduction to this thesis (section 1.3.2), not all SIAH1 interacting proteins are targets for SIAH1 mediated ubiquitination and breakdown as SIAH proteins can bind cofactors/adaptors which bridge the interaction between SIAH and its target for destruction. For example APC and SIP function as bridging proteins, physically linking SIAH with β-catenin, resulting in β-catenin ubiquitination and degradation (Liu et al., 2001). SIP contains a recognised SIAH1 binding domain and binds to the SIAH SBD, however its stability is unaffected by this interaction (Matsuzawa et al., 2001; House et al., 2003).

However, proteins which interact with the substrate binding domain of SIAH1, contain a conserved SIAH binding motif and, more importantly, are notably reduced when co-expressed with SIAH1, are likely to be targets for SIAH1 mediated degradation.

Taking into consideration the data so far, the most likely candidates for SIAH1 targeted destruction identified from the SIAH1 testes yeast 2-hybrid screen include, PHC2, a polycomb protein which is part of a multimeric, chromatin associated complex involved in homeotic gene regulation; NELF-A, a component of the negative elongation factor

complex which negatively regulates RNA polymerase II; ASPP1, a protein required for the induction of apoptosis by p53-family proteins; and ZC3H11A, a recently identified member of the mRNA export complex, known as the TREX complex (Dufu et al., 2010).

Further mapping of the SIAH1 binding site in ZC3H14 and ZC3H11A revealed a potential SIAH1 binding site in the ZC3H11A SIAH1-interacting region however, no obvious motif was found in ZC3H14 when the ClustalW alignment method was used.

The SIAH binding motif has only been identified in around half of the functionally diverse SIAH binding proteins so far (Santelli et al., 2005). Proteins in which no obvious motif has been identified include substrates such as Synaptophysin, mGlutR1 (House et al., 2003), TRIM proteins (Fanelli et al., 2004) and cofactors such as APC (House et al., 2003). It is possible that there is a different consensus motif in these SIAH interacting proteins and ZC3H14. However, further mapping of the SIAH interacting region in these proteins, alignment analysis and mutational analysis is required.

Chapter 4. Further investigation into the SIAH1:NELF-A interaction

4.1 Introduction

As a result of our previous studies, NELF-A, one of the hits from the SIAH1 yeast 2-hybrid screen, was found to interact specifically with the SIAH1 substrate binding domain. NELF-A contains a putative conserved SIAH binding motif and levels of NELF-A-GFP fusion protein were notably reduced when co-expressed with SIAH1, comparable to the published SIAH1 substrate, human T-STAR. Each piece of evidence to date implied that NELF-A was a target for SIAH1-mediated degradation.

The NELF-A protein is a member of a highly conserved, multi-subunit complex known as the negative elongation factor (NELF) protein complex. This complex is composed of four subunits. These are named the A subunit (66kDa), B subunit (62kDa), C/D subunits (60/59kDa), and the E subunit (46kDa), all of which appear to be ubiquitously expressed (Mariotti et al., 2000; Narita et al., 2003). NELF-C/D are translation variants of the same mRNA (Gilchrist et al., 2008).

The importance of the NELF complex is highlighted by the implication of some of its subunits in the etiology of various diseases. NELF-A is encoded by the *WHSC2* gene which was first identified as a candidate gene for Wolf-Hirschhorn syndrome, a multiple malformation disorder characterised by a range of developmental defects (Wright et al., 1999). NELF-B, also known as COBRA1 (cofactor of BRCA1), is a breast/ovarian cancer susceptibility gene (Ye et al., 2001; Narita et al., 2003; Aiyar et al., 2004) and reduced NELF-B expression correlates with poor prognosis in breast cancer (Sun et al., 2008a). RNAi against NELF-E in *Drosophila* has been shown to cause developmental defects or lethality depending on where the RNAi was expressed. Thus like NELF-A, absence of NELF-E also affects development (Enerly et al., 2002).

In vitro biochemical and tissue culture based studies have demonstrated that this multi-subunit complex acts together with DRB-sensitivity inducing factor (DSIF) and stalls elongating RNA polymerase II (RNAPII), resulting in a pause in transcription (Yamaguchi et al., 1999; Yamaguchi et al., 2002). Transcription is the process through which a DNA sequence is copied to produce a complementary RNA, and transcription of protein coding genes is carried out by the multi-subunit enzyme RNAPII. The NELF complex and DSIF achieve transcriptional pausing by binding to RNAPII and nascent

RNA via their various subunits (summarised in Figure 13) (Narita et al., 2003; Yung et al., 2009).

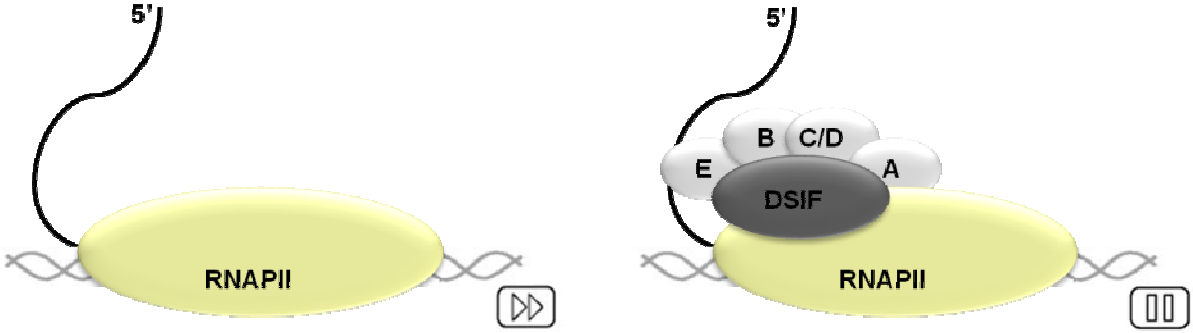

Figure 13. NELF- and DSIF- induced stalling of elongating RNAPII. NELF subunits are light grey. The functionally active NELF complex consists of a heterotetramer of one of each subunit bound to each other and to other factors in the configuration shown. NELF-A binds to elongating RNAPII on one surface and to NELF-C on another, while NELF-B is sandwiched between NELF-C and NELF-E and another surface of NELF-E binds to short nascent RNA transcripts protruding from the active site of RNAPII. The tethering of the NELF-E to nascent transcript and elongation complex restricts the movement of RNAPII. Figure compiled from information from Narita et al., (2003) and Yung et al., (2009).

It is often assumed that RNAPII initiation is the rate-limiting step in gene expression, however it is emerging that the elongation step of transcription is a crucial control point in transcriptional regulation for a subset of genes, requiring the recruitment of multiple proteins. Hence, the identification of potential regulators of this level of gene expression is of great interest. Mechanisms controlling transcriptional elongation are reviewed by Shilatifard (2004); Saunders et al., (2006) and Price (2008).

Generally, NELF and DSIF pause elongating RNAPII approximately 20-50 base pairs downstream from the transcription start site, after transcription initiation and promoter clearance (Wu et al., 2005; Gilchrist et al., 2008; Lee et al., 2008a). Genes which contain these poised polymerases are designated 'potentially active' and studies which have measured the distribution of poised RNAPII across the *Drosophila* and human genomes have revealed that that they predominantly locate to developmental control genes, such as those encoding homeodomain proteins and genes which respond to developmental or environmental cues (e.g., wnt, notch and TGFβ) (Aida et al., 2006; Gilchrist et al., 2008). Thus the NELF complex plays a very important role in regulating the pattern of genes expressed during development and differentiation, however very little is known of how this complex is manipulated to give rise to selective gene activation or repression.

As the *Siah1a* mutant mouse is growth retarded and the male mouse is sterile, Siah1a evidently plays an important role in regulating cell growth and differentiation. Thus it is possible that SIAH proteins may mediate an additional layer of transcriptional regulation of the various NELF- regulated developmental control genes by modulating stability of NELF-A and the NELF complex.

We wanted to further characterise the SIAH1:NELF-A interaction and determine whether or not SIAH1 could regulate NELF-A stability *in vivo*. To do this, the SIAH binding site in NELF-A was mapped and further investigated *in vivo* via GST pull down. Experiments were carried out in order to determine whether or not NELF-A was ubiquitinated and endogenous NELF-A protein was analysed in mouse testes tissue and *Siah* deficient cells. We also wanted to establish whether or not the other members of the Siah family could regulate NELF-A stability and to do this, levels of NELF-A-GFP fusion protein were monitored when each of the three murine Siah proteins were over-expressed.

4.2 Assay to determine whether or not GFP-tagged NELF-A is regulated by the proteasome

The *in vivo* degradation assay described in chapter 3 (section 3.5.3) revealed that levels of NELF-A-GFP fusion protein were notably reduced when co-expressed with SIAH1. However, as noted in the discussion (chapter 3, section 3.7), this observed reduction may be due to SIAH1 mediated poly-ubiquitination of NELF-A-GFP and proteasomal breakdown, or it may be a result of reduced expression due to competition for transcriptional and translational machinery when both expression plasmids are present in the cell.

To distinguish between these two possibilities, the stability of NELF-A-GFP fusion protein was assayed in the presence and absence of the peptide aldehyde MG132, a potent inhibitor of proteasome function. If NELF-A-GFP is targeted by SIAH1 for proteasomal breakdown then we would expect levels of the protein to stabilise in the presence of MG132.

Essentially, the *in-vivo* degradation assay described in chapter 3 (section 3.5.3) was repeated. NELF-ApGFP3 and SIAH1pCDNA3 were co-transfected into HEK293 cells

with a GFP expression vector internal standard to show the relative amount of the NELF-A-GFP fusion protein. 24 hours after transfection cells were incubated with or without the proteasome inhibitor MG132 for 7 hours. Cell extracts were then analysed by Western blot probing with GFP antisera (Figure 14).

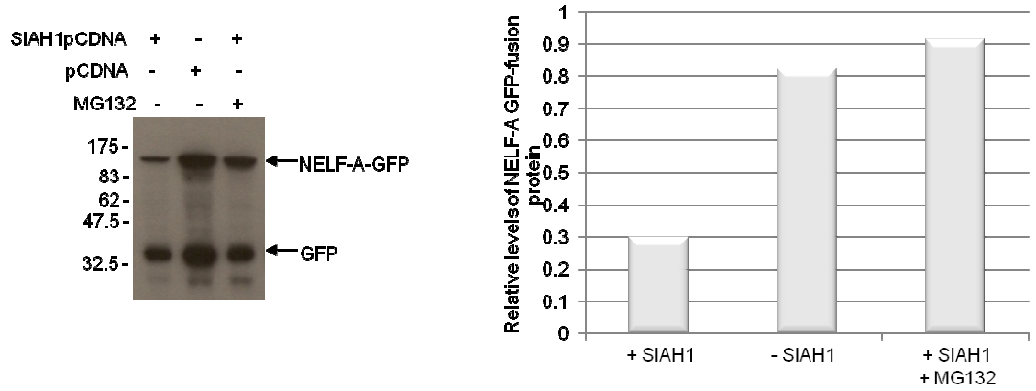

Figure 14. GFP-tagged NELF-A is stabilised by MG132. 24 hours after transfection, cells were incubated with or without 40µM MG132 for 7 hours. Cell lysates were prepared and samples were separated on 10% SDS PAGE. Levels of GFP-tagged NELF-A were measured by immunoblotting with α-GFP and HRP-conjugated anti-mouse secondary antibody. The migration of molecular weight markers is indicated on the left of the Western. The graph shows the relative amount of NELF-A-GFP fusion protein in each of the co-transfections.

Consistent with regulation by a proteasome dependent mechanism, NELF-A-GFP fusion protein was more stable with MG132 incubation when co-expressed with SIAH1.

4.3 Comparison of the human and mouse NELF-A protein sequence

Given that human NELF-A is a SIAH1 substrate, our next question was could the same protein interaction take place in the mouse and perhaps contribute to the *Siah1a*$^{-/-}$ mutant phenotype. As mentioned in the introduction to this thesis (section 1.4), an investigation into the interaction between T-STAR and SIAH1 by Venables and colleagues (2004) revealed that human T-STAR efficiently bound to SIAH1 resulting in its proteasomal degradation. However, mouse T-STAR was neither bound nor degraded by SIAH1. Comparative sequence analysis of mouse T-STAR with the SIAH1-binding region in human and primate T-STAR proteins revealed that the SIAH binding motif evolved specifically in the primate lineage and is absent in the mouse. Hence, defects in modulation of T-STAR protein stability by SIAH1 could not help explain the mouse *Siah1a*$^{-/-}$ mutant phenotype.

It was previously reported that the *WHSC2* gene, encoding NELF-A, is a highly conserved gene with the human and mouse genes showing 84.2% identity at the nucleotide level and the encoded proteins are 93.3% identical at the amino acid level (Wright et al., 1999). In order to determine whether or not the putative SIAH1 binding site identified in NELF-A (chapter 3, section 3.4) was conserved between humans and mice, the human and mouse NELF-A protein sequences were aligned using ClustalW (Figure 15). This revealed that unlike T-STAR, the predicted SIAH1 binding site identified in NELF-A is identical in humans and mice.

```
Mouse   MASMRESDTGLWLHNKLGATDELWAPPSIASLLTAAVIDNIRLCFHRLSSAVKLKLLLGT 60
Human   MASMRESDTGLWLHNKLGATDELWAPPSIASLLTAAVIDNIRLCFHGLSSAVKLKLLLGT 60
        ********************************************* *************

Mouse   LHLPRRTVDEMKAALMDIIQLATLDSDPWVLMVADILKSFPDTGSLNLDLEEQNPNVQDI 120
Human   LHLPRRTVDEMKGALMEIIQLASLDSDPWVLMVADILKSFPDTGSLNLELEEQNPNVQDI 120
        ************.***:*****:*************************:***********

Mouse   LGELREKVSECEASAMLPLECQYLNKNALTTLAGPLTPPVKHFQLKRKPKSATLRAELLQ 180
Human   LGELREKVGECEASAMLPLECQYLNKNALTTLAGPLTPPVKHFQLKRKPKSATLRAELLQ 180
        ********.**************************************************

Mouse   KSTETAQQLKRSAGVPFHAKGRGLLRKMDTTTPLKGIPKQAPFRSPTTPSVFSPSGNRTP 240
Human   KSTETAQQLKRSAGVPFHAKGRGLLRKMDTTTPLKGIPKQAPFRSPTAPSVFSPTGNRTP 240
        ************************************************:******:*****

Mouse   IPPSRTPLQKERGVKLLDISELNTVGAGREAKRRRKTLDTEVVEKPTKEETVVENATPDY 300
Human   IPPSRTLLRKERGVKLLDISELDMVGAGREAKRRRKTLDAEVVEKPAKEETVVENATPDY 300
        ****** *:*************: ***************:******:*************

Mouse   AAGLVSTQKLGSLNSEPTLPSTSYLPSTPSVVPASSYIPSSETPPAPPSREASRPPEEPS 360
Human   AAGLVSTQKLGSLNNEPALPSTSYLPSTPSVVPASSYIPSSETPPAPSSREASRPPEEPS 360
        **************.**:*****************************.************

Mouse   APSPTLPTQFKQRAPMYNSGLSPATPAPAAPTSPLTPTTPPAVTPTAQTPPVAMVAPQTQ 420
Human   APSPTLPAQFKQRAPMYNSGLSPATPTPAAPTSPLTPTTPPAVAPTTQTPPVAMVAPQTQ 420
        *******:******************:**********:******:**:*************

Mouse   APAPVQQQPKKNLSLTREQMFAAQEMFKTANKVTRPEKALILGFMAGSRENPCPEQGDVI 480
Human   APA--QQQPKKNLSLTREQMFAAQEMFKTANKVTRPEKALILGFMAGSRENPCQEQGDVI 478
        ***  ********************************************** ******

Mouse   QIKLSEHTEDLPKADGQGSTTMLVDTVFEMNYATGQWTRFKKYKPMTNVS 530
Human   QIKLSEHTEDLPKADGQGSTTMLVDTVFEMNYATGQWTRFKKYKPMTNVS 528
        ************************************************
```

Figure 15. Sequence alignment between human and mouse NELF-A protein. The alignment was generated using ClustalW. The putative SIAH binding motif is highlighted by the red box. . "*"residues represent those that are identical the alignment. ":" represent conserved substitutions and "." represent semi-conservative substitutions.

4.4 Immunodetection of NELF-A in mouse tissues

WHSC2 expression was analysed in human tissues by Mariotti and colleagues (2000) via Northern blot. They found it was expressed in all human tissues examined and was most abundant in the heart and placenta. Narita et al., (2003) also examined expression of *WHSC2* and the other three NELF subunits by Northern blot and again found they were expressed in all human tissues examined. To our knowledge, however, NELF-A protein abundance in both human and mouse tissues has not been analysed.

As SIAH proteins affect protein rather than mRNA stability we hoped to gain an insight of the relative stability of NELF-A protein in varying tissues by comparing NELF-A protein levels with the published mRNA expression results. In order to analyse this, a NELF-A specific antibody was purchased (Santa Cruz, H-240). Due to the limited availability of human tissues samples we sought to analyse protein levels of NELF-A in various murine tissues. Although the NELF-A polyclonal antibody was raised against amino acids 92-300 mapping near the N-terminus of NELF-A of human origin we were confident that it would detect both human and mouse proteins due to the high degree of protein sequence identity (see alignment Figure 15).

Various mouse tissues were dissected and homogenised in 2x sample loading buffer. Samples were then boiled and proteins were separated by 7% SDS-PAGE. NELF-A protein abundance was analysed by Western blot probing with the α-NELF-A polyclonal antibody. For a loading control, the blot was also probed with a β-actin specific antibody (Figure 16).

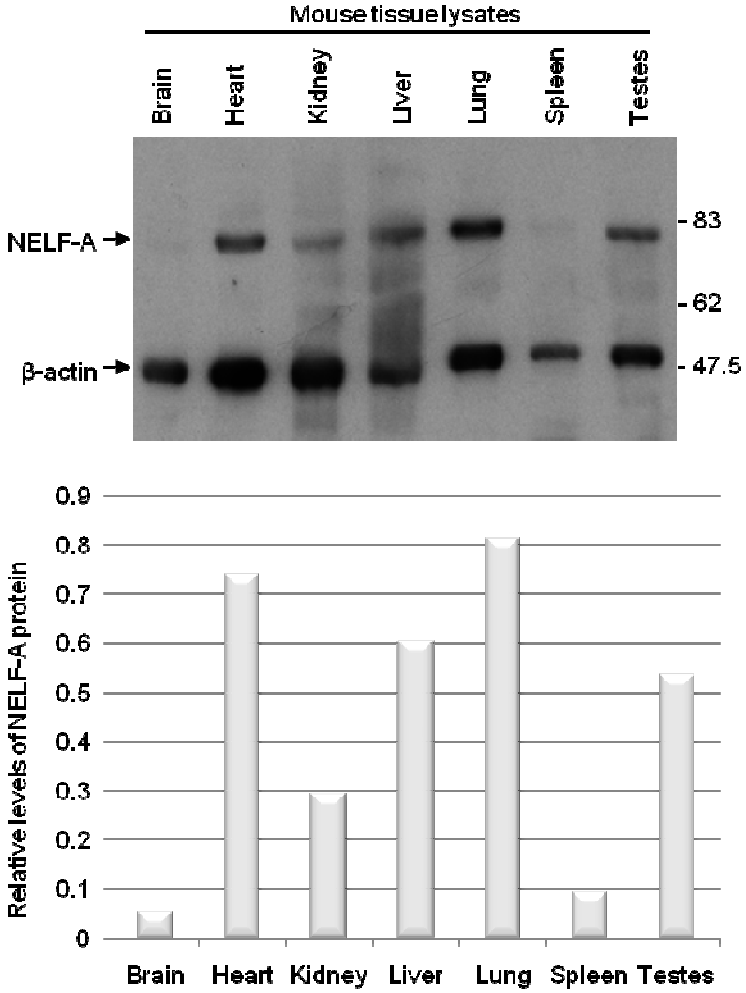

Figure 16. Analysing abundance of NELF-A protein in multiple mouse tissues. Tissue lysates were prepared, and the level of NELF-A was measured by immunoblotting with α-NELF-A and anti-β-actin antibodies. Antibody binding was detected using HRP-conjugated α-rabbit secondary antibody. The migration of molecular weight markers is indicated on the right. The graph shows the relative amount of NELF-A protein in each tissue compared to the β-actin loading control.

NELF-A protein was most abundant in mouse lung, heart, liver and testis. Protein levels were moderate in the kidney and NELF-A was least abundant in the brain and spleen. In contrast to this result, although no quantitative data is shown, the Northern blot published by Mariotti et al., (2000) shows that NELF-A mRNA levels in the human brain are higher than or approximately equal to those in the liver, lung and kidney. This may imply that NELF-A protein is less stable in the brain, potentially due to rapid turnover by the proteasome in these tissues. Alternatively, the *WHSC2* gene encoding NELF-A may be differentially expressed in mouse and human tissues.

4.5 Immunodetection of NELF-A in mouse testes

As discussed previously, the murine Siah1a protein is known to play an essential role in male germ cell development as targeted deletion of this gene results in meiotic arrest during spermatogenesis. To further investigate Siah1 expression during meiosis, Venables and colleagues (2004) performed Western blots with a SIAH1 antibody on extracts from different purified mouse germ cell populations. The SIAH1 antibody used could detect both human SIAH1 and mouse Siah1a proteins as they differ by only one amino acid. They found Siah1 was strongly expressed in spermatocytes (meiotic cells) but not spermatids (post-meiotic cells).

As noted in the introduction (chapter 1, section 1.3) mice contain a second, almost identical copy of the *Siah1a* gene, *Siah1b*. This gene however, resides on the X chromosome which is shut down during meiosis. Therefore the Siah1 protein expressed in murine spermatocytes is likely to represent Siah1a, not Siah1b.

Our initial analysis of NELF-A protein expression in various mouse tissues confirmed that NELF-A was expressed in the testes which is consistent with its isolation from the testis cDNA library used for the SIAH1 yeast 2-hybrid screen. In order to determine whether or not Siah1 and NELF-A protein were present in the same cell types in the testis, the precise localisation of NELF-A protein was analysed in mouse testes sections by immunohistochemistry.

Murine testis sections (prepared by Dr Ingrid Ehrmann, IHG, Newcastle University) were dewaxed and microwaved in citrate buffer to expose antigens. Sections were then stained using the α-NELF antibody and the DAB detection system (see methods, section 2.3.7). Staining was visualised by light microscopy (Figure 17).

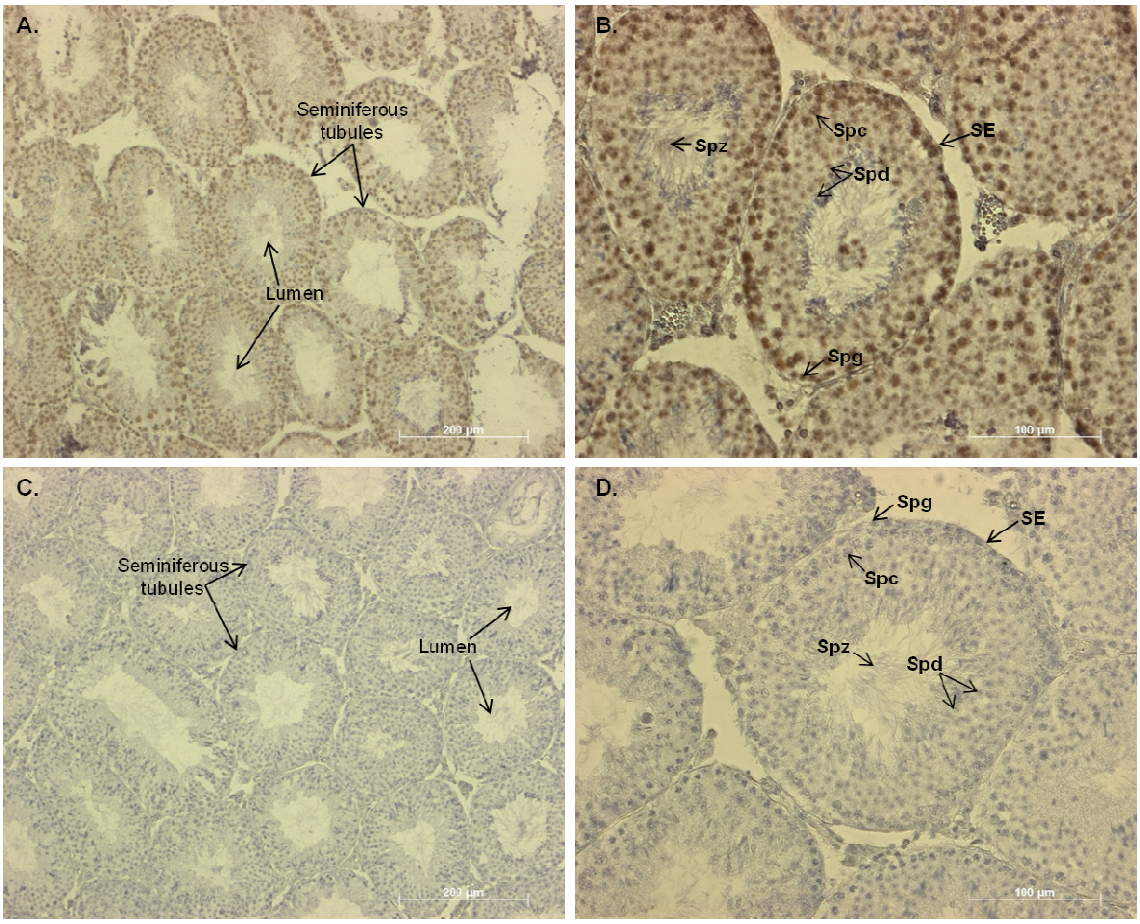

Figure 17. Images of testis sections from wild-type mice immunostained with NELF-A. (A and B) Mouse testis sections were probed with NELF-A antisera and NELF-A was detected using biotin-conjugated α-rabbit secondary antibody and the DAB system. Brown staining indicates NELF-A protein, and blue staining is the haematoxylin counterstain which stains nuclei. (C and D) Mouse testes sections stained with biotin-conjugated α-rabbit secondary antibody alone and haematoxylin counterstained. Scale bars are equal to 200µm in A and C and 100µm in B and D. SE: seminiferous epithelium; Spg: spermatogonia; Spc: spermatocyte; Spd: Spermatids at differing stages of differentiation, including round and elongating spermatids; Spz: spermatozoon.

It was clear from the images presented in Figure 17 that NELF-A protein was present in the nuclei of a large proportion of developing germ cells within the testes. The nuclear localisation is consistent with NELF-A's role as a regulator of RNAPII. To gain a clearer picture of the specific populations of germ cells in which NELF-A was present, the images were sent to Professor Philippa Saunders (MRC Human Reproductive Sciences Unit, Edinburgh, UK) a specialist in male germ cell development. Professor Saunders concluded that NELF-A protein was present in the nuclei of pachytene spermatocytes and round spermatids, and was absent in elongate spermatids and most spermatogonia. The pachytene stage occurs during meiosis I (primary spermatocytes) and is the point where spermatocytes begin to synthesise large amounts of mRNAs and

proteins permitting them to sustain two consecutive rounds of cell division (Geremia et al., 1977; Monesi et al., 1978).

Thus unlike Siah1a which seems to be expressed mainly in meiotic cells (i.e. spermatocytes) NELF-A is expressed in both meiotic and mitotic cells. Since Siah1a and NELF-A are co-expressed in a subset of cells it is possible that Siah1a could regulate NELF-A in these cell types. Determination of the precise points at which Siah1a and NELF-A expression is switched on and off during spermatogenesis however, would require more in depth analysis. Unfortunately, the SIAH1 antibodies available to us did not work by Western blot or immunohistochemistry, therefore we were unable to co-stain the testes sections.

4.6 Mapping the SIAH1 binding site in NELF-A

Analysis of the NELF-A protein sequence revealed a putative SIAH binding site encompassing amino acids 381-405 which is conserved between humans and mice (see section 4.3). To determine which part of NELF-A is recognised by SIAH1, four constructs containing different regions of NELF-A were generated by PCR and tested in a directed yeast 2-hybrid assay for their ability to bind SIAH1 protein.

4.6.1 Generation of partial NELF-A constructs

NELF-A was divided into four regions – the N-terminal region (amino acids 1-248, using primers WHSC2-F and WHSC2(744)R), the central region (amino acids 248-317, using primers WHSC2(744)F and WHSC2(951)B), the C-terminal region including the PST-rich domain (amino acids 317-528, using primers WHSC2(951)F and WHSC2-B), and the PST-rich domain alone (amino acids 317-427, using primers WHSC2(951)F and WHSC2(1281)B) (see Figure 18). The PCR products were then digested with *Eco*RI/*Xho*I and ligated into complementary digested sites in the pGADT7 yeast 2-hybrid vector. The ligations were then re-cleaved with *Bam*HI followed by dialysis. 1µl of each of the ligation mixes was then transformed into *E. coli* DH5α cells by electroporation. The resultant transformation mix was then plated out onto LB plates containing ampicillin and incubated at 37ºC overnight. Colonies were screened by PCR using a vector specific forward primer (T7-F) and an insert specific reverse primer. Insert positive colonies were further grown in LB-ampicillin overnight before plasmid

purification. To confirm that the pGADT7 clones contained the correct sequences, each construct was sequenced from the 5′ end using the T7-F sequencing primer.

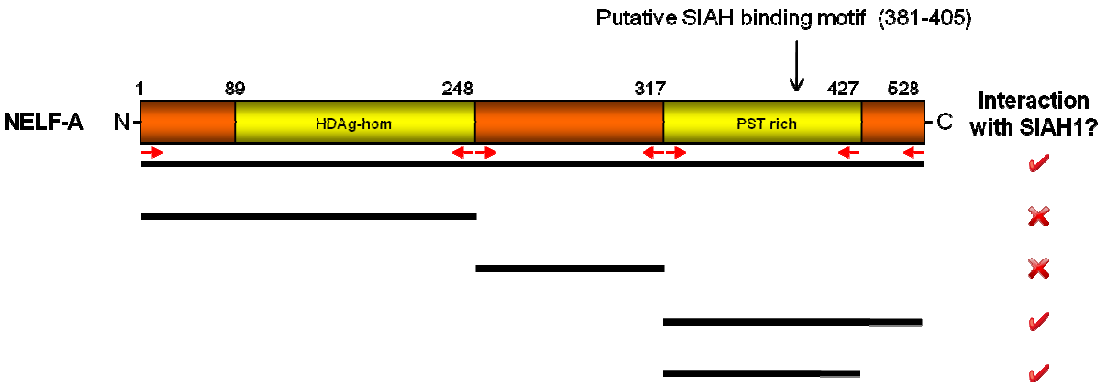

Figure 18. Schematic diagram of the NELF-A protein and summary of yeast 2-hybrid results. The N-terminal HDAg homology region (amino acids 89 to 248) is essential for interaction with RNAPII and the C-terminal half of the protein includes a region which is rich in proline (P), serine (S), and threonine (T) residues. The putative SIAH binding motif (amino acids 381-405) lies within this PST-rich region (↓). Smaller constructs outlined below were cloned independently into the pGADT7 vector, and were assayed for an interaction with SIAH1 via the yeast 2-hybrid assay. Primers used for cloning are shown as red arrows.

4.6.2 Mapping the NELF-A:SIAH1 interacting region using the yeast 2-hybrid assay

The four partial NELF-ApGADT7 clones shown in Figure 18 were tested against the pGBKT7 vector alone to assay for auto-activation, and against full length SIAH1-pGBKT7. As a positive control, full length NELF-ApACTII was tested against full length SIAH1-pGBKT7. Results are presented in Figure 19.

	NELF-A Full length (pACTII)	NELF-A constructs in pGADT7 (amino acids)			
		NELF-A (1-248)	NELF-A (248-317)	NELF-A (317-427)	NELF-A (317-528)
SIAH1pGBKT7	++	-	-	+++	+++
pGBKT7	-	-	-	-	-

Figure 19. Mapping of the NELF-A interaction domain with SIAH1. Full length SIAH1-pGBKT7 was tested against partial NELF-A constructs to identify the interacting region. Empty bait plasmid, pGBKT7, was used as a control to test for auto-activation of prey plasmids. Filters stained with X-Gal are shown. Positive interactions manifest as blue colonies while if no interaction is present, the colonies remain white or red. Key, +++ strong interaction, positive blue colour within 10 minutes, ++ positive blue colour observable within 30 minutes, + positive blue colour observable within 1 hour, - no noticeable interaction after 2 hours of exposure.

A strong, positive interaction with SIAH1 was detected with constructs 317-427 and 317-528. This mapped to the PST-rich region of the NELF-A protein. This is the region of the protein which contains the putative SIAH1 degron motif that we previously identified (chapter 3, section 3.4). Negative results for interaction between the empty pGBKT7 vector and the various NELF-A regions in pGADT7 confirmed that the positive results were not due to auto-activation by the Gal4 AD-NELF-A fusions alone.

4.7 Assaying the NELF-A:SIAH2 interaction via yeast 2-hybrid

Some SIAH substrates such as DCC are targeted for proteolytic degradation by both SIAH1 and SIAH2 proteins (Hu et al., 1997b). However in some cases, the biochemical functions SIAH1 and SIAH2 are unique to the individual family member. For example the central regulator of cellular responses to stress and cytokines, TRAF2, is targeted for proteasomal degradation by SIAH2 but not SIAH1 (Habelhah et al., 2002). Identifying substrates which are uniquely degraded by SIAH1 may help explain why, in contrast to the *Siah2* mutant, which is largely phenotypically normal, the *Siah1a* mutant mouse is growth retarded and males are sterile.

Therefore SIAH2 was assayed for its ability to interact with NELF-A via yeast 2-hybrid. A SIAH2 clone was available in pACTII, which is a Gal4 activation domain plasmid (Venables et al., 2004). In order to test whether or not SIAH2 interacts with NELF-A, full length NELF-A and its partial sequences needed to be transferred from pGADT7 (as this is also a Gal4 activation domain plasmid) to the pGBKT7 vector, which contains the Gal4 DNA binding domain sequence.

NELF sequences were amplified by PCR and digested as previously described (see section 4.6.1). In this case however, products were ligated into *Eco*RI/*Sal*I sites of the pGBKT7 yeast 2-hybrid vector. Ligations were re-cleaved with *Sal*I, transformed into *E. coli* DH5α and the transformations were plated out on LB agar containing Kanamycin.

To confirm that positive clones contained the correct sequence, each construct was sequenced. Each NELF-A construct was then tested for ability to interact with SIAH2 in a yeast 2-hybrid assay. Results are presented in Figure 20.

	NELF-A constructs in pGBKT7 (amino acids)				
	NELF-A Full length	NELF-A (1-248)	NELF-A (248-317)	NELF-A (317-427)	NELF-A (317-528)
SIAH2pACTII	- 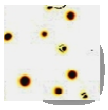	- 	- 	+++ 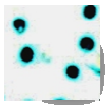	+++ 
pACTII	- 	- 	- 	- 	++ 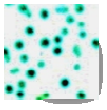

Figure 20. Mapping of the NELF-A interaction domain with SIAH2. Full length SIAH2-pACTII was tested against partial NELF-A constructs to identify the interacting region. Empty bait plasmid, pACTII, was used to test for auto-activation of prey plasmids. Filters stained with X-Gal are shown. Positive interactions manifest as blue colonies while if no interaction is present, the colonies remain white or red. Key, +++ strong interaction, positive blue colour within 1 hour, ++ positive blue colour observable within 2 hours, - no noticeable interaction after 24 hours of exposure.

The full length NELF-A protein did not interact with SIAH2, however the minimal PST-rich domain (amino acids 317-427) containing the SIAH binding motif did. Often, sub-domains of proteins interact better than full length clones, perhaps due to the lack of certain folding constraints. In the yeast 2-hybrid system, the full-length fusion proteins may not fold correctly consequently altering their confirmation. Alternatively, in order to interact, they may require certain post-translational modifications (e.g. phosphorylation or glycosylation), which may not occur properly, or at all in the yeast system. Also, some proteins, when expressed in yeast, are not be targeted to the nucleus, they may be toxic to the cell, or they may also be unstable and degraded by yeast proteins. Thus, it remains possible that SIAH2 and NELF-A interact *in vivo*. The C-terminal (amino acids 317-528) region of NELF-A was found to auto-activate when cloned in frame with the activation domain of Gal4 (encoded for by empty pACTII).

4.8 Confirmation of the interaction between NELF-A and SIAH1 *in vitro*

The next step was to confirm that the interaction between NELF-A and SIAH1 was a genuine molecular interaction, caused by direct protein-protein contact rather than any yeast bridging proteins. This was achieved via a GST *in vitro* pull-down assay. Firstly, the PST-rich region of NELF-A was cloned into the pGEX5X1 vector to create a GST-fusion gene. The encoded fusion protein was then expressed in *E. coli* BL21 cells, and used to specifically pull down radiolabelled, *in vitro*-translated, SIAH1. A similar experiment was previously carried out to confirm the interaction between SIAH1, and the RG-rich region of human T-STAR containing the SIAH1 binding site (Venables et al., 2004). Because this was known to work, T-STAR(RG) was used as a positive control.

4.8.1 Generation of partial NELF-A-GST fusion protein

The PST-rich region of NELF-A (amino acids 317-427) which was found to interact with SIAH1 via yeast 2-hybrid was amplified by PCR from the NELF-ApACTII clone (using primers WHSC2(951)F and WHSC2(1281)B) and cloned into the *Eco*RI/*Xho*I sites of the pGEX5X1 GST fusion vector. To confirm that the pGEX5X1 clone contained the correct sequence, it was sequenced from the 5′ end using the pGEX5 sequencing primer. T-STAR(RG) was previously cloned into pGEX5X1 (Venables et al., 2004). Both recombinant plasmids were then transformed into *E. coli* BL21 cells, via the calcium chloride transformation procedure and were expressed overnight using Instant TB medium (see methods, section 2.3.8). Total BL21 cell lysate samples from the overnight cultures are shown in Figure 21A.

The molecular weight of the T-STAR RG-rich domain and the NELF-A PST-rich domain was estimated using the Scansite tool (see methods, section 2.6.3). The predicted molecular weight of T-STAR(RG) was 8kDa, and NELF-A(317-427) was 11.5kDa (both predictions were based on the absence of phosphate groups). GST is a 25kDa protein, therefore the expected sizes of the T-STAR(RG) and NELF-A(317-427) GST-fusion proteins were 33kDa and 36.5kDa, respectively.

Strong bands for T-STAR(RG)-GST and NELF-A(317-427)-GST were evident in the overnight induction samples showing that the GST-fusion proteins expressed well (see overnight (O/N) culture lanes in Figure 21). The proteins migrated a little slower than

their expected molecular weight, however proteins often run a little larger or smaller than their calculated molecular weight and deviations of up to 5kDa are not unusual.

4.8.2 Testing solubility and purification of T-STAR and NELF-A GST-fusion proteins

For use in a GST-pull-down assay, it is important that the GST fusion protein is soluble. Hence, bacterial cell pellets from the overnight cultures were lysed and sonicated, followed by a 10 minute centrifugation step to pellet any insoluble material (see methods, section 2.3.8.3). To test solubility, samples of total cell lysate, taken before the centrifugation step, and samples of soluble supernatant, taken after centrifugation, were analysed on a coomassie-stained SDS-PAGE gel (Figure 21A).

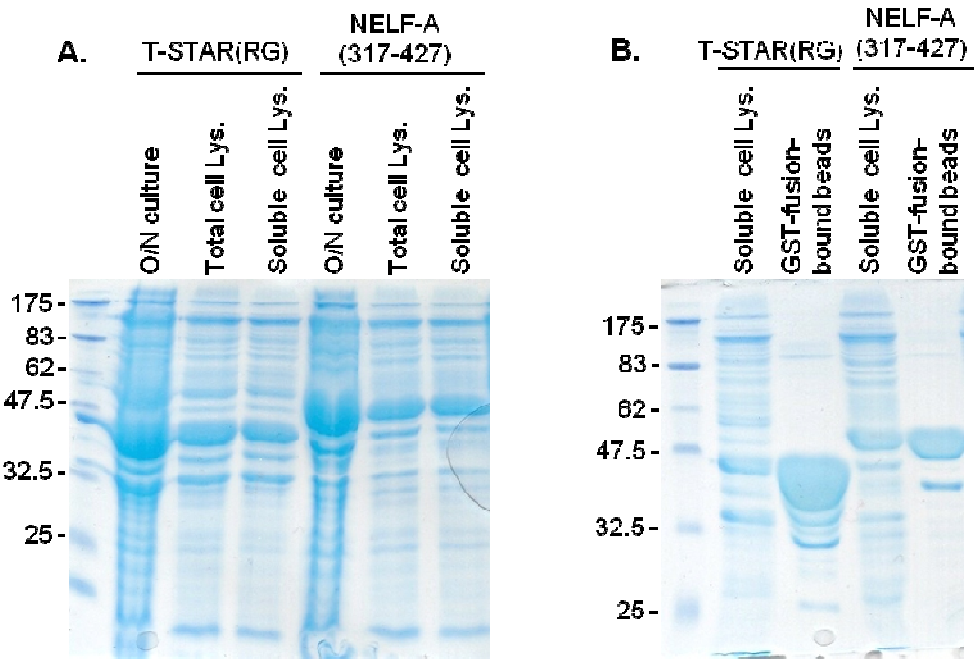

Figure 21. Testing solubility of the T-STAR(RG) and NELF-A(317-427) GST fusion proteins and purification using glutathione agarose. (A) Samples taken after the overnight (O/N) induction are shown along with total BL21 cell lysates and soluble cell lysates expressing GST fusion proteins. (B) GST-fusion proteins bound to glutathione agarose. Samples were boiled in 2X loading buffer and analysed on a coomassie stained, 10% SDS-PAGE gel. The sizes of molecular weight markers in kDa are indicated on the left.

For both fusion proteins, strong bands of the approximate expected size were present in both the non-pelleted, total cell lysate, and in the soluble supernatant from the centrifuged sample (Figure 21A), confirming that both fusion proteins were soluble.

These proteins were then purified from the soluble cell lysates using glutathione agarose beads (methods, section 2.3.8.3). To check purification, a sample of GST-fusion-bound beads were again analysed via SDS-PAGE (Figure 21B). Evidently, incubation with glutathione agarose beads, resulted in isolation of large amounts of T-STAR(RG)-GST and NELF-A(317-427)-GST.

4.8.3 In vitro transcription and translation of SIAH1

The SIAH1pGBKT7 plasmid (encoding the full length SIAH1 coding sequence, downstream of a T7 promoter) was used as a template to generate radiolabelled SIAH1 protein via an *in vitro* transcription and translation technique (see methods, section 2.3.4). A T7 Luciferase control plasmid was also used to make luciferase protein for a negative control. Both products were analysed by SDS-PAGE and autoradiography (see input lanes in Figure 22). Strong bands of the expected size of full length SIAH1 (34kDa) and Luciferase (61kDa) proteins were detected.

4.8.4 In vitro pull-down

Equal amounts of radiolabelled SIAH1 and luciferase were added to equal amounts of T-STAR and NELF-A GST-fusion bound agarose beads. Glutathione agarose beads attached to GST alone were used as a negative control. Samples were incubated for 1 hour, with rotation at room temperature, to allow protein binding. The beads were then pelleted by centrifugation and washed to remove any unbound protein. Reactions were analysed on an SDS-PAGE gel and visualised by autoradiography (Figure 22).

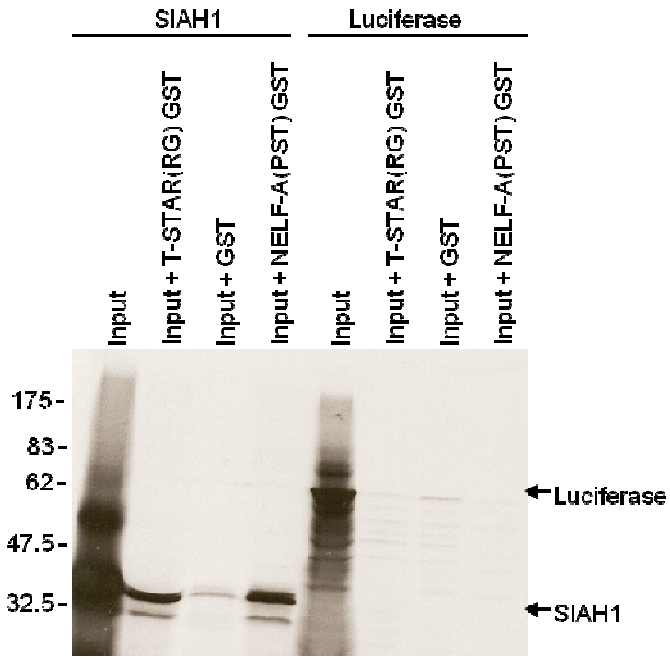

Figure 22. *In vitro* pull-down of radiolabelled SIAH1 by T-STAR and NELF-A. Glutathione agarose beads bound to GST fusions of the RG-rich region of T-STAR and the PST-rich region of NELF-A were added to *in vitro*-translated SIAH1 or luciferase proteins. After binding, samples were washed, boiled and separated by SDS-PAGE prior to autoradiography. T-STAR(RG) and NELF-A(PST) fusion proteins efficiently pulled down *in vitro*-translated SIAH1.

The positive control, T-STAR(RG)-GST-fusion protein efficiently pulled down radiolabelled SIAH1, as expected. A similar signal was evident with the NELF-A(317-427)GST fusion protein. This is consistent with the yeast 2-hybrid data, showing that the PST-rich region of NELF-A is capable of binding full length SIAH1 protein. The weaker lower bands may be due to translational initiation at secondary methionine codons (AUG) within the SIAH1 coding sequence. The stronger, upper bands appear to be the correct size for full length SIAH1. The negative control, GST alone, pulls down a small amount of SIAH1 protein, however the signal is negligible compared to that of T-STAR(RG) and NELF-A(317-427). Under the same conditions, only minor amounts of the negative control luciferase protein were pulled down by each GST-fusion protein.

4.9 Assay for SIAH1-mediated ubiquitination of NELF-A in cultured cells

Confirmation of the specific interaction between SIAH1 and NELF-A *in vitro* and results from our *in vivo* degradation assays (section 4.2) implied that this interaction resulted in proteasomal degradation of over-expressed NELF-A-GFP fusion protein. If this was indeed the case, then we would presume that this was mediated by polyubiquitination.

To test this possibility, ectopically expressed NELF-A-GFP fusion protein was immunoprecipitated using the GFP antibody after co-expression with or without SIAH1 and incubation with the proteasome inhibitor MG132 to prevent degradation of ubiquitinated protein.

In the experiments described, one 6 well plate of approximately 60% confluent HEK293 cells were used for each immunoprecipitation. Two plates were transfected with NELF-ApGFP3 alone, and in another two plates NELF-ApGFP3 was co-expressed with SIAH1pCDNA. 24 hours after transfection one of each of these plates of cells was treated with the proteasome inhibitor MG132 for 5 hours. By immunoprecipitating NELF-A-GFP fusion protein from cells in which SIAH1 was not overexpressed we aimed to establish whether or not there was sufficient endogenous SIAH1 activity in the cell to mediate NELF-A-GFP ubiquitination.

Following confirmation of GFP fluorescence, all plates were harvested and cell lysates prepared (see methods 2.3.10). Half of the cell lysate from each transfection were incubated with the α-GFP antibody overnight and the other half without antibody as a negative control. The following day cell lysates +/- GFP antibody were incubated with protein A Dynabeads and immunoprecipitated. Immunoprecipitates were then subjected to Western blot analysis using α-GFP antibody to confirm the IP was successful (Figure 23A).

As shown in Figure 23A NELF-A-GFP appears to be stabilised when MG132 was present (compare lanes 1 with 2 and 2 with 3), however there appears to be more NELF-A-GFP when co-expressed with SIAH1 (compare lanes 1 with 3 and 2 with 4). It is important to bear in mind, that there is no loading control on this Western. Therefore, we cannot ascertain anything with regards to protein levels from this IP. Interestingly, a higher molecular-weight smear characteristic of polyubiquitinated products was detected in all four IP lanes and this smear was strongest in cells in which SIAH1 was co-expressed and cells were treated with MG132. This was consistent with the hypothesis that SIAH1 mediates polyubiquitination of NELF-A-GFP fusion protein.

In order to confirm that the observed smear was due to ubiquitinated NELF-A-GFP fusion protein, the blot was stripped and re-probed with an anti-ubiquitin antibody. However, despite re-running samples, repeating Westerns and testing varying

concentrations of antibody we failed to detect any protein on these immunoprecipitations using the ubiquitin antibody (data not shown). As we did not have a positive control for this experiment (an expression construct for a proven SIAH1 target for polyubiquitination), we were unable to determine whether this was because NELF-A-GFP was not ubiquitinated or if it was simply due to the antibody having deteriorated.

In an attempt to resolve this issue, we utilised an HA-tagged ubiquitin expression construct, HA-UbpCDNA3 (purchased from Professor Yue Xiong, Lineberger Cancer Centre, University of North Carolina, USA) and the experiment described above was repeated. This time however, the HA-UbpCDNA3 was co-transfected and cells were incubated with the proteasome inhibitor MG132 for 6 hours rather than 5 in the hope that more ubiquitinated species would accumulate, making it easier to detect. Again, immunoprecipitates were then subjected to Western blot analysis using α-GFP antibody to ensure that NELF-A-GFP immunoprecipitated successfully (Figure 23B).

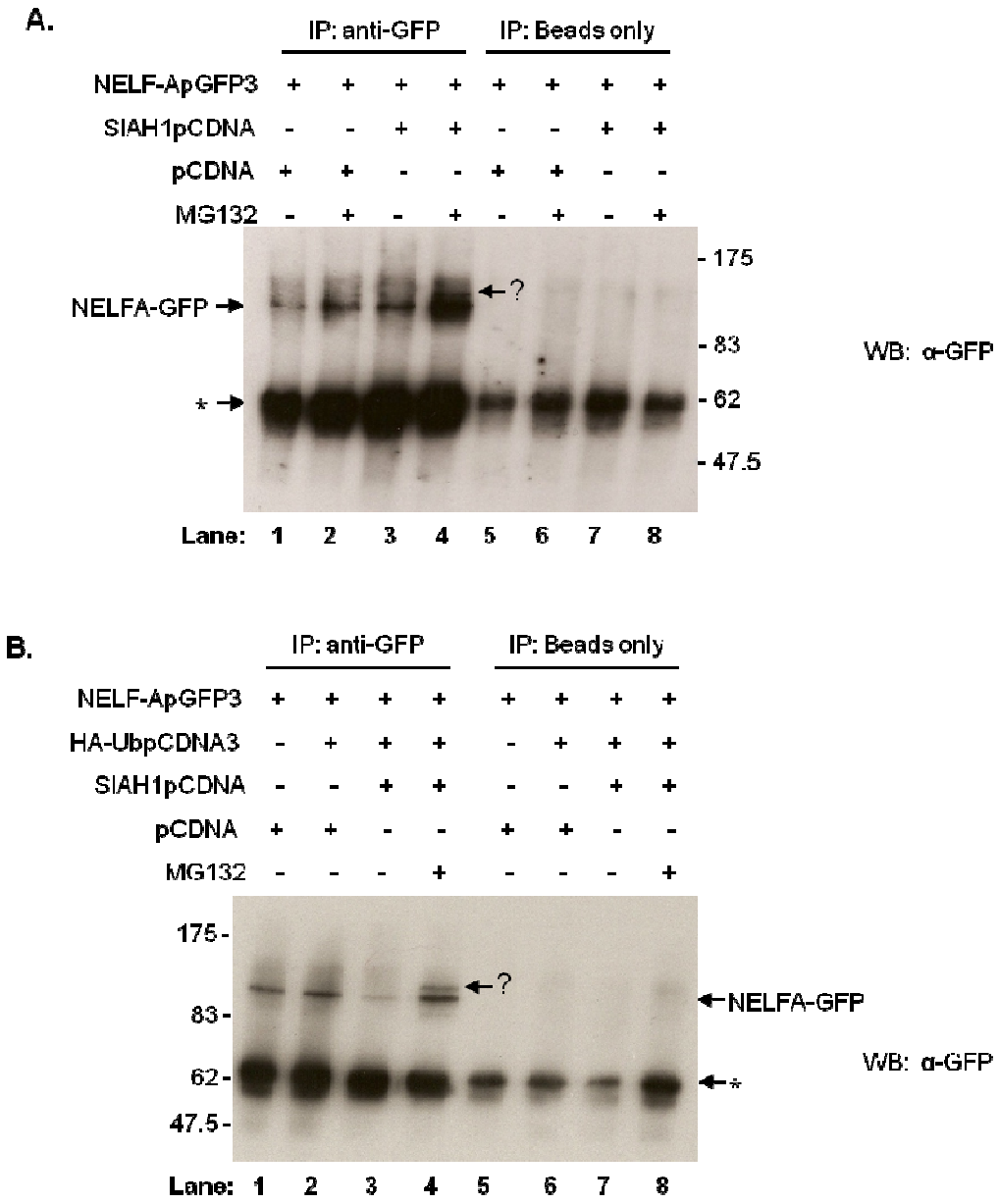

Figure 23. Immunoprecipitation of NELF-A-GFP fusion protein in attempt to detect SIAH1 mediated ubiquitination of ectopically expressed NELF-A. (A) HEK293 cells were co-transfected with NELF-ApGFP3 and SIAH1pCDNA or empty pCDNA vector in the minus SIAH1 controls. 24 hours after transfection cells were incubated in the presence or absence of 50µM MG132 for 5 hours. (B) HEK293 cells were co-transfected with NELF-ApGFP3, SIAH1pCDNA5 and HA-UbpCDNA3 as indicated. 24 hours after transfection cells were incubated in the presence or absence of 60µM MG132 for 6 hours. In both experiments lysates were immunoprecipitated with α-GFP antibody and Protein A Dynabeads or beads only as a negative control. After washing, samples were eluted by boiling in sample loading buffer. Immunoprecipitates and controls were separated on 7% SDS PAGE followed by immunoblotting with α-GFP and HRP-conjugated α-mouse secondary antibody to visualise NELF-A-GFP. The asterisks highlight non-specific bands. The question marks highlight the higher molecular weight NELF-A-GFP band observed when both NELF-ApGFP3 and SIAH1pCDNA were co-expressed and cells were incubated with MG132.

Similar to the previous experimental result (Figure 23A), it was clear that levels of NELF-A-GFP fusion protein were again stabilised in the presence of the proteasome

inhibitor MG132 (compare lanes 3 and 4 in Figure 23B) and a higher molecular weight band was also clearly observed (highlighted by the arrow and question mark). In order to determine whether or not the band represented a ubiquitinated form of NELF-A-GFP protein, this Western was stripped and re-probed with an α-HA antibody. However, once again we failed to detect any bands on these samples using the α-HA antibody despite repeated attempts (data not shown).

Therefore this data showed that the NELF-A-GFP fusion protein was modified in the presence of the proteasome inhibitor when SIAH1 was co-expressed, however we were unable to confirm that this modification was due to addition of a ubiquitin tag.

4.10 Assay for GFP-tagged NELF-A:RNAPII interaction in the presence/absence of SIAH1

As mentioned in the introduction to this chapter, the four subunits of the NELF complex interact with one another, DRB-sensitivity inducing factor (DSIF) and RNA polymerase II (RNAPII) to stall elongating RNAPII (summarised in Figure 13). The NELF-A protein in particular has been shown to be essential for RNAPII binding and transcriptional pausing, associating with RNAPII via its HDAg homology region (amino acids 89-248, see Figure 18) (Yamaguchi et al., 2001; Narita et al., 2003).

In our previous experiment we found that overexpression of SIAH1 results in modification (possibly ubiquitination) of NELF-A-GFP fusion protein. This led us to hypothesise that this modification could affect the ability of NELF-A to associate with RNAPII and/or other subunits of the NELF complex. In order to test this hypothesis and determine whether or not the NELF-A-GFP fusion protein and/or its modified species were able to interact with RNAPII *in vivo*, HEK293 soluble cell lysates (input), immunoprecipitations (IP: anti-GFP antibody) and controls (IP: protein A Dynabeads only) from the experiment described in the previous section (4.9) were subject to SDS-PAGE and Western blot probing with an antibody specific to the carboxy-terminal domain (CTD) of RNAPII (Figure 24).

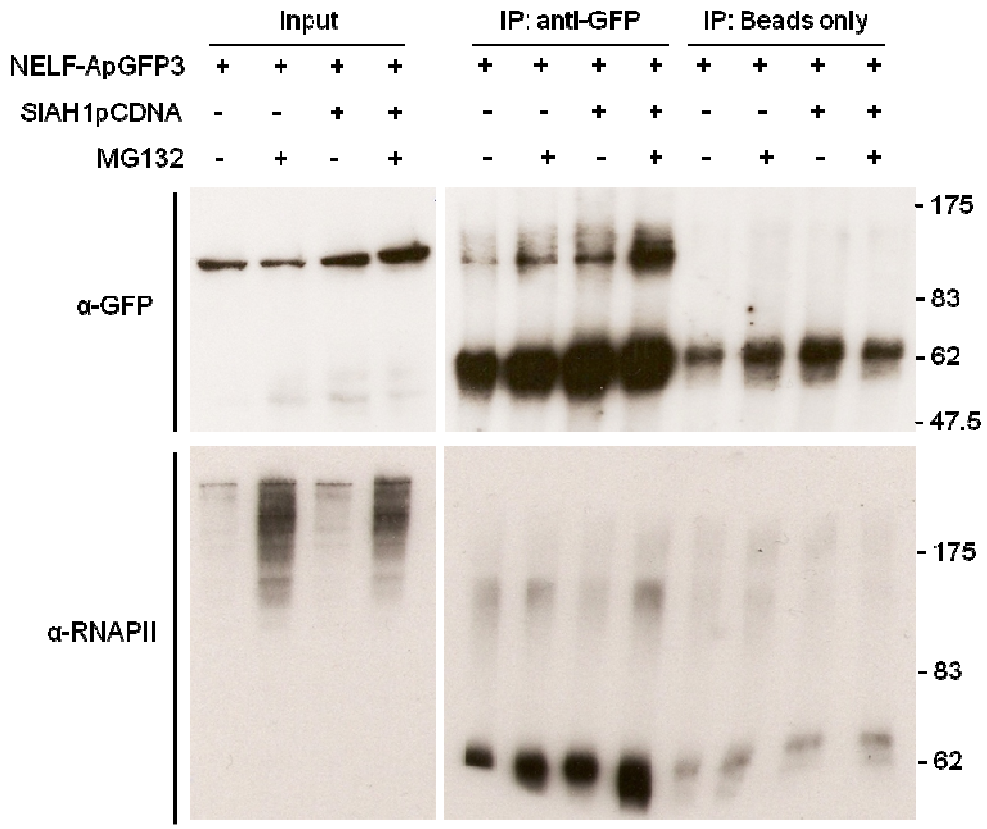

Figure 24. Testing co-immunoprecipitation of NELF-A-GFP and RNAPII in HEK293 cells. HEK293 cells were co-transfected with NELF-ApGFP3 and SIAH1pCDNA or empty pCDNA vector in the minus SIAH1 controls. 24 hours after transfection cells were incubated in the presence or absence of 50µM MG132 for 5 hours, then harvested and cell lysates prepared. Soluble HEK293 cell lysates were incubated either with or without α-GFP antibody and protein A Dynabeads. After washing, samples were eluted by boiling in sample loading buffer. Soluble cell lysates (input), and IP samples were separated on 7% SDS PAGE and probed with α-GFP and HRP-conjugated α-mouse secondary antibody (upper blots). Blots were then stripped and re-probed with α-RNAPIICTD and α-mouse HRP-conjugated secondary antibodies (lower blots). The migration of molecular weight markers is indicated on the right.

RNAPII, running above the 175kDa marker was detected in the soluble HEK293 cell lysates (input) and it was evident that treatment with the proteasome inhibitor MG132 resulted in RNAPII stabilisation. This was not unexpected as a number of studies have shown that stalled or arrested RNAPII is ubiquitinated and degraded (Somesh et al., 2005; Somesh et al., 2007). The smears observed are likely to represent breakdown products of RNAPII as they are more stable in the presence of MG132.

There was no RNAPII detected in the NELF-A-GFP IP lanes. Therefore, in this experiment, ectopically expressed NELF-A-GFP fusion protein did not co-immunoprecipitate with RNAPII, either when co-expressed with SIAH1 or in the presence of MG132. It remains possible that these proteins form a complex *in vivo*,

however, the amount of NELF-A-GFP immunoprecipitated may be insufficient to detect this interaction.

4.11 Analysing NELF-A stability and localisation in *Siah1a*$^{-/-}$*2*$^{-/-}$ cells

In experiments to date in this thesis, the effect of SIAH1 on target protein stability has been investigated through over-expression studies. To further characterise the physiological function of SIAH proteins and understand how they affect NELF-A protein stability *in vivo*, we utilised mouse embryonic fibroblasts (MEFs) which lack *Siah1a* and *Siah2* genes. Murine embryonic fibroblasts derived from wild-type embryos and *Siah1a*$^{-/-}$*Siah2*$^{-/-}$ embryos were kindly supplied by Professor David Bowtell (Peter MacCallum Cancer Centre, Australia). Generation of these MEFs is described in Frew et al., (2002).

4.11.1 Siah gene expression analysis in Siah1a$^{-/-}$*2*$^{-/-}$ *cells*

Before commencing with analysis of NELF-A protein abundance in wild-type and *Siah1a*$^{-/-}$*2*$^{-/-}$ cells we first wanted to ensure the cells were the correct genotype and confirm that the *Siah1a*$^{-/-}$*2*$^{-/-}$ cells lack *Siah2* and *Siah1a* mRNA transcripts. To do this reverse transcriptase PCR (RT-PCR) analysis was performed. Primers were designed to amplify the region between the targeting construct and the Siah1a and Siah2 coding sequence (Figure 25).

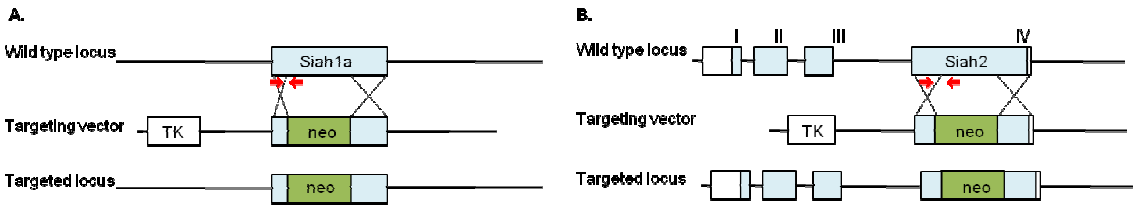

Figure 25. *Siah1a* and *Siah2* gene targeting strategy summarised from Dickins et al., (2002) and Frew et al., (2003). (A) The *Siah1a* coding region resides on a single exon. The targeting vector was designed to replace the coding region with a neomycin resistance gene, leaving only the first 22 codons intact. (B) The *Siah2* gene was inactivated by insertion of a neomycin resistance gene into exon IV. This insertion truncates the Siah2 protein reading frame at codon 180. The primers used for RT-PCR are shown as red arrows. For *Siah1a*, the forward primer (Siah1a-F) lies within the first 66 nucleotides (encoding the first 22 codons) of the coding region and the reverse primer (Siah1a-R) is within the coding sequence which was replaced by the neomycin resistance gene. The *Siah2* forward primer (Siah2-F) lies within the first 540 nucleotides (encoding the first 180 codons) of the coding region and again the reverse primer (Siah2-R) is within the coding sequence which is replaced by the neomycin resistance gene. The Siah1a and Siah2 RT-PCRs were expected to yield products of 153 and 214 nucleotides, respectively.

To establish whether or not *Siah1a* and *Siah2* were expressed in the MEFs, RNA was extracted from the wild-type and the *Siah1a*$^{-/-}$*2*$^{-/-}$ cells. For a positive control, RNA was extracted from mouse testes tissue as expression of both *Siah1a* and *Siah2* in murine testis has been reported (Della et al., 1995; Venables et al., 2004). Expression was measured by RT-PCR and results are presented in Figure 26A.

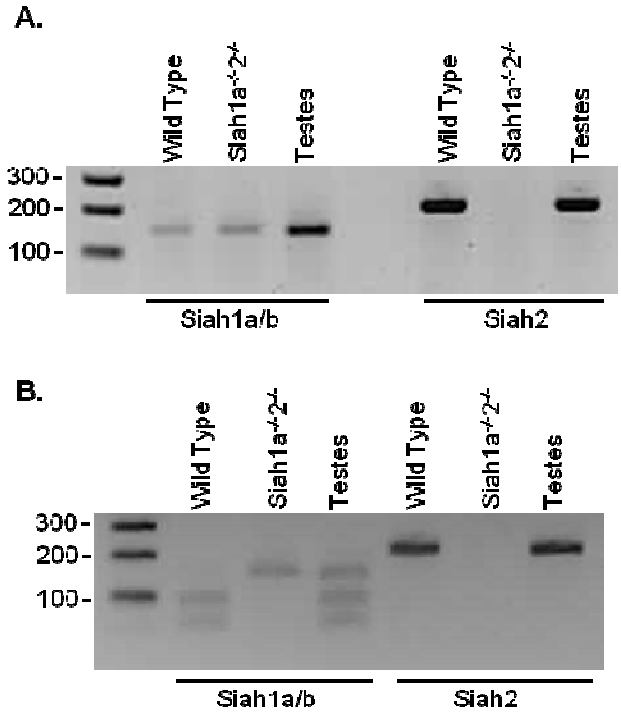

Figure 26. Analysis of *Siah1a* and *Siah2* expression in murine embryonic fibroblasts and murine testes. (A) RNAs were analysed by RT-PCR using Siah1a-F, Siah1a-R and Siah2-F, Siah2-R. (B) *Msp*I digest of RT-PCR products. *Msp*I cuts the *Siah1a* 153bp PCR product into 99bp and 54bp fragments. *Msp*I does not cut *Siah1b* or *Siah2*. All samples were analysed by electrophoresis on 2% agarose gels. The DNA markers are shown on the left.

RT-PCR analysis confirmed the absence of *Siah2* mRNA in *Siah1a*$^{-/-}$*2*$^{-/-}$ cells (Figure 26A). However the presence/absence of *Siah1a* required further investigation. Unlike humans, which have two *SIAH* genes (*SIAH1* and *SIAH2*), mice have three highly conserved *Siah* genes *Siah1a*, *Siah1b* and *Siah2* (see chapter 1, section 1.3). As you can see from the *Siah1a*/*1b* alignment presented in Figure 27, these genes encode very similar proteins. Due to the high degree of similarity of the *Siah1a* and *Siah1b* gene coding sequences, it is very likely that the Siah1a primers amplified the *Siah1b* coding sequence.

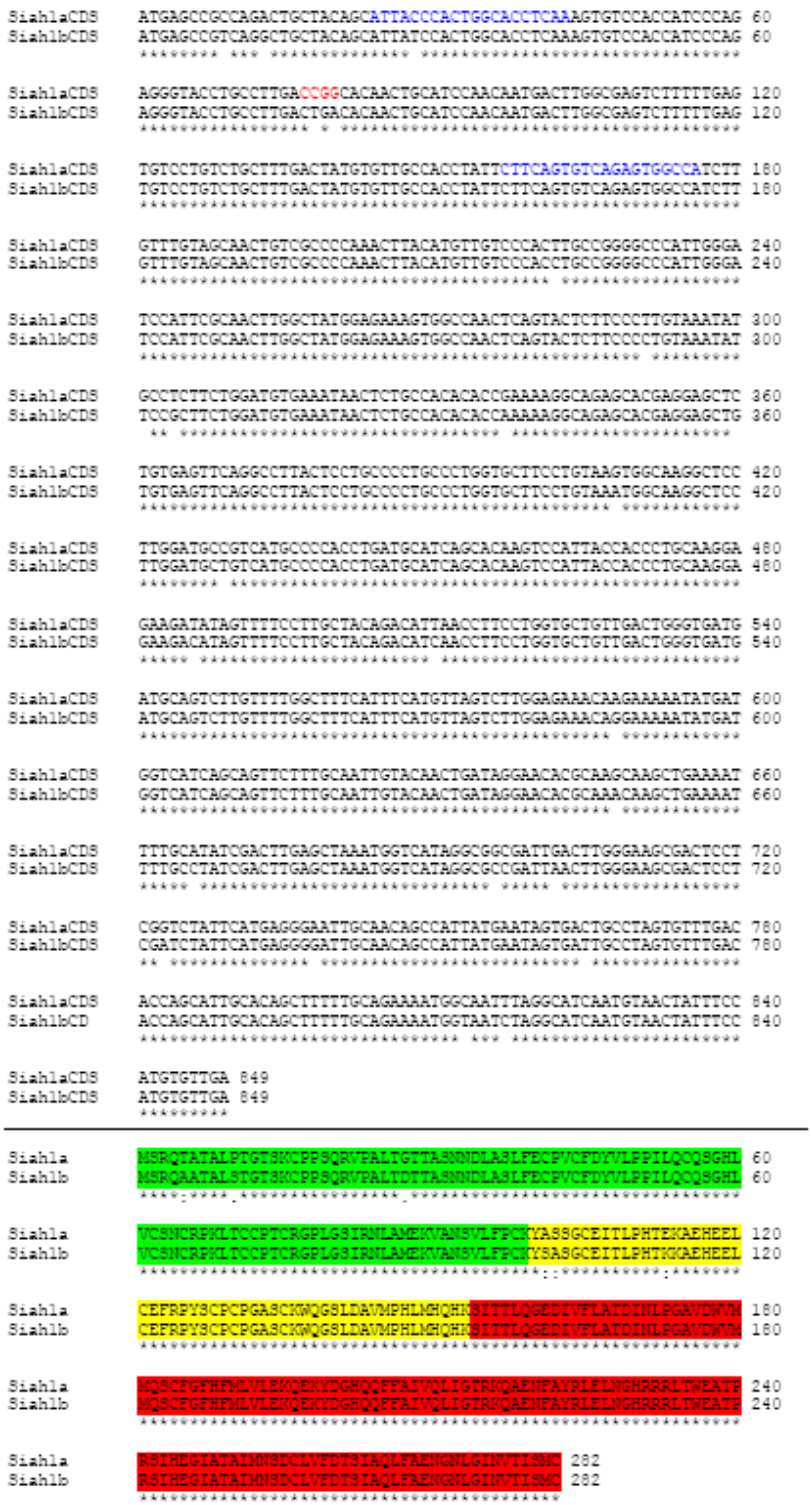

Figure 27. Sequence alignment between murine Siah1a and Siah1b. The nucleotide sequence alignments are presented in the upper panel and the protein sequence is shown below. The Siah1a-F and Siah1a-R primers used for RT-PCR and the *Msp*I site (CCGG) are highlighted. Both Siah1a and Siah1b are 282-amino-acid proteins with 97% homology. "*" residues are identical in both proteins. ":" represents a conserved substitution and "." represents a semi-conservative substitution. The RING finger domain (amino acids 1-99) is highlighted in green. The zinc-finger region (amino acids 99-153) is highlighted in yellow and the substrate binding domain (amino acids 153-282) is highlighted in red.

In order to distinguish between *Siah1a* and *Siah1b* PCR products, a varying restriction enzyme site in the *Siah1a* and *Siah1b* coding sequences was identified. There is an *Msp*I restriction enzyme site present within the *Siah1a* amplified coding region, which is absent in *Siah1b* (Figure 27). Therefore the RT-PCR products were digested with *Msp*I (Figure 26B). This *Msp*I digest (Figure 26B) showed that, as expected, the double knock out MEFs do not express *Siah1a* and the 153bp band observed represents *Siah1b*. It also confirms that all 3 murine *Siah* genes are expressed in the testes.

To further confirm the identity of the *Siah1a* RT-PCR product shown in Figure 26A, the PCR product was purified using the Qiagen PCR purification kit and sequenced. Approximately 100bp of sequence was obtained from the 5′ end using the Siah1a-F primer. A BLAST search revealed that this PCR product matched the *Siah1b* coding sequence.

Interestingly, the *Siah1b* RT-PCR product appeared to be stronger in the double knockout MEFs than in the wild-type cells and once the products were digested with *Msp*I the 153bp *Siah1b* band appeared to be absent in the wild-type cells (Figure 26B). This led us to speculate that in the absence of *Siah1a* and/or *Siah2*, *Siah1b* expression is up-regulated in order to compensate for the lack of Siah function. To further analyse *Siah1b* expression in the wild-type and *Siah1a*$^{-/-}$*2*$^{-/-}$ MEFs, *Siah1b* specific primers were designed for RT-PCR. The forward primer was designed from the *Siah1b* 5′UTR, which has no homology to *Siah1a* and the reverse primer from within the coding sequence. For a loading control, *HPRT* (*Hypoxanthine Phosphoribosyltransferase*) specific primers were also designed as the *HPRT* gene is reported as a constitutively expressed housekeeping gene (Pernas-Alonso et al., 1999). It was ensured that both sets of primers had the same annealing temperature and they were designed to span an intron allowing us to distinguish between gDNA and RNA.

RNA was extracted from four separate cell harvests of wild-type and the *Siah1a*$^{-/-}$*2*$^{-/-}$ cells and *Siah1b* expression was measured by RT-PCR using the *Siah1b* and *HPRT* specific primers. Results are presented in Figure 28.

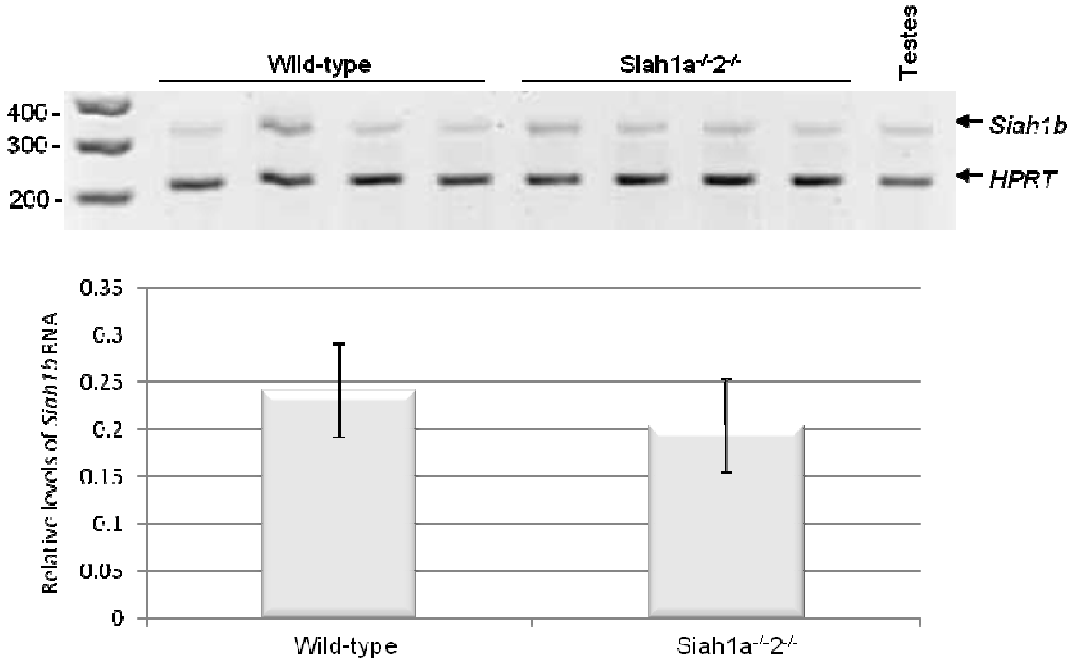

Figure 28. Analysis of *Siah1b* expression in murine embryonic fibroblasts and murine testes. (A) RNA from four separate cell harvests were analysed by RT-PCR using Siah1b-F, Siah1b-R and HPRT-F, HPRT-R primers. Samples were separated on a 2% agarose gel. The DNA markers are shown on the left. The graph shows the relative amount of Siah1b mRNA in wild-type and the *Siah1a*$^{-/-}$*2*$^{-/-}$ MEFs. Data is presented as the mean ± SD and is representative of the four cell harvests shown.

The *Siah1b* specific RT-PCR analysis revealed that there was no significant difference in *Siah1b* expression in wild-type and *Siah1a*$^{-/-}$*2*$^{-/-}$ cells.

4.11.2 NELF-A stability in Siah1a$^{-/-}$*2*$^{-/-}$ *cells*

If SIAH1 and potentially SIAH2 were primarily responsible for controlling levels of NELF-A in the cell, then we would expect to find elevated levels of NELF-A protein in cells which lack *Siah1a* and *Siah2*.

In order to determine whether or not this was the case, and to establish whether or not the stability of NELF-A protein in the MEFs was dependent on the proteasome, confluent T25 flasks of wild-type and *Siah1a*$^{-/-}$*2*$^{-/-}$ MEFs were incubated with the proteasome inhibitor MG132 for 5 hours. Control samples (minus MG132) were also harvested and lysed in 2x sample loading buffer. Total cell lysates were separated by SDS-PAGE and analysed by Western blot (Figure 29) probing with the antibody specific to NELF-A and α-tubulin for a loading control.

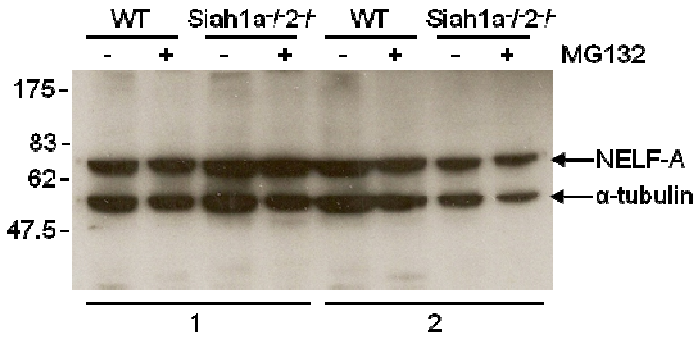

Figure 29. NELF-A protein levels in Siah deficient MEFs. Exponentially growing wild-type and *Siah1a*$^{-/-}$*2*$^{-/-}$ mutant MEFs were incubated with or without 60μM MG132 for 5 hours. Cell lysates were prepared, and the level of NELF-A was measured by immunoblotting with α-NELF-A antibody, and an anti-α-tubulin antibody for a loading control. Antibody binding was detected using HRP-conjugated α-rabbit and α-mouse secondary antibodies, respectively. Two separate cell harvests (1-2) are presented. The migration of molecular weight markers is indicated on the left.

Germani et al., (2000) report that α-tubulin is a SIAH1 interacting protein, however they found no evidence of variation in α-tubulin levels in cells over-expressing SIAH1 and no difference in the presence of proteasome inhibitors. This was consistent with our results and so α-tubulin was considered to be a suitable loading control. When comparing NELF-A protein abundance in wild-type and *Siah1a*$^{-/-}$*2*$^{-/-}$ MEFs, steady state levels appear similar (Figure 29). Clearly there was little difference in NELF-A protein in wild-type cells compared to *Siah1a*$^{-/-}$*2*$^{-/-}$ null cells and NELF-A protein stability was not affected by incubation with the proteasome inhibitor, MG132.

4.11.3 Comparison of NELF-A distribution in wild-type and Siah1a$^{-/-}$*2*$^{-/-}$ *MEFs*

In order to gain some insight as to whether or not NELF-A was in some way differentially regulated in the presence and absence of Siah proteins, precise localisation of endogenous NELF-A protein was visualised by immunofluorescence. Wild-type and *Siah1a*$^{-/-}$*2*$^{-/-}$ null MEFs were fixed in methanol and stained with the α-NELF-A antibody (Figure 30).

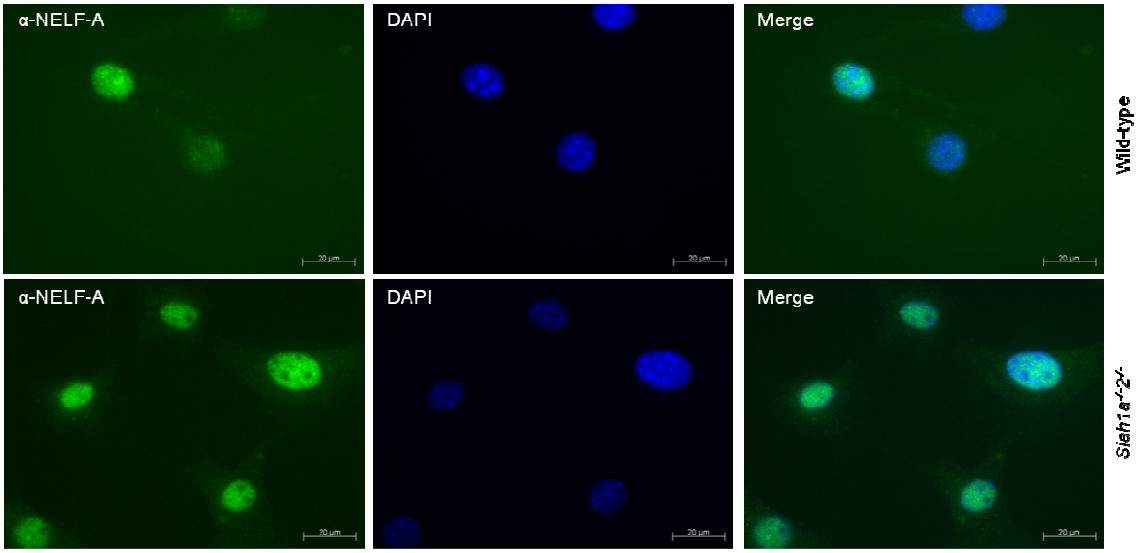

Figure 30. Localisation of NELF-A in wild-type and *Siah1a*$^{-/-}$*2*$^{-/-}$ MEFs. Cells were fixed, permeabilised and stained with α-NELF-A. NELF-A was visualised with an Alexa Flour-488 (green) conjugated α-rabbit secondary antibody. DNA was visualised with DAPI (blue). Images were generated by fluorescence microscopy. Scale bars represent 20μM.

Consistent with previous studies on NELF-localisation, NELF-A protein localised to the nucleus, although a small amount of cytoplasmic staining was observed. There did not appear to be any difference in NELF-A localisation in wild-type or *Siah1a*$^{-/-}$*2*$^{-/-}$ null cells.

4.12 *Siah1b* expression in mouse tissues

As mentioned in the introduction to this thesis (section 1.3) three highly conserved murine *Siah* genes have been identified (*Siah1a*, *Siah1b* and *Siah2*), whereas only two human homologs, *SIAH1* and *SIAH2*, have been identified (Della et al., 1993). So far, investigations have focused primarily on the human SIAH1:NELF-A protein interaction. Analysis of *Siah* gene expression in the *Siah1a*$^{-/-}$*2*$^{-/-}$ double knockout MEFs showed that these cells express *Siah1b* (section 4.11.1). *Siah1b* knockout mice have been reported to have an embryonic lethal phenotype suggesting, although this gene is murine-specific, it plays an essential role in development (Frew et al., 2002). Given that the Siah1a and Siah1b proteins are very similar (see alignment Figure 27), we speculated that they are likely to have overlapping functions and Siah1b could provide sufficient Siah activity in the *Siah1a*$^{-/-}$*2*$^{-/-}$ cells to allow normal stability of NELF-A.

Aside from the phenotype of the *Siah1b* knockout which was briefly noted in the study by Frew et al., (2002), Siah1b is rarely mentioned in the literature and no Siah1b

substrates have been reported. This is possibly because this is a murine specific gene and its high sequence homology to *Siah1a* makes it difficult to distinguish between the two. As we were confident that the primers used for RT-PCR in section 4.11.1 were specifically amplifying *Siah1b*, we used these to analyse *Siah1b* expression in various mouse tissues.

RNA was extracted from various murine tissues by Miss Emily Jones (MSc Medical Genetics student, IHG, Newcastle University) and *Siah1b* expression was analysed by RT-PCR using the Siah1b and HPRT specific primers. Results are presented in Figure 31.

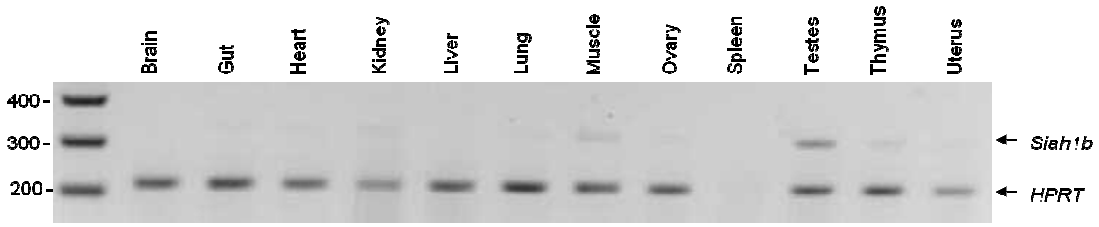

Figure 31. Analysis of *Siah1b* expression in multiple mouse tissues. RNA from the tissues shown was analysed by RT-PCR using Siah1b-F, Siah1b-R and HPRT-F, HPRT-R primers. Samples were analysed by electrophoresis on a 2% agarose gel. The DNA markers are shown on the left.

RT-PCR results revealed that *Siah1b* was predominantly expressed in the murine testes. Weak expression was also detected in muscle, thymus and kidney. Thus, unlike the other Siah proteins which are reportedly ubiquitously expressed, *Siah1b* expression appears to be restricted to particular tissues. Its elevated expression in the testes suggested that Siah1b, like Siah1a, may play an important role in the testes. This result however was quite surprising as the *Siah1b* gene resides on the X chromosome and most of the gene activity on the X chromosome is shut down in male meiotic cells. Thus, either the *Siah1b* gene remains active during meiosis or the expression detected is from the non-meiotic cells in the testes.

4.13 Assaying murine Siah mediated degradation of NELF-A in cultured cells

To determine whether or not NELF-A stability is controlled by Siah1b we performed an experiment analogous to the SIAH1 degradation assay described in chapter 3 (section 3.5.3). In this case, the NELF-A-GFP fusion construct was co-transfected into HEK293 cells with empty GFP-expression vector and either a *Siah1a*, *Siah1b* or *Siah2* eukaryotic

expression construct. The levels of NELF-A-GFP fusion protein could then be assayed in the presence/absence of the murine Siah homologs (1a, 1b and 2). *Siah1a* and *Siah2* eukaryotic expression constructs (in the pKH3 vector) were previously provided by Professor David Bowtell (Peter MacCallum Cancer Centre, Australia). These constructs encode the full length *Siah1a*/*Siah2* coding sequence, downstream of a human cytomegalovirus (CMV) promoter. A *Siah1b* expression construct, however, was not available, which we therefore created.

4.13.1 Generation of Siah1b mammalian expression construct

Siah1b was PCR amplified from a full length clone purchased from the mammalian genome collection (*Siah1b* image ID; 30053109) using primers Siah1b(F) and Siah1b(R). PCR products were digested with *Eco*RI/*Xho*I and ligated into complementary sites in pCDNA3.1, a mammalian expression plasmid which also contains a CMV promoter. The ligation was re-cleaved with *Eco*RV, followed by dialysis, transformation and selection on ampicillin-LB plates. Colonies were screened by PCR using Siah1b(F) and pCDNArev. Insert positive colonies were further grown overnight before plasmid purification. To confirm that the pCDNA clone contained the correct *Siah1b* sequence it was sequenced from the 5′ end using the T7-F primer.

4.13.2 In vivo murine Siah degradation assay using HEK293 cells

In order to determine which of the murine Siah proteins affect NELF-A stability, NELF-ApGFP3 and the murine *Siah* expression plasmids (*Siah1a*-pKH3, *Siah1b*-pCDNA, *Siah2*-pKH3) were co-transfected into HEK293 cells with the GFP expression vector to show the relative amount of the NELF-A-GFP fusion protein. *SIAH1*-pCDNA was also tested as a positive control. Cell extracts were analysed by Western blot and probed with GFP antibody. To ensure the murine Siah proteins and the human SIAH1 protein were being expressed and were functional, the same experiment was carried out using a known SIAH1 substrate, T-STAR (Venables et al., 2004). Results are presented in Figure 32.

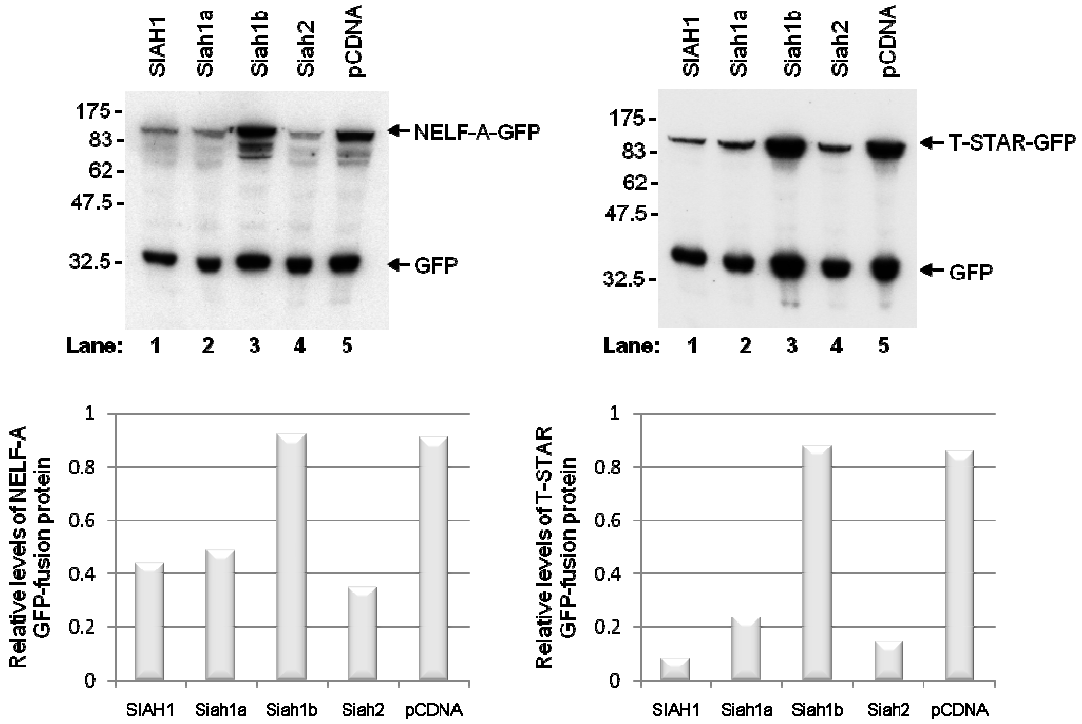

Figure 32. Western blot analysis of co-transfection assays to monitor the stability of NELF-A and T-STAR GFP-fusion proteins in the presence of murine Siah proteins in HEK293 cells. NELF-ApGFP3 and the murine *Siah* expression plasmids (*Siah1a*-pKH3, *Siah1b*-pCDNA, *Siah2*-pKH3) were co-transfected into HEK293 cells along with empty GFP expression vector. Cells were harvested 24 hours after transfection. Cell lysates were separated on 7% SDS PAGE and analysed by Western blot. Blots were probed with α-GFP antibody and HRP-conjugated anti-mouse secondary antibody. The migration of molecular weight markers is indicated on the left. The graphs show the relative amount of the GFP-fusion proteins in each of the co-transfections.

As expected, levels of NELF-A and T-STAR GFP-fusion proteins were reduced in the presence of human SIAH1 (compare lanes 1 and 5). A similar affect was observed in the presence of the murine Siah1a and Siah2 proteins. However, co-expression of Siah1b did not appear to have any effect on NELF-A or T-STAR protein stability. This suggested that either Siah1b was not functional as an E3 ubiquitin ligase, or that it was not efficiently expressed. Since the expression vectors used encoded non-tagged Siah1a, Siah1b and Siah2 proteins it was not possible to confirm that they were expressed.

4.13.3 In vivo murine Siah degradation assay using 3T3 cells

Considering Siah1a and Siah1b proteins are highly homologous, we were surprised to find that these proteins did not have a similar affect on NELF-A and T-STAR GFP-fusion stability. Given that Siah1b is a murine specific protein, and no equivalent *Siah1b* gene

has been identified in humans, we speculated that this protein may require a murine specific partner protein to target substrates for degradation which is not present in HEK293 cells. Alternatively, because Siah1b is not normally expressed in HEK293 cells, it may mis-localise. In order to determine whether or not this was the case, the *in vivo* murine Siah degradation assay described above (section 4.13.2) was repeated in a mouse cell line. As we had previously shown that Siah1b is expressed in murine embryonic fibroblasts (section 4.11.1) we chose to use mouse embryonic fibroblast 3T3 cells for this experiment. Results are presented in Figure 33.

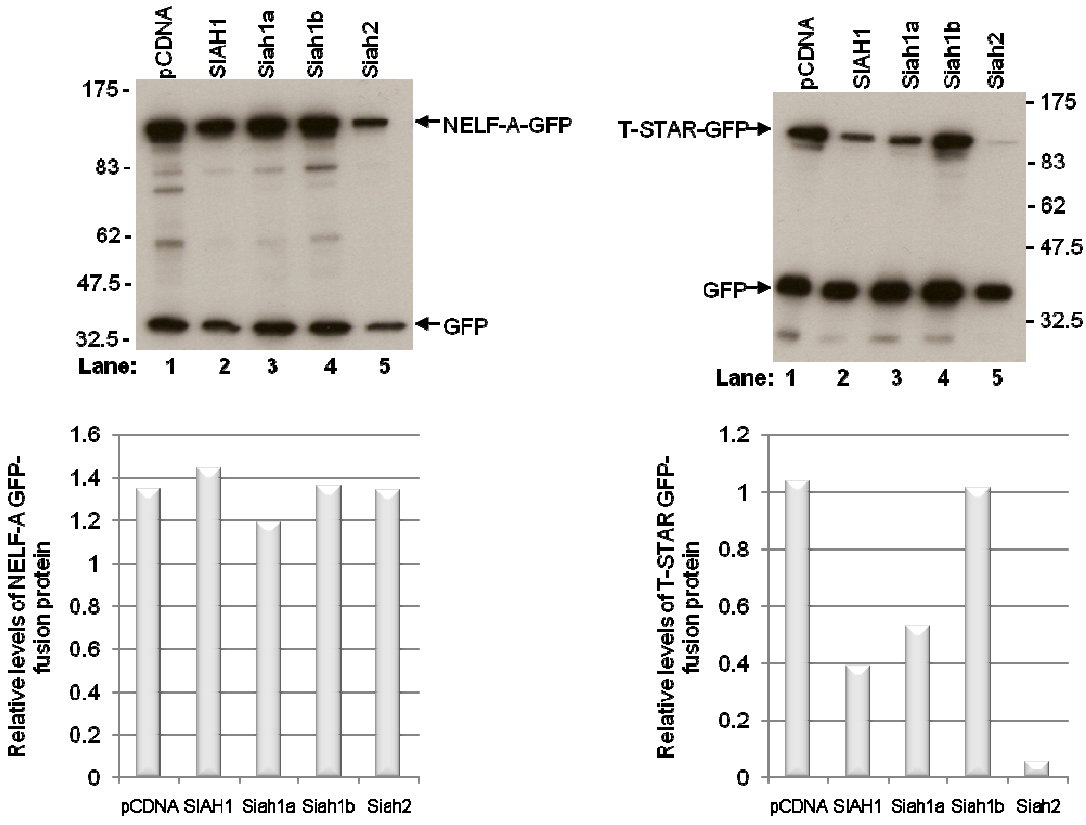

Figure 33. Westerns of co-transfection assays to monitor the stability of NELF-A and T-STAR GFP fusion proteins in the presence of murine Siah proteins in 3T3 cells. Cells were harvested 24 hours after transfection. Cell lysates were separated on 7% SDS PAGE and analysed by Western blot. Blots were probed with α-GFP antibody and HRP-conjugated anti-mouse secondary antibody. The migrations of molecular weight markers are shown and the graphs show the relative amount of the GFP-fusion proteins in each of the co-transfections.

Again, as in HEK293 cells, Siah1b did not appear to have any effect on the stability of NELF-A or T-STAR GFP-fusion proteins in the murine 3T3 cell line (compare lanes 1 and 4). In this experiment, neither SIAH1, Siah1a or Siah2 appeared to affect NELF-A-GFP stability, however they efficiently de-stabilised the T-STAR GFP-fusion protein. It

is possible that SIAH1, Siah1a and Siah2 require a co-factor protein to target NELF-A for degradation which is not expressed in 3T3 cells. However this experiment was only performed once therefore repeats of this experiment are required to confirm this observation.

4.13.4 Generation of FLAG-tagged murine Siah proteins

Results to date from our transient expression experiments revealed that Siah1a and Siah2 proteins efficiently destabilised the ectopically expressed NELF-A and T-STAR GFP-fusion proteins but no effect on protein stability was observed for Siah1b. This could be for several reasons, for example, Siah1b may not function as an E3 ubiquitin ligase, or alternatively, it may not being efficiently expressed in cells. Due to the lack of Siah specific antibodies, we were unable to determine whether or not the Siah proteins were being efficiently expressed. To remedy this we chose to tag Siah1a, Siah1b and Siah2 with the FLAG epitope. The three murine *Siah* genes were cloned into both the N-terminal and C-terminal p3XFLAG-CMV expression vectors as we were concerned that adding the FLAG epitope to either the C-terminal substrate binding domain or the N-terminal RING finger domain may affect Siah function.

Murine Siah primers were designed to ensure the FLAG peptide sequence would be in frame with the *Siah* coding sequences. For cloning into the N-terminal FLAG vector, reverse primers included the Siah STOP codon and for cloning in the C-terminal FLAG vector, the STOP codon was omitted. Due to the very high sequence homology/similarity between the *Siah1a* and *Siah1b* coding sequences, the same reverse primers were used for cloning (see appendix for further primer and cloning information).

Siah1b was amplified from the full length Siah1b image clone (ID; 30053109) and *Siah1a* and *Siah2* were amplified from the Siah1a-pKH3 and Siah2-pKH3 vectors, respectively. PCR products were digested with *Eco*RI/*Xba*I and ligated into complementary sites in the N-terminal and C-terminal vectors p3XFLAG-CMV. The ligations were re-cleaved with *Bgl*II, followed by dialysis, transformation into *E. coli* DH5α cells and selection on ampicillin-LB plates. Colonies were screened by PCR using CMV-F and the Siah specific reverse primers. Plasmids were purified from insert positive colonies and then sequenced to ensure they contained the correct sequence.

4.13.5 In vivo degradation assay using murine Siah-FLAG tagged clones.

In order to determine whether or not the murine Siah-FLAG tagged clones were functional the experiment described in section 4.13.2 was repeated. This time however, the cells were co-transfected with NELF-ApGFP3 and the FLAG-tagged Siah clones and in the minus Siah controls (-) empty FLAG vector was co-transfected. Also, because SIAH1 protein is known to regulate its own stability (Hu et al., 1999; Lorick et al., 1999), we also assayed Siah-FLAG protein and NELF-A-GFP protein stability in the presence and absence of the proteasome inhibitor MG132. 24 hours after transfection HEK293 cells expressing the FLAG-tagged Siah proteins and NELF-A-GFP were treated with or without MG132 for 6 hours before they were harvested. Again, cell extracts were analysed by Western blot and probed with the α-GFP antibody. To ensure that the Siah-FLAG fusion proteins were being expressed the blot was re-probed with α-FLAG antibody. Results are presented in Figure 34.

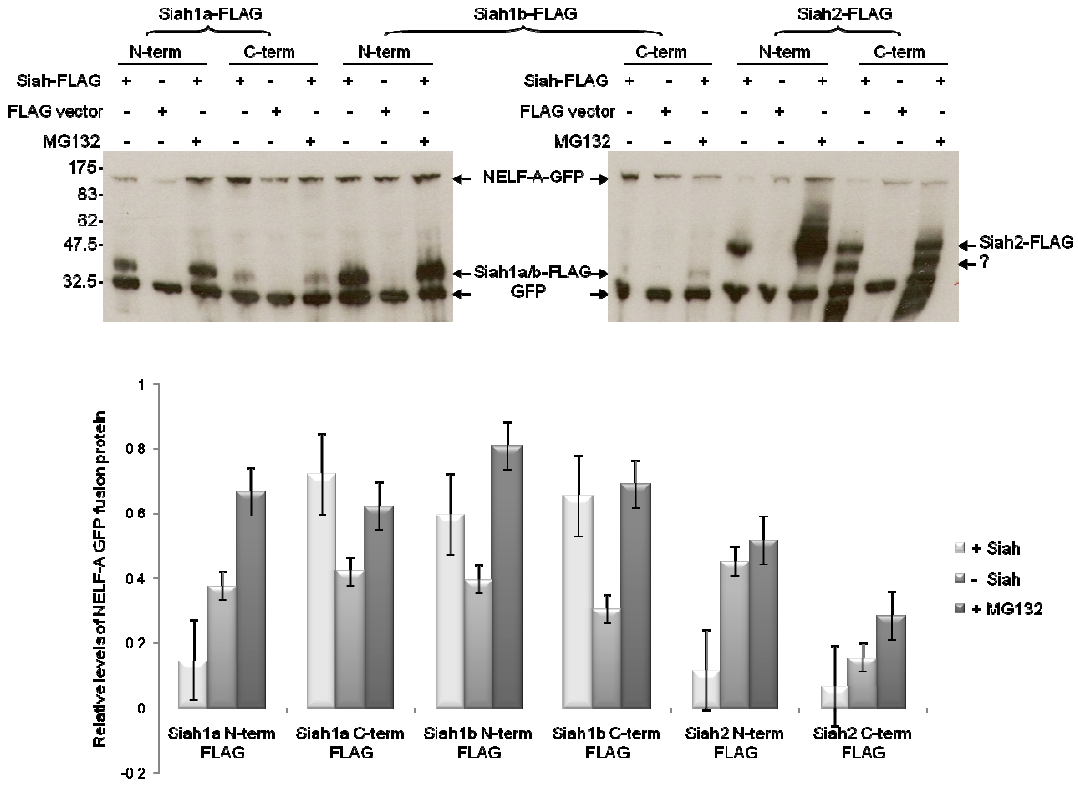

Figure 34. Westerns of co-transfection assays to monitor the stability of NELF-A-GFP fusion proteins in the presence of murine Siah FLAG-tagged proteins in HEK293 cells. 24 hours after transfection, cells were incubated with or without 60μM MG132 for 6 hours. Cell lysates were prepared and samples were separated on 12% SDS PAGE. Levels of GFP-tagged NELF-A and FLAG-tagged Siah proteins were measured by immunoblotting with α-GFP and α-FLAG primary antibodies and HRP-conjugated anti-mouse secondary antibody. The migration of molecular weight markers is indicated on the

left of the Westerns. The graph shows the relative amount of the GFP-fusion proteins in each of the co-transfections. The data in the graphs is presented as the mean ± SE and is representative of two experiments.

Both Siah1a and Siah1b are 282-amino-acid proteins and have a molecular weight of 31kDa. Siah2 is a slightly larger 325-amino acid protein with a molecular weight of 34kDa. We can see from Figure 34 that addition of the 3xFLAG epitopes (which consists of 22 amino acids, DYKDHDGDYKDHDIDYKDDDDK) shifts protein migration by ~10kDa as expected and the Siah FLAG-tagged proteins migrate just above the GFP loading control band.

From the graph (Figure 34) we can see that in the presence of N-terminal-FLAG tagged Siah1a and Siah2, NELF-A-GFP stability is reduced. However, when co-expressed with C-terminal FLAG-tagged Siah1a, and both N- and C-terminal-FLAG tagged Siah1b, levels of NELF-A-GFP are elevated compared to minus Siah controls. Co-expression with the C-terminal Siah2 had no effect on NELF-A-GFP stability. As expected, NELF-A-GFP protein was stabilised by MG132 consistent with it being regulated by a proteasome dependent mechanism.

Aside from NELF-A-GFP protein stability, it was clear from the Western that the Siah1a and Siah2 N-terminal-FLAG tagged proteins were stabilised by MG132, whereas the C-terminal clones and both the Siah1b clones were not. Therefore addition of the FLAG-tag to the C-terminal SBD domain prevents Siah1a and Siah2 from auto-regulating themselves and NELF-A-GFP. It perhaps not surprising that the C-terminal FLAG-tagged clones do not affect NELF-A-GFP stability as addition of the FLAG-tag to the substrate binding domain of the protein is likely to interfere with ligase-substrate interaction. The N-terminal FLAG-tagged proteins however are functional in de-stabilising NELF-A-GFP and in regulating their own stability.

Again, these experiments support our previous data showing that Siah1b does not regulate the stability of NELF-A-GFP fusion protein. As a result of using the FLAG epitope to detect expression levels of transfected Siah proteins we were certain that they were being efficiently expressed. We also found that unlike Siah1a and Siah2, Siah1b does not auto-regulate its own stability suggesting that Siah1b is not functioning as an E3 ligase.

4.14 Assay for Siah1b:NELF-A interaction

Our *in vivo* degradation assays show that Siah1b, unlike Siah1a, does not affect the stability of T-STAR- or NELF-A-GFP fusion proteins. Given that Siah1a and Siah1b contain the exact same substrate binding domain, it seemed surprising that they do not have similar targets or function. We therefore wanted to determine whether or not Siah1b could actually interact with NELF-A and T-STAR. In order to do this, a Siah1b yeast 2-hybrid construct containing the full length Siah1b sequence was generated and tested via a directed yeast 2-hybrid assay for its ability to bind to the SIAH1 interacting proteins NELF-A and T-STAR.

4.14.1 Generation of Siah1b yeast 2-hybrid construct

Siah1b was amplified by PCR and digested as described previously (section 4.13.1). The digested PCR product was ligated into complementary *Eco*RI/*Sal*I sites in the pGBKT7 Y2H vector. The ligation was re-cleaved with *Sal*I, followed by dialysis, transformation and selection on Kanamycin-LB plates. Colonies were screened by PCR using the T7-F primer and Siah1b(R). Insert positive colonies were further grown overnight before plasmid purification.

4.14.2 Testing for Siah1b:NELF-A interaction via yeast 2-hybrid

The Siah1b pGBKT7 clone expresses full length Siah1b as a fusion protein with the DNA binding domain of Gal4. This protein was tested for its ability to interact with full length NELF-A and T-STAR via a yeast 2-hybrid assay (NELF-A and T-STAR clones in the pACTII Y2H vector were previously isolated by Dr Julian Venables). The full length SIAH1 protein was also tested to act as a positive control. Results are presented in Figure 35.

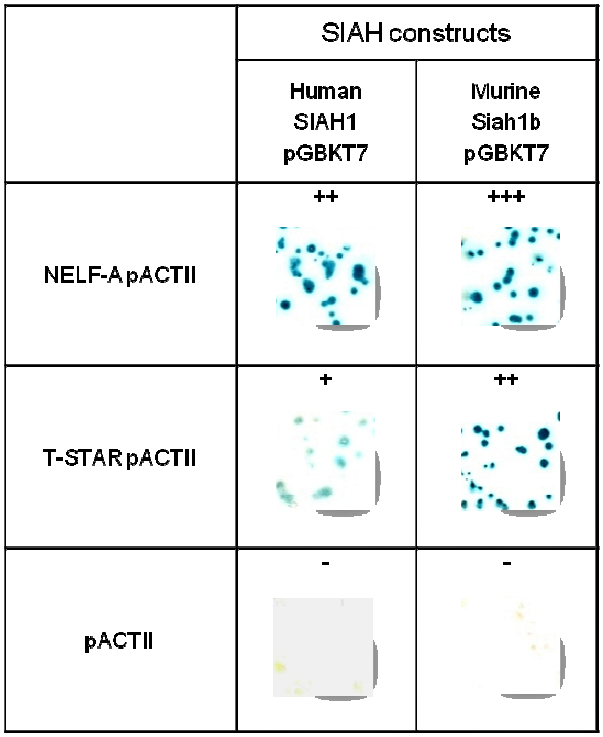

Figure 35. Testing for interaction with Siah1b. Siah1b-pGBKT7 was assayed for its ability to interact with NELF-A and T-STAR. SIAH1-pGBKT7 was tested as a positive control. Empty bait plasmid, pACTII, was used to test for auto-activation of Siah1b-pGBKT7. Filters stained with X-Gal are shown. Key, +++ strong interaction, positive blue colour within 30 minutes, ++ positive blue colour observable within 1 hour, + positive blue colour within 24 hours, - no noticeable interaction after 24 hours of exposure.

As expected, an interaction between the human SIAH1 protein and NELF-A and T-STAR was detected. The SIAH1pGBKT7, NELF-A and T-STAR-pACTII constructs were previously tested for auto-activation and proven not to auto-activate (see chapter 3, section 3.2). A strong interaction between Siah1b, NELF-A and T-STAR was also observed and a negative result for interaction between the empty pACTII vector and the Siah1b-pGBKT7 construct shows that this construct does not auto-activate.

4.15 Testing Siah1b mediated-inhibition of NELF-A degradation

The Siah1b yeast 2-hybrid result shows that Siah1b can bind to NELF-A and T-STAR, however unlike the other Siah proteins it does not target these proteins for degradation. In the *in vivo* degradation assay using the FLAG-tagged Siah constructs (section 4.13.5) we also observed that levels of NELF-A-GFP fusion protein were in fact elevated when co-expressed with Siah1b compared to the minus Siah controls (whereby empty FLAG-vector was co-transfected). These results prompted us to hypothesise that by binding to

NELF-A, Siah1b may inhibit the binding of other Siah proteins and hence prevent its degradation.

It is also possible that Siah1b inhibits Siah1a and Siah2 activity by forming a heterodimer. Siah proteins have been shown to form homo- or heterodimers with other Siah proteins through their C-terminal domain (Hu et al., 1999). Recently, a novel splice variant of human SIAH1, designated as SIAH-1S (Mei et al., 2007), was identified and it was found that SIAH-1S was able to interact with SIAH1 to form a heterodimer or with itself to form a homodimer. However, unlike SIAH1:SIAH1, neither SIAH1:SIAH1-1S nor SIAH-1S:SIAH-1S could degrade the previously identified SIAH substrate, β-catenin. Thus, SIAH-1S acts as a dominant-negative inhibitor of SIAH1.

To determine whether or not Siah1b was inhibiting Siah-mediated degradation, expression plasmids encoding murine Siah genes were co-transfected in pair-wise combinations along with NELF-ApGFP3, and the levels of NELF-A-GFP fusion protein were analysed.

In this experiment, NELF-ApGFP3 and equal amounts of either SIAH1pCDNA3, Siah1a-pKH3, Siah1b-pCDNA, or Siah2-pKH3 were co-transfected in varying combinations into HEK293 cells. The GFP expression vector was also transfected to act as an internal standard and show the relative amount of the NELF-A-GFP fusion protein. 24 hours after transfection, and upon confirmation of GFP fluorescence, cells were harvested and cell extracts were analysed by Western blot and probed with GFP antisera (Figure 36).

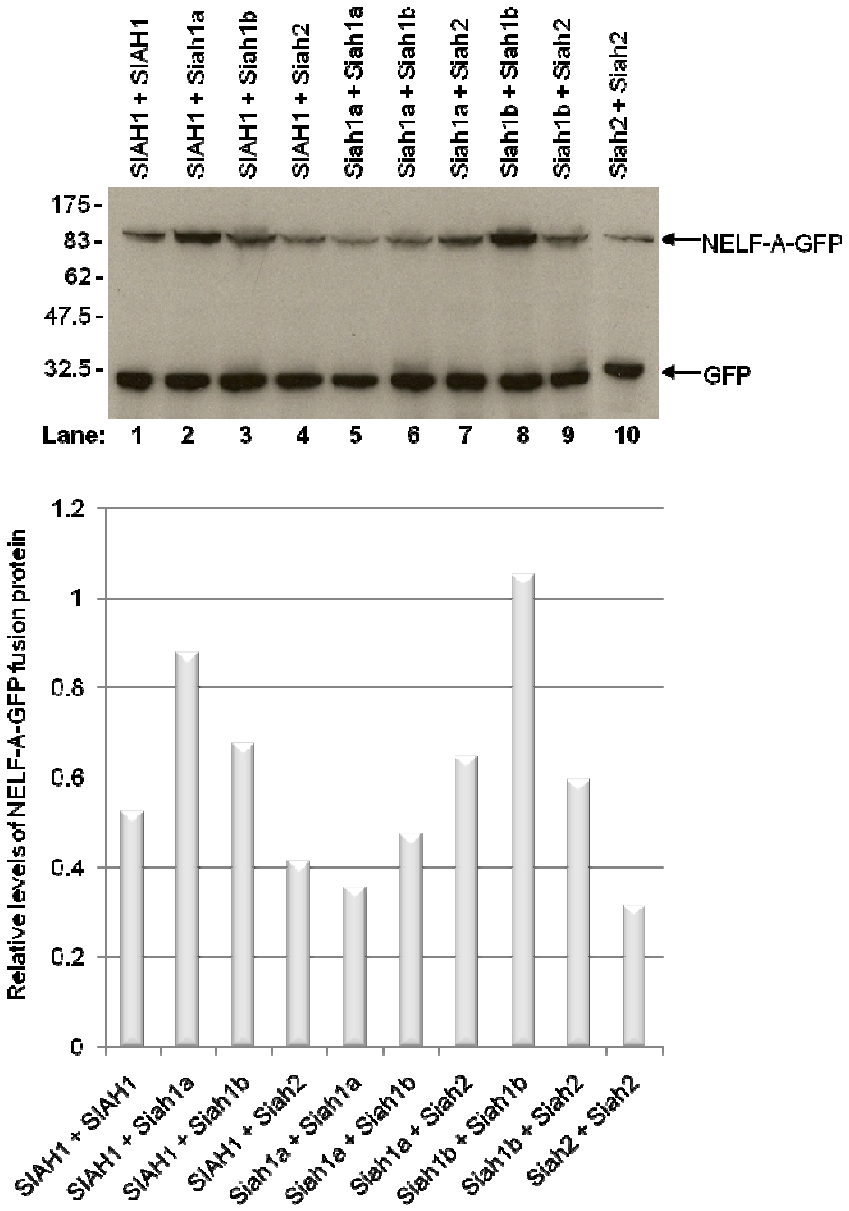

Figure 36. Examining the stability of NELF-A-GFP fusion protein in the presence of pair wise combinations of ectopically expressed Siah proteins. 24 hours after transfection, cell lysates were prepared and samples were separated by 10% SDS PAGE and analysed by Western blot. Levels of GFP-tagged NELF-A were assayed by probing with α-GFP and HRP-conjugated anti-mouse secondary antibodies. On the left of the Western the migrations of molecular weight markers are shown. The graph shows the relative amount of NELF-A-GFP fusion protein in each of the co-transfections in the Western presented.

It was clear from this assay that NELF-A-GFP fusion protein was most abundant in cells co-transfected with a double dose of the Siah1b expression vector (lane 8) and was least abundant in cells co-transfected with either a double dose of Siah1a or Siah2 expression vectors (lanes 5 and 10). Although there is no negative control in this experiment (e.g. cells transfected with empty expression vector), results are consistent with previous

experiments whereby Siah1a and Siah2 efficiently degrade NELF-A-GFP and Siah1b does not. When Siah1b is co-expressed with SIAH1, Siah1a or Siah2, levels of NELF-A-GFP are approximately equal to or more than that observed with the SIAH1/SIAH1, Siah1a/Siah1a and Siah2/Siah2 pairs. Therefore, the data suggests that Siah1b may have inhibitory effect on SIAH1, Siah1a or Siah2 mediated degradation of NELF-A-GFP, however the basis of this requires further investigation.

4.16 Immunoprecipitation of murine Siah-FLAG tagged proteins

Results to date implied that N-terminal FLAG-tagged Siah1a and Siah2 target NELF-A-GFP fusion protein for proteasome-mediated destruction. In an attempt to determine whether or not the ectopically expressed Siah proteins functionally interact with endogenous NELF-A protein, we utilised the Siah FLAG-epitope in order to carry out an immunoprecipitation experiment.

To assay for an *in vivo* interaction with NELF-A, each of the N-terminal FLAG-tagged Siah clones were transfected into HEK293 cells. Because ligase-substrate interactions *in vivo* are likely to be transient, immunoprecipitations were carried out in the presence and absence of the proteasome inhibitor, MG132. In previous experiments we had shown that N-terminal FLAG-tagged Siah1a and Siah2 were stabilised by MG132 which then strengthens the likelihood of detecting an interaction (section 4.13.5). 24 hours after transfection HEK293 cells expressing the N-terminal FLAG-tagged Siah proteins were treated with or without MG132 for 6 hours. Cells were harvested and FLAG-tagged proteins were immunoprecipitated using α-FLAG affinity resin (see methods, section 2.3.11). Immunoprecipitated samples were washed, electrophoresed on 10% SDS-PAGE, and analysed by Western blot, firstly probing with a monoclonal antibody against the FLAG epitope to determine whether or not the IP was successful (Figure 37).

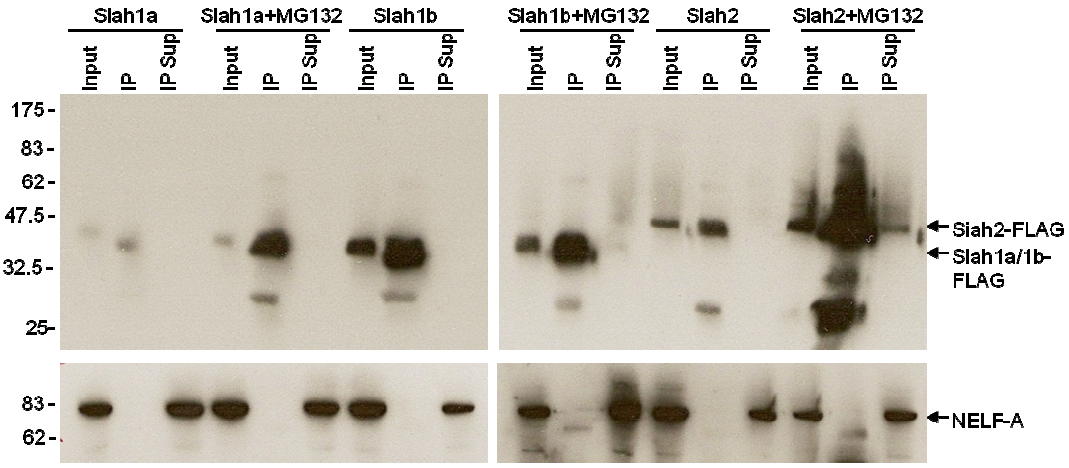

Figure 37. Immunoprecipitation of N-terminal FLAG-tagged murine Siah proteins and testing for co-immunoprecipitation with endogenous NELF-A. 24 hours after transfection, cells were incubated with or without 60µM MG132 for 6 hours. Cell lysates were then prepared and incubated with α-FLAG affinity resin. After washing, samples were boiled, electrophoresed on a 10% SDS-polyacrylamide gel and analysed by immunoblotting with α-FLAG antibody and HRP-conjugated anti-mouse secondary antibody (upper blot). The blots were then re-probed with α-NELF-A antibody and HRP-conjugated anti-rabbit secondary antibody (lower blot). The migration of molecular weight markers is shown on the left.

It was clear from the Western probed with α-FLAG antibody (Figure 37, upper blot) that Siah1a, Siah1b and Siah2 immunoprecipitated successfully. Consistent with previous experimental results, the Siah1a and Siah2 immunoprecipitations were more efficient in the presence of MG132 showing that these proteins auto-regulate their own stability, whereas Siah1b did not.

The Siah1a protein band differs slightly in size when comparing the input and IP lanes in both the presence and absence of MG132. This was often observed in IP experiments and suggests that the protein has been modified in some way (e.g. de-phosphorylation, de-ubiquitination etc) as a result of immunoprecipitation. Alternatively, the migration of bands may be affected by the varying buffers/salt concentrations in the input and immunoprecipitation samples. Also, a lower molecular weight band running just below the 32.5kDa marker was evident in each of the IP lanes. Because this band was present in the IP lanes only it is likely that this is an artefact from the α-FLAG affinity resin.

To determine whether or not endogenous NELF-A protein interacts with the FLAG-tagged Siah proteins, the same blot was then re-probed with α-NELF-A antibody. The 83kDa NELF-A band was clearly observable in the input and IP supernatant lanes, and absent from the IP lanes, thus NELF-A did not co-immunoprecipitate with ectopically

expressed Siah proteins, neither in the presence or absence of MG132. This is perhaps not surprising given that the Siah-NELF-A interaction is likely to be transient.

4.17 Mutating Siah1b

As shown in the Siah1a/1b alignment (Figure 27), there are only six amino acid differences between the Siah1a and Siah1b proteins (summarised in Table 11). Three of these amino acid differences locate to the N-terminal RING-finger domain of the protein and the other three amino acid differences locate to the central zinc finger region.

To determine whether there was a particular residue or residues responsible for rendering Siah1b non-functional with regard to controlling NELF-A-GFP stability, site-directed mutagenesis was performed to make point mutations and thus sequentially revert each of the 6 differing amino acids which have accumulated in Siah1b since it diverged from Siah1a.

Amino acid	Siah1a	Siah1b	Protein domain
5	T - Threonine	A – Alanine	RING-Finger Domain
10	P – Proline	S – Serine	
27	G - Glycine	D – Aspartic Acid	
101	A - Alanine	S – Serine	Zinc –Finger Region
102	S – Serine	A – Alanine	
113	E – Glutamic Acid	K – Lysine	

Table 11. Amino acid differences between Siah1a and Siah1b.

To make each of the 6 point mutations, two oligonucleotide primers were designed, each primer pair complementary to opposite strands of the Siah1b-FLAG vector. These oligonucleotide primers were then extended during temperature cycling by *PfuTurbo* DNA polymerase (see methods, section 2.1.12). *PfuTurbo* DNA polymerase replicates both plasmid strands with high fidelity without displacing the mutant oligonucleotide primers. Following temperature cycling, the products were then treated with *Dpn*I, an endonuclease which specifically cuts methylated and hemimethylated DNA. *Dpn*I therefore digests the parental DNA template, leaving the newly synthesised mutation-containing DNA intact. Each DNA product containing the desired mutation was then purified using the Qiagen PCR purification kit and transformed into *E. coli* DH5α cells by electroporation. The resultant transformation mix was then plated out on LB plates

containing the selective antibiotic ampicillin and incubated at 37ºC overnight. Plasmids were purified from colonies and mutations were verified by DNA sequencing.

4.17.1 Assaying ability of Siah1b mutants to degrade NELF-A in vivo

To determine whether any of the six single amino acid substitutions between the Siah1a and Siah1b proteins were responsible for the differing activity with regard to controlling NELF-A-GFP fusion protein stability, each of the Siah1b mutants described in the previous section were co-transfected with the NELF-ApGFP3 expression plasmid into HEK293 cells, and the levels of NELF-A-GFP fusion protein were analysed.

As a positive control the N-terminal FLAG-tagged Siah1a expression vector was co-transfected and in the minus Siah control (-) empty FLAG vector was co-transfected. The GFP expression vector was also transfected to act as an internal standard and show the relative amount of the NELF-A-GFP fusion protein. 24 hours after transfection and upon confirmation of GFP fluorescence, cells were harvested and cell extracts were analysed by Western blot probing with α-GFP antibody and α-FLAG antibody to ensure the Siah proteins were being efficiently expressed (Figure 38).

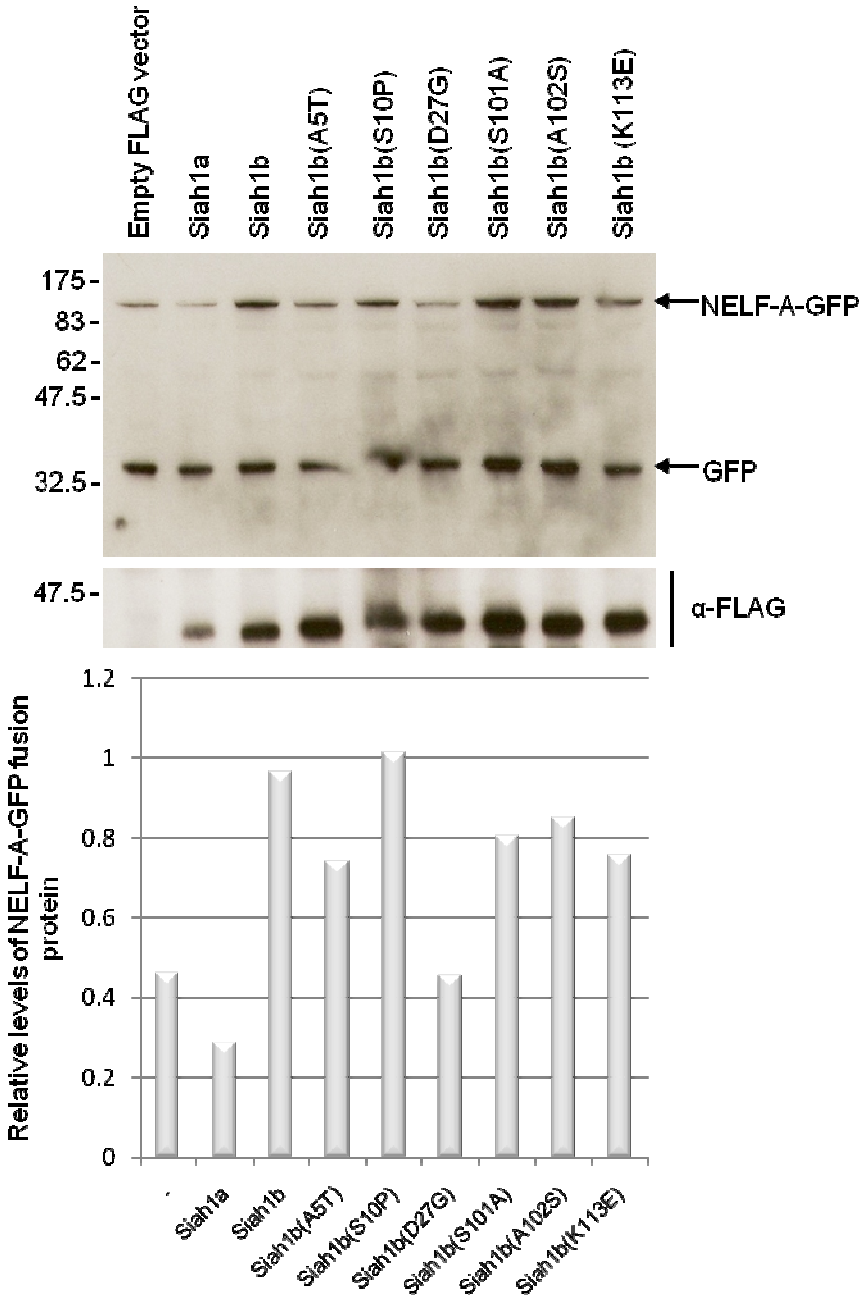

Figure 38. Co-transfection experiment to assay the ability of Siah1b mutants to degrade NELF-A-GFP fusion protein in HEK293 cells. 24 hours after transfection, cell lysates were prepared. Samples were separated by 10% SDS-PAGE and analysed by Western blot. Levels of GFP-tagged NELF-A were assayed by probing with α-GFP and HRP-conjugated anti-mouse secondary antibodies. To visualise Siah protein expression, the blot was re-probed with α-FLAG antibody and HRP-conjugated anti-mouse secondary antibody (lower blot). On the left of the Western the migrations of molecular weight markers are shown. The graph shows the relative amount of NELF-A-GFP fusion protein in each of the co-transfections compared to the GFP loading control.

Co-expression of none of the six different Siah1b mutants resulted in a reduction of NELF-A-GFP protein levels to the equivalent level of that observed when co-expressed with the functional E3 ligase Siah1a, however a reduction was observed when co-

expressed with Siah1b mutant D27G. In contrast, NELF-A-GFP protein was more stable when co-expressed with Siah1b and mutants A5T, S10P, S101A, A102S and K113E when compared to the minus Siah control (-). Although repeats of this experiment are required in order to determine whether or not these results are statistically significant, preliminary results suggest that a single amino acid substitution is not solely responsible for the differing functional activity between Siah1a and Siah1b.

4.17.2 Assaying ability of Siah1b mutants to auto-regulate themselves

As noted in the literature and consistent with our findings, the SIAH1 protein targets itself for proteasomal degradation. Studies by Hu and Fearon (1999) revealed that an intact N-terminal RING finger domain is essential for this function as point mutations and deletion of the RING finger domain lead to stabilisation of the SIAH1 protein. As a result of our experiments, we found that the murine Siah1a and Siah2 proteins also auto-regulate their own stability, however the closely related Siah1b protein did not. Because three of the six differing amino acids between Siah1a and Siah1b locate to the RING finger domain (Table 11), we speculated that these differences were responsible for the observed differences in stability.

To investigate whether or not the six amino acid substitutions between Siah1a and Siah1b proteins could affect Siah1b stability, levels of FLAG-tagged wild-type Siah1b and the Siah1b mutants were measured in the presence and absence of the proteasome inhibitor MG132.

The N-terminal FLAG tagged Siah1b clones were co-transfected with empty GFP vector to act as transfection and loading control into HEK293 cells. N-terminal FLAG-tagged Siah1a was also transfected as a positive control as we had previously shown that this protein is stabilised by MG132. 24 hours after transfection HEK293 cells expressing the N-terminal FLAG-tagged Siah proteins were treated with or without MG132 for 6 hours. Following confirmation of GFP fluorescence cells were harvested and subjected to SDS-PAGE and Western blot analysis (Figure 39).

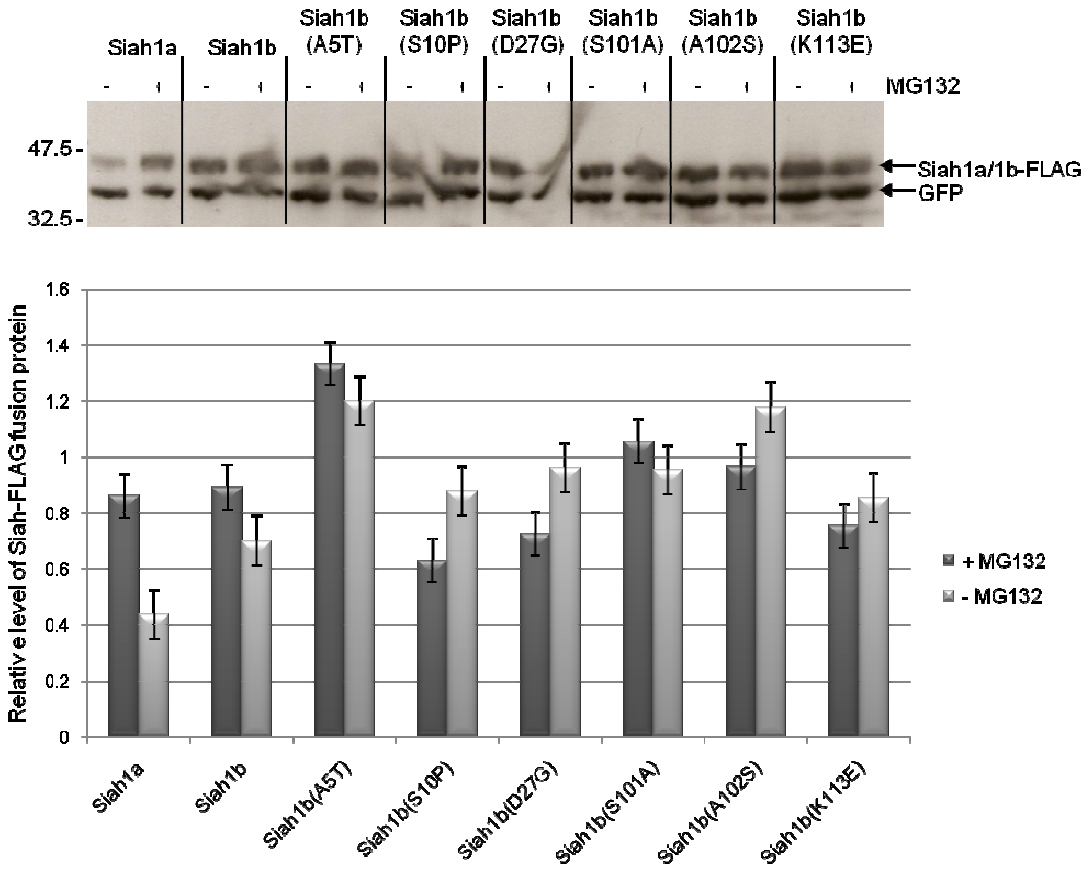

Figure 39. Co-transfection assay to monitor the stability of Siah1b mutants. 24 hours after transfection, cells were incubated with or without 60µM MG132 for 6 hours. Cell lysates were prepared and samples were separated by 10% SDS-PAGE. Levels of FLAG-tagged Siah proteins and the GFP loading control were measured by immunoblotting with α-FLAG and α-GFP primary antibodies, and HRP-conjugated anti-mouse secondary antibody. The migration of molecular weight markers is indicated on the left of the Western. The graph shows the relative amount of the FLAG-tagged Siah protein in the presence and absence of the proteasome inhibitor MG132. The data in the graphs is representative of an average of two Westerns and is presented as the mean ± SE.

A number of samples in the Western shown in Figure 39 did not separate well (particularly Siah1b D27G). Therefore samples were electrophoresed a second time on 10% SDS-PAGE and were again analysed by Western blot (Western not shown). Both Westerns were analysed using ImageQuant (Version 5.2) and an average of results is presented in the graph in Figure 39. As expected, the Siah1a protein was stabilised in the presence of MG132. A slight stabilisation was also observed for Siah1b, however this was negligible comparable to Siah1a. Levels of Siah1b mutants A5T, S101A and K113E were unaffected by the addition of MG132, whereas mutants S10P, D27G and A102S appeared to be more stable in the absence MG132.

Overall these experimental results imply that the individual reversion of each of the six amino acid changes in Siah1b, which have accumulated since it diverged from Siah1a, were insufficient to restore its ability to target itself for proteasomal degradation.

4.18 Summary and discussion

At the beginning of this chapter we hypothesised that Siah proteins may mediate an additional layer of transcriptional regulation of the various NELF- regulated developmental control genes by modulating stability of NELF-A. Thus, in order to further characterise the SIAH1:NELF-A interaction and determine whether or not Siah proteins regulate NELF-A stability *in vivo* we carried out a number of experiments. These included mapping of the SIAH binding site in NELF-A and confirmation via GST pull down; IP experiments to determine whether or not NELF-A was ubiquitinated; analysis of NELF-A protein localisation in mouse testes tissue and Siah deficient cells and analysis of NELF-A stability in the presence of the murine family of Siah proteins

We confirmed that a genuine molecular interaction occurred *in vitro,* mapping to the PST-rich region of NELF-A which contains a conserved SIAH binding motif. SIAH2, the SIAH1 homolog also bound to the PST-rich region of NELF-A, but not the full-length protein in a yeast 2-hybrid experiment. Consistent with this, Narita and colleagues (2003) aiming to better understand the interactions of the NELF complex at a molecular level found that C-terminal deletions of NELF-A, including the PST-rich region, did not affect the assembly of the NELF complex, however they hypothesised that this region may contribute to the stability of the DSIF/NELF/RNAPII complex.

The stability of NELF-A-GFP fusion protein was found to be dependent on the proteasome as protein levels increased in the presence of the proteasome inhibitor MG132. Since this data suggested that SIAH1 targeted NELF-A-GFP for proteasomal degradation, immunoprecipitation experiments were carried out to investigate whether or not SIAH1 mediates ubiquitination of NELF-A-GFP fusion protein. Results from these experiments however remained inconclusive. A modified, larger molecular weight NELF-A-GFP fusion protein was detected when SIAH1 was co-expressed and MG132 was present. However, due to lack of a suitable positive control, we were unable to determine whether or not this modification was a result of ubiquitination.

I would like to note that ubiquitination of proteins is inherently difficult to detect. This is due to the rapid proteasomal degradation of ubiquitinated species and also, ubiquitination can often be rapidly reversed by the action of a large family of deubiquitinating enzymes (DUBs). Although we addressed the problem of the proteolytic activities of the proteasome by using the inhibitor MG132, there may be DUBs in the cell that specifically de-ubiquitinate NELF-A. The majority of DUBs are cysteine proteases, therefore addition of cysteine protease inhibitors to the cell may improve our chances of detecting modified substrates.

Also, as noted in the introduction to this thesis (section 1.2.1) various polyubiquitin chain types have been described and it is unlikely that ubiquitin antibodies are able to detect free-ubiquitin, mono-ubiquitin and the various types of polyubiquitin chain conjugates with equal affinity. Thus, it is possible that a different ubiquitin antibody would detect the modified NELF-A-GFP species. Proteins modified with polyubiquitin chains are usually detected as higher molecular weight smears on Western blots, however we observed a discrete higher molecular weight band (Figure 23). If this is indeed a result of modification with ubiquitin then the presence of a discrete band suggests that the protein was mono or di-ubiquitinated rather than polyubiquitinated. The ubiquitin monomer has a molecular weight of 8.6kDa, therefore it is possible that the observed higher molecular weight band could represent a mono or di-ubiquitin tagged protein. In general, SIAH proteins are reported to polyubiquitinate substrates, however there was one exception published by Lee et al., (2008b) whereby SIAH1 was found to facilitate the mono and di-ubiquitination of α-synuclein which is commonly found in neurodegenerative inclusion bodies. SIAH1-mediated ubiquitination of α-synuclein did not target it for degradation by the proteasome, but instead appeared to promote α-synuclein aggregation.

Another possibility is that the NELF-A-GFP protein was modified by a ubiquitin like protein (see introduction, section 1.2.2). For example, modification with the UBL SUMO has been shown to affect protein stability, however, a distinct set of E1, E2 and E3 enzymes appear to be required for sumoylation. It is interesting to note though that SIAH1 and SIAH2 were found to interact with UbcH9, an E2 enzyme that catalyzes conjugation of SUMO, not ubiquitin, via yeast 2-hybrid (Desterro et al., 1997; Hu et al., 1997b). Although there is no evidence in the literature of SIAH proteins facilitating sumoylation, it is an intriguing possibility. It is also possible that other pathways may be

activated in the presence of SIAH1 and MG132 which results in a differing type of post-translational modification of NELF-A-GFP (e.g. phosphorylation).

Although SIAH1 was able to efficiently target ectopically expressed NELF-A for proteasomal degradation, analysis of endogenous levels of NELF-A protein in HEK293 cells revealed that endogenous protein was stable and unaffected by both MG132 incubation and SIAH1 over expression (data not shown). We were also unable to detect an interaction between FLAG-tagged Siah proteins and endogenous NELF-A via co-immunoprecipitation. These results suggest that these proteins do not interact under normal cellular conditions. It is possible that SIAH proteins may serve to limit NELF-A only at certain stages in the cell cycle. Interestingly, a study by Yung et al., (2009) which followed the movement of fluorescently labelled NELF-A via live cell fluorescence microscopy showed that NELF bodies were present in the nucleus throughout most of the cell cycle, except that they disappeared shortly before entering mitosis and reappeared after completion of cytokinesis. Therefore it would be interesting to monitor NELF-A protein levels throughout the cell cycle.

Alternatively, SIAH proteins may simply serve to target NELF-A which is in excess of cellular requirements. It is likely that the majority of NELF-A within the cell is present with the NELF complex, inaccessible to SIAH proteins. There may be some sort of trigger required that results in dissolution of the NELF complex to make NELF-A accessible to SIAH1-mediated ubiquitination.

Investigation in to NELF-A protein localisation in the testes revealed that NELF-A was present in pachytene spermatocytes and round spermatids and experiments by Venables et al., (2004) revealed that Siah1a is also expressed in spermatocytes, but not spermatids. Potentially, Siah1a regulates NELF-A which is being expressed in spermatocytes and once Siah1a expression is switched off in the spermatids, NELF-A is stable. The precise points at which Siah proteins and NELF-A are present during meiosis I and/or meiosis II however is unknown, and further investigation is required.

Analysis of NELF-A protein in the MEFs by Western and cell staining revealed that steady-state levels of NELF-A were similar in wild-type and the *Siah1a*$^{-/-}$*2*$^{-/-}$ null cells. This showed that the NELF-A protein was not exclusively regulated by either Siah1a and/or Siah2. In the absence of Siah proteins alternative pathways or other regulators of

NELF-A may be activated or it may be subject to degradation by another E3 ligase. There are a number of acknowledged Siah substrates which have been found to be regulated by alternate pathways and E3 ligases other than SIAH proteins. β-catenin, for example, was primarily believed to be regulated by the Wnt signalling pathway, however Matsuzawa and Reed (2001) and Liu et al., (2001) later found that β-catenin could also be destroyed by SIAH1 (Polakis 2001). HIPK2, another SIAH1 target, has also been shown to be regulated by alternate ubiquitin ligases, including WSB-1 and Fbx3 (Choi et al., 2008; Shima et al., 2008), and it appears that HIPK2 is regulated by multiple E3 ligases according to cellular needs (Kim et al., 2009).

We initially predicted that the most likely candidate to additionally control NELF-A protein in the mouse was the Siah1a murine homolog, Siah1b. Analysis of *Siah1b* expression in mouse tissues and MEFs revealed that *Siah1b* was most highly expressed in the testes and was expressed in both wild-type and *Siah1a*$^{-/-}$*2*$^{-/-}$ null cells. This prompted us to hypothesise that Siah1b could replace Siah function and compensate for the lack of Siah1a and Siah2 in the *Siah1a*$^{-/-}$*2*$^{-/-}$ null cells. However, our *in vivo* degradation assays revealed that Siah1b, unlike SIAH1, Siah1a and Siah2, had no affect on GFP-tagged NELF-A or T-STAR stability. Also, unlike the other Siah proteins Siah1b did not auto-regulate its own stability.

Given that Siah1a and Siah1b proteins are so similar it was surprising to find that Siah1b had diverged in function. The six amino acid differences between Siah1a and Siah1b reside in the RING finger domain and the central zinc finger region. There are no amino acid differences between the SIAH1, Siah1a and Siah1b substrate binding domains, thus it was not unexpected to find that Siah1b, like SIAH1 also bound to NELF-A and T-STAR in the yeast 2-hybrid assay.

It is unlikely that the amino acid changes that have accumulated in Siah1b simply render this protein non-functional, as in an attempt to generate Siah1b knockout mice, Bowtell and colleagues found that Siah1b was essential for viability during embryonic development (Frew et al., 2002). As Siah1b was capable of binding to NELF-A we hypothesised that Siah1b may act as a competitor and play an important role in the cell by preventing Siah1/2-mediated degradation.

The RING finger domain binds to E2 ubiquitin-conjugating enzymes and functions as part of a scaffold to optimally position substrate and E2 for ubiquitin transfer (Hu et al., 1999; Zheng et al., 2000). As a result of these varying residues it is possible that Siah1b binds to differing E2s or other modifying enzymes which are perhaps absent from HEK293 and murine 3T3 cells. Alternatively, the Siah1b RING finger and/or zinc finger region may bind to a protein which prevents or inhibits its ability to bind to and ubiquitinate particular substrates. It is also possible that Siah1b protein may have evolved to assist in the conjugation of UBL proteins, rather than ubiquitin.

Individual reversion of each of the six amino acid changes which have accumulated in Siah1b since it diverged from Siah1a had no affect on Siah1b's auto-regulatory activity. With regard to controlling NELF-A-GFP stability, co-expression the six different Siah1b mutants did not decrease NELF-A-GFP protein levels to the equivalent level of that observed when co-expressed with Siah1a, however a reduction was observed when co-expressed with Siah1b mutant D27G. Although repeats of this experiment are required in order to determine whether or not this is a statistically significant result, preliminary results suggest that multiple amino acid differences between Siah1a and Siah1b are responsible for their differing activities.

Co-expression of none of the six different Siah1b mutants resulted in a reduction of NELF-A-GFP protein levels to the equivalent level of that observed when co-expressed with the functional E3 ligase Siah1a, however a reduction was observed when co-expressed with Siah1b mutant D27G. In contrast, NELF-A-GFP protein was more stable when co-expressed with Siah1b and mutants A5T, S10P, S101A, A102S and K113E when compared to the minus Siah control (-). Although repeats of this experiment are required in order to determine whether or not these results are statistically significant, preliminary results suggest that a single amino acid substitution is not solely responsible for the differing functional activity between Siah1a and Siah1b.

Overall these experiments revealed that SIAH1, Siah1a and Siah2 proteins but not Siah1b preferentially down-regulate the levels of ectopically expressed NELF-A protein and the endogenous cellular NELF-A protein was largely stable under parallel conditions. Also, we were unable to detect an interaction between NELF-A-GFP and RNAPII by immunoprecipitation and we suspect that the GFP-tagged NELF-A protein does not participate in the formation of a functional NELF complex.

It remains possible that Siah proteins, excluding Siah1b, do mediate transcriptional regulation by modulating stability of NELF-A and the NELF complex. However, further understanding of what triggers disassociation of the NELF complex is required.

Chapter 5. Further investigation into the interaction between SIAH1 and the tumour suppressor proteins ASPP1 and ASPP2

5.1 Introduction

One of the interacting proteins identified in the SIAH1 yeast 2-hybrid screen included a tumour suppressor protein known as ASPP1 (Apoptosis Stimulating Protein of p53). In chapter 3 ASPP1 was found to interact specifically with full length SIAH1 protein, it contained a conserved SIAH binding motif and levels of ASPP1-GFP fusion protein were notably reduced when co-expressed with SIAH1. Therefore, evidence to date implied that ASPP1 was a target for SIAH1-mediated degradation.

The ASPP1 protein, encoded by the *PPP1R13B* gene, is a member of a family of proteins that share common domains at their N-termini, including an ankyrin-repeat domain, an SH3 domain and proline rich domain (hence, ASPP is also an acronym for the ankyrin repeats, SH3 domain, and proline rich domains that characterise the family). The family consists of three members, ASPP1, ASPP2 and iASPP, reviewed by Sullivan and Lu, (2007).

ASPP1 and ASPP2, also known as 53BP1 and 53BP2/53BP2L (made from splicing variants of the same gene) were originally identified in a yeast 2-hybrid screen aiming to identify p53 interactors, and were shown to bind to wild-type but not mutant p53 protein *in vitro* (Iwabuchi et al., 1994). They were later found to interact with p53 *in vivo* and regulate its activity (Samuels-Lev et al., 2001). Subsequently, ASPP1 and ASPP2 were found to interact with other key proteins involved in apoptosis and cell growth. These include the p53 family members, p63 and p73 (Bergamaschi et al., 2004; Robinson et al., 2008), the apoptotic regulator Bcl-2 (Naumovski et al., 1996), p65, a subunit of the apoptotic regulator NFκB (Yang et al., 1999), and APCL (Nakagawa et al., 2000) among others (see Table 12 in chapter 6 for a comprehensive list of ASPP1 and ASPP2 interacting proteins). To date however, the most studied function of the ASPP family proteins is their ability to bind to and regulate p53. ASPP1 and ASPP2 are activators of p53-dependent apoptosis but not cell cycle arrest (Samuels-Lev et al., 2001). They bind to the DNA binding domain of p53 and enhance its ability to selectively bind to promoters of pro-apoptotic genes and stimulate their expression (Iwabuchi et al., 1998; Samuels-Lev et al., 2001; Patel et al., 2008) . The mechanism of how they accomplish this however, is not clear. It may be achieved by changing the protein conformation of p53 itself or by recruiting other transcription factors or chromatin remodelling enzymes.

In contrast, the third ASPP family member, iASPP, is a key inhibitor of p53-mediated apoptosis, summarised in Figure 40 (Bergamaschi et al., 2003).

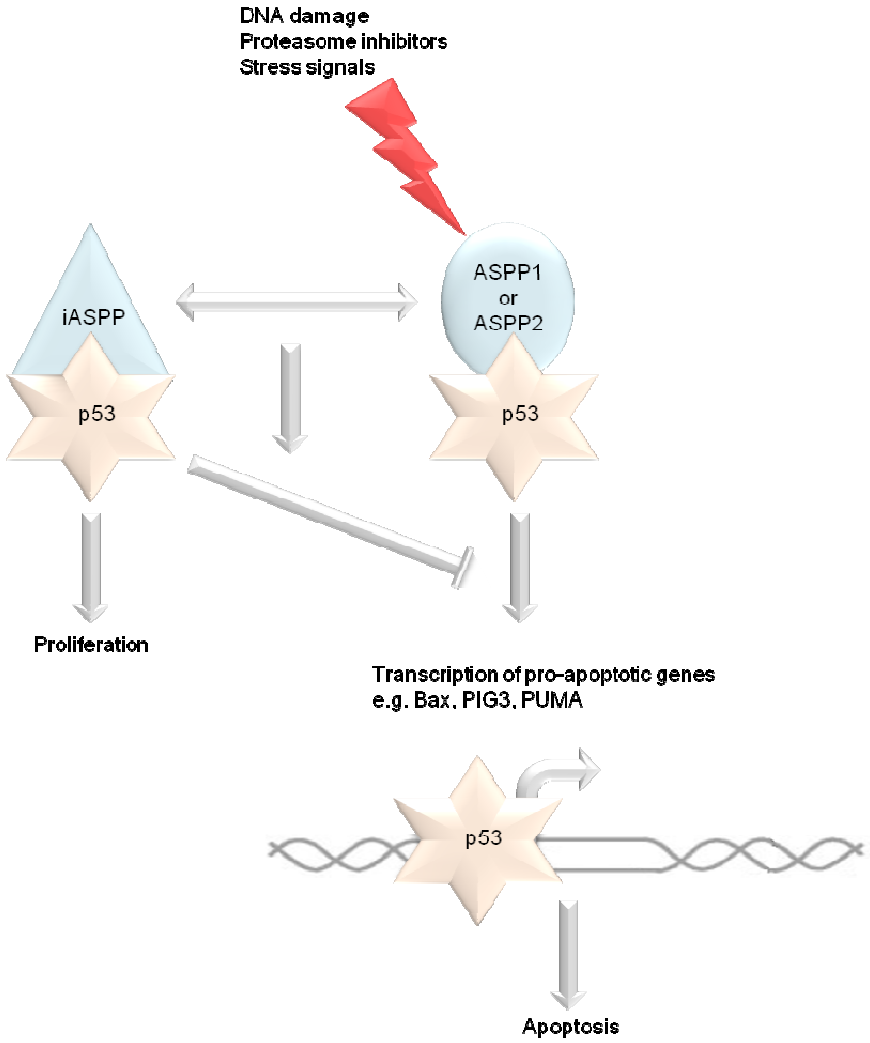

Figure 40. Regulation of p53-dependent apoptosis by ASPP proteins. After stress such as DNA damage, p53 is up regulated and stabilised. Binding of ASPP1 or ASPP2 results in transactivation of pro-apoptotic genes such as Bax and PIG3 resulting in cell death. iASPP prevents this, instead allowing proliferation to occur. Figure modified from Braithwaite et al., (2006).

The most common p53 mutations observed in human cancer map to the 200-amino acid core DNA binding domain which overlaps with the ASPP binding region. Elucidation of the crystal structure of the C-terminal portion of ASPP2 bound to the p53 core domain revealed that a number of these frequently mutated residues in p53 disrupt the ASPP2:p53 interaction (Gorina et al., 1996). Thus, this interaction plays an important role in p53 cancer biology and one mechanism by which wild-type p53 is tolerated in human cancer is through loss of ASPP activity. Both ASPP1 and ASPP2 are frequently down-regulated in human breast cancer (Samuels-Lev et al., 2001), leukaemia (Liu et al.,

2004) and tumour cell lines (Liu et al., 2005). Low ASPP2 mRNA levels have also been linked to poor clinical outcome in lymphoma patients (Lossos et al., 2002) and ASPP2 heterozygous mice are tumour prone (Kampa et al., 2009a).

Given the pro-apoptotic functions of ASPP1 and ASPP2, it must be important to keep ASPP activity in check as any disruption may result in impaired apoptosis and tumour formation. Much of the literature on the ASPP proteins focuses predominately on ASPP2, and a number of publications have shown that ASPP2 levels increase following UV irradiation and treatment with the clinically utilised bortezomib and chemotherapy agents which induce DNA damage (Lopez et al., 2000; Zhu et al., 2005). However, the mechanisms controlling ASPP1 and ASPP2 protein levels and function are poorly understood.

As discussed in the introduction to this thesis (section 1.3.3) SIAH1 is a p53 inducible gene and appears to play a role in the p53-mediated response. A number of groups observed that overexpression of SIAH1 often results in apoptosis or cell cycle arrest however the exact way in which SIAH1 controls the outcome is undefined. It is possible that SIAH1 contributes to the decision by regulating levels of the pro-apoptotic protein ASPP1.

Interestingly, a report published by Zhu and colleagues (2005) revealed that ASPP2 was regulated by a proteasome dependent mechanism. They found that treatment of cells with proteasomal inhibitors increased ASPP2 protein levels but not RNA and they also showed that ASPP2 was ubiquitinated. The E3 ligases responsible for ASPP2 ubiquitination however remain unknown. Given that ASPP1 and ASPP2 share 48% identity (Slee et al., 2003) we were keen to further characterise the interaction between SIAH1 and ASPP1 and we also wanted to determine whether or not SIAH1 could regulate ASPP2 stability.

In this chapter I describe experiments which address these issues. Levels of ASPP2-GFP fusion protein were monitored when SIAH1 was overexpressed and the ASPP2 protein sequence was analysed for the presence of a SIAH binding site. The SIAH1 interacting regions were mapped in both ASPP1 and ASPP2 and in order to gain a better idea of how SIAH proteins regulate ASPP stability *in vivo*, an ASPP1 polyclonal antibody was purified and levels of endogenous ASPP1 protein were analysed in Siah deficient cells.

5.2 Assay to determine whether or not GFP-tagged ASPP1 and ASPP2 are regulated by SIAH1 and the proteasome

Previous experiments suggested that ASPP1-GFP was modulated by proteasomal degradation as levels of ASPP1-GFP fusion protein were reduced when co-expressed with the E3 ubiquitin ligase, SIAH1 (chapter 3, section 3.5.3). Given that the ASPP1 and ASPP2 proteins are 48% similar, and Zhu and colleagues (2005) revealed that ASPP2 was regulated by a proteasome dependent mechanism, we hypothesised that SIAH1 may also target ASPP2 for proteasomal breakdown. In order to analyse this ASPP1pGFP3, ASPP2pGFP3 and SIAH1pCDNA3 were co-transfected into HEK293 cells. The GFP expression vector was also co-transfected to show the relative amounts of GFP-tagged ASPP protein. 24 hours after transfection, cells were incubated with or without the proteasome inhibitor MG132 for 7 hours. Cell extracts were then analysed by Western blot (Figure 41).

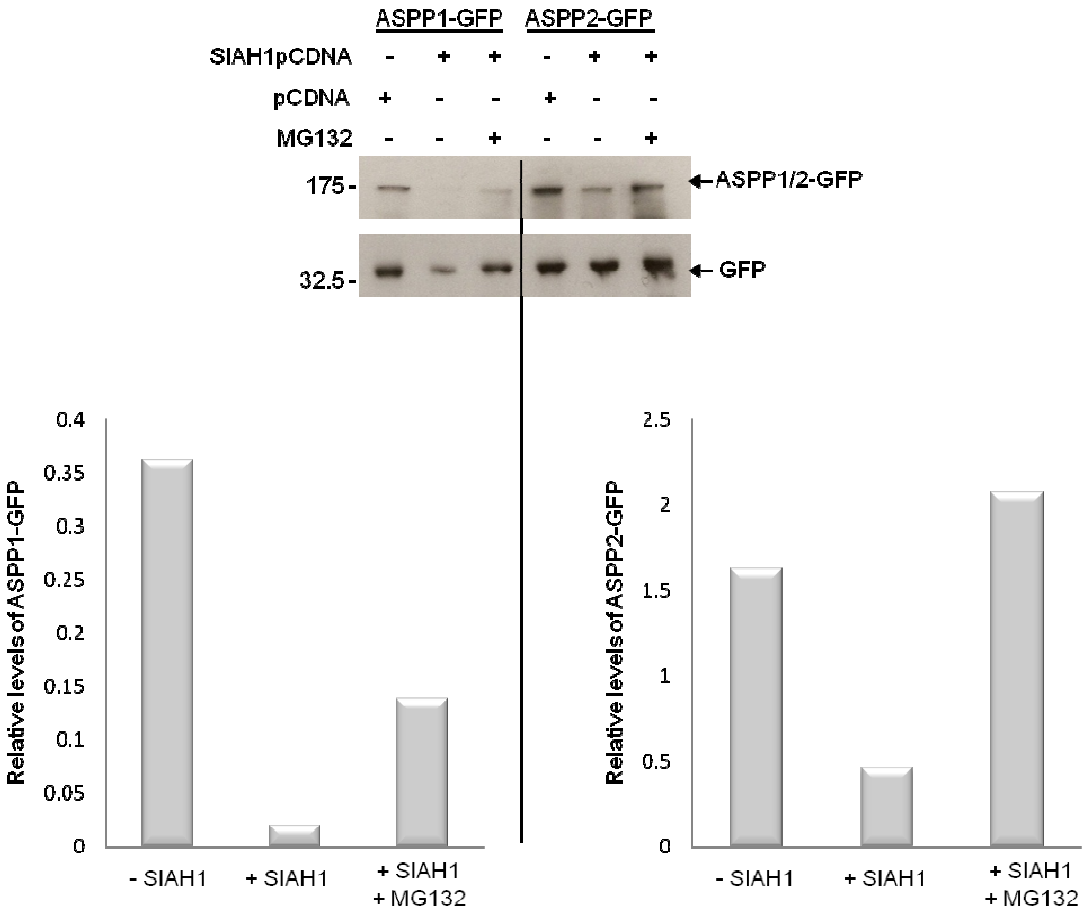

Figure 41. GFP-tagged ASPP1 and ASPP2 are stabilised by MG132. 24 hours after transfection, cells were incubated with or without 60µM MG132 for 7 hours. Cell lysates were prepared and samples were

separated on 7% SDS PAGE. Levels of GFP-tagged ASPP were measured by immunoblotting with α-GFP and HRP-conjugated anti-mouse secondary antibody. The migration of molecular weight markers is indicated on the left of the Western. The graphs show the relative amount of the GFP-fusion protein in each of the co-transfections.

Consistent with our previous results, co-expression with SIAH1 resulted in reduced ASPP1-GFP stability and a similar effect was observed on the stability of ASPP2-GFP. Also ASPP1- and ASPP2-GFP fusion proteins were stabilised in the presence of MG132. Therefore these results suggest that SIAH1 targets both of these proteins for proteasomal breakdown.

5.3 Analysis of ASPP2 protein sequence for presence of a SIAH-binding motif

Results from our *in vivo* degradation assay described in section 5.2 suggest that SIAH1 can target the ASPP2 protein for proteasomal breakdown. This prompted us to analyse the ASPP2 protein sequence in order to determine whether or not it contains a SIAH-binding motif. Sequence analysis was performed using ClustalW as described previously (chapter 3, section 3.4).

```
DCC          -------------------------SEEAPSRTIPTACVRPTHPLRSF------------
OBF-1        -------------------------HASSGAAPAPTAVVLPHQPLATY------------
SIP          -------------------------KAELLDNEKPAAVVAPITTGYTV------------
TIEG1        -------------------------NVEAARKNIPCAAVSPNRSKCER------------
ASPP2        PKPAGQQPRVLLSPSIPSVGQDQTLSPGSKQESPPAAAVRPFTPQPSKDTLLPPFRKPQT 480
```

Figure 42. Sequence alignment of the SIAH binding motif in recognised SIAH interacting proteins and ASPP2. Alignments were generated with ClustalW. Identical residues in the core motif are highlighted in red columns. Only the sequence encompassing the identified SIAH binding motif is shown.

The ClustalW alignment revealed that the ASPP2 protein contains the precise 'PxAxVxP' core SIAH binding motif encompassing amino acids 445-468 (Figure 42). We then went on to confirm that this predicted binding motif was completely conserved between humans and mice by aligning the human and mouse ASPP2 protein sequences using ClustalW (Figure 43).

```
Human        TVVPSMGTKPKPAGQQPRVLLSPSIPSVGQDQTLSPGSKQESPPAAAVRPFTPQPSKDTL 471
Mouse        IAATSVGAKLKPAGPQARMLLSPGAPSGGQDQVLSPASKQESPPAAAVRPFTPQPSKDTF 599
              ...*:*:* **** *.*:****. ** ****.***.**********************:
```

Figure 43. Partial sequence alignment between the human and mouse ASPP2 proteins. Alignment

was generated using ClustalW. Only the sequence encompassing the identified SIAH binding motif (red box) is shown. "*"residues represent those that are identical in the alignment. ":" represent conserved substitutions and "." represent semi-conservative substitutions.

5.4 Mapping the SIAH1 binding site in ASPP2

Analysis of the ASPP2 protein sequence revealed that it contained a precise SIAH binding motif (between amino acids 445-468) which was conserved between humans and mice (see Figure 43). To determine which part of the ASPP2 protein was bound by SIAH1, partial constructs containing the N-terminal and C-terminal regions of ASPP2 were generated and the encoded proteins were tested for their ability to interact with SIAH1 in a directed yeast 2-hybrid assay.

5.4.1 Generation of partial ASPP2 yeast 2-hybrid constructs

ASPP2 was divided in to two halves, an N-terminal half, including amino acids 1-556, and a C-terminal half, including amino acids 556-1005. This was achieved via PCR using an *ASPP2* expression plasmid encoding the full length *ASPP2* CDS as a PCR template (gift from Professor Xin Lu, Ludwig Institute for Cancer Research, University of Oxford, UK). PCR products were cloned into the pGADT7 vector (see appendix for primer and cloning information). To confirm that the pGADT7 clones contained the correct sequence, both constructs were sequenced from the 5′ end using the T7-F sequencing primer.

5.4.2 Mapping the SIAH1 interacting region in ASPP2 via yeast 2-hybrid

The two ASPP2pGADT7 clones described above were tested against the pGBKT7 vector alone, to assay for auto-activation, and against full length SIAH1-pGBKT7. Results are from the yeast 2-hybrid assay presented in Figure 44 and are summarised in Figure 48.

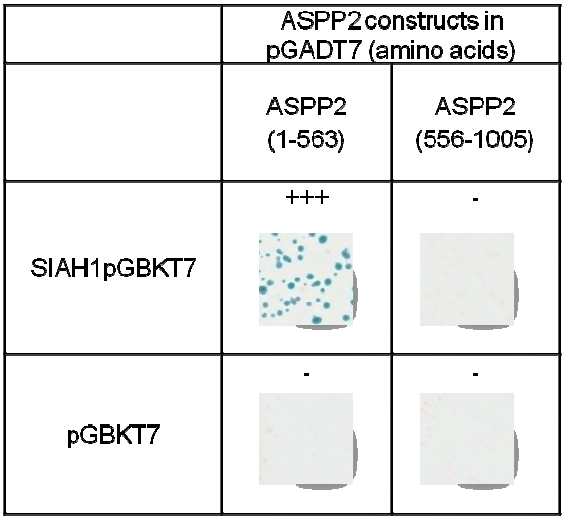

Figure 44. Mapping the SIAH1 interaction region in ASPP2. Full length SIAH1-pGBKT7 was tested against two partial ASPP2 constructs to identify the interacting region. Empty bait plasmid, pGBKT7 was used to test for auto-activation of prey plasmids. Filters stained with X-Gal are shown. Positive interactions manifest as blue colonies while when no interaction is present, the colonies remain white or red. Key, +++ strong interaction, positive blue colour within 30 minutes, ++ positive blue colour observable within 1 hour, + positive blue colour observable within 4 hours, - no noticeable interaction after 24 hours of exposure.

A strong, positive interaction with SIAH1 was detected with the N-terminal ASPP2 construct (amino acids 1-563). It is this half of the protein which contains the SIAH-binding motif previously identified (section 5.3). Negative results for an interaction between the empty pGBKT7 vector and the two ASPP2-pGADT7 clones confirmed that the positive result was not due to auto-activation by the Gal4-activation domain ASPP2 fusions alone.

5.5 Mapping the SIAH1-binding site in ASPP1

Previous analysis of the ASPP1 protein sequence revealed a putative conserved version of the SIAH-binding site encompassing amino acids 420-444 (see chapter 3, section 3.4). In order to determine whether or not this putative SIAH1 binding site was conserved between humans and mice, the human and mouse ASPP1 protein sequences were aligned using ClustalW (Figure 45). This revealed that unlike the motif identified in ASPP2, the putative motif in ASPP1 was only partially conserved between humans and mice.

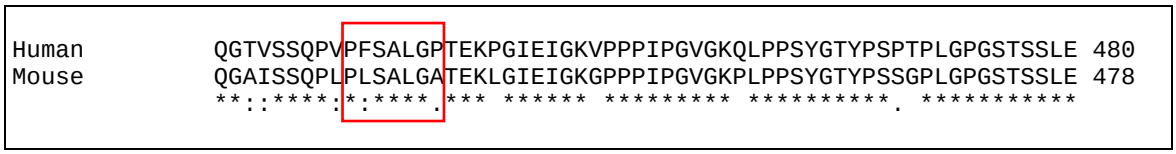

Figure 45. Partial sequence alignment between the human and mouse ASPP1 proteins. Alignment was generated using ClustalW. Only the sequence encompassing the putative SIAH binding motif which is highlighted by the red box is shown. "*"residues represent those that are identical in the alignment. ":" represent conserved substitutions and "." represent semi-conservative substitutions.

5.5.1 Mapping the SIAH1 interacting region in ASPP1 via yeast 2-hybrid

In order to determine which part of ASPP1 was recognised by SIAH1, Dr Jared Thornton previously generated partial ASPP1 yeast 2-hybrid constructs (Thornton 2005) and tested these in a directed yeast 2-hybrid assay for their ability to interact with full-length SIAH1. I repeated this assay in order to confirm results and further map the interacting region. Results are presented in Figure 46.

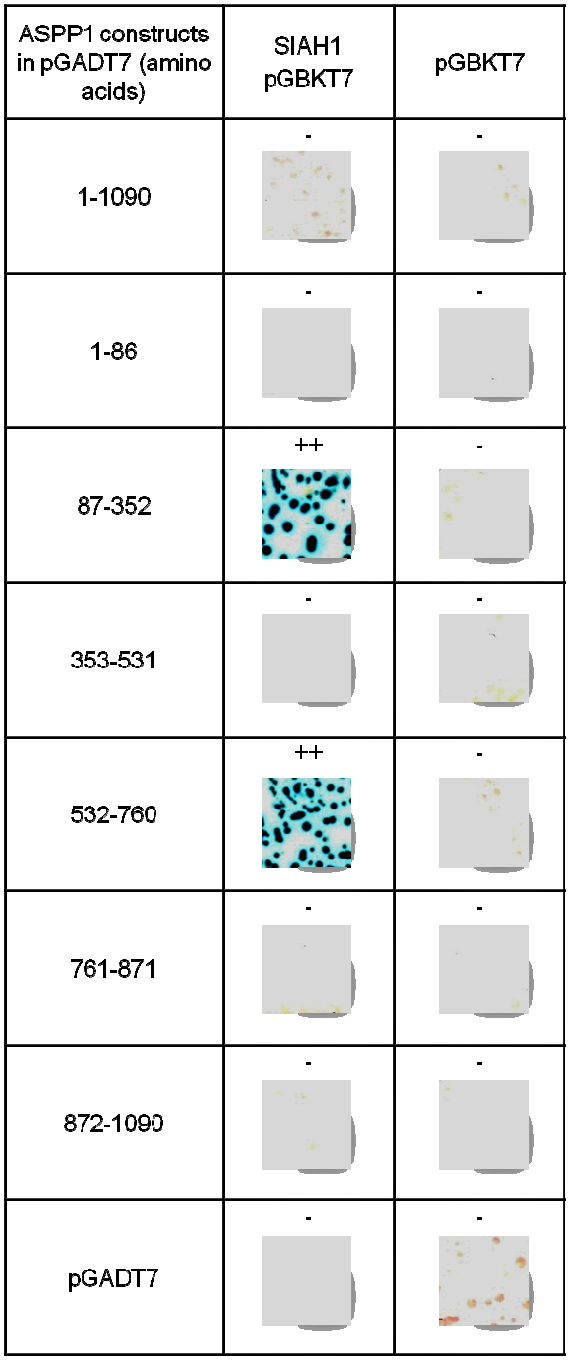

Figure 46. Mapping the SIAH1 interaction domains in ASPP1. Full length SIAH1-pGBKT7 was tested against partial ASPP1 constructs to elucidate the interacting region. Empty bait plasmid, pGBKT7, was used to test for auto-activation of prey plasmids. Filters stained with X-Gal are shown. Positive interactions manifest as blue colonies while colonies remain white or red when there is no interaction. Key, +++ strong interaction, positive blue colour within 10 minutes, ++ positive blue colour observable within 30 minutes, + positive blue colour observable within 1 hour, - no noticeable interaction after 24 hours of exposure.

Surprisingly, no interaction was detected between full length ASPP1 and SIAH1 in this assay. However, this was detected in the yeast 2-hybrid assay described in chapter 3,

sections 3.2 and 3.3. The only difference between these two assays is that the ASPP1 coding sequence was in the pACTII plasmid rather than pGADT7, both of which contain the Gal4 activation domain fused to ASPP1 CDS. It is possible that the pGADT7 clone had deteriorated. SIAH1 however, was also pulled out of a yeast 2-hybrid screen aiming to identify ASPP1 interacting proteins in the testes (see next chapter, section 6.2), thus we were confident that the full length proteins interact and this was an anomalous result.

Two different regions of ASPP1, amino acids 87-352 and 532-760, were found to interact with SIAH1 and this was consistent with Dr Jared Thornton's results (Thornton 2005). Negative results for an interaction between the empty pGBKT7 vector and the various ASPP1 fragments in pGADT7 confirmed that the positive interactions were not due to auto-activation by the Gal4-activation domain ASPP1 fusions alone.

5.5.2 Confirmation of the interaction between ASPP1 and SIAH1 in vitro

It was confirmed that the ASPP1:SIAH1 interactions were genuine molecular interactions by BSc students Anthony J. Cutts and Robin Humphrey (Human Genetics, Newcastle University) who performed an *in vitro* GST pull-down assay (data not shown). They cloned the two SIAH1 interacting ASPP1 fragments (amino acids 87-352 and 532-760) into the pGEX5X1 vector to create GST-fusion proteins. They then expressed these in *E. coli* BL21 cells and used these to specifically pull down radiolabelled, *in vitro*-translated SIAH1. Therefore, we were confident that the ASPP1:SIAH1 interactions detected in our yeast 2-hybrid assay were due to direct protein-protein contact rather than yeast bridging proteins.

5.6 Further mapping of the SIAH1 binding site in ASPP1

Previous experiments confirmed that SIAH1 interacts with amino acids 87-352 and 532-760 of ASPP1. However, the original analysis of the ASPP1 protein sequence for the presence of a SIAH-binding motif identified a putative site within amino acids 420-444 (chapter 3, section 3.4), which lies in-between the two SIAH1 interacting fragments.

In order to further narrow down the SIAH1 binding sites in ASPP1, constructs containing different regions of the two interacting fragments were generated and tested for their ability to interact with SIAH1 in the yeast 2-hybrid system.

5.6.1 Generation of partial ASPP1 yeast 2-hybrid constructs

The two SIAH1 interacting fragments (87-352 and 532-760) were divided into two regions by PCR. An ASPP1-V5 expression plasmid encoding the full length ASPP1 CDS was used as a template for PCR (gift from Professor Xin Lu, Ludwig Institute for Cancer Research, University of Oxford, UK). The 87-352 SIAH1 interacting region was divided into amino acids 86-216 and 208-355. The 532-760 SIAH1 interacting region was divided into amino acids 525-620 and 613-760 (see appendix for primer and cloning information). Each PCR product was cloned into the pGADT7 vector and we confirmed that the pGADT7 clones contained the correct sequences by sequencing from the 5′ end using the T7-F sequencing primer.

5.6.2 Further mapping of the SIAH1 interacting region in ASPP1 via yeast 2-hybrid

Each construct described above was then tested for interaction with full length SIAH1 protein in a directed yeast 2-hybrid assay. Full length ASPP1 was also tested as a positive control. Results are shown in Figure 47.

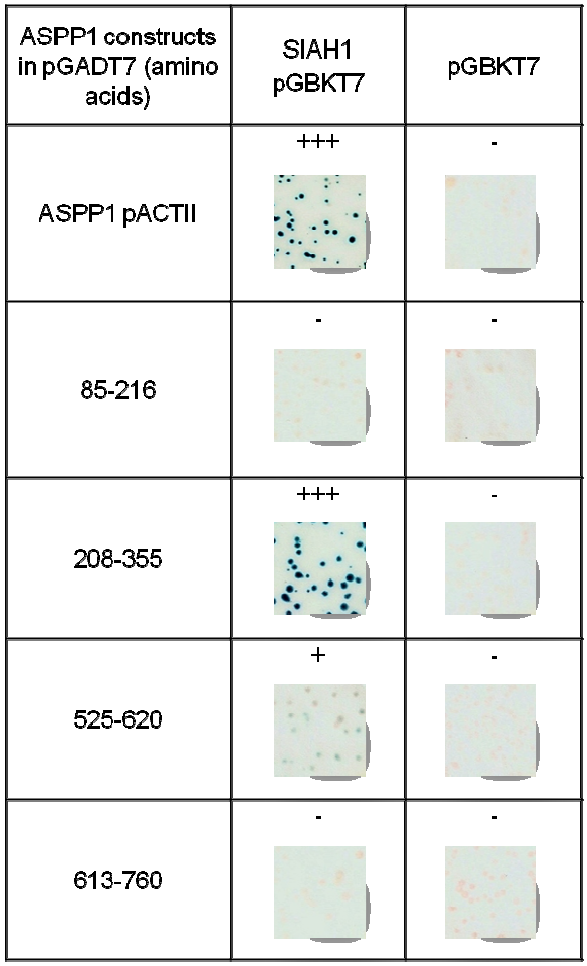

Figure 47. Further mapping the SIAH1 interaction region in ASPP1. Full length SIAH1-pGBKT7 was tested against partial ASPP1 constructs to further narrow down the interacting region. Empty bait plasmid, pGBKT7, was used to test for auto-activation of prey plasmids. Filters stained with X-Gal are shown. Positive interactions manifest as blue colonies while colonies remain white or red when there is no interaction. Key, +++ strong interaction, positive blue colour within 30 minutes, ++ positive blue colour observable within 1 hour, + positive blue colour observable within 4 hours, - no noticeable interaction after 24 hours of exposure.

SIAH1 interacted strongly with full length ASPP1 and amino acids 208-355, and a weak interaction was detected with amino acids 525-620. Results are summarised in Figure 48.

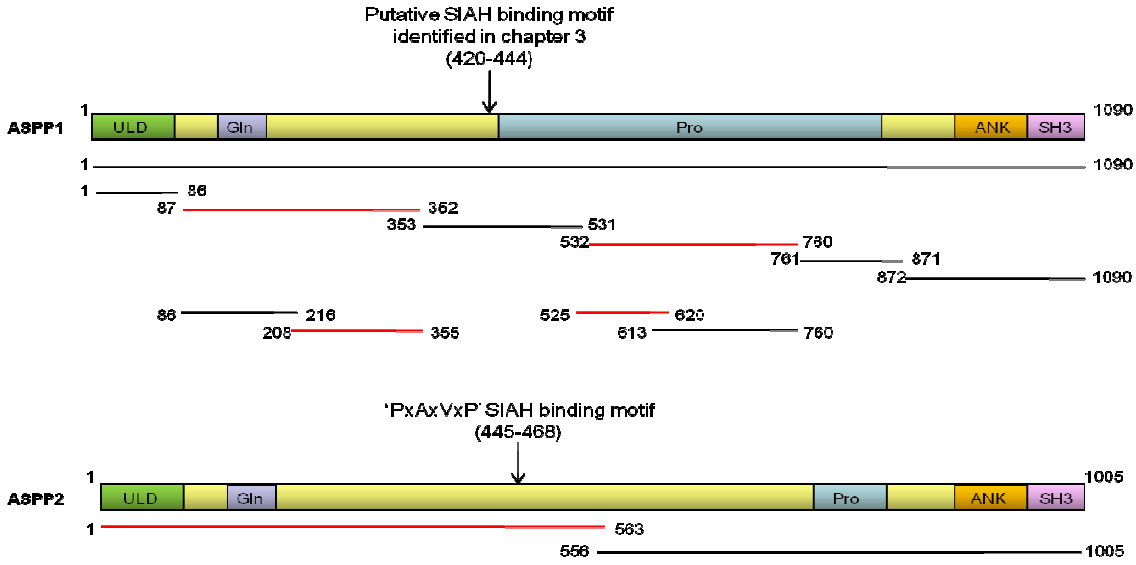

Figure 48. Schematic diagram of the ASPP1 and ASPP2 proteins and summary of the yeast 2-hybrid results. ASPP1 and ASPP2 proteins have a similar modular structure and the domain organisation of both proteins is shown. Domains include ubiquitin-like (ULD), glutamine-rich (Gln), proline-rich (Pro), ankyrin repeats (ANK) and Src homology 3 (SH3) domains. Smaller constructs outlined below were assayed for an interaction with SIAH1 via yeast 2-hybrid. SIAH1 interacting fragments are red.

Sequence analysis was performed in order to determine whether or not there was a degenerate SIAH1 binding motif present in the two ASPP1 SIAH1-interacting fragments. Again, fragments of four SIAH binding proteins containing a confirmed SIAH binding motif were aligned with ASPP1(208-355) and ASPP1(525-620) using ClustalW (see chapter 3, section 3.4). No clear SIAH binding motif was identified in either of these fragments (data not shown). However when the full length ASPP1 and ASPP2 protein sequences were aligned, the precise SIAH1 binding motif present in ASPP2 aligns within the 525-620 ASPP1 region which interacts weakly with SIAH1 via yeast 2-hybrid (Figure 49). Therefore SIAH1 may interact with both ASPP1 and ASPP2 in similar regions.

```
ASPP1         IQQRIS--------------VPPSPTYPPAGPPAFPAGDSKPELPLTVAIRPFLADKG-S 562
ASPP2         LSTVVPSMGTKPKPAGQQPRVLLSPSIPSVGQDQTLSPGSKQESPPAAAVRPFTPQPSKD 469
              :.  :.              *  **: *..*     : .** * * :.*:*** .: . .
```

Figure 49. Partial sequence alignment between ASPP1 and ASPP2 proteins. Alignment was generated using ClustalW. Only the sequence encompassing the SIAH binding motif identified in ASPP2 (red box) is shown. "*"residues represent those that are identical in the alignment. ":" represent conserved substitutions and "." represent semi-conservative substitutions.

5.7 ASPP1 polyclonal antibody purification

Experiments to date revealed that levels of both GFP-tagged ASPP1 and ASPP2 were notably reduced when co-expressed with SIAH1 and this effect was reversed by proteasome inhibition. In order to determine whether or not SIAH proteins normally target ASPP proteins for proteasomal degradation *in vivo*, we wanted to examine levels of endogenous ASPP proteins.

Unfortunately an ASPP2 antibody was not available to us. However, a polyclonal antibody specific to ASPP1 was previously generated by Dr Jared Thornton and it was formerly shown to work well on Western blots (Thornton 2005). This antibody was raised in sheep by injecting a GST-tagged ASPP1 specific epitope (amino acids 357-532). Due to limited stocks of the purified antibody however, I first had to re-affinity purify the polyclonal antibody from crude serum.

Total IgG was first separated from sheep serum (injected with purified ASPP1(357-532)-GST protein) by Agata Rozanska (IHG, Newcastle University) using caprylic acid. Epitope-specific antibodies were then affinity purified against an ASPP1-histidine fusion peptide coupled to a SulfoLink column (see methods, section 2.3.9.2). By using a His-tagged peptide derived from the pET32 vector (encoding the same ASPP1 specific epitope, amino acids 357-532) rather than the GST-tagged immunising peptide we ensured that the purified IgG was specific to the ASPP1 epitope, not the GST-tag.

5.7.1 Purification of ASPP1(357-532) His-fusion protein

The ASPP1(357-532)pET32a plasmid was transformed into *E. coli* BL21 cells via the calcium chloride transformation procedure (see methods, section 2.3.8.1). The pET32a plasmid contains six His-tag peptides fused with the thioredoxin protein. The empty vector was also transfected as a positive control. Single colonies were selected and expression was induced overnight in Instant TB medium (see methods, section 2.3.8.2). Total BL21 cell lysate samples from the overnight cultures are shown in Figure 50A. Following induction strong bands were observed corresponding to the predicted size of either ASPP1(357-532)-His-thioredoxin (approximately 35kDa) or His-thioredoxin (approximately 20kDa).

A solubilisation assay was previously carried out by Dr Jared Thornton showing that the ASPP1 epitope was predominantly soluble under native conditions (Thornton 2005). To ensure this was the case, lysed cells were centrifuged to pellet any insoluble material. After centrifugation, samples of soluble supernatant were taken and analysed on a SimplyBlue stained SDS-PAGE gel (Figure 50B). Bands of the correct size were present in the soluble fraction, indicating that as expected both proteins were soluble.

The His-tagged ASPP1(357-532) peptide was then purified from soluble cell lysate using ProCatch His resin under native conditions (see methods, section 2.3.8.4). The peptide was then eluted with imidazole, which displaces histidine and the elution process was repeated three times to recover as much of the purified peptide as possible. To check purification, a sample of each elution was analysed via SDS-PAGE (Figure 50C). It was clear that sufficient amounts of pure ASPP1(357-532)-His protein were obtained for subsequent purification of α-ASPP1-specific IgG.

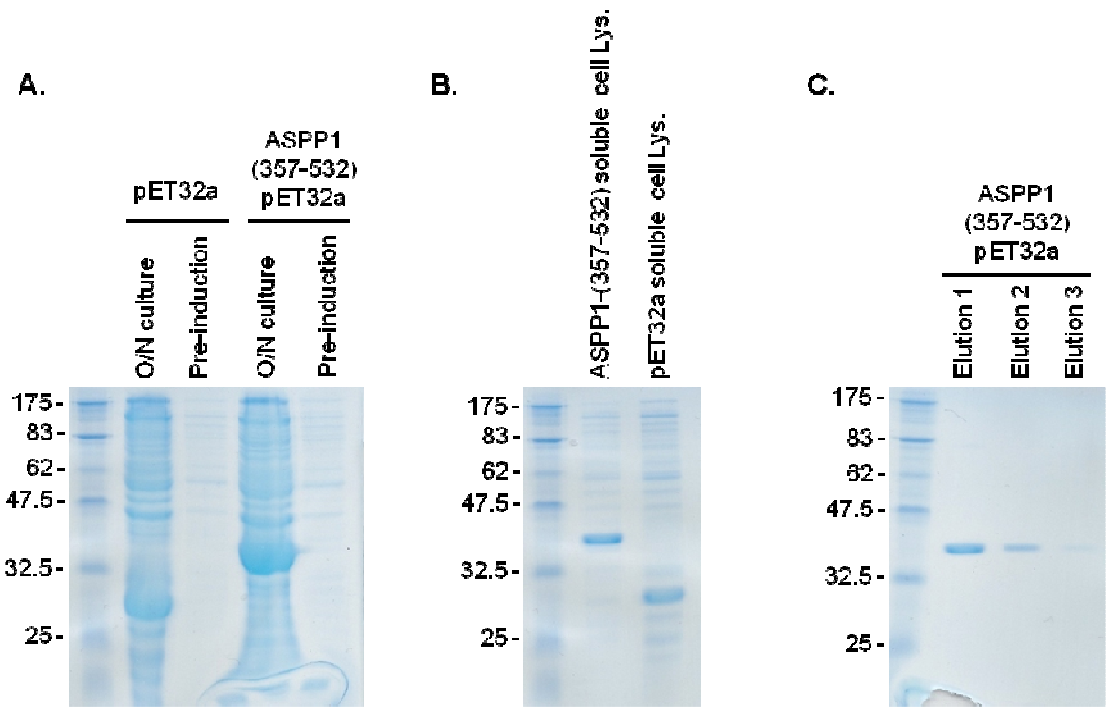

Figure 50. Preparation of the His-tagged ASPP1 antigenic peptide for affinity purification. (A) Bacterial expression of the ASPP1(357-532)-His fusion peptide. ASPP1(357-532)pET32a and empty pET32a plasmids were transformed into *E. coli* BL21 bacteria. Transformed bacteria were cultured and expression from the plasmids was induced overnight using instant TB medium. Before (pre-induction) and after the induction (O/N culture), aliquots of BL21 cells were harvested, lysed in 2X loading buffer, resolved on 10% SDS-PAGE and visualised with SimplyBlue SafeStain. (B) Testing solubility of His-fusion peptides. Induced cells lysates were subject to centrifugation and the soluble supernatant was visualised on the SimplyBlue stained gel. (C) Purification of the ASPP1(357-532)-His peptide. The peptide was purified using ProCatch His resin. After washing, bound peptide was eluted by adding 1ml of

elution buffer. The elution process was repeated three times and protein samples from each elution were analysed by SDS-PAGE. Molecular weight markers are indicated on the left of each gel.

5.7.2 ASPP1-specific IgG purification

Purified ASPP1(357-532)-His fusion protein was reduced with DTT to provide free sulfhydryls for linking the peptide to a SulfoLink column. ASPP1(357-532)-His was bound to the SulfoLink agarose and washed to wash off any un-bound protein (see methods, section 2.3.9.2).

Caprylic acid-purified total IgG (purified by Agata Rozanska, IHG) was passed through the ASPP1-epitope coated column. The column was then washed before elution of α-peptide specific antibodies first under acidic conditions followed by neutralisation of the column and subsequent elution under alkaline conditions. Fractions were collected, immediately neutralised and assayed for protein content via a Bradford assay (see methods, section 2.3.9.2). High levels of IgG protein eluted in acid fractions 3 and 4. Positive fractions were dialysed overnight against 1X PBS. Sodium azide was added (final concentration 0.05%) to the purified IgG to prevent bacterial infection and glycerol was added (final concentration 10%) to prevent freeze/thaw damage.

5.7.3 Characterisation of the α-ASPP1 antiserum by Western blotting and pre-absorption

Following purification, acid fractions 3 and 4 were tested for their ability to recognise full length ASPP1 by Western blot. Total protein was prepared from non-transfected HEK293 cells and cells transfected with the ASPP1pGFP3 expression plasmid. Proteins were electrophoresed on 7% SDS-PAGE followed by immunoblotting with the α-ASPP1 antibody (Figure 51).

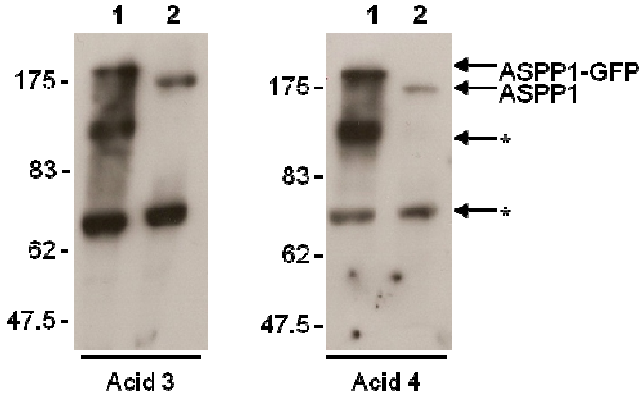

Figure 51. Analysis of the α-ASPP1 antiserum, acidic fractions 3 and 4 by Western Blot. Fractions 3 and 4 eluted from the SulfoLink column under acidic conditions were tested against HEK293 cells transfected with ASPP1-GFP (Lane 1), or non-transfected HEK293 cells (Lane 2). Protein samples were boiled, electrophoresed on a 7% SDS-polyacrylamide gel and analysed by immunoblotting with α-ASPP (1 in 500 dilution) and HRP-conjugated anti-sheep secondary antibody. On the left of the Westerns the migrations of molecular weight markers are shown. The asterisks highlight potential smaller ASPP1 isoforms or ASPP1 degradation products.

The α-ASPP1 antibody fractions 3 and 4 detected three protein bands in cells transfected with ASPP1-GFP and two protein bands in non-transfected cells (Figure 51). Clear bands were observed at the expected sizes for both the endogenous ASPP1 protein and ASPP1-GFP fusion protein (expected sizes 175kDa and 202kDa respectively) and these were detected with approximate equal affinity with both the acidic fractions. The smaller protein bands (*) were also observed with Dr Jared Thornton's purified α-ASPP1 antibody (Thornton, 2005). It is likely that these are ASPP1 degradation products or are representative of proteins made from alternatively spliced ASPP1 transcripts. However, these bands may also be due to the antibody binding non-specifically to a different protein.

Following detection of a protein of the expected size of ASPP1 and ASPP1-GFP fusion protein in non-transfected and transfected cells, pre-absorption assays were carried out to determine if the detected protein was indeed ASPP1 (see methods, section 2.3.9.3). If the protein bands resulted from the α-ASPP1 antiserum recognising ASPP1 protein, then prior binding of the antiserum to the ASPP1(357-532)-His fusion peptide before immunoblotting should eliminate or diminish the signal. This pre-absorption assay was carried out by pre-incubating the α-ASPP1 antiserum with ProCatch His resin coated with the ASPP1(357-532)-His fusion protein. As a control, a mock pre-absorption assay was carried out using an unrelated peptide, an RBM-histidine peptide attached to

ProCatch His resin which was used to generate an α-RBM antibody (Elliott et al., 1998). Both acid fractions 3 and 4 were tested on a Western blot of non-transfected and transfected HEK293 cells (transfected with ASPP1-GFP). Results are presented in Figure 52.

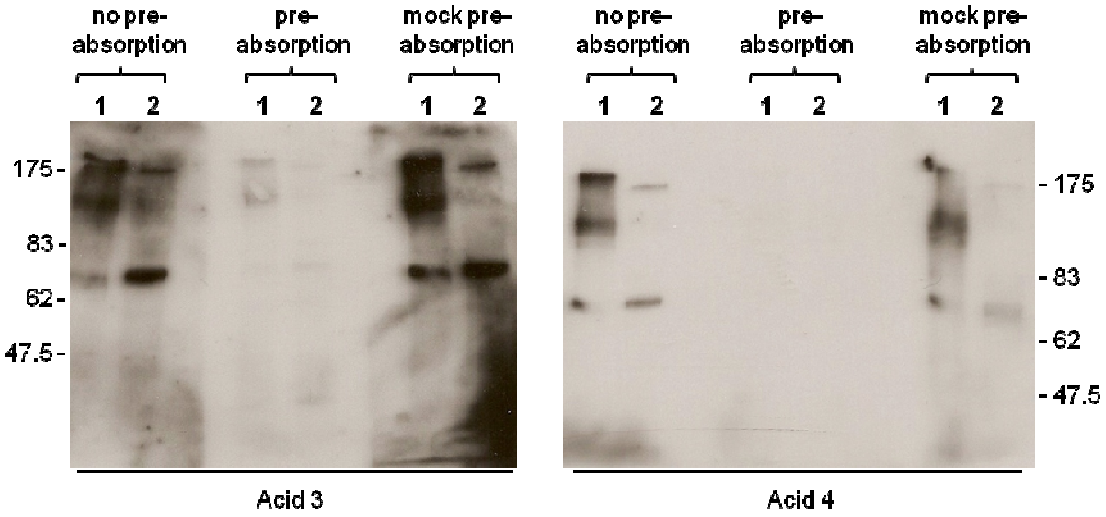

Figure 52. Western blots of pre-absorption assays to test the specificity of the α-ASPP1 antiserum, acidic fractions 3 and 4. Total protein from HEK293 cells transfected with ASPP1-GFP (lane 1) and non-transfected cells (lane 2) were prepared, resolved on 7% SDS-PAGE and analysed by Western blotting. Blots were probed with α-ASPP1 antiserum (no pre-absorption), the α-ASPP1 antiserum pre-incubated with the ASPP1(357-532)-His fusion coated resin (pre-absorption), and the α-ASPP1 antiserum pre-incubated with an RBM-histidine fusion coated resin (mock pre-absorption). Antibody binding was detected using a HRP-conjugated α-sheep secondary antibody.

Upon pre-absorption with the ASPP1(357-532)-His coated resin, no bands were observable for acid fraction 4 and a substantial decrease in band intensity was observed with acid fraction 3 (Figure 52). Therefore, this implies that the bands detected in non-transfected and transfected HEK293 cells are specific to the ASPP1 protein.

Mock pre-absorption with the ProCatch His resin coated in RBM-His peptide had no effect on the detection of ASPP1 using acid fraction 3. This further confirmed that the loss of signal in the pre-absorbed assay was due to the specific sequestration of the antibody by the epitope and not non-specific binding to the ProCatch His resin. Band intensity however was decreased when acid fraction 4 was mock pre-absorbed which may be due to poor protein transfer in this region of the gel during Western blotting. A stronger signal was observed when using α-ASPP1 acid fraction 3 therefore this antibody was used in subsequent experiments.

5.8 Analysing ASPP1 stability in *Siah1a*$^{-/-}$*2*$^{-/-}$ cells

Since we purified the α-ASPP1 polyclonal antibody which detected both ASPP1 and ASPP1-GFP on Western blot, we utilised this to examine endogenous ASPP1 protein levels in *Siah1a*$^{-/-}$*Siah2*$^{-/-}$ mouse embryonic fibroblasts (MEFs). These cells were introduced in the previous chapter and were used to analyse the stability of NELF-A protein (see chapter 4, section 4.11). By comparing ASPP1 protein levels in wild-type and *Siah* null cells we hoped to determine whether or not Siah proteins were primarily responsible for targeting ASPP1 for proteasomal degradation *in vivo*.

Confluent T75 flasks of wild-type and double mutant MEFs were harvested and lysed in 2x sample loading buffer. Total cell lysates were subject to SDS-PAGE and were analysed by Western blot (Figure 53) probing with the α-ASPP1 antibody.

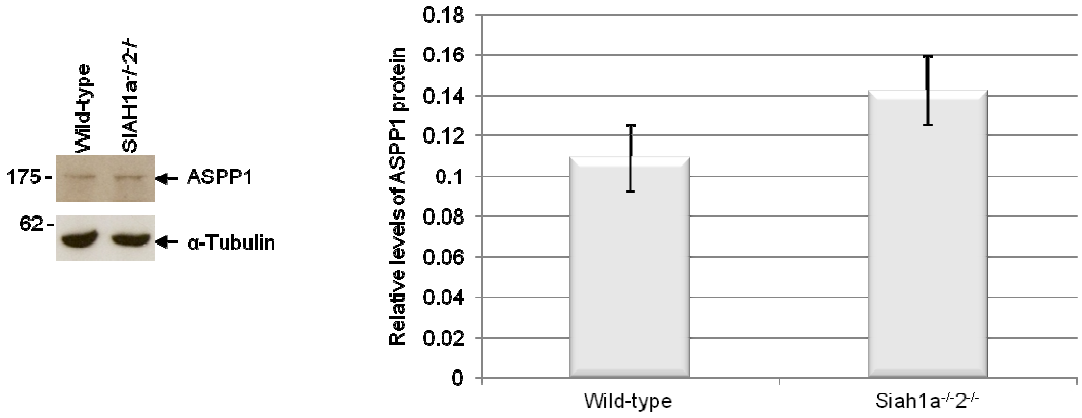

Figure 53. ASPP1 protein levels in Siah deficient MEFs. Cell lysates from wild-type and *Siah1a*$^{-/-}$*2*$^{-/-}$ mutant MEFs were prepared, and the level of ASPP1 was measured by immunoblotting with α-ASPP1 antibody and HRP-conjugated α-sheep secondary antibody. The migration of molecular weight markers is indicated on the left of the Western. The graph shows the relative amount of ASPP1 protein in wild-type and mutant MEFs compared to the α-tubulin loading control. Data is presented as the mean ± SE and is representative of 3 separate cell harvests.

When comparing ASPP1 protein abundance in wild-type and *Siah1a*$^{-/-}$*2*$^{-/-}$ MEFs by Western blot, steady state levels appeared similar. To gain a more quantitative result, four separate cell harvests were subjected to Western blot analysis (a representative Western shown in Figure 53) and protein levels were quantified using ImageQuant (Version 5.2). These results, presented in the graph in Figure 53, show that there is a trend towards increased ASPP1 stability in *Siah1a*$^{-/-}$*2*$^{-/-}$ null cells. However further

analysis is required in order to determine whether or not this result is of statistical significance.

5.9 Summary and discussion

In order to determine whether or not SIAH1 could regulate both ASPP1 and ASPP2 protein stability, levels of GFP-tagged ASPP1 and ASPP2 were analysed in the presence and absence of SIAH1. We found that ASPP1- and ASPP2-GFP tagged proteins were reproducibly destabilised by co-expression of human SIAH1, and protein destabilisation was MG132-sensitive, indicating this resulted from SIAH1-mediated targeting to the proteasome. Analysis of the ASPP2 protein sequence revealed that it contained the precise SIAH binding motif which is found in a number of known SIAH-interacting proteins (House et al., 2003), and we mapped the SIAH1:ASPP2 interaction to the N-terminal half of ASPP2 which contains this motif. These findings support the study published by Zhu et al., (2005) who report that proteasomal degradation modulates ASPP2 protein levels and apoptotic function. The ASPP1 protein was not mentioned in this study and prior to our studies the regulatory mechanism controlling ASPP1 stability, and the E3 ligases responsible for targeting ASPP2 for proteasomal degradation, were unknown.

Further characterisation of the SIAH1:ASPP1 interaction via yeast 2-hybrid mapping revealed that there were two regions of ASPP1 capable of interacting with SIAH1. Sequence comparison between full length ASPP1 and ASPP2 proteins indicated that the binding site identified in ASPP2 overlaps with one of the ASPP1:SIAH1 interacting fragments (amino acids 525-620) containing a conserved version of this motif. No obvious SIAH1 binding motif was found in the second ASPP1:SIAH1 interacting fragment (amino acids 208-355), suggesting that there is an unknown secondary SIAH binding motif present in ASPP1. Although the interaction between SIAH1 and the ASPP1 interacting fragments were confirmed via GST-pull down by BSc students Anthony J. Cutts and Robin Humphrey (Human Genetics, Newcastle University), it is unknown as to whether SIAH1 could simultaneously interact with both of these regions of ASPP1 *in vivo*.

Both ASPP1 and ASPP2 proteins have a similar modular structure. They both contain an ubiquitin-like (ULD) domain and glutamine-rich (Gln) domain at their N-terminus and proline-rich, ankyrin-repeat and SH3 domains at their C-terminus (see Figure 48). The C-terminal region is highly conserved amongst all of the ASPP family members (ASPP1, ASPP2 and iASPP) and interactions with all known ASPP1 and ASPP2 interacting proteins (including p53 and Bcl2) are mediated through the ankyrin repeats and SH3 domains (Naumovski et al., 1996; Trigiante et al., 2006). The N-terminal domain is only conserved between ASPP1 and ASPP2 and not much is known about what this region of the protein does except that it is required for pro-apoptotic function (Samuels-Lev et al., 2001). Tidow and colleagues (2007), who solved the structure of the ASPP2 N-terminal domain by NMR, suggest that the N-terminus is responsible for binding to other proteins in the apoptotic network. Interestingly, unlike all of the known ASPP1 and ASPP2 interactors, we found that SIAH1 binds to the proline-rich domain of ASPP1 and the N-terminal regions of the ASPP1 and ASPP2 proteins. Thus SIAH proteins may be able to interact with ASPP1 and ASPP2 whilst they are in a complex with other proteins resulting in their polyubiquitination and proteasomal degradation.

While it has been established that the ASPP2 protein is ubiquitinated, as would be expected for a proteasomal substrate, this remains to be determined for ASPP1. Zhu and colleagues (2005) show that it is the central region of ASPP2 which is ubiquitinated and this region is rich in lysine residues that could serve as ubiquitin conjugation sites. Consistent with their findings, the SIAH binding motif we identified in ASPP2 also locates to the central region (amino acids 445-468).

In order to gain a better idea of how SIAH proteins regulate ASPP stability *in vivo*, ASPP1 protein levels were analysed in the wild-type and the *Siah1a*$^{-/-}$*2*$^{-/-}$ null MEFs using the ASPP1 polyclonal antibody which we purified. Western blot analysis revealed that there was slightly more ASPP1 protein in the *Siah1a*$^{-/-}$*2*$^{-/-}$ null cells compared to the wild-type controls. These observations suggest that Siah1a and/or Siah2 are directly involved in regulating ASPP1 stability however more repeats of this experiment are required to determine whether or not this will achieve statistical significance.

It is of interest to note that the ASPP1:SIAH1 interaction was originally identified in the SIAH1 testes yeast 2-hybrid screen and analysis of ASPP1 localisation in mouse testes

section by Dr Jared Thornton found that it was expressed in round spermatids and spermatocytes (Thornton et al., 2006). Given that spermatocytes were found to apoptose after meiotic arrest in the *Siah1a*$^{-/-}$ mutant mouse (Dickins et al., 2002) it is possible that in the absence of Siah1a in testes, ASPP1 protein accumulates and promotes apoptosis.

As a result of our experiments, our data suggests that ASPP1, like ASPP2, is also regulated by the proteasome and that the E3 ligase SIAH1 may be candidate in controlling this process. However the signals which promote these interactions and subsequent degradation remain to be determined.

Chapter 6. The ASPP1 interacting proteome

6.1 Introduction

As discussed in the introduction to the previous chapter, ASPP1 and ASPP2 have been reported to bind to and modulate the behaviour of p53 and its family members, p63 and p73 (Bergamaschi et al., 2004; Robinson et al., 2008). In addition to p53, several other ASPP interacting proteins have been identified, many of which are involved in modulating apoptosis and cell growth (summarised in Table 12). The majority of these interacting proteins were identified as ASPP2 or 53BP2 (a splicing variant of ASPP2) interacting partners and often determination of a potential interaction with ASPP1 was not studied.

Putative Interactor	Interaction identified with ASPP1/ASPP2/53PB2	Putative function or pathway interaction	References
E2F1, E2F2, E2F3	ASPP1 and ASPP2 promoters	E2F1, E2F2 and E2F3 are transcription factors which bind to the ASPP1 and ASPP2 promoters and up regulate their expression	(Chen et al., 2004; Fogal et al., 2005; Hershko et al., 2005)
PP1γ_1	53BP2	53BP2 inhibits PP1 phosphatase activity	(Helps et al., 1995)
p53, p63, p73	53BP2, ASPP1, ASPP2	ASPP1 and ASPP2 stimulate p53, p63 and p73 transcriptional activity and apoptotic function	(Iwabuchi et al., 1994; Samuels-Lev et al., 2001; Bergamaschi et al., 2004)
14-3-3's	ASPP2/53BP2	ASPP2/53BP2 associate with 14-3-3 proteins during interphase, however the functional outcome of this association is unknown	(Meek et al., 2004)
APCL	53BP2	APCL appears to regulate cytoplasmic location of 53BP2	(Nakagawa et al., 2000)
APP-BP1	ASPP2	ASPP2 is a negative regulator of the neddylation pathway through specific interaction with APP-BP1	(Chen et al., 2003)
Bcl-2	53BP2	Hinders cell cycle progression/induces apoptosis through the mitochondrial cell death pathway	(Naumovski et al., 1996; Takahashi et al., 2005)
DDA3	ASPP2	ASPP2/DDA3 interaction appears to inhibit ASPP2 stimulation of p53 apoptotic signalling	(Sun et al., 2008b)
Ddx42p	ASPP2	This DEAD box protein inhibits ASPP2 apoptotic induction	(Uhlmann-Schiffler et al., 2009)
HCV core protein	53BP2/ASPP2	Hepatitis C virus core protein inhibits p53-mediated apoptosis by blocking the interaction between p53 and ASPP2	(Cao et al., 2004)
IRS1	53BP2	53BP2 interacts with and modulates the insulin signals mediated by insulin receptor substrate-1	(Hakuno et al., 2007)
p65, a subunit of NFκB	53BP2	53BP2 may act as a NFκB inhibitor and control NFκBs role in apoptosis	(Yang et al., 1999; Benyamini et al., 2009)
YAP1	53BP2	Functional association between 53BP2 and Yes-associated protein is undefined	(Espanel et al., 2001)
dCsk	*Drosophila* ASPP (dASPP)	dASPP binds to and positively regulates dCsk (C-terminal Src kinase)	(Langton et al., 2007)
SAM68	ASPP1	The ASPP1:SAM68 interaction appears to be restricted to human germ cells, may be involved in regulation of alternative splicing	(Thornton et al., 2006)

Table 12. Published ASPP1, ASPP2 and/or 53BP2 interacting proteins. 53BP2 is a short form splicing variant of ASPP2.

Our experimental results reported in chapter 5 imply that ASPP1 and ASPP2 are regulated at the post-transcriptional level by the E3 ubiquitin ligase SIAH1, and we speculate that targeted degradation of ASPP proteins represents an important mechanism

in regulating activation of the apoptotic programme. However, despite the identification of a number of ASPP interacting protein partners which are apoptotic regulators the exact mechanism by which ASPP1 and ASPP2 stimulate apoptosis remain elusive.

One conundrum surrounding ASPP protein function is that ASPP1 and ASPP2 appear to locate to the cytoplasm in cell lines and mouse tissue (Samuels-Lev et al., 2001; Thornton 2005; Thornton et al., 2006) whereas p53 and its target genes are located in the nucleus. In order to bind to p53 and its family members and stimulate their ability to activate expression of pro-apoptotic genes then presumably ASPP1 and ASPP2 need to translocate to the nucleus.

In an attempt to better understand ASPP1 function, and to identify pathways which modulate ASPP1 function in the cytoplasm and possible translocation to the nucleus, we set out to identify its major protein binding partners. Firstly positive hits from an ASPP1 yeast 2-hybrid screen carried out by Dr Jared Thornton (Thornton 2005) were analysed in order establish the identity of potential interactors. Dr Jared Thornton screened a human testis cDNA library as ASPP1 was found to be highly expressed in testis tissue and surprisingly, in contrast to cell culture and mouse tissues, ASPP1 was nuclear in human germ cells (Thornton et al., 2006).

As well as elucidating the ASPP1 binding partners from the testes yeast 2-hybrid screen we also performed immunoprecipitation experiments in order to get a better understanding of ASPP1 function *in vivo*. Both endogenous and ectopically expressed FLAG-tagged ASPP1 proteins were immunoprecipitated and co-immunoprecipitating proteins were analysed by mass spectronomy. Further co-immunoprecipitation experiments were carried out in order to verify the main interactors. By taking together the yeast 2-hybrid results and the proteomics results, we hoped to gain a better understanding of protein networks in which ASPP1 is involved.

6.2 Analysis of ASPP1 yeast 2-hybrid hits

To determine the identity of the positive hits from Dr Jared Thornton's yeast 2-hybid screen, prey plasmids were isolated from positive yeast colonies by MSc student Febin Roy (Human Genetics, Newcastle University), and sequenced from the 5′ end using the pACT25 primer. BLAST searches were carried out with the sequence data to determine

which proteins were encoded by the positive hits. Thirty informative sequences were obtained. Results are summarised in Figure 54.

Gene Symbol	Accession number	Protein name	Number of Hits
CLU	P10909	Clusterin	4
COPB1	P53618	Coatomer subunit beta	3
COL1A2	P08123	Collagen alpha-2(I) chain	2
HCFC2	Q9Y5Z7	Host cell factor 2	2
SIAH1	Q8IUQ4	Seven in absentia homolog 1	2
SYNJ2	O15056	Synaptojanin-2	2
ZMYM2	Q9UBW7	Zinc finger MYM-type protein 2	2
C20orf96	Q9NUD7	Uncharacterised protein C20orf96	1
CEP350	Q5VT06	Centrosome-associated protein 350	1
DIP2A	Q14689	Disco-interacting protein 2 homolog A	1
FTMT	Q8N4E7	Ferritin, mitochondrial	1
GTPBP4	Q9BZE4	GTP binding protein 4	1
HLA-A	Q09160	HLA class I histocompatibility antigen, A-1 alpha chain	1
NCOR1	O75376	Nuclear receptor corepressor 1	1
PPP1CC	P36873	protein phosphatase PP1-gamma catalytic subunit	1
PRM2	P04554	Protamine-2	1
SMC3	Q9UQE7	Structural maintenance of chromosomes protein 3	1
SPATS1	Q498A3	Spermatogenesis-associated serine-rich protein 1	1
UBAP1	Q9NZ09	Ubiquitin-associated protein 1	1
ZMYND19	Q96E35	Zinc finger MYND domain-containing protein 19	1

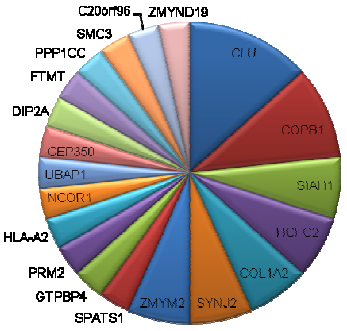

Figure 54. Positive 'hits' from the ASPP1 yeast 2-hybrid screen. Table shows results from BLAST database searches with sequences obtained from positive hits. The number of representative hits for each protein is shown and summarised in the pie chart.

By analysing the clone sequences from the multiple hits, two independent cDNA constructs were identified out of the four clusterin (CLU) clones and, out of all the other multiple hits, only COPB1 and COL1A2 were found to derive from two independent cDNAs. Double-hit results obtained for Clusterin, COPB1 and COL1A2 gave us more confidence that these proteins were genuine biological interactors however this may also be due to high levels of expression of these proteins in the testes and hence an abundance of these clones in the cDNA library. A brief summary of these principal interactors follows:

Clusterin (CLU)

Clusterin is a ubiquitously expressed glycoprotein with an apparent involvement in a variety of biological processes including DNA repair, cell cycle regulation, and more

interesting with regard to the ASPP1 interaction, apoptotic cell death. There are two known isoforms of clusterin; a nuclear isoform (nCLU) which appears to be pro-apoptotic (Yang et al., 2000; Leskov et al., 2003) and a secretory isoform (sCLU) which is, in contrast, pro-survival (Shannan et al., 2007). sCLU is the major secreted product of Sertoli cells (Clark et al., 1997) in the testes and it has been shown to have a protective effect against apoptosis in the murine testes after heat exposure (Bailey et al., 2002). Despite extensive research on clusterin in the testes and other organs, how exactly the secretory and nuclear isoforms exert their protective/pro-apoptotic affects remains unknown.

Coatomer protein complex, subunit beta 1 (COPB1)

COPB1 is a subunit of the coatomer protein complex which associates with the Golgi apparatus and is involved in intracellular protein transport (Lee et al., 2004). It also appears to maintain the physical integrity of Golgi, as it lines the surface of Golgi membranes creating a protein 'scaffold' (Gaynor et al., 1998). Interestingly, breakdown of the Golgi apparatus is an early event during apoptosis (Mukherjee et al., 2007).

Collagen alpha-2(I) chain (COL1A2)

Collagen alpha-2(I) chain is one of the chains which constitutes type I fibrillar collagen. Collagens are secreted by connective tissue cells, forming a major part of the extracellular matrix, and type I collagen is the commonest form of collagen in the human body. *Col1a2* expression in germ cells of immature and adult mouse testis is believed to play a potential role in mediating the detachment and migration of germ cells during spermatogenesis (He et al., 2005).

6.2.1 Testing the protein interaction between ASPP1 and Clusterin in mouse testes

Having established that an interaction between clusterin and ASPP1 occurs in yeast *in vitro*, and due to clusterin having identifiable characteristics which overlap with ASPP1 function, we chose to further investigate this interaction. Firstly, we wanted to ascertain whether or not this interaction actually takes place *in vivo*. To do this we utilised the α-ASPP1 antibody previously generated (see previous chapter, section 5.7) to immunoprecipitate ASPP1 from testes tissue. Although the ASPP1:CLU interaction was identified using a human testes cDNA library, we used mouse testes tissue due to human

testes tissue being in short supply and also since ASPP1 has been found to be highly expressed in mouse testes (Thornton et al., 2006).

Cell lysate was prepared from two murine testes and endogenous ASPP1 protein was immunoprecipitated using α-ASPP1 antibody and protein A Dynabeads (see methods, section 2.3.10). As the α-ASPP1 antibody was raised in sheep, control immunoprecipitations were carried out using total IgG which I prepared from crude sera from the pre-immune ASPP1 sheep (see methods, section 2.3.9). Mouse testes soluble lysate (input), ASPP1- and sheep IgG- immunoprecipitates and IP supernatants were analysed by SDS-PAGE and Western blot (Figure 55).

To ensure that the IP was successful, and that the ASPP1 antibody was immunoprecipitating a protein of the correct size, the Western blot presented in Figure 55 was probed with the α-ASPP1 antibody. The presence of a strong ASPP1 band running at the 175kDa marker in the ASPP1 IP lane and its absence from the negative control Sheep IgG IP showed that the ASPP1 protein had immunoprecipitated efficiently. A number of distinct smaller bands were seen, particularly in the input and IP supernatant lanes (*). These are often observed when using this particular antibody for Western blot (see previous chapter, Figures 51 and 52) and are likely to be either ASPP1 degradation products or are representative of proteins made from alternatively spliced ASPP1 transcripts. It is possible that the antibody may also cross-react with a non-specific protein, however results from the pre-absorption assay described in Chapter 5 (section 5.7.3), suggest that the bands detected are specific to ASPP1 protein. The full length ASPP1 protein runs at the 175kDa marker. The strong ~62kDa bands present in the IP lanes are likely to be IgG heavy chain.

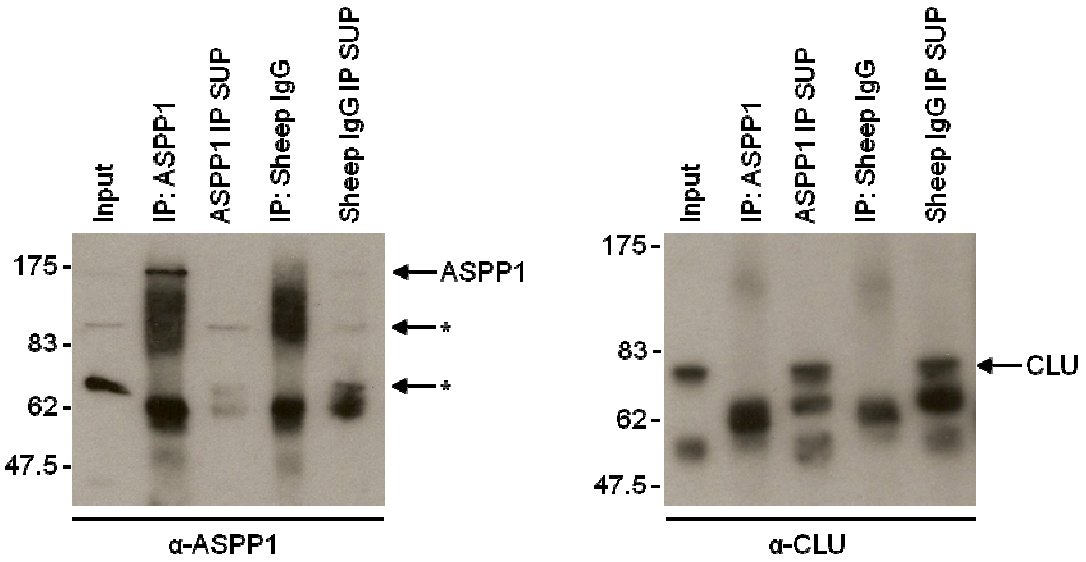

Figure 55. Testing co-immunoprecipitation of ASPP1 and CLU in mouse testes tissue. Soluble mouse testes tissue lysates were incubated with either α-ASPP1 antibody or sheep IgG and Protein A Dynabeads. After washing, samples were eluted by boiling in sample loading buffer. Mouse testes soluble cell lysates (Input), immunoprecipitates (IP) and IP supernatants were separated on 7% SDS PAGE and probed with α-ASPP1 and α-CLU antisera. Antibody binding was detected using an HRP-conjugated α-sheep and HRP-conjugated α-goat secondary antibodies, respectively. The migration of molecular weight markers is indicated on the left. The asterisk highlight potential smaller ASPP1 isoforms or ASPP1 degradation products.

To determine whether or not ASPP1 and CLU interact in mouse testes, the same samples were ran on a second polyacrylamide gel and analysed by Western blot using a α-CLU antibody (gift from Dr Arturo Sala, UCL, London, UK). Clusterin is synthesised as a 449 amino acid polypeptide with a molecular weight of 70kDa. This 70kDa band is clearly observable in the input and IP supernatant lanes, and absent from the IP. The lower molecular weight bands are likely to be the Clusterin α/β-subunits as the 449 amino acid precursor peptide is post-translationally cleaved to give α and β subunits which associate via disulphide bonds. Therefore, in this IP experiment ASPP1 and clusterin do not appear to co-immunoprecipitate. It is possible that the amount of ASPP1 protein immunoprecipitated was insufficient to detect association between the two proteins. As we have no positive control for this experiment it remains feasible that ASPP1 and clusterin associate in murine testes.

6.2.2 Testing protein interaction between ASPP1 and p53 in mouse testes

Although p53 was not pulled out of the ASPP1 yeast 2-hybrid human testes screen, this does not necessarily mean that these proteins do not interact *in vivo*. In order to interact,

ASPP1 and/or p53 may require modification which may only occur in mammalian cells, not yeast. Also, the yeast 2-hybrid screen was not saturating. We therefore wanted to determine whether or not ASPP1 and p53 interact in mouse testes. To do this, Sheep-IgG and ASPP1 IPs were separated by SDS-PAGE and analysed by Western blot probing with an antibody specific to p53 (Figure 56).

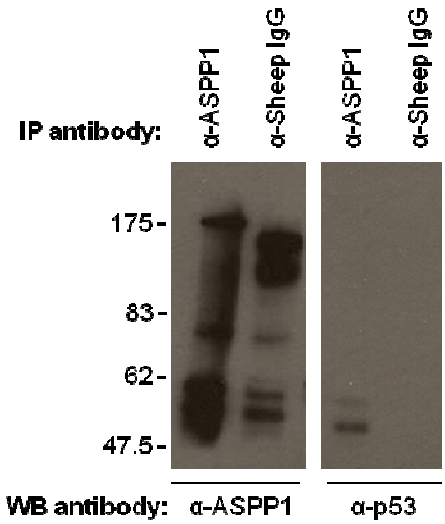

Figure 56. Co-immunoprecipitation of ASPP1 and p53 in mouse testes tissue. Soluble mouse testes tissue lysates were incubated with either α-ASPP1 antibody or sheep IgG and Protein A Dynabeads. After washing, samples were eluted by boiling in sample loading buffer, separated by SDS-PAGE and probed with α-ASPP1 and α-p53. Antibody binding was detected using a HRP-conjugated α-sheep and HRP-conjugated α-mouse secondary antibodies, respectively. The migration of molecular weight markers is indicated on the left.

A clear p53 band, running just above the 47.5kDa marker, is present in the ASPP1 IP lane and absent from the control. This result shows that ASPP1 and p53 associate in murine testes tissue however further investigation is required to determine whether or not these two proteins directly interact with one another.

6.3 Identifying endogenous ASPP1 interacting proteins by mass spectrometry

One limitation of the yeast 2-hybrid screen is that it identifies pairs of protein interactions, hence it does not reveal much about the nature of the complexes in which these proteins interact. Thus in order to identify protein complexes in which ASPP1 is involved we carried out a large scale immunoprecipitation experiment, whereby endogenous ASPP1 protein was pulled down from cells and co-immunoprecipitating proteins were determined by mass spectrometry.

Given the tumour suppressor and oncogenic activities of ASPP1, identification of ASPP1 interacting proteins and regulators may have therapeutic implications. Therefore, rather than studying ASPP1 interacting proteins in mouse testes, we wanted to focus on ASPP1 interacting proteins in human cells, as proteins and signalling pathways that govern ASPP1 function may vary between humans and mice.

Due to the inherent problems in using human tissue we chose to use a human cell line, allowing us to bulk up cell number and isolate as much ASPP1 protein as possible. We chose to use Saos2 cells, an osteosarcoma cell line, as we had previously found that ASPP1 was expressed at reasonable levels in these cells (data not shown).

6.3.1 Saos2 ASPP1 immunoprecipitation

Saos2 cell lysate was prepared from forty confluent T75 flasks. Proteins were immunoprecipitated using protein A Dynabeads, the α-ASPP1 antibody and Sheep IgG control (see methods, section 2.3.10). Saos2 soluble lysate (Input) ASPP1- and sheep IgG-IPs were first subjected to SDS-PAGE and Western blot analysis (Figure 57A). By probing with the α-ASPP1 antibody it was evident that ASPP1 immunoprecipitated successfully from Saos2 cells.

The remaining ASPP1 and Sheep IgG IP samples were then resolved on a 4-12% gradient gel and proteins were visualised with SimplyBlue SafeStain (Figure 57B). It was clear from the stained gel that there were many more proteins present in the ASPP1 IP lane compared to the Sheep IgG control IP. A faint band running at the 175kDa marker was predicted to be ASPP1 protein.

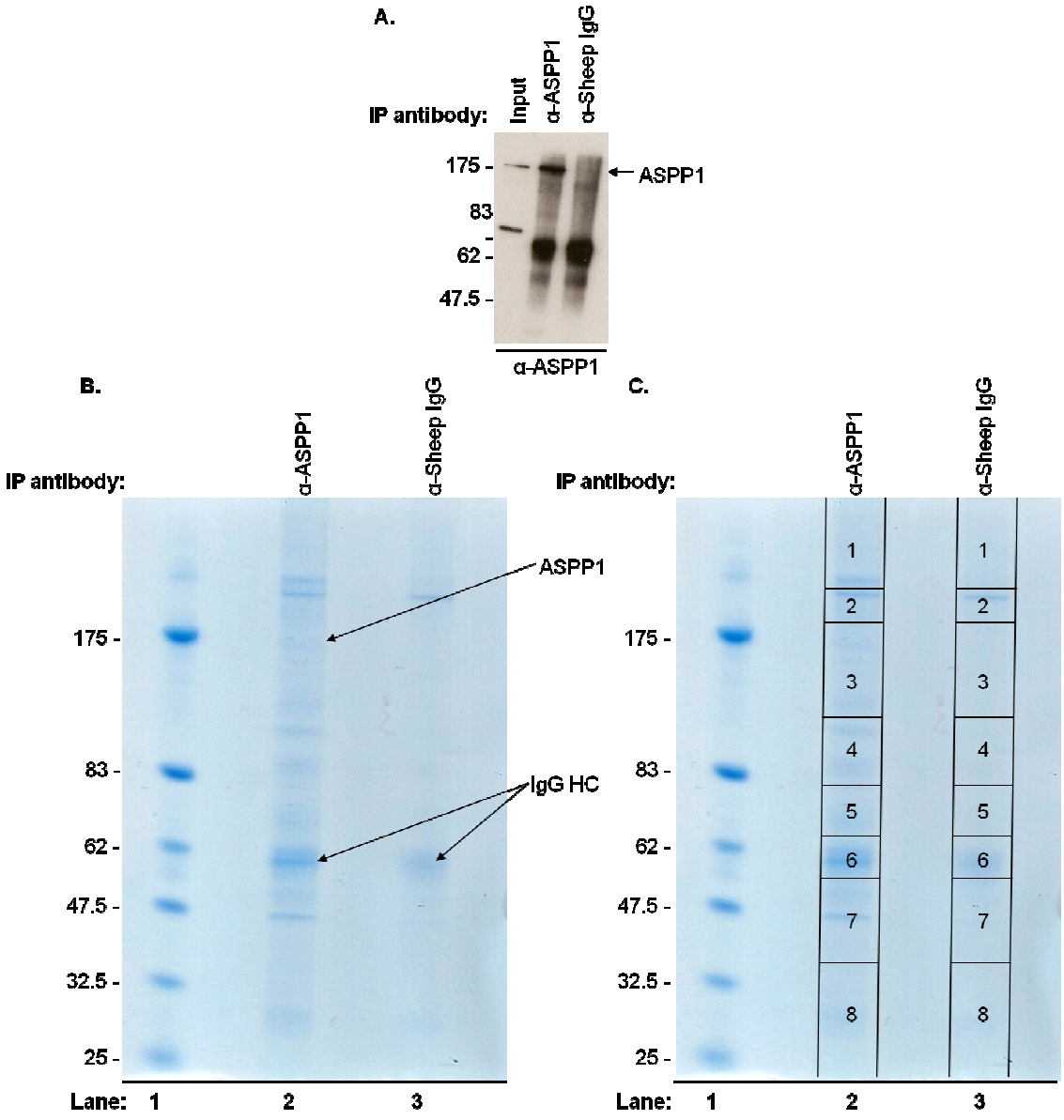

Figure 57. Immunoprecipitation of ASPP1 in Saos2 cells. Forty confluent T75 flasks of Saos2 cells were harvested, cell lysates prepared and incubated with α-ASPP1/Sheep IgG and dynabeads. After washing, samples were eluted by boiling in sample loading buffer. (A) Saos2 soluble cell lysate (Input) and immunoprecipitates were separated on 7% SDS PAGE and probed with α-ASPP1. (B) Remaining IP samples were resolved by SDS-PAGE (NuPAGE 4-12% Bis-Tris Gel) and ASPP1 and Sheep IgG interacting proteins were visualised by staining with SimplyBlue. Molecular weight size markers are shown on the left and in lane 1. (C) To determine protein identities the ASPP1 IP and control lanes were cut up in the fashion outlined.

6.3.2 Mass spectrometry results

To determine the identities of the ASPP1 interacting proteins, the two lanes (control Sheep IgG IP and ASPP1 IP) were divided into 8 slices as indicated in Figure 57C. The 8 slices were digested with trypsin, peptides were eluted and samples were analysed by liquid chromatography-mass spectronomy (LCMS). The digest was carried out by Karen

Lowden, the MS analysis by David Blinco, and the data analysis by Dr Achim Treuman, all members of the North East Proteome Analysis Facility (NEPAF), Newcastle University.

Proteins pulled down with the α-ASPP1 antibody are listed in Table 13. Proteins that were detected only in the ASPP1 IP lane, not in the control lane, are shown.

Gel slice	Swiss-Prot entry name	Accession number	Gene name	Protein ID	Nominal mass Mr
1	PYR1_HUMAN	P27708	CAD	CAD	242.8
1, 2, 3, 8	SC16A_HUMAN	O15027	SEC16A	Sec16A	233.4
1, 2, 3, 4	PLPL6_HUMAN	Q8IY17	PNPLA6	NTE	149.9
3	IQEC2_HUMAN	Q5JU85	IQSEC1	ARF-GEP$_{100}$	161.6
3	CYFP1_HUMAN	Q7L576	CYFIP1	CYPFIP1	145.1
3, 4, 6	ASPP1_HUMAN	Q96KQ4	PPP1R13B	ASPP1	119.5
3	SC24C_HUMAN	P53992	SEC24C	Sec24C	118..2
4	SC23A_HUMAN	Q15436	SEC23A	Sec23A	86.1
4	GRP75_HUMAN	P38646	HSPA9	Hsp70-9	73.6
4	HS71L_HUMAN	P34931	HSPA1L	Hsp70-Hom	70.3
6	RTN4_HUMAN*	Q9NQC3	RTN4	RTN4	129.9
6	TBA1A_HUMAN	Q71U36	TUBA1A	TUBA1A	50.1
6	PP1A_HUMAN	P62136	PPP1CA	PP1c$_{\alpha}$	37.5
6	CA198_HUMAN*		Uncharacterised protein		36.3
6	YBOX1_HUMAN	P67809	YBX1	YBX1	35.9
6, 7	SEC13_HUMAN	P55735	SEC13	Sec13	35.5
6	SYPL1_HUMAN*	Q16563	SYPL1	SYPL1	28.5
6, 7	ODO2_HUMAN	P36957	DLST	DLST	48.6
7	SCAM3_HUMAN	O14828	SCAMP3	SCAMP3	38.3
7	SCAM1_HUMAN	O15126	SCAMP1	SCAMP1	37.9
7	KCD15_HUMAN	Q96SI1	KCTD15	KCTD15	31.9
7	HAX1_HUMAN	O00165	HAX1	HAX-1	31.6
7	DIPA_HUMAN	Q15834	CCDC85B	DIPA	22.1
8	TCP4_HUMAN	P53999	SUB1	PC4	14.4
8, 4	DCD_HUMAN*	P81605	DCD	Dermcidin	11.3

Table 13. ASPP1-interacting proteins identified by LCMS in Saos2 cells. Identifications of uncertain significance are highlighted*. The BLAST search with CA198 did not indicate homology with any other human protein.

Interestingly, ASPP1 was identified in slices 3, 4 and 6. We would expect to pull full length ASPP1 protein out of slice 3 as this includes the 175kDa region. It is possible that the ASPP1 protein identified in slices 4 and 6 represent the smaller molecular weight bands that are often picked up on Westerns which we suspect are alternate ASPP1 isoforms or degradation products (see chapter 5, section 5.7.3). A number of other proteins, including Sec16A and NTE (Neuropathy target esterase), were also identified in multiple slices in the ASPP1 IP lane. Again it is possible that these may represent alternate isoforms of differing molecular weight, or these proteins may have degraded and we may be detecting smaller degradation products. Indeed multiple splice forms of

Sec16 have been identified which are expressed together in the same tissues (Watson et al., 2006).

In order to get an overall idea of the cellular processes in which ASPP1 is involved, the proteins identified by mass spectrometry were grouped according to their primary function and cellular locations upon preliminary assessment of the literature (summarised in Figure 58).

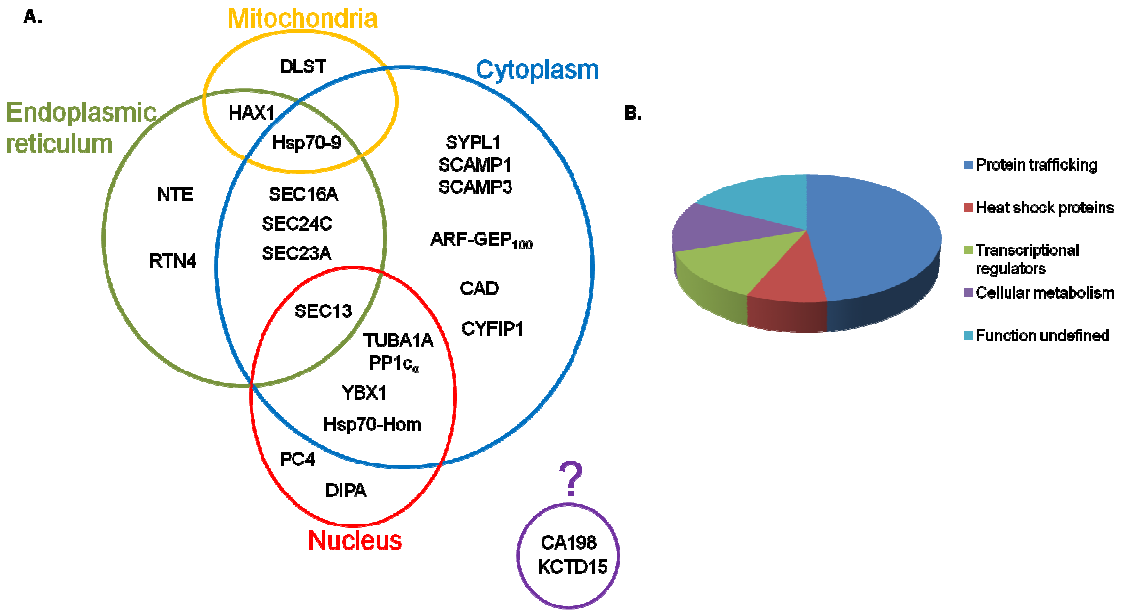

Figure 58. Summary of cellular location (A) and function (B) of ASPP1-interacting proteins in Saos2 cells. Sec13, Sec23A and Sec24C are components of the COPII coat protein complex, which transports proteins within the cell. They locate to the endoplasmic reticulum (ER) and associated vesicles in the cytoplasm. Sec16A locates to discrete locations on the ER membrane known as ER exit sites and acts as a scaffold for assembly of the COPII coat. It can however cycle on and off the ER membrane (Watson et al., 2006; Iinuma et al., 2007). Sec13 has also been observed to shuttle between the nucleus and the cytoplasm (Enninga et al., 2003). Neuropathy target esterase (NTE) is an ER resident phospholipase which is important in regulating ER-cargo traffic (Li et al., 2003a). ARF-GEP$_{100}$ is a guanine nucleotide-exchange factor which locates to the cytosol and is involved in endosomal membrane trafficking (Someya et al., 2001). The Secretory carrier-associated membrane proteins, SCAMP1 and SCAMP3 and synaptophysin-like protein 1 (SYPL1) locate to cytoplasmic transport vesicles. They often co-localise and participate in post-Golgi trafficking (Haass et al., 1996; Windoffer et al., 1999). TUBA1A, α-tubulin is a major constituent of microtubules. Microtubules are found in both the cytoplasm, where they form part of the cytoskeleton, and the nucleus, where they constitute the mitotic spindle. Cytoplasmic FMR1-interacting protein 1 (CYFIP1) is a cytosolic protein which regulates the actin cytoskeleton and appears to play a role in endosomal membrane trafficking from the Golgi (Anitei et al., 2010). PP1c$_{\alpha}$ (protein phosphatase 1 catalytic subunit alpha) is a catalytic subunit of a major eukaryotic phosphatase enzyme. It can be found in both the cytoplasm and nucleus. It is highly mobile in cells and can relocalise via interactions with other proteins (Cohen 2002). Heat shock 70 kDa protein 1-like (Hsp70-Hom) is predominantly cytoplasmic however, it appears to move to the nucleus in response to the stress of heat shock (Fourie et al., 2001). Heat shock 70 kDa protein 9 (Hsp70-9) resides in multiple subcellular sites including mitochondria, ER, plasma membrane, cytoplasmic vesicles and cytosol (Wadhwa et al., 2002a). Dihydrolipoamide succinyltransferase (DLST) is a mitochondrial enzyme involved in the Krebs cycle (Nakano et al., 1994). The CAD enzyme localises to the cytoplasmic compartment and participates in pyrimidine biosynthesis (Chaparian et al., 1988). HCLS1-associated protein X-1 (HAX-1) is mainly localised in mitochondria and to a lesser extent in ER and nuclear envelope (Suzuki et al., 1997). Reticulon-4 (RTN4) is an ER membrane

protein with unknown function (van de Velde et al., 1994). DIPA is a nuclear protein which plays a role in regulation of gene expression and cell proliferation (Bezy et al., 2005; Du et al., 2006). PC4 is a transcriptional regulator which locates to the nucleus (Conesa et al., 2010). YBX1 is a multi-functional protein which localises in both the cytoplasm and nucleus. It translocates to the nuclear compartment following cytotoxic stress (Koike et al., 1997) where it can act as a transcription factor. The function and subcellular localisation of the potassium channel tetramerisation domain containing 15 protein (KCTD15) is unknown. CA198 is also an uncharacterised protein.

This dataset clearly suggests that ASPP1 interacts with the protein transport machinery in the cell, implying ASPP1 plays a role in protein trafficking. A number of transcriptional regulators, metabolic enzymes and heat shock proteins were also identified. These proteins locate to both the cytosol and nucleus, and some reportedly shuttle between these cellular compartments.

6.3.3 Testing protein interaction between ASPP1 and alpha tubulin in Saos2 cells

One of the ASPP1-interacting proteins identified by mass spectrometry was α-tubulin (Gene name *TUBA1A*). Tubulin is the primary building block of microtubules which function as structural and mobile elements in intracellular transport, mitosis, flagella movement and the cytoskeleton. Tubulin is a heterodimer consisting of an alpha- and beta-tubulin subunit, both of which have a molecular weight of approximately 50kDa.

In an attempt to confirm the ASPP1:α-tubulin interaction, the IP experiment was repeated, this time using 36 T75 flasks of confluent Saos2 cells. However, upon repeating the experiment and probing the samples after Western blotting with an anti-α-tubulin antibody, α-tubulin protein was not detected as co-immunoprecipitating with ASPP1 (Figure 59).

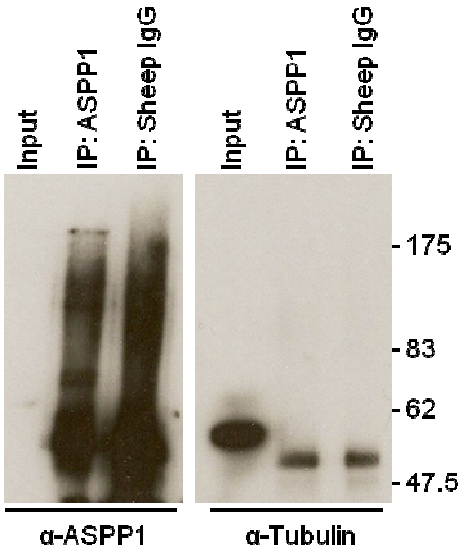

Figure 59. Testing co-immunoprecipitation of ASPP1 and α-tubulin in Saos2 cells. Soluble Saos2 cell lysate was incubated with either α-ASPP1 antibody or sheep IgG and Protein A Dynabeads. After washing, samples were eluted by boiling in sample loading buffer. Soluble Saos2 cell lysate (Input), and immunoprecipitates (IP) were separated on 7% SDS PAGE and probed with α-ASPP1 and α-tubulin. Antibody binding was detected using HRP-conjugated α-sheep and HRP-conjugated α-mouse secondary antibodies, respectively. The migration of molecular weight markers is indicated on the right.

6.3.4 Analysing the ASPP1:Sec16A interaction

A number of Sec proteins were pulled down specifically in the Saos2 ASPP1-IP. The Sec genes were first identified in a genetic screen in *Saccharomyces cerevisiae* aimed at identifying mutants that are defective in protein secretion (Deshaies et al., 1987; Deshaies et al., 1989). The Sec proteins identified by mass spectrometry in this screen interact with one another to form a large protein complex known as the COPII coat which is responsible for transporting proteins synthesised in the endoplasmic reticulum (ER) to the Golgi. For further information on COPII assembly and function see the review by Hughes and Stephens (2008).

Four Sec proteins, Sec13, Sec16A, Sec23A and Sec24C were identified in this screen suggesting that ASPP1 is somehow involved in this step of intracellular transport. In order to further investigate this we acquired an antibody and GFP-fusion construct specific to, and encoding, one of these proteins, Sec16A. Generation of this antibody and construct is described in Watson et al., (2006) and they were kindly given to us by Dr David Stephens (University of Bristol, UK).

Sec16A is a large (234kDa) protein which is bound to the cytosolic surface of the endoplasmic reticulum (ER) (Watson et al., 2006). It has been shown to be tightly associated with ER exit sites (ERES), which are long-lived, ribosome free sub-domains of the ER that are specialised for the production of COPII transport vesicles (Watson et al., 2006).

Firstly we wanted to determine whether or not ASPP1 and Sec16A co-localise in the cell. Presumably if these proteins directly interact with one another then full or partial co-localisation should be observed. Unfortunately, we were unable to detect either endogenous or over expressed Sec16A by Western using the α-Sec16A antibody suggesting it had deteriorated. We therefore decided to utilise the Sec16A-GFP construct to analyse cellular location.

6.3.3.1 Sec16A-GFP localisation

To ensure the Sec16A-GFP construct expressed and localised as expected, Sec16A-GFP alone was transfected into HeLa cells and incubated for 24 hours before checking for GFP fluorescence. Following confirmation of GFP expression, the cells were fixed in methanol and fluorescence images were taken using the DAPI and FITC channels on a Zeiss Axiovert fluorescent microscope (Figure 60).

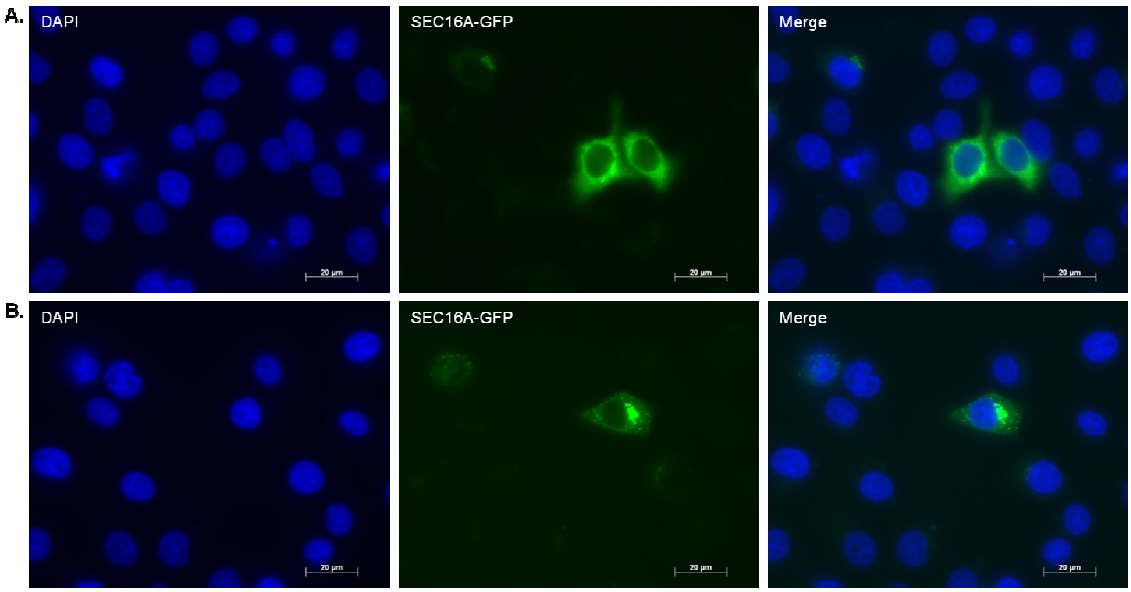

Figure 60. Fluorescence images of typical distributions of Sec16A-GFP in HeLa cells. 24 hours after transfection cells were fixed with methanol. The individual DAPI and FITC channels and a merge of both channels are shown. Nuclei are represented by blue DAPI stain. Scale bars represent 20µm. A) Transfected cells showing general cytoplasmic and perinuclear localisation of Sec16A-GFP. B) Transfected cell showing accumulation of perinuclear Sec16A-GFP with multiple small cytoplasmic concentrations.

In some cases we found Sec16A-GFP looked rather punctate (Figure 60B) while in others it seemed quite continuous around the nuclear envelope (Figure 60A). This is consistent with previous reports on Sec16A localisation. Watson et al., (2006) analysed localisation of both endogenous and GFP-tagged Sec16A. They observed both a membrane bound (ERES) pool in the juxtanuclear area, and a cytosolic pool, and they suggested Sec16A recycles on and off the ER membrane. Similarly, Iinuma et al., (2007) analysed Sec16A localisation using a Sec16A specific antibody and found in some cases it had a punctate pattern, with some concentration at the perinuclear region, and in other cases they found Sec16A exhibited diffuse cytosolic staining.

6.3.3.2 Endogenous ASPP1, ASPP1-V5 and Sec16A-GFP localisation

As our analysis of Sec16A-GFP localisation corresponded with previously published reports we utilised this construct to determine whether or not ASPP1 and Sec16A co-localise in the cell. Previous experiments analysing ASPP1 localisation using ectopically expressed V5-tagged ASPP1 and a α-V5 antibody worked well (data not shown). Therefore Sec16A-GFP was co-transfected into HeLa cells along with equal amounts of an ASPP1-V5 expression plasmid (gift from Professor Xin Lu, Ludwig Institute for Cancer Research, University of Oxford, UK). 24 hours after transfection cells were fixed, permeabilised and stained with the α-V5 antibody (Figure 61).

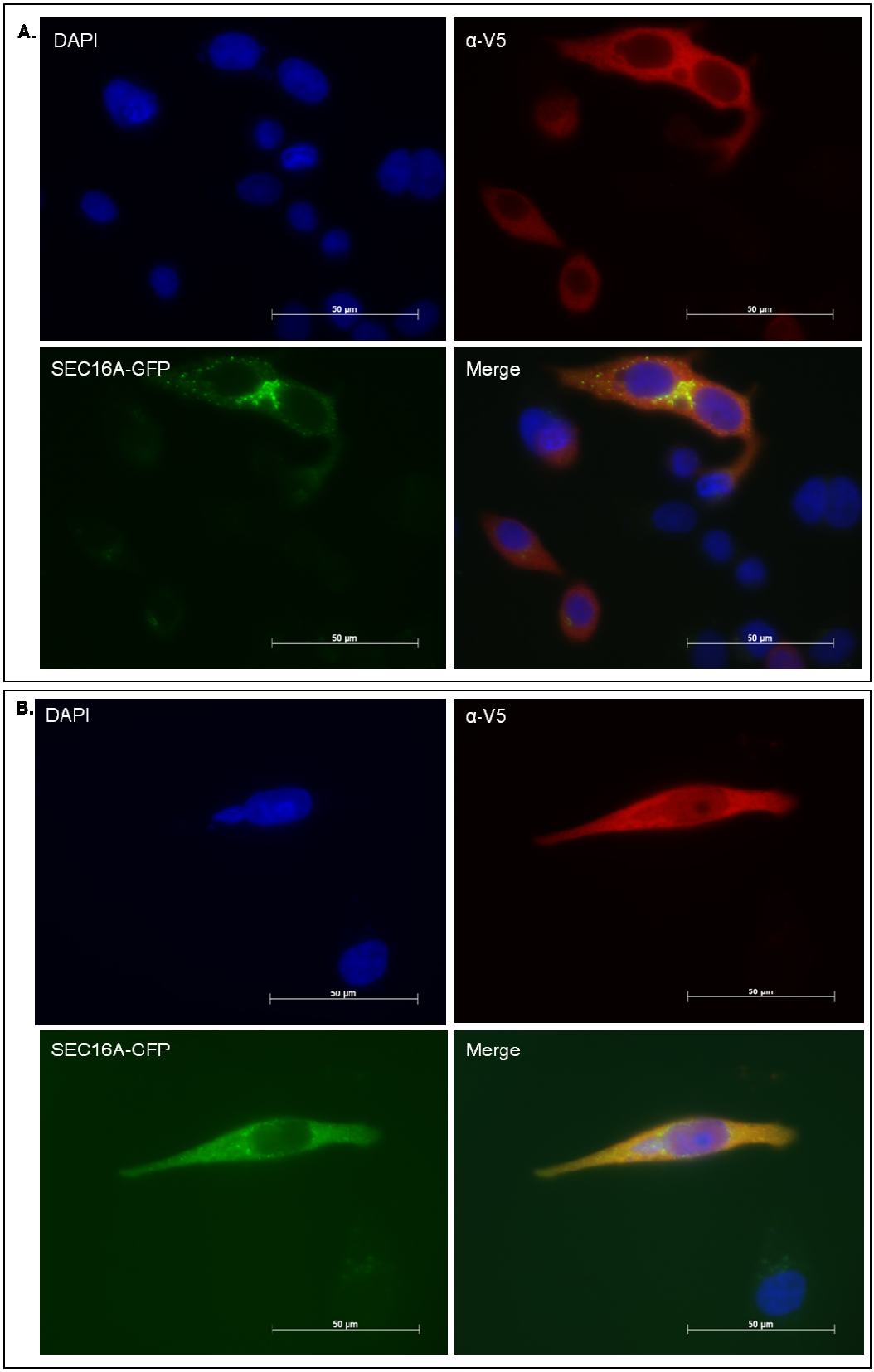

Figure 61. Localisation of ectopically expressed ASPP1-V5 and Sec16A-GFP in HeLa cells. 24 hours after transfection cells were fixed, permeabilised and stained with the α-V5 antibody. ASPP1-V5 was visualised with an Alexa Flour 594 (red) conjugated α-mouse secondary antibody. DNA was visualised with DAPI (blue) and Sec16A-GFP via FITC. (A) Transfected cells showing accumulation of perinuclear Sec16A-GFP with multiple small cytoplasmic concentrations. (B) Transfected cells showing general cytoplasmic localisation of Sec16A-GFP. Scale bars represent 50µm.

ASPP1-V5 had a general cytoplasmic distribution, which is consistent with previous reports (Thornton 2005). Again both punctate, cytoplasmic and perinuclear localisation of Sec16A-GFP was observed (Figure 61A and B). Despite the primary cytoplasmic localisation of both proteins, the bulk of ASPP1 and Sec16A-GFP did not co-localise (Figure 61A). In some cells however, partial overlap of proteins was observed (Figure 61B).

6.3.3.3 Sec16-GFP Immunoprecipitation

Visualisation of ASPP1 and Sec16A-GFP by immunofluorescence suggested that in some cells there appeared to be partial co-localisation. In order to test for protein-protein interactions we attempted to immunoprecipitate ectopically expressed Sec16A-GFP from HEK293 cells using the α-GFP antibody.

In one experiment Sec16A-GFP was transfected alone in attempt to determine whether or not endogenous ASPP1 immunoprecipitates with Sec16A-GFP. In a second experiment Sec16A-GFP was co-transfected with ASPP1-V5, to determine whether or not both proteins needed to be over-expressed in order to detect an interaction. One six well plate of HEK293 cells was used for each immunoprecipitation. 24 hours after transfection, and upon confirmation of GFP fluorescence, cell lysates were prepared. Half of the cell lysate from each transfection was incubated with the α-GFP antibody and the other half without any antibody as a negative control. After an overnight incubation lysates +/- GFP antibody were incubated with Protein A Dynabeads and immunoprecipitated (see methods, section 2.3.10).

To determine whether or not the Sec16A-GFP IP was successful, immunoprecipitates were first separated by SDS-PAGE and subject to Western blot analysis, probing with the α-GFP antibody (Figure 62). Unfortunately, after repeated attempts, even though Sec16A-GFP was being expressed efficiently (see input lane in Figure 62) I was unable to immunoprecipitate any notable amount of Sec16A-GFP. Blots shown in Figure 62 were stripped and re-probed with ASPP1 antibody and V5 antibody in the hope that enough Sec16A-GFP had immunoprecipitated to detect ASPP1/ASPP1-V5 co-immunoprecipitation. However, neither endogenous nor ectopically expressed ASPP1 were present in the IP lanes. We did note that expression of Sec16-A GFP was reduced when co-expressed with ASPP1-V5.

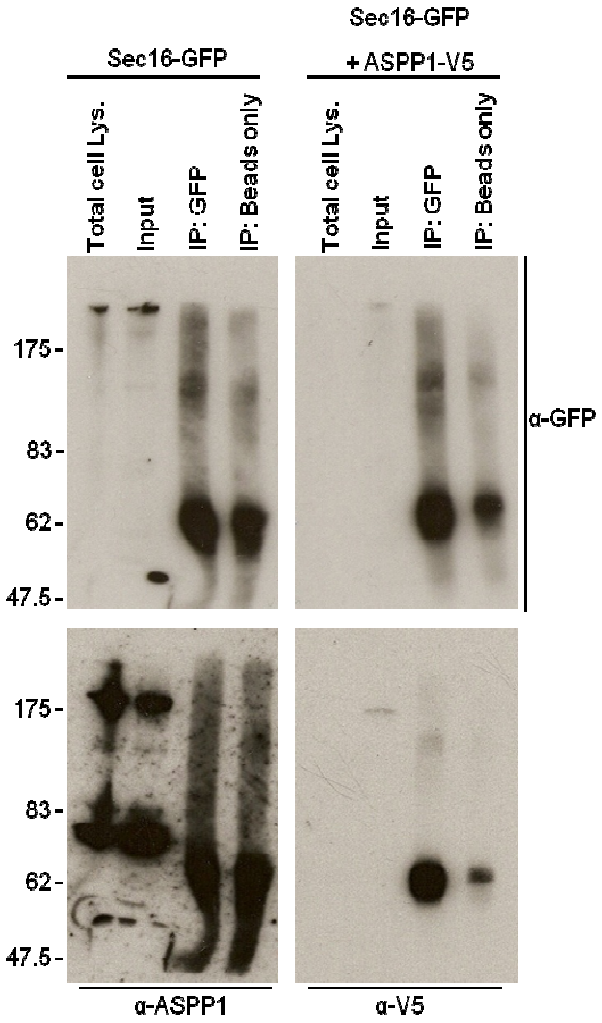

Figure 62. Testing co-immunoprecipitation of Sec16A-GFP, endogenous ASPP1 and ectopically expressed ASPP1-V5 in HEK293 cells. Soluble HEK293 cell lysate was incubated either with or without α-GFP antibody and Protein A Dynabeads. After washing, samples were eluted by boiling in sample loading buffer. Total HEK293 cell lysate, soluble cell lysate (input), and immunoprecipitates (IP) were separated on 7% SDS PAGE and probed with α-GFP and HRP-conjugated α-mouse secondary antibody to visualise Sec16A-GFP. Blots were then stripped and re-probed with either α-ASPP1 or α-V5, and α-sheep and HRP-conjugated α-mouse secondary antibodies, respectively. The migration of molecular weight markers is indicated on the left.

6.4 Generation of an inducible ASPP1 HEK293 cell line

In order to further follow up on the mass spectrometry results obtained for the endogenous ASPP1 Saos2 IP, rather than obtaining antibodies to each of the hits and repeating IP experiments, we wanted to analyse ASPP1 interactors in a second human cell line with the hope that we would identify common interacting proteins, giving us a better indication of the protein complexes in which ASPP1 is involved.

One of the main problems encountered when trying to identify ASPP1 interacting proteins endogenously was the inherently low ASPP1 expression/protein level. Despite

using large quantities of cells (which are time consuming and expensive to grow and maintain), the amount of ASPP1 protein immunoprecipitated was small. As a result, we were unable to distinguish any specific ASPP1 interacting protein bands on the SimplyBlue stained gel and expensive high sensitivity analysis was necessary. Also, due to low ASPP1 abundance we were less likely to identify low abundance interactors. In order to isolate large amounts of ASPP1 protein and assay interacting proteins, we wanted to create a stable ASPP1-inducible cell line, whereby we could 'switch on' ASPP1 expression in order to produce large amounts of ASPP1 protein. To do this we utilised the Flp-In HEK293 cell line (Invitrogen).

This system permits the generation of stable, tetracycline-regulated, inducible cell lines by taking advantage of a *Saccharomyces cerevisiae* derived DNA recombination system. This DNA recombination system utilises a recombinase enzyme called Flp and a FRT site which serves as a binding and cleavage site for the Flp recombinase.

To generate an inducible cell line, the gene of interest is cloned into a specialised Flp-In expression vector (pCDNA5) which is co-transfected with a plasmid encoding Flp recombinase (pOG44) into Flp-In HEK293 cells. These cells are engineered to continually express the Tet repressor and they contain a stably integrated FRT site in their genome. Co-expression of the Flp-In expression vector containing the gene of interest, and the Flp recombinase, results in targeted integration of the expression vector in the same locus in every cell.

The Flp-In expression vector is designed so that the gene of interest is expressed under the control of a tetracycline inducible promoter. Hence, addition of tetracycline to the culture medium ensures homogeneous and high level gene expression.

Firstly, we needed to clone the ASPP1 cDNA sequence into the specialised inducible expression vector. We utilised a modified version of this vector (pCDNA5-FLAG) which was kindly given to us by Dr Andrew Knox (Institute for Cell and Molecular Biosciences, Newcastle University, UK). Dr Andrew Knox cloned a 2x FLAG Tag and a His-Tag between the *Kpn*I and *Bam*HI sites of pCDNA5 thus creating an in-frame N-terminal FLAG-His-fusion protein. Addition of the epitope tags bypasses the need for an efficient antibody specific to the expressed protein for purification and analysis purposes.

We know from previous experience that α-FLAG affinity resin (Sigma) immunoprecipitates FLAG fusion proteins very efficiently, therefore we wanted to utilise this in the hope that it would be a more efficient method to pull down large amounts of ASPP1 protein.

6.4.1 Cloning ASPP1 into the pCDNA5-FLAG vector

To construct ASPP1-FLAGpCDNA5, full length ASPP1 was amplified by PCR (from the ASPP1-V5 construct) using primers ASPP1-F(*Bgl*II) and ASPP1-R(*Xho*I). Due to the size of the amplification product (3.4Kb) a high fidelity DNA polymerase (Phusion Taq) was used as well as a longer extension period (3.5 minutes). The *Bgl*II/*Xho*I digested PCR product was then ligated into complementary sites in pCDNA5-FLAG before selection on ampicillin-LB plates. Colonies were then screened by PCR using an ASPP1-specific forward primer (ASPP1(1839)F) and a pCDNA5 specific reverse primer (BGHrev). Insert positive colonies were further grown overnight before plasmid purification. To ensure that the pCDNA5-FLAG clone contained the correct full length ASPP1 sequence, it was sequenced from both the 5′ end 3′ ends using the ASPP1-F(*Bgl*II) and BGHrev primers, respectively.

6.4.2 Stable transfection of Flp-In HEK293 cells with ASPP1-FLAGpCDNA5

The pCDNA5-FLAG vector containing the ASPP1 coding sequence was then co-transfected with pOG44 into Flp-In HEK293 cells (see methods, section 2.5.5). The Flp-In HEK293 cells were kindly given to us by Dr Nicholas Watkins (ICaMB, Newcastle University, UK). When co-transfected, the Flp recombinase is expressed from pOG44 and catalyses a homologous recombination event between the FRT sites in the host cell line and the pCDNA5-FLAG expression vector, resulting in the integration of ASPP1-FLAGpCDNA5 into the genome. As a negative control, cells were co-transfected with the empty pCDNA5-FLAG vector and pOG44.

Approximately forty eight hours after transfection, stably transfected cells were selected for by adding the selective antibiotic hygromycin B to the culture medium. The pCDNA5-FLAG vector contains a hygromycin resistance gene, therefore integration of the expression construct confers hygromycin resistance to the cells.

Over the following weeks, dead cells were removed by washing, the medium was changed and hygromycin selection was maintained. Cells were monitored for the development of clonal colonies daily and after approximately two weeks of selection, ASPP1-FLAGpCDNA5 and pCDNA5-FLAG colonies were selected and re-plated.

Once hygromycin clones were selected and sufficiently established we were then ready to induce ASPP1-FLAG expression.

6.4.3 Testing induction of ASPP1-FLAG

Before commencing with the FLAG-IP we first wanted to ensure that the ASPP1-FLAG protein expressed efficiently and determine the time point at which to harvest cells for IP. Considering ASPP1 is a reported pro-apoptotic protein, we wanted to check whether continually elevated levels resulted in cell death.

A 6 well plate of ASPP1 Flp-In HEK293 cells and pCDNA5 Flp-In control cells were grown to ~60% confluence. To induce expression, tetracycline was added to each well (final concentration 1μg/ml). Over the next 3 days cells were harvested every 12 hours. Harvested cells were lysed and subjected to SDS-PAGE and Western blot. Blots were probed with the α-FLAG antibody and α-tubulin (Figure 63).

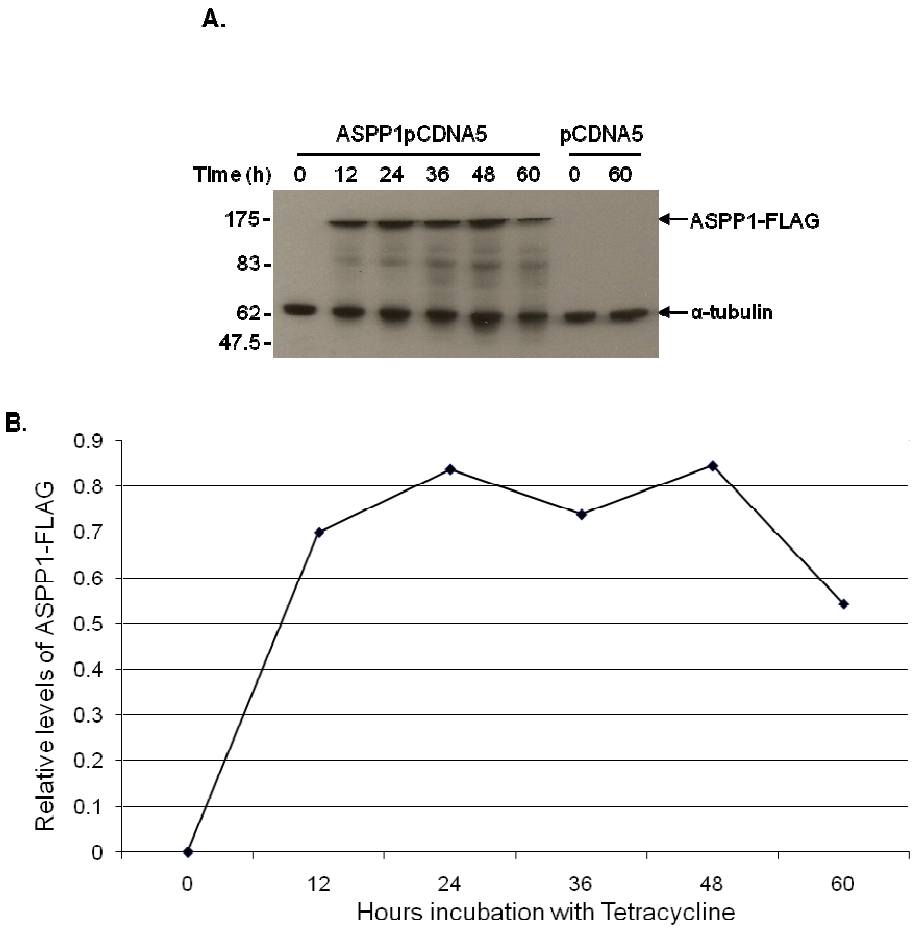

Figure 63. Induction of ASPP1-FLAG expression in Flp-In HEK293 cells. (A) Cell lysates were prepared every 12 hours after addition of 1µg/ml of tetracycline, and the level of ASPP1-FLAG was measured by immunoblotting with α-FLAG antibody and α-tubulin for a loading control. Both antibodies were detected using the HRP-conjugated α-mouse secondary antibody. Two separate cell harvests (0 hour and 60 hours) of the negative control pCDNA5-only stable cells are also presented. The migration of molecular weight markers is indicated on the left. (B) The graph shows the relative amount of ASPP1-FLAG protein compared to the α-tubulin loading control.

The Western shows that the ASPP1-FLAG protein band migrated at a molecular weight consistent with the size of the ASPP1 protein (175kDa), and it was clear that ASPP1-FLAG was efficiently expressed 12 hours after tetracycline addition. Maximal ASPP1-FLAG protein levels were observed at the 24 hour and 48 hour time points (see graph in Figure 63). Also, after 60 hours cells looked healthy, implying that elevated ASPP1 expression was not having a detrimental effect.

6.4.4 Immunoprecipitation of ASPP1-FLAG

Cell lysate was prepared from two confluent T75 flasks of both ASPP1-FLAGpCDNA5 and control cells which had been induced with tetracycline for 48 hours. FLAG-fusion

protein was immunoprecipitated using α-FLAG affinity resin (see methods, section 2.3.11).

The resulting samples from the FLAG immunoprecipitations were firstly analysed by Western to ensure the ASPP1-FLAG fusion protein was immunoprecipitating efficiently (Figure 64A). A strong ASPP1-FLAG band was detected with α-FLAG antibody in the IP lane from the ASPP1-FLAGpCDNA5 cells. ASPP1-FLAG was also present in the IP supernatant showing us that an ample amount of tagged ASPP1 protein was expressed. This band was absent from our control IP using the cells containing the empty pCDNA5-FLAG construct, as expected. Remaining IP samples were resolved on a 4-12% gradient gel and protein was visualised with SimplyBlue SafeStain (Figure 64B).

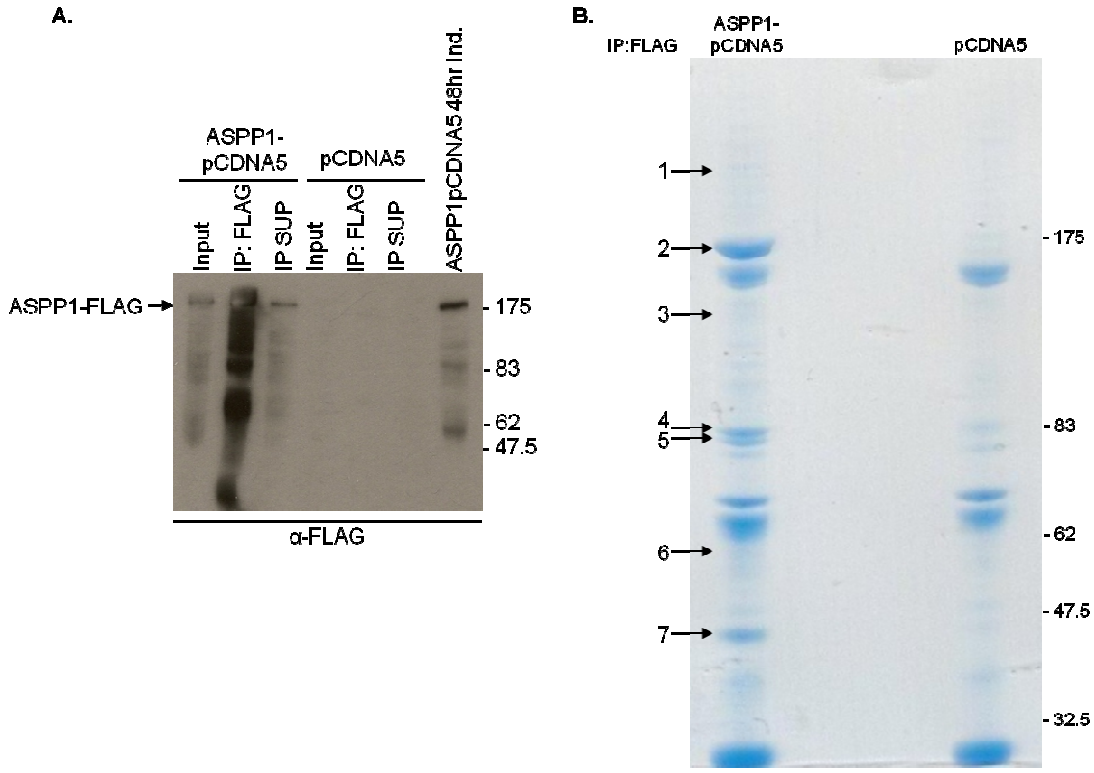

Figure 64. Immunoprecipitation of ASPP1-FLAG fusion protein. (A) After 48 hours, induced cell lysates were prepared and incubated with α-FLAG affinity resin. After washing, samples were boiled, electrophoresed on a 7% SDS-polyacrylamide gel and analysed by immunoblotting with α-FLAG antibody. (B) FLAG immunoprecipitation samples resolved on a NuPAGE 4-12% Bis-Tris protein gel and stained with SimplyBlue. Numbered protein bands (1-7) were excised from the gel and subjected to analysis by mass spectrometry. The migration of molecular weight markers is indicated on the right.

The immunoprecipitating ASPP1-FLAG fusion protein was clearly observable on the stained gel (band 2). In comparison to our endogenous ASPP1 IP in Saos2 cells (see Figure 57), this IP was much more efficient.

6.4.5 Analysis of ASPP1-FLAG interactors by mass spectrometry

Protein bands specific to the ASPP1-FLAG IP were predicted to result from proteins that specifically co-immunoprecipitated with the ASPP1-FLAG fusion protein. Protein bands 1-7 were chosen as they were the strongest in intensity compared to the FLAG only control IP lane (Figure 64B). We also included the suspected ASPP1-FLAG band (Band 2). To determine the identity of these proteins, the seven bands were excised from the gel and digested with trypsin using the Trypsin profile IGD Kit (see methods 2.3.12). Samples were then subjected to mass spectrometry analysis by Dr Kaveh Emami at the North East Proteome Analysis Facility, Newcastle upon Tyne.

Of the seven bands sent for peptide mass fingerprinting, six were positively identified (Figure 65). The significance threshold was set at $p<0.05$.

Band	Swiss-Prot entry name	Accession number	Gene name	Protein ID	Peptides matched	Nominal mass Mr	Sequence coverage
1	No significant hits to report						
2	ASPP1_HUMAN	Q96KQ4	PPP1R13B	ASPP1	27	119492	24%
3	HSP74_HUMAN	P34932	HSPA4	Hsp74	3	94240	9%
	ASPP1_HUMAN	Q96KQ4	PPP1R13B	KIAA0771	3	103002	7%
4	HSP7C_HUMAN	P11142	HSPA8	Hsc70	27	70761	31%
5	HSP71_HUMAN	P08107	HSPA1A	HSP72	22	69995	25%
6	YBOX1_HUMAN	P67809	YBX1	YBX1	5	35964	28%
7	PP1B_HUMAN	P62140	PPP1CB	PP1cβ	5	37225	9%

Figure 65. Proteomic analysis of ASPP1-FLAG interacting proteins. The identities of ASPP1-FLAG interacting proteins are listed in the table. Swiss-Prot names and primary accession numbers for proteins are shown. The distribution of identified peptides (highlighted red) matching the protein sequence for each band is shown.

There were no proteins identified in band 1. As expected, band 2 was correctly identified as ASPP1, however, ASPP1 was also identified in band 3. Again, it is possible that this may be an alternate ASPP1 isoform or a product of proteolytic degradation. Alternatively this may be the result of cross-contamination when cutting bands 2 and 3.

There were three different heat shock proteins positively identified from bands 3, 4 and 5, Hsp74, Hsc70 and Hsp72. Protein band 6 was identified as Y box binding protein 1 (YBX1), which was also pulled out in the endogenous ASPP1 IP in Saos2 cells, and band 7 was identified as Protein phosphatase 1 beta ($PP1c_{\beta}$).

By SimplyBlue staining, the levels of co-precipitated Hsc70, Hsp72 and $PP1c_{\beta}$ were approximately half the level of immunoprecipitated ASPP1-FLAG, and there was considerably less Hsp74 and YBX1 present.

A brief description of each of the ASPP1-FLAG interactors identified in this experiment follows. The cellular function of each of these proteins is discussed further in the discussion.

Heat shock 70 kDa protein 4 (HSP74)

Protein band 3, which ran between the 175 and 83 kDa markers, was positively identified as Heat shock 70 kDa protein 4 (HSP74). This protein, encoded by the *HSPA4* gene, was originally reported as a member of the heat shock protein 70 family (Fathallah et al., 1993). However, it was later found to belong to the Hsp110 family and is equivalent to the mouse apg-2 protein (Kaneko et al., 1997).

Heat shock 70 kDa protein 8 (Hsc70)

Band 4, running just below the 83 kDa marker, was identified as Hsc70. Hsc70 is a 74kDa protein encoded by the *HSPA8* (*heat shock 70kDa protein 8*) gene. Two alternatively spliced variants have been characterised to date. When analysing the sequence coverage of the peptides identified in this band, one of the peptides was specific to isoform 1, the larger of the two isoforms with an extra 153 amino acids in the N-terminal half of the protein. We cannot rule out the possibility that isoform 2 is also present in this band, however it is likely that this smaller isoform would migrate faster.

Heat shock 70 kDa protein 1A/1B (Hsp72)

Band 5, another strong band running closely with the Hsc70 band, was identified as heat shock 70kDa protein 1, another member of the heat shock protein 70 family, often known as Hsp72 or Hsp70. It is a 70kDa protein which is encoded by the *HSPA1A* gene.

Y box binding protein 1 (YBX1)

Band 6, migrating below the 62kDa marker, was identified as Y-box binding protein 1 (YBX1). YBX1, encoded by the *NSEP1* gene, is member of the cold shock family of proteins that contain a highly conserved nucleic acid binding motif. It is a 47kDa protein which can bind to double-stranded and single-stranded DNA and RNA. It is involved in a variety of cellular functions including regulation of transcription, DNA repair and stress responses to extracellular signals. The multiple functions of YBX1 are reviewed by Kohno et al., (2003). YBX1, like ASPP1, has also been shown to interact with p53 and regulate its activity (Okamoto et al., 2000).

Protein phosphatase (PP1)-beta catalytic subunit (PP1c$_\beta$)

Band 7, a strong band, corresponded to PP1c$_\beta$. This protein, encoded by the *PPP1CB* gene, is one of the three catalytic subunits of the serine/threonine- protein phosphatase 1. PP1 is known to be involved in the regulation of a variety of cellular processes (see summary and discussion for further information).

6.4.6 Testing protein interaction between ASPP1 and Hsp72

To confirm the novel protein-protein interaction detected between ASPP1 and Hsp72, the ASPP1-FLAG IP experiment was repeated. Again, ASPP1 Flp-In HEK293 cells and control cells were induced for 48 hours, cell lysates prepared and incubated with FLAG-affinity resin. Immunoprecipitates were subjected to immunoblot analysis. Probing with α-FLAG revealed that ASPP1-FLAG immunoprecipitated efficiently as expected. The Western was then stripped and re-probed with an α-Hsp72 antibody (Figure 66) which was kindly given to us by Professor Anne Dickinson (Haematological Sciences, Institute of Cellular Medicine, Newcastle upon Tyne).

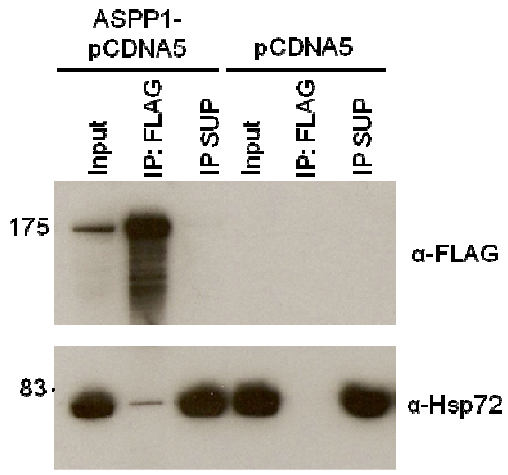

Figure 66. Co-immunoprecipitation of ASPP1-FLAG and Hsp72 in Flp-In HEK293 cells. 48 hours after tetracycline induction, cell lysates were prepared and incubated with α-FLAG affinity resin. After washing, samples were boiled, electrophoresed on a 7% SDS-polyacrylamide gel, and subjected to Western blotting. The blot was first probed with α-FLAG antibody to ensure the IP was successful. The blot was then stripped and re-probed with α-Hsp72. In both cases, antibody binding was detected using a HRP-conjugated α-mouse secondary antibody. The migration of molecular weight markers is indicated on the left.

A Hsp72 band was clearly present in the ASPP1-FLAG IP and absent from the control thus confirming that ASPP1-FLAG and Hsp72 co-immunoprecipitate. Comparing the Hsp72 band in the IP and IP supernatant lanes (IP SUP) shows that only a small proportion of the Hsp72 protein present in the cell was pulled down in the ASPP1-FLAG complex.

6.4.7 Testing protein interaction between ASPP1 and YBX1

Considering YBX1 was identified in both the Saos2 and Flp-In HEK293 screens, and given it is a p53 interacting protein with a role in apoptosis, we were keen to follow up on this interaction. We therefore acquired a YBX1-specific antibody, a kind gift from Professor Anthony Braithwaite (Children's Medical Research Unit, University of Sydney, Australia). Generation of this antibody is described in Cohen et al., (2009). In order to confirm the interaction detected between ASPP1 and YBX1, the ASPP1-FLAG IP samples and the endogenous ASPP1 IP from Saos2 cells, presented in Figures 66 and 59 respectively, were electrophoresed on a 10% polyacrylamide gel and analysed by Western blot using the α-YBX1 antibody (Figure 67).

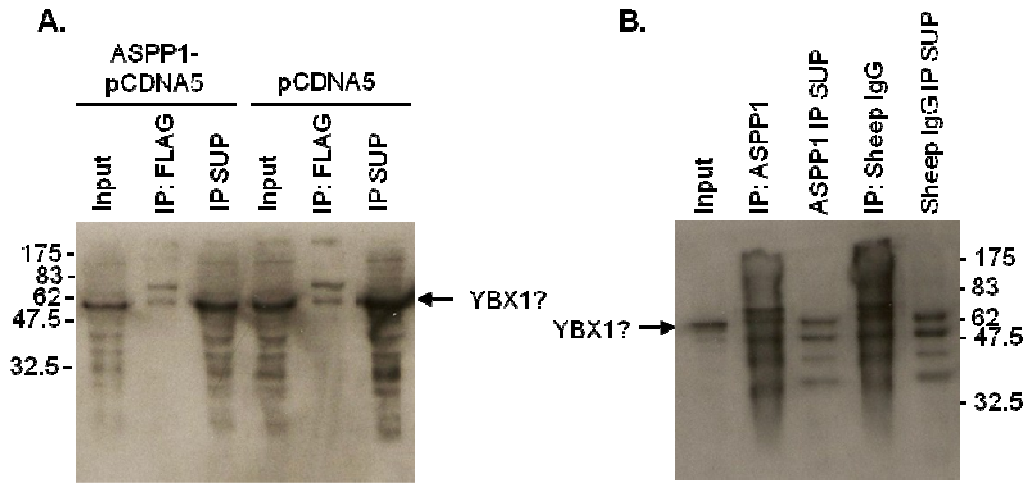

Figure 67. Testing co-immunoprecipitation between ASPP1 and YBX1. (A) FLAG-IP samples from the Flp-In293s and (B) endogenous ASPP1 IP from Saos2 cells were ran on a 10% SDS-polyacrylamide gel and probed with α-YBX1 and HRP-conjugated α-rabbit secondary.

A band of the expected size (~47kDa) was clearly visible in the input and IP supernatant lanes in both the ASPP1-FLAG, and control immunoprecipitations (Figure 67A). A faint band of approximately equal size is observable in both the ASPP1-FLAG IP and pCDNA5-FLAG IP lanes. A similar result was observed with the Saos2 IP (Figure 67B). This suggests that YBX1 is interacting non-specifically with the FLAG epitope and the Sheep IgG antiserum. However, only proteins which were present in the Saos2 ASPP1-IP and absent from the Sheep IgG control were included in our dataset (Table 13) thus it is unlikely that this is YBX1. It is possible that these bands are IgG heavy chain as this has a molecular weight of approximately 50kDa. Thus, although we cannot conclude from these Westerns that ASPP1 and YBX1 interact nor can we exclude the possibility.

6.5 Summary and discussion

In attempt to identify the major binding partners of ASPP1 and better understand how ASPP1 functions *in vivo* we analysed positive hits from an ASPP1 yeast 2-hybrid screen and took a proteomic approach to elucidate proteins co-immunoprecipitating with both endogenous and ectopically expressed ASPP1.

Twenty ASPP1 interacting proteins were identified from the human testes cDNA library yeast 2-hybrid screen. Two of these proteins, the E3 ubiquitin ligase SIAH1 and the protein phosphatase PP1cγ were previously identified ASPP1 interactors. The ASPP1:SIAH1 interaction was detected in both the SIAH1 and ASPP1 testes yeast 2-

hybrid screens (carried out by Dr Julian Venables and Dr Jared Thornton, respectively), however SIAH1 was not found to co-immunoprecipitate with ASPP1 from Saos2 cells or Flp-In HEK93 cells. It is tempting to speculate that the ASPP1:SIAH1 interaction may be specific to human testes, however the SIAH1:ASPP1 interaction *in vivo* is likely to be transient hence it is unlikely that we would pull SIAH1 down in complex with ASPP1.

The remaining 18 proteins identified in the yeast 2-hybrid screen represented novel interactors. A number of these proteins are highly expressed in the testes and appear to play an important role in spermatogenesis. For example, clusterin is produced abundantly by the Sertoli cells which line the walls of the seminiferous tubules. It is associated with both apoptosis and cell survival and is often proposed as a regulator of germ cell fate.

We were unable to detect an interaction between clusterin and ASPP1 when ASPP1 protein was immunoprecipitated from mouse testes tissue (Figure 55). However, although ASPP1 is expressed in the same germ cell types in human and murine testes, in humans ASPP1 locates to the nucleus and in mice it is cytoplasmic (Thornton et al., 2006). Therefore it is possible that the ASPP1-CLU interaction occurs only in the human testes.

Other proteins identified with a role in spermatogenesis included SPATS1 (spermatogenesis associated serine rich-1 protein), a highly conserved testis-specific protein which appears to play an important role in meiosis (Capoano et al., 2010), and Protamine 2, which is one of the most abundant nuclear sperm proteins found in humans and mice. Protamines replace histones during spermatogenesis and are essential for DNA condensation and stabilisation in the sperm head (Carrell et al., 2007).

Thus, results from the yeast 2-hybrid screen imply that ASPP1 may play an important role in germ cell development in the testes. This is consistent with ASPP1 being a SIAH1 regulated protein as the murine homolog, Siah1a, is essential for germ cell development.

In order to further characterise ASPP1 function *in vivo,* and identify protein complexes in which ASPP1 was involved, proteins co-immunoprecipitating with endogenous ASPP1 from Saos2 cells, and with ectopically expressed FLAG-tagged ASPP1 from the

inducible Flp-In HEK293 cells, were elucidated by mass spectrometry and as a result of these experiments a diverse set of interacting proteins were identified.

One common hit from all 3 of the ASPP1 screens were the catalytic subunits of protein phosphatase 1 (PPI), a major eukaryotic serine/threonine specific phosphatase. The ASPP-PP1 interaction was previously identified by Helps and colleagues (1995) who showed that 53BP2, the C-terminal 528 amino acids of ASPP2, can inhibit PP1 activity. ASPP1 and ASPP2 are approximately 49% homologous, with the highest regions of homology at their N- and C-terminal ends, thus it was not unexpected that ASPP1 would also interact with PP1.

Four mammalian PP1 catalytic (PP1c) gene products have been identified, designated $PP1c_{\alpha}$, $PP1c_{\beta}$, $PP1c_{\gamma1}$ and $PP1C_{\gamma2}$, the latter two arising from alternative splicing. The catalytic subunits have ~90% amino acid sequence identity. Through their interaction with various proteins, the PP1 subunits are believed to control an array of cellular functions, including gene transcription, translation, RNA splicing, metabolism, cell cycle progression, and apoptosis. The multifunctional roles of PP1 are reviewed by Cohen (2002), Garcia et al., (2003) and Ceulemans and Bollen (2004).

Intriguingly, three different PP1 catalytic subunits were pulled out of each of our ASPP1 screens (Table 14). PP1cγ was identified in the testes yeast 2-hybrid screen, $PP1c_{\alpha}$ in the Saos2 screen, and $PP1c_{\beta}$ in the Flp-In 293 screen. The original ASPP-PP1 interaction published by Helps et al., (1995) was identified via yeast 2-hybrid using the catalytic subunit, $PP1\gamma_1$, and they confirmed this interaction *in vitro*. Owing to the high level of amino acid sequence conservation of the catalytic subunits, it is perhaps not surprising that we found ASPP1 interacts with each of them. Also, PP1c isoforms possess distinct tissue distribution and subcellular locations (Shima et al., 1993; Andreassen et al., 1998) which may explain why we pulled out different isoforms in each of our screens.

Gene Symbol	Description	Protein ID	Identified ASPP1:PP1c interaction
PPP1CA	Protein phosphatase 1, catalytic subunit, alpha isoform	$PP1c_{\alpha}$	ASPP1 IP in Saos2 cells
PPP1CB	Protein phosphatase 1, catalytic subunit, beta isoform	$PP1c_{\beta}$	ASPP1-FLAG IP in Flp-In HEK293 cells
PPP1CC	Protein phosphatase 1, catalytic subunit, gamma isoform	$PP1c_{\gamma1}$/$PP1c_{\gamma2}$	Human testes Y2H screen and Helps et al., 1995

Table 14. The *PP1c* genes and protein products. The catalytic subunits identified in the ASPP1-protein

interactor screens are shown.

Interestingly, the PP1cγ_2 isoform is predominantly expressed in the testes and we identified the gamma isoform in our testes yeast 2-hybrid screen (Vijayaraghavan et al., 1996). PP1cγ_2 is a key enzyme in mammalian spermatozoa and a number of regulatory proteins that regulate PP1cγ_2 in spermatozoa have been identified (Chakrabarti et al., 2007). Targeted disruption of the *Ppp1cc* gene, which encodes both the PP1cγ_1 and PP1cγ_2 isoforms results in male infertility in mice (Varmuza et al., 1999). Chakrabarti et al., (2007) studied the localisation of the PP1 isoforms in murine testes and observed that PP1cγ_2 was prominently expressed in the cytoplasm of secondary spermatocytes, round spermatids, and elongating spermatids, whereas expression was weak or absent in spermatogonia, and interstitial cells. Similarly, analysis of ASPP1 localisation in mouse testes by Thornton et al., (2006) revealed that ASPP1 is present in the cytoplasm of round spermatids and is absent in the elongating spermatids and spermatogonia.

Given that ASPP1 and PP1cγ_2 are present at elevated levels in mouse testes, are expressed at similar stages of spermatogenesis and Helps et al., (1995) demonstrate that ASPP2 can affect PP1 activity, it is possible that ASPP1 may add to the list of PP1cγ_2 regulatory proteins in the mouse testes. As noted earlier, ASPP1 is found in the nuclei rather than the cytoplasm in human testes therefore it would be interesting to analyse PP1cγ expression in human testes too. We can also propose that ASPP1 is a regulator of PP1c$_\alpha$ in Saos2 cells and PP1c$_\beta$ in HEK293 cells.

It is also worth noting that Helps et al., (1995) found that ASPP2 appears to bind to PP1 more strongly than to p53 and they also showed that PP1 and p53 cannot bind simultaneously, thus suggesting that ASPP2 is more likely to exist in a complex with PP1 in the cell than with p53. As a PP1 catalytic subunit was pulled out in the FLAG-ASPP1 IP from Flp-In HEK293 cells and HEK293 screens, this may indicate why p53 was absent from this set of ASPP1 interactors. Saos2 cells are a p53 null cell line therefore it was no surprise that p53 was not detected in the endogenous ASPP1-IP from Saos2 cells.

As well as PP1c, a number of Sec proteins were pulled down in the endogenous ASPP1 IP from Saos2 cells. Sec proteins and a small GTPase (Sar1) collaborate to form the COPII complex which is the primary vesicle coat complex used to transport newly synthesised proteins from the ER to the Golgi apparatus. Also, one of the double hits from the ASPP1 yeast 2-hybrid screen was COPB1 (coatomer protein complex, subunit

beta 1) which a subunit of the COPI complex which mediates Golgi-to-ER protein trafficking. The protein components of the COP complexes are listed in Table 15 and the mechanism of COPII coat formation is summarised in Figure 68. For in depth reviews on COPII coat formation and function see Lee and Miller (2007), Hughes and Stephens (2008), and Budnik and Stephens (2009).

Vesicle	Coat and Adaptor Proteins	Small GTP-Binding protein	Transport step
COPI	COP α, β, β1, γ, δ, ε, ζ	ARF	Golgi to ER
COPII	Sec23/Sec24 complex, Sec13/Sec31 complex, Sec16	Sar1	ER to Golgi

Table 15. Protein components of COPI and COPII vesicles. The coats of COPI and COPII vesicles consist of large protein complexes composed of varying individual protein subunits. Budding is initiated by recruitment of a small GTP-binding protein to a patch of membrane. Proteins identified as ASPP1 interactors in our studies are highlighted.

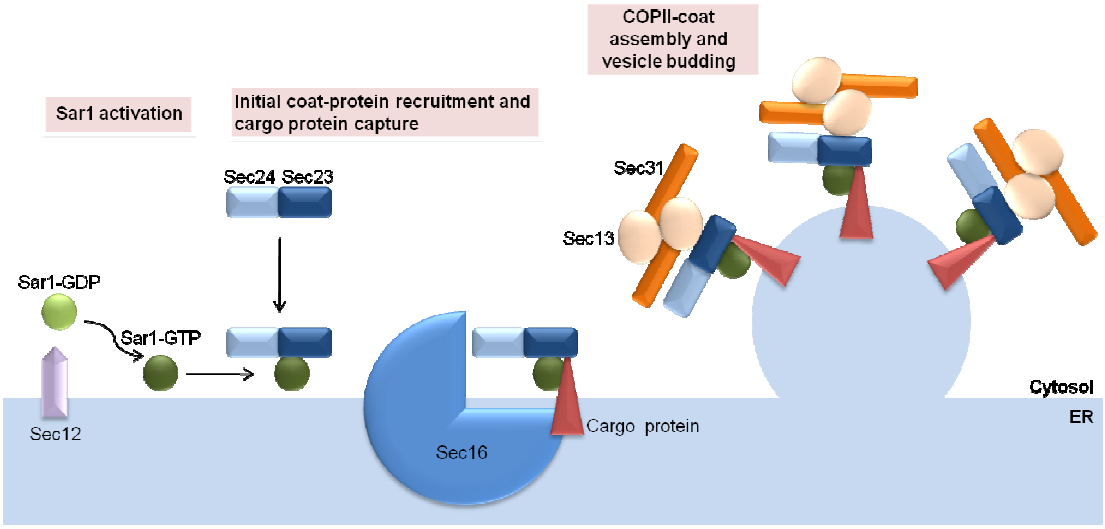

Figure 68. Schematic depiction of the COPII coat machinery mediating ER cargo export. COPII assembly on ER membranes initiates with the transmembrane protein Sec12. Inactive GDP-bound Sar1 is attracted to the cytosolic side of the endoplasmic reticulum (ER) by Sec12. Sec12 functions as a guanine nucleotide exchange factor (GEF) and mediates nucleotide exchange of GTP on Sar1. The GTP-bound form of Sar1 then recruits the Sec23/Sec24 heterodimer, an adaptor complex that recognises sorting-peptide motifs on membrane bound cargo proteins. This in turn binds the Sec13/Sec31 complex which constitutes the coat framework of COPII coated vesicles. The Sec23/24-Sec13/31-Sar1 complexes then coalesce to form a much larger complex which deforms the membrane enough to bud a vesicle off. Sec16 appears to plays a central role organising COPII formation functioning as a scaffold for assembly of the vesicle coat. Figure re-drawn with modification from Roy et al., (2006).

Although four Sec proteins were identified by mass spectronomy it is unlikely that ASPP1 interacts specifically with all four of these proteins. A relatively stable interaction with either one of these proteins may be sufficient to pull down all of these COPII components.

We were unable to detect an association between ASPP1 and Sec16A by IP and immunofluorescence studies showed they may partially co-localise. This suggests that ASPP1 may be specifically interacting with other Sec proteins which are not bound to the ER membrane. It is also possible that the ASPP1-Sec16A interaction is cell cycle specific or dependent on activation of a particular intracellular signalling pathway.

As well as the Sec proteins, α–tubulin was also detected in the complex pulled down with the ASPP1 antibody. COPII coated packages which bud from the ER translocate via microtubules to the Golgi. Thus microtubules function as 'railroad tracks'. The ASPP1-COPII complexes pulled down in this IP are indeed likely to be in association with microtubules hence α-tubulin, a major constituent of microtubules, was also pulled down.

Although we were unable to detect co-immunoprecipitation between ASPP1 and α-tubulin upon repeat of the IP, judging by the Western blot less ASPP1 protein was pulled down in the repeated experiment (compare Figure 57A and Figure 59). Therefore, in this instance there may be so little α-tubulin being pulled down in this complex that we are unable to detect it by Western.

A number of other proteins were also identified which are likely to play an important role in protein trafficking. For example, neuropathy target esterase (NTE), a phospholipaseB enzyme tethered to the cytoplasmic face of the ER, plays an important role in regulating vesicular transport (Li et al., 2003b; Zaccheo et al., 2004). On a similar theme, a protein called Synaptojanin-2 was pulled out of the ASPP1 yeast 2-hybrid screen. Synaptojanin 2 is a regulatory lipid phosphatase enzyme which also appears to be involved in distinct vesicle trafficking and signal transduction pathways in mammalian cells (Malecz et al., 2000). Other identified proteins with a role in endosomal trafficking include ARF-GEP_{100} (encoded by the *IQSEC1* gene) (Someya et al., 2001; D'Souza-Schorey et al., 2006), SCAMP1, SCAMP3 (Castle et al., 2005), CYFIP1 (Cytoplasmic FMRP-Interacting Protein 1) and SYLP1 (Synaptophysin-like protein 1, often called Pantophysin) (Haass et al., 1996; Egea et al., 2006).

Co-immunoprecipitation of ASPP1 and various proteins involved in ER-Golgi trafficking and post-Golgi trafficking suggests that ASPP1 plays a functional role in protein transport. Alternatively, ASPP1 may simply be exported from the ER and transported to the Golgi for processing in COPII vesicles and then directed to another destination in the cell via the post-Golgi network.

A number of Heat shock proteins (HSPs) were pulled down in the Saos2 and Flp-In HEK293 immunoprecipitations (summarised in Table 16). Heat shock proteins are a class of highly conserved, functionally related proteins many of which are expressed when cells are exposed to elevated temperatures or other stress so that they can protect protein substrates against conformational damage, aggregation and denaturation. Many HSPs, however, are synthesised in the absence of stress and are involved in a variety of cellular functions such as folding of newly synthesised proteins, transport of proteins between cellular compartments, activity control of regulatory proteins, assembly and disassembly of protein complexes, and assistance of proteolytic degradation (Becker et al., 1994; Hartl 1996; Daugaard et al., 2007). Also, HSPs often play key regulatory roles in apoptosis as the events of cell stress and cell death are not surprisingly linked and a number of HSPs have been reported to act as, or interact with, both anti-apoptotic and pro-apoptotic proteins. For a review on HSPs and apoptosis see Garrido et al., (2001).

Gene Symbol	Description	Protein ID	Identified ASPP1:HSP interaction
HSPA9	Heat shock 70 kDa protein 9	Hsp70-9	ASPP1 IP in Saos2 cells
HSPA1L	Heat shock 70 kDa protein 1-like	Hsp70-Hom	
HSPA4	Heat shock 70 kDa protein 4	Hsp74	ASPP1-FLAG IP in Flp-In HEK293 cells
HSPA8	Heat shock 70 kDa protein 8	Hsc70	
HSPA1A	Heat shock 70 kDa protein 1A	Hsp72	

Table 16. Heat shock proteins identified in the ASPP1-protein interaction screens.

Hsp72 was pulled down in the ASPP1-FLAG immunoprecipitation and we confirmed this interaction by Western (Figure 66). Hsp72 is a ubiquitously expressed heat shock protein, but it is also known to be up regulated after exposure to a variety of cellular stresses (Wu et al., 1985; Hartl 1996). Park et al., (2002) reported that Hsp72 can negatively regulate apoptosis by binding to and inhibiting the function of ASK1 (apoptosis signal-regulating kinase 1), a widely expressed serine-threonine kinase that induces apoptosis. Potentially Hsp72 may have a similar inhibitory effect on ASPP1's pro-apoptotic function. Also Hsp70-9, which was pulled down with ASPP1 from Saos2 cells, has been reported to interact with wild type p53 and this interaction is believed to promote sequestration of p53 in the cytoplasm, inhibiting its nuclear activity (Wadhwa et al., 1998; Wadhwa et al., 2002b). Thus, HSPs may bind to ASPP1 and sequester it in the cytoplasm, preventing its pro-apoptotic activities in the nucleus, much like Hsp70-9 does with p53. In response to cell stress, Hsp70-Hom and Hsp74 may assist in transporting

ASPP1 into the nucleus, as these proteins have been shown to re-localise from the cytosol to the nucleus after heat shock (Milner et al., 1990; Kaneko et al., 1997; Fourie et al., 2001). The regulatory mechanisms that control the translocation of these HSPs into the nucleus, however, are unknown. Alternatively, HSPs may bind to partially translated or newly synthesised ASPP1 and contribute to its efficient folding. They may assist in ASPP1 stabilisation or prevent ASPP1 aggregation during both normal cellular conditions and adverse conditions. ASPP1 is a relatively large protein implying it is likely to need assistance in assembly. They may also transport old or excess ASPP1 protein, which may have been tagged for degradation by SIAH1, to the proteasome.

Despite the high sequence homology of the individual HSPs pulled down in our IPs, they appear to reside in varying subcellular compartments and display functional diversity. It is likely that the functional consequence of the interaction between ASPP1 and HSPs is dependent on the individual HSP, and a number the scenarios suggested above may take place simultaneously.

A number of transcriptional regulators were also identified in our screens, including DIPA (delta-interacting protein A), PC4 (positive co-activator-4) and YBX1 (Y-box binding protein 1). DIPA regulates gene expression and cell proliferation by interacting with various transcription factors (Bezy et al., 2005; Du et al., 2006; Iwai et al., 2007). PC4, like ASPP1, has been reported to interact with p53 and enhance p53 dependent apoptosis (Banerjee et al., 2004). EMSA experiments carried out by Banerjee et al., (2004) show that PC4 stimulates the sequence-specific DNA binding of p53 and they demonstrate that PC4 induces expression of the p53-targeted pro-apoptotic gene, *Bax*. Similarly, chromatin immunoprecipitation (ChIP) assays carried out by Samuels-Lev et al., (2001) show that ASPP1 and ASPP2 can selectively stimulate the binding of p53 to the promoters of pro-apoptotic genes, such as *Bax* and *PIG3*. Thus, ASPP1 and PC4 appear to function in a similar manner and potentially cooperate with one another.

YBX1, commonly referred to as YB-1, was positively identified in both the endogenous ASPP1 IP and the ASPP1-FLAG IP. YBX1 has also been shown to directly associate with p53 and again this association activates the binding activity of p53 to its consensus sequence (Okamoto et al., 2000). However, in contrast to PC4 and ASPP proteins, YBX1 prevents p53 from inducing apoptosis by selectively preventing p53 from transactivating pro-apoptotic genes, including *Bax* (Homer et al., 2005). We were unable

to confirm the ASPP1:YBX1 interaction by Western using a YBX1 antibody as we suspect that IgG heavy chain and the YBX1 protein are migrating similarly. Thus, further analysis is required to resolve this issue.

In addition to transcriptional regulators, HSPs and several protein transport machinery proteins, there were several other proteins pulled down in the Saos2 IP, some of which are metabolic enzymes (e.g. DLST and CAD) and some of whcih whose functions are unknown (e.g. RTN4, HAX-1 and KCTD15).

Overall, the ASPP1-protein interaction screens revealed that ASPP1 interacts with diverse set nuclear and cytoplasmic proteins. In comparison to the ASPP1 interacting proteins identified in Saos2 and Flp-In HEK293 cells, a rather different set of interactors was identified in the testes yeast 2-hybrid screen. Contrasting cellular location is likely to affect potential binding partners as ASPP1 is nuclear in human testes and cytoplasmic in mouse tissues and cell lines. ASPP1 therefore, is likely to have a different function in human testes compared to other tissues It is also important to bear in mind that one of the limitations of the yeast 2-hybrid system is that spurious interactions are sometimes detected that are not displayed by proteins in their native environment. Synthetically made fusion proteins may not be able to fold properly and/or proteins may not be correctly modified in yeast in comparison to mammalian tissue, consequently altering their properties. Also, interactions detected in yeast may not occur in mammalian tissues due to the possibility of cell-specific or subcellular compartment specific expression of detected prey proteins. Therefore all yeast 2-hybrid results must be dealt with caution, and interactions must be validated in the appropriate biological system. The ASPP1 interacting proteins we have most confidence in are PP1c, which was previously identified by Helps and colleagues (1995), and Hsp72, as we were able to verify this interaction by Western (Figure 66). Further investigation is required in order to confirm that the remaining interactors identified in these screens are genuine molecular interactors *in vivo*. Never the less, the diverse set of interacting proteins identified in these studies implicate ASPP1 involvement in a range of cellular processes, as well as apoptosis.

Chapter 7. Concluding remarks and future work

Since the initial characterisation of the mammalian Siah family in the mid 90's, and the realisation that Siah proteins are key regulators of protein turnover, a multitude of Siah interacting proteins have been identified (see Tables 1 and 2 in the introduction to this thesis). Siah proteins regulate a diverse set of substrates and as a result they have been implicated in a number of cellular processes (Figure 69).

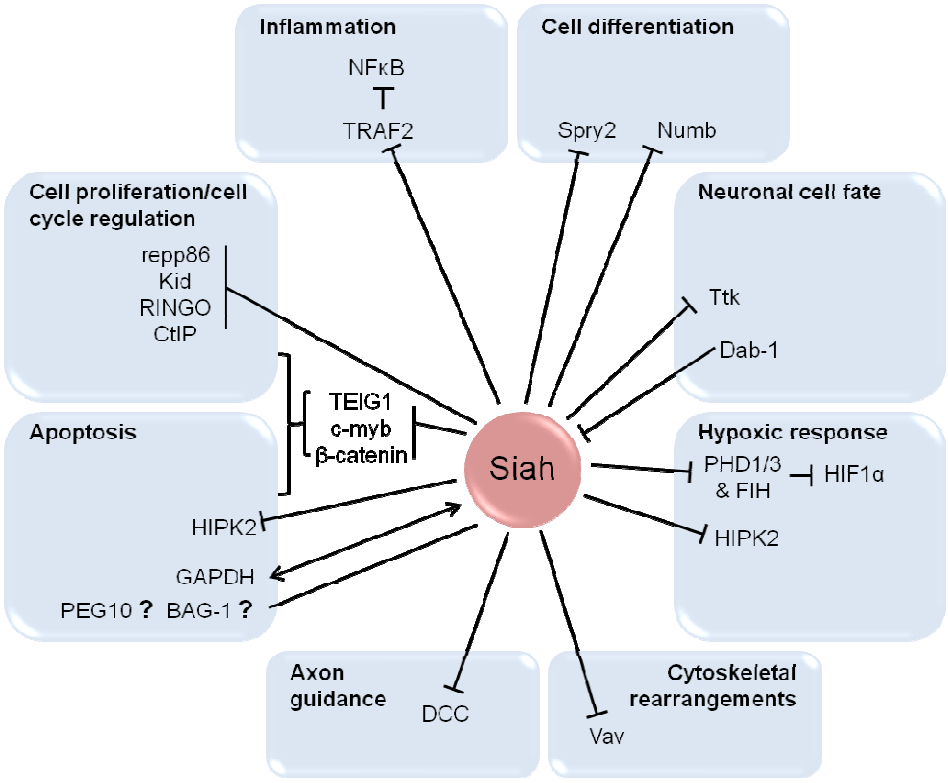

Figure 69. Pathways involving Siah family proteins. The *Drosophila* Sina protein controls R7 photoreceptor development by targeting the transcription repressor tramtrack (Ttk) for degradation. Mammalian Siah family proteins have been implicated in the degradation of many proteins including PHD and FIH, negative regulators of hypoxia signalling; HIPK2, the protein kinase with a key role in the hypoxic response and apoptosis; DCC, the netrin receptor which controls axonal patterning and cell migration; β-catenin, c-myb and TEIG1, transcriptional regulators involved in apoptosis and cell proliferation; repp86, a component of the mitotic spindle which plays a role in cell cycle progression; Kid, a microtubule binding protein involved in mitosis; RINGO, a cell cycle regulator; CtIP, a transcriptional regulator involved in cellular proliferation; TRAF2, the signal transducer which in turn leads to diminished NFκB activation; Spry2, a negative regulator of RAS signalling involved in cell growth and differentiation; NUMB, a membrane protein which plays a role in the determination of cell fate during development. Mammalian Siah proteins also bind to Vav, a guanine nucleotide exchange factor which regulates cytoskeletal reorganisation and suppress its function. An interaction with GAPDH leads to Siah stabilisation and promotion of apoptosis. Interactions with the inhibitors of apoptosis PEG10 and BAG-1 have also been observed, however the outcomes of these interactions are not clear. Figure redrawn with modification from House et al., (2009).

Generation of *Siah1a* and *Siah2* knockout mice were valuable in establishing the significance of the role Siah proteins play in these cellular processes and, although *Siah2*$^{-}$

$^{/-}$ mice were phenotypically normal, it was revealed that Siah1a had a novel role in the testes as *Siah1a* null male mice were sterile (Dickins et al., 2002). Thus, to better understand SIAH1 function in the testes, the primary aim of this thesis was to characterise a number of SIAH1 interacting proteins identified in a yeast 2-hybrid screen of a human testes cDNA library and determine whether or not any of these proteins were targets for SIAH1-mediated degradation. If so, we could then speculate on the consequences of the SIAH1 interaction on cellular processes. The experimental approaches taken to characterise each interaction and our findings have been discussed at the close of each chapter. Here, the major discoveries from this study are summarised and the future direction this research may take is considered.

Initial analysis of the eight SIAH1 yeast 2-hybrid hits revealed that the most likely targets for SIAH1 mediated degradation were PHC2, a polycomb protein which is part of a large chromatin associated complex involved in the stable repression of genes during early development; NELF-A, a component of the NELF complex which regulates transcription of developmental control genes by stalling RNA polymerase II; ASPP1, an apoptosis promoting protein, which is dependent on its interaction with p53; and ZC3H11A, a zinc finger protein with unknown function.

Whist writing this thesis, the SIAH1:PHC2 interaction was published by Wu and colleagues (2010). They identified this interaction in a SIAH1 yeast 2-hybrid screen of a human foetal brain cDNA library. Therefore the SIAH1:PHC2 interaction is unlikely to be exclusive to the testes. Similar to our findings they report that PHC2 interacts with the C-terminal domain of SIAH1. They recognise the same SIAH-binding motif that we identified (Chapter 3, section 3.4) and show that deletion of the motif abrogates the interaction. They also provide evidence to show that SIAH1 mediates PHC2 ubiquitination and targets it for proteasomal degradation. Confirmation of the SIAH1:PHC2 interaction implies that SIAH1 has a role during early development. By regulating the stability of PHC2, SIAH1 may in turn regulate the expression of *Hox* genes which are repressed by the Polycomb complex. Regulation of PHC2 by SIAH1 may be important in the testes as large numbers of genes involved in spermatogenesis are differentially expressed during germ cell development and so their expression must be tightly controlled. Potentially a subset of genes essential for successful germ cell production might be repressed by the polycomb complex and so Siah1a may be required to degrade PHC2 to permit their expression.

Further analysis of the SIAH1:NELF-A interaction (Chapter 4) via transient transfection assays and monitoring of endogenous protein levels in *Siah1a*$^{-/-}$*Siah2*$^{-/-}$ fibroblasts revealed that SIAH1 predominantly targets over-expressed NELF-A-GFP fusion protein for degradation, and endogenous NELF-A protein was largely unaffected. These results suggest that SIAH proteins preferentially target excess proteins which might not be present within intracellular complexes. In the study by Wu and colleagues (2010) mentioned above, they solely analyse ectopically expressed FLAG-tagged PHC2 protein when co-expressed with SIAH1 and endogenous PHC2 is not studied. Thus, it is possible that SIAH proteins also preferentially degrade excess PHC2 which is not part of the polycomb chromatin associated complex. So why should proteasome mediated destruction of certain excess protein components be important? We speculate that this homeostatic control of protein levels might be a particularly important component of gene expression in the testis which has high levels of general transcription. Due to the many cellular differentiation events that occur during spermatogenesis, many gene products are required, more than at any other time during development. High levels of general transcription are also thought to be associated with efficient DNA repair processing during recombination (Hackstein et al., 2000). Potentially many of the mRNAs which are translated into protein are surplus to requirements and are hence targets for proteasomal degradation. Any defect in this homeostatic control mechanism may therefore manifest in the infertility shown by *Siah1a*$^{-/-}$ mice. However, more generally this data also strongly suggests that an important trigger for SIAH1-mediated protein degradation of endogenous proteins sequestered in complexes will be the dissolution of these intracellular protein complexes to make target proteins accessible to SIAH1-mediated ubiquitination.

An investigation into the effect of the murine family of Siah proteins on the stability of NELF-A-GFP revealed that Siah1a and Siah2 proteins target NELF-A for degradation but Siah1b does not. Nor was Siah1b able to autoregulate its own stability like Siah1a and Siah2. This was a surprising result as Siah1a and Siah1b are much more similar to each other than to Siah2 in terms of protein sequence. We also analysed the effect of the murine family of Siah proteins on the stability of PHC2- and ASPP1-GFP fusion proteins and similar results were obtained (data not shown in this thesis). Thus, Siah1a and Siah2 target an overlapping, heterologous set of target proteins for proteasome-mediated destruction, but Siah1b does not.

The finding that one Siah1 protein rather than two is sufficient in humans and rats (see section 1.3 in the introduction to this thesis) suggests that the Siah1b protein has little or no role in the mouse. However, Siah1b is being maintained under purifying selection (Dr Michael Jackson, IHG, Newcastle University, unpublished observations), *Siah1b* is activated during p53-mediated apoptosis (Amson et al., 1996; Fiucci et al., 2004), and *Siah1b*$^{-/-}$ mutant mice exhibit an embryonic lethal phenotype (Frew et al., 2002). Therefore, Siah1b clearly has an important role in the mouse as it is essential for viability during embryonic development, but this seems to be outside targeting proteins for proteasomal degradation.

In the literature, most Siah protein studies have focused on either human SIAH1 or SIAH2 and mouse Siah1a or Siah2 and, as far as we are aware, no Siah1b interacting proteins or target proteins have been identified. To our knowledge, we are the first to report that Siah1b has functionally diverged.

Further analysis of the interaction between SIAH1 and the pro-apoptotic protein ASPP1 (Chapter 5) revealed that SIAH1 is a likely E3 ligase candidate responsible for controlling the stability of both ASPP1 and its homologue ASPP2, which was previously found to be regulated by a proteasome dependent mechanism. Detection of elevated levels of ASPP1 in meiotic and post meiotic male germ cells by Thornton et al., (2006) suggests that this protein may play an important role in germ cell development. Indeed, apoptosis of spermatogenic cells is an essential homeostatic process in the testes, maintaining the correct proportion of germ cells and somatic cells and eliminating any defective or damaged gametes (Print et al., 2000). If ASPP1 is involved in this homeostatic process then the finding that SIAH1 regulates ASPP1 stability suggests that SIAH1 might inhibit ASPP1-dependent apoptosis in the testis. Contrarily, SIAH1 has been shown to activate apoptosis (discussed in sections 1.3.3 and 1.3.4 in the introduction to this thesis). It is possible that activation of apoptosis by SIAH1 is via an ASPP1-independent pathway and that SIAH1-mediated degradation of ASPP1 is a method by which various pro-apoptotic signals are regulated. However, protein interaction screens carried out to identify major ASPP1 protein binding partners revealed that ASPP1 bound/co-immunoprecipitated with a diverse array of proteins implying ASPP1 is a multifunctional protein with a role in many cellular pathways (Chapter 6). Thus, SIAH1 mediated degradation of ASPP1 is likely to have downstream effects on multiple pathways and cellular processes, as well as apoptosis.

Much of the literature on the ASPP proteins focuses predominately on ASPP2, and the majority of ASPP interacting proteins identified are ASPP2 interactors (Table 12, Chapter 6). Due to the identification of various ASPP2 interacting partners, it is becoming increasingly recognised that ASPP2 may have many other functions in the cell beyond enhancing apoptosis (Kampa et al., 2009b). To our knowledge this is the first comprehensive study aimed at identifying ASPP1 interacting partners and, as a result, we also found that ASPP1, like ASPP2, appears to be involved in a perplexing range of biological pathways. The ASPP1 protein interaction network elucidated in this study is surmised in Figure 70. Aside from PP1c, we did not identify any of the published ASPP2 interacting partners in our ASPP1 protein interaction screens (Table 12, Chapter 6). This suggests that, aside from promoting apoptosis via their interaction with p53 and family members, ASPP1 and ASPP2 also have distinct roles in the cell.

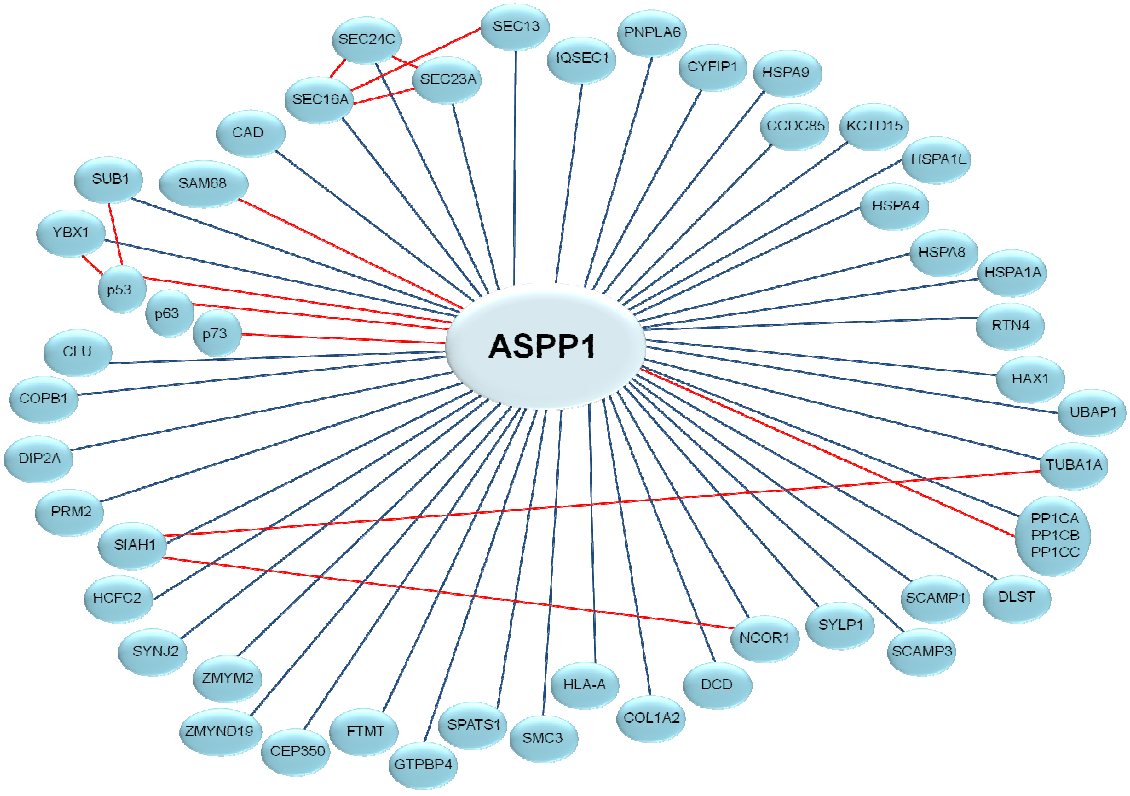

Figure 70. ASPP1 interacting proteome. Previously identified interactions are depicted by red lines. Blue lines represent interactions identified in this study. It is likely that some of the proteins identified in our ASPP1 protein interaction screens also interact with one another, however only the interactions identified upon my assessment of the literature are shown.

Despite identification of SIAH1 targets, PHC2, NELF-A and ASPP1, all of which potentially play an important role in germ cell development in the testes and also in other tissues, the signals which trigger SIAH-mediated degradation of these proteins *in vivo* are

yet to be determined. It is becoming increasingly recognised that Siah proteins do not function constitutively in the cell, but rather are recruited into action by certain signals. For example, Siah2 has been shown to primarily target TRAF2 for degradation, but only in response to stress (Habelhah et al., 2002). Habelhah and colleagues (2002) compared TRAF2 abundance in wild-type and *Siah2*$^{-/-}$ MEFs and found that there was a limited difference in TRAF2 protein levels between wild-type and *Siah2* null cells under normal growth conditions. In response to stress however, in the form of actinomycin D treatment (a DNA intercalator which inhibits transcription), there was a marked decrease in the half-life of TRAF2 in wild type MEFs compared with *Siah2*$^{-/-}$ cells. It would therefore be interesting to analyse NELF-A and ASPP1 stability in MEFs subjected to particular stress stimuli.

As well as cell stress, there are many other potential pathways and signals that may trigger SIAH-mediated degradation. Due to SIAH proteins interacting with such a diverse set of substrates it is likely that signals and triggers for degradation vary depending on the substrate. In order to better understand when and where SIAH proteins initiate degradation, and what the downstream consequences are, further knowledge of ASPP1 function and the triggers for dissolution of the NELF complex is required.

The function of the murine specific Siah1b protein also remains to be determined. Due to the only amino acid differences between Siah1a and Siah1b proteins residing in the RING finger and zinc finger regions it will be of interest to determine which E2 enzymes these proteins interact with, as recent evidence indicates that it is the E2 enzyme which dictates the type of ubiquitin modification that will occur on the substrate (Ikeda et al., 2008). Potentially, Siah1b may assist in either protein monoubiquitination, polyubiquitination of atypical ubiquitin chains or conjugation of UBL proteins which instead of targeting proteins for degradation may alter protein function or localisation (discussed in sections 1.2.1 and 1.2.2 in the introduction to this thesis). Also, due to the *Siah1b* knock out having an embryonic lethal phenotype (Frew et al., 2002), creation of a conditional *Siah1b* knock out would help clarify Siah1b function in different tissues and in varying stages of development.

Moreover, now that we have identified a large number of candidate ASPP1 interacting proteins, many of which are highly intriguing, interactions need to be verified *in vivo* and the functional implications of these interactions remain to be determined. The PP1c

interaction was verified previously and we were able to confirm the ASPP1:Hsp72 interaction by co-immunoprecipitation. However, it is unlikely that all of the ASPP1 interactors identified are genuine physiological binding partners. Never the less, in order to better understand ASPP1 function in the nucleus, and the mechanisms by which ASPP1 itself stimulates apoptosis, it may be interesting to follow up on the interaction with the p53 interacting transcriptional regulators PC4 and YBX1 (discussed in the summary and discussion in Chapter 6). ASPP1 and PC4 specifically promote p53-dependent apoptosis and YBX1 acts in an opposite manner, specifically preventing p53-dependent apoptosis. Interestingly, prior to this study it was hypothesised in a review by Braithwaite et al., (2006) that the outcome of the p53 response may be determined by the relative concentrations of YBX1 and ASPP proteins in the nucleus. Presumably the more YBX1 present in the nucleus, the more likely apoptosis is to be inhibited and the more ASPP1/2 present, the more apoptosis is promoted. If this is indeed the case, there must be some sort of control mechanism regulating the amount of ASPP1 and YBX1 translocating to the nucleus. Like ASPP1, YBX1 is predominantly cytoplasmic, however it translocates to the nucleus in response to cytotoxic stress and DNA damage (Koike et al., 1997). Therefore, it would also be interesting to monitor ASPP1 localisation after cytotoxic stress. We did perform some preliminary studies whereby ASPP1-V5 localisation was analysed by cell staining before and after UV treatment and results suggest that ASPP1 translocates to the nucleus similarly to YBX1 (data not shown). Further analysis of the ASPP1, PC4 and YBX1 protein interaction network identified in this study may provide further insight into how these proteins dictate how p53 behaves.

As a number of proteins involved in protein trafficking were identified in the ASPP1 protein interaction screens then ASPP1's role in COPII coat formation, ER-Golgi and post-Golgi protein trafficking also requires further investigation. One way to better understand ASPP1 roles in protein transport may be to construct recombinant genes encoding ASPP1 and COPII chimeric fluorescent proteins and monitor their migration in the cell in real time. The interaction between ASPP1 and the various heat shock proteins also requires further investigation in order to determine the functional consequences of these interactions. As we confirmed the interaction between ASPP1 and Hsp72 by co-immunoprecipitation (Chapter 6, section 6.4.6) it would be interesting to do some co-staining in order to determine whether these proteins co-localise and if this interaction is

affected by cytotoxic damage such as UV. A model of ASPP1 function based on the interacting proteome identified in this study is presented in Figure 71.

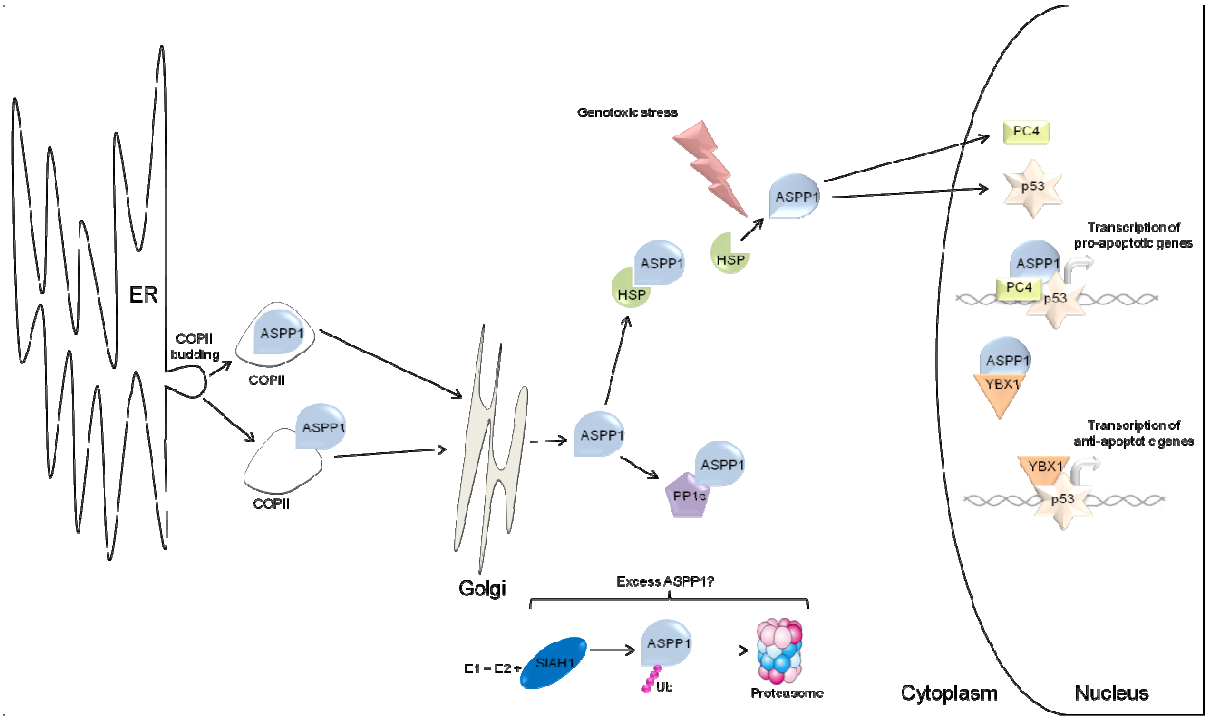

Figure 71. A model of ASPP1 function in the cell. This figure summarises our protein interaction data discussed in the text. One might envisage that ASPP1 carries out activities in the cytoplasm that are part of the normal cell physiology, possibly regulating PP1 activity or assisting in protein transport in COPII vesicles which bud from the ER. Alternatively, ASPP1 may be transported in the cell within COPII vesicles to the Golgi for processing, and sorting. ASPP1 may be sequestered in the cytoplasm by heat shock proteins or support HSP cellular function, for example assisting in control of regulatory proteins or assembly and disassembly of protein complexes. Any ASPP1 in excess of cellular requirements may be targeted for proteasomal degradation by SIAH1. Upon genotoxic stress/or other exogenous signals, ASPP1 may translocate into nucleus potentially with the aid of HSPs. In the nucleus ASPP1 may associate with PC4 and p53 to promote transcription of pro-apoptotic genes. It may also bind to YBX1 in order to sequester it away from anti-apoptotic promoters. The cellular decision to promote cell growth or undergo programmed cell death may be dependent on the relative levels or activity of ASPP1 and YBX1 in the nucleus.

Clearly, identifying the proteins that interact with the E3 ubiquitin ligase SIAH1, and the tumour suppressor protein ASPP1, has provided an important first step towards our understanding of the functional responsibilities of these proteins in the cell. However, as is often the case with scientific research, many unanswered questions remain. No doubt further understanding of the triggers of SIAH-mediated degradation will lead to fascinating discoveries on how SIAH proteins contribute to development by regulating NELF-A, ASPP1 and PHC2 stability. In addition, further analysis of the ASPP1 interacting partners identified will lead to new and interesting discoveries on how ASPP1 functions in the cell and a better understanding of ASPP1 function is also likely to lead to

an expansion in our understanding of the downstream effects of SIAH-mediated degradation.

Appendix A. Primers used for PCR

Primer name	Target	Sequence (5′-3′)	Site	Purchased from
ASPP1(252)F	ASPP1	AAAAAAAAAGAATTCTCCCCAACTGAGAACAGTGAA	*Eco*RI	Sigma
ASPP1(624)F	ASPP1	AAAAAAAAAGAATTCAATCTGTCTGCTGAAATAGAAAGG	*Eco*RI	Sigma
ASPP1(624)R	ASPP1	AAAAAAAAACTCGAGCCTTTCTATTTCAGCAGACAGATT	*Xho*I	Sigma
ASPP1(1050)R	ASPP1	AAAAAAAAACTCGAGTCCGGCACTGGGAACCTG	*Xho*I	Sigma
ASPP1(1575)F	ASPP1	AAAAAAAAACATATGCCAAGTCCCACGTACCCG	*Nde*I	Sigma
ASPP1(1839)F	ASPP1	AAAAAAAAACATATGTTACCTTCGGGTTCAACCTCT	*Nde*I	Sigma
ASPP1(1839)R	ASPP1	AAAAAAAAACTCGAGAGAGGTTGAACCCGAAGGTAA	*Xho*I	Sigma
ASPP1(2259)R	ASPP1	AAAAAAAAACTCGAGATTGTCCACATCGGCCAAGGT	*Xho*I	Sigma
ASPP1-F(BglII)	ASPP1	AAAAAAAAAGATCTATGATGCCGATGATATTAACTGTTT	*Bgl*II	IDT
ASPP1-R-(XhoI)	ASPP1	AAAAAAAACTCGAGTCAGGCGAGTGTTCGCTGT	*Xho*I	IDT
ASPP2-F	ASPP2	AAAAAAAAACATATGATGGATCTGACTCTTGCTGAAC	*Nde*I	Sigma
ASPP2-R	ASPP2	AAAAAAAAACTCGAGTCAGGCCAAGCTCCTTTGTCT	*Xho*I	Sigma
ASPP2(1668)F	ASPP2	AAAAAAAAACATATGCCTGTTTCTTCAGTTCAGGAG	*Nde*I	Sigma
ASPP2(1668)R	ASPP2	AAAAAAAAACTCGAGCTCCTGAACTGAAGAAACAGG	*Xho*I	Sigma
BGHrev	BGH seq	TAGAAGGCACAGTCGAGG	-	MWG
CMV-F	CMV prom	CGCAAATGGGCGGTAGGCGTG	-	Eurogentec
HPH2F	PHC2	AAAAAAAAACAATTGGACATGACCTCAGGGAACG	*Mfe*I	Eurogentec
HPH2B	PHC2	AAAAAAAAACTCGAGCTAGGAGTCCTTGAGCATGC	*Xho*I	Eurogentec
KIAA0663F	ZC3H11A	AAAAAAAAAGAATTCACAGGAGTTGACATCACTAAAATTC	*Eco*RI	Eurogentec
KIAA0663B	ZC3H11A	AAAAAAAAACTCGAGTTCAGCTATCAATCATTTCTGTAG	*Xho*I	Eurogentec
KIAA0663(1638)F	ZC3H11A	AAAAAAAAAGAATTCACAGGAGTTGACATCACTAAAATTC	*Eco*RI	VHBio
KIAA0663(2034)F	ZC3H11A	AAAAAAAAAGAATTCGTCATTGCCGCTGTGAAGC	*Eco*RI	VHBio
KIAA0663(2100)R	ZC3H11A	AAAAAAAAACTCGAGCGGGACAACAGCCACAGC	*Xho*I	VHBio
KIAA0663(1875)F	ZC3H11A	AAAAAAAAAGAATTCGGGATTGGAGACTCATTATTGAAT	*Eco*RI	Sigma
KIAA0663(1875)R	ZC3H11A	AAAAAAAAACTCGAGATTCAATAATGAGTCTCCAATCCC	*Xho*I	Sigma
Limkain-β2F	CCDC92	AAAAAAAAAGAATTCCTGGAGGAGCTGAAGGCC	*Eco*RI	Eurogentec
Limkain-β2B	CCDC92	AAAAAAAAAGCGGCCGCCTTCACACAGTTCTGTCCGTC	*Not*I	Eurogentec
pACT25-F	pACTII	CGCGTTTGGAATCACTACAGGGAT	-	MWG
pCDNArev	pGFP3	CTAGAAGGCACAGTCGAGGCT	-	MWG
pGEX5	pGEX5X1	GGCAGATCGTCAGTCAGTCACGA	-	MWG
PUF60F	SIAH1BP1	AAAAAAAAAGAATTCACGGCGACCATAGCTCTCC	*Eco*RI	Eurogentec
PUF60B	SIAH1BP1	AAAAAAAAACTCGAGTCACGCAGAGAGGTCACTGT	*Xho*I	Eurogentec
SIAH95-F	SIAH1	AAAAAAAAGAATTCCTTTTCCCCTGTAAATATGCGT	*Eco*RI	MWG
SIAH155-B	SIAH1	AAAAAAAACTCGAGAATGGACTTATGCTGATGCATC	*Xho*I	MWG
SIAH153-F	SIAH1	AAAAAAAAGAATTCAAGTCCATTACCACCCTACAGG	*Eco*RI	MWG
SIAH1 protein-B	SIAH1	AAAAAAACTCGAGTCAACACATGGAAATAGTTACAT	*Xho*I	MWG
Siah1a-F(FLAG)	Siah1a	AAAAAAAAAGAATTCAATGAGCCGCCAGACTGCTA	*Eco*RI	IDT
Siah1b/a-R(FLAG)	Siah1b/a	AAAAAAAAATCTAGAACACATGGAAATAGTTACATTGATG	*Xba*I	IDT
Siah1b(F)	Siah1b	AAAAAAAAAGAATTCATGAGCCGTCAGGCTGCT A	*Eco*RI	VHBio
Siah1b(R)	Siah1b	AAAAAAAAACTCGAGTCAACACATGGAAATAGTTACATTGA	*Xho*I	VHBio
Siah1b-F(FLAG)	Siah1b	AAAAAAAAAGAATTCAATGAGCCGTCAGGCTGCTA	*Eco*RI	IDT
Siah1b-R(FLAG)	Siah1b	AAAAAAAAATCTAGATCAACACATGGAAATAGTTACATTGA	*Xba*I	IDT
Siah2-F(FLAG)	Siah2	AAAAAAAAAGAATTCAATGAGCCGCCCGTCCTC	*Eco*RI	IDT
Siah2-R(FLAG)+STOP	Siah2	AAAAAAAAATCTAGATCACTGACAGCATGTAGATATCG	*Xba*I	IDT
Siah2-R(FLAG)-STOP	Siah2	AAAAAAAAATCTAGACTGACAGCATGTAGATATCGTG	*Xba*I	IDT
T7-F	T7 prom	TAATACGACTCACTATAGGG	-	Eurogentec
Uk-p68F	ZC3H14	AAAAAAAAAGATATCAAGTTCCACAGAAACAGACACTTC	*Eco*RV	Eurogentec
Uk-p68B	ZC3H14	AAAAAAAAACTCGAGCTATTCGCTGGTTTGAGGTCG	*Xho*I	Eurogentec
UKp68(1449)F	ZC3H14	AAAAAAAAAGAATTCCAAGAGTCGGGGATGAAGACT	*Eco*RI	Sigma
UKp68(1449)R	ZC3H14	AAAAAAAAACTCGAGAGTCTTCATCCCCGACTCTTG	*Xho*I	Sigma
UKp68(1122)F	ZC3H14	AAAAAAAAACATATGGTTCCACAGAAACAGACACTTC	*Nde*I	VHBio
UKp68(1662)F	ZC3H14	AAAAAAAAACATATGAAGGGACTCAGAGGTCTCC	*Nde*I	VHBio
UKp68(1782)R	ZC3H14	AAAAAAAAACTCGAGACAAGCAGGCCAGTACTTGCA	*Xho*I	VHBio
VAPAF	VAPA	AAAAAAAAAGAATTCATGGCGTCCGCCTCAGG	*Eco*RI	Eurogentec
VAPAB	VAPA	AAAAAAAAACTCGAGCTACAAGATGAATTTCCCTAGAAAG	*Xho*I	Eurogentec
WHSC2F	WHSC2	AAAAAAAAAGAATTCGAGAGCGACACGGGCCT	*Eco*RI	Eurogentec
WHSC2B	WHSC2	AAAAAAAAACTCGAGCTAGGACACATTGGTCATGGG	*Xho*I	Eurogentec
WHSC2(744)F	WHSC2	AAAAAAAAAGAATTCCTGCGGAAGGAACGAGGTG	*Eco*RI	Eurogentec
WHSC2(744)B	WHSC2	AAAAAAAAACTCGAGCAGCAGCGTCCTGGAAGG	*Xho*I	Eurogentec
WHSC2(951)F	WHSC2	AAAAAAAAAGAATTCGCGCTGCCCTCCACGAG	*Eco*RI	Eurogentec
WHSC2(951)B	WHSC2	AAAAAAAAACTCGAGAGGCTCATTGTTCAGGGACC	*Xho*I	Eurogentec
WHSC2(1281)B	WHSC2	AAAAAAAAACTCGAGAGGCTGCTGCTGAGCAGG	*Xho*I	Eurogentec

Appendix B. Plasmids used in this thesis

Gene	Vector	Selective Antibiotic	Source/Cloning method
ASPP1	pACTII	Ampicillin	Julian Venables, unpublished data
ASPP1	pCDNA5-FLAG	Ampicillin	PCR amplification from ASPP1-V5 clone using ASPP1-F(*Bgl*II) and ASPP1-R-(*Xho*I) incorporating *Bgl*II and *Xho*I restriction sites. Ligated into complementary sites in the pCDNA5-FLAG vector.
ASPP1	pGFP3	Ampicillin	Thornton 2005
ASPP1	pV5	Ampicillin	Gift from Professor Xin Lu, University of Oxford, UK
ASPP1(357-532)Epi	pET32a	Ampicillin	Thornton, 2005
ASPP1(1-1090)	pGADT7	Ampicillin	Thornton, 2005
ASPP1(1-86)	pGADT7	Ampicillin	Thornton, 2005
ASPP1(87-352)	pGADT7	Ampicillin	Thornton, 2005
ASPP1(353-531)	pGADT7	Ampicillin	Thornton, 2005
ASPP1(532-760)	pGADT7	Ampicillin	Thornton, 2005
ASPP1(761-871)	pGADT7	Ampicillin	Thornton, 2005
ASPP1(872-1090)	pGADT7	Ampicillin	Thornton, 2005
ASPP1(86-216)	pGADT7	Ampicillin	PCR amplification from ASPP1-V5 clone using ASPP1(252)F and ASPP1(624)R incorporating *Eco*RI and *Xho*I restriction sites. Ligated into complementary sites in the pGADT7 vector.
ASPP1(208-355)	pGADT7	Ampicillin	PCR amplification from ASPP1-V5 clone using ASPP1(624)F and ASPP1(1050)R incorporating *Eco*RI and *Xho*I restriction sites. Ligated into complementary sites in the pGADT7 vector.
ASPP1(525-620)	pGADT7	Ampicillin	PCR amplification from ASPP1-V5 clone using ASPP1(1575)F and ASPP1(1839)R incorporating *Nde*I and *Xho*I restriction sites. Ligated into complementary sites in the pGADT7 vector.
ASPP1(613-760)	pGADT7	Ampicillin	PCR amplification from ASPP1-V5 clone using ASPP1(1839)F and ASPP1(2259)R incorporating *Nde*I and *Xho*I restriction sites. Ligated into complementary sites in the pGADT7 vector.
ASPP2	pGFP3	Ampicillin	Jared Thornton, unpublished data
ASPP2 (1-563)	pGADT7	Ampicillin	PCR amplification from ASPP2-V5 clone using ASPP2-F and ASPP2(1668)R incorporating *Nde*I and *Xho*I restriction sites. Ligated into complementary sites in the pGADT7 vector.
ASPP2 (556-1005)	pGADT7	Ampicillin	PCR amplification from ASPP2-V5 clone using ASPP2(1668)F and ASPP2-R incorporating *Nde*I and *Xho*I restriction sites. Ligated into complementary sites in the pGADT7 vector.
HA-Ubiquitin	pCDNA3	Ampicillin	Purchased from Professor Yue Xiong, University of North Carolina, USA
KIAA0663 (ZC3H11A)	pACTII	Ampicillin	Venables, unpublished data
KIAA0663 (ZC3H11A)	pGFP3	Ampicillin	PCR amplification from pACTII using KIAA0663-F and KIAA0663-B primers incorporating *Eco*RI and *Xho*I restriction sites. Ligated into complementary site in pGFP3 vector.
Limkain-β2 (CCDC92)	pACTII	Ampicillin	Venables, unpublished data
Limkain-β2 (CCDC92)	pGFP3	Ampicillin	PCR amplification from pACTII using Limkainβ2-F and Limkainβ2-B primers incorporating *Eco*RI and *Not*I restriction sites. Ligated into complementary site in pGFP3 vector.
PHC2	pACTII	Ampicillin	Venables, unpublished data
PHC2	pGFP3	Ampicillin	PCR amplification from pACTII using HPH2-F and HPH2-B primers incorporating *Mfe*I and *Xho*I restriction sites. Ligated into complementary site in pGFP3 vector.
Sec16A	pEGFP	Kanamycin	Dr David Stephens (University of Bristol, UK). Watson et al., 2006
SIAH1	pGBKT7	Kanamycin	Venables et al., 2004
SIAH1(153+)	pGADT7	Ampicillin	Venables, unpublished data
SIAH1(153+)	pGBKT7	Kanamycin	PCR amplification from SIAH1pGADT7 using SIAH153-F and SIAH1 protein-B primers incorporating *Eco*RI and *Xho*I restriction sites. Ligated into complementary sites in the pGBKT7 vector.
SIAH1	pCDNA3.1	Ampicillin	Venables et al., 2004
SIAH1(-98)	pGBKT7	Kanamycin	Venables et al., 2004
SIAH1(99-155)	pGADT7	Ampicillin	Venables, unpublished data

SIAH1(99-155)	pGBKT7	Kanamycin	PCR amplification from pGADT7 using SIAH195-F and SIAH155-B primers incorporating *Eco*RI and *Xho*I restriction sites. Ligated into complementary sites in the pGBKT7 vector.
Siah1a	pKH3	Ampicillin	Gift from Professor David Bowtell, Peter MacCallum Cancer Centre, Melbourne, Australia
Siah1a(N-FLAG)	p3XFLAG(N)	Ampicillin	PCR amplification from Siah1a-pKH3 using Siah1a-F(FLAG) and Siah1b-R(FLAG) primers incorporating *Eco*RI and *Xba*I restriction sites. Ligated into complementary sites in the p3XFLAG(N) vector.
Siah1a(C-FLAG)	p3XFLAG(C)	Ampicillin	PCR amplification from Siah1a-pKH3 using Siah1a-F(FLAG) and Siah1b/a-R(FLAG) primers incorporating *Eco*RI and *Xba*I restriction sites. Ligated into complementary sites in the p3XFLAG(C) vector.
Siah1b	pCDNA3.1	Ampicillin	PCR amplification from a full length Siah1b clone (*Siah1b* image ID; 30053109) using Siah1b(F) and Siah1b(R) primers incorporating *Eco*RI and *Xho*I restriction sites. Ligated into complementary sites in the pCDNA3.1 vector.
Siah1b	pGBKT7	Kanamycin	PCR amplification from a full length Siah1b clone (*Siah1b* image ID; 30053109) using Siah1b(F) and Siah1b(R) primers incorporating *Eco*RI and *Xho*I restriction sites. Ligated into complementary sites in the pGBKT7 vector.
Siah1b(N-FLAG)	p3XFLAG(N)	Ampicillin	PCR amplification from a full length Siah1b clone (*Siah1b* image ID; 30053109) using Siah1b-F(FLAG) and Siah1b-R(FLAG) primers incorporating *Eco*RI and *Xba*I restriction sites. Ligated into complementary sites in the p3XFLAG(N) vector.
Siah1b(C-FLAG)	p3XFLAG(C)	Ampicillin	PCR amplification from a full length Siah1b clone (*Siah1b* image ID; 30053109) using Siah1b-F(FLAG) and Siah1b/a-R(FLAG)primers incorporating *Eco*RI and *Xba*I restriction sites. Ligated into complementary sites in the p3XFLAG(C) vector.
Siah2	pKH3	Ampicillin	Gift from Professor David Bowtell, Peter MacCallum Cancer Centre, Melbourne, Australia
Siah2(N-FLAG)	p3XFLAG(N)	Ampicillin	PCR amplification from a full length Siah2-pKH3 using Siah2-F(FLAG)and Siah2-R(FLAG)+STOP primers incorporating *Eco*RI and *Xba*I restriction sites. Ligated into complementary sites in the p3XFLAG(N) vector
Siah2(C-FLAG)	p3XFLAG(C)	Ampicillin	PCR amplification from a full length Siah2-pKH3 using Siah2-F(FLAG)and Siah2-R(FLAG)-STOP primers incorporating *Eco*RI and *Xba*I restriction sites. Ligated into complementary sites in the p3XFLAG(C) vector
SIAH2	pACTII	Ampicillin	Venables et al., 2004
SIAH1BP1	pACTII	Ampicillin	Venables, unpublished data
SIAH1BP1	pGFP3	Ampicillin	PCR amplification from pACTII using PUF60-F and PUF60-B primers incorporating *Eco*RI and *Xho*I restriction sites. Ligated into complementary sites in the pGFP3 vector.
T-STAR	pGFP3	Ampicillin	Venables et al., 2004
T-STAR(RG)	pGEX5X1	Ampicillin	Venables et al., 2004
Uk-p68 (ZC3H14)	pACTII	Ampicillin	Venables, unpublished data
Uk-p68 (ZC3H14)	pGFP3	Ampicillin	PCR amplification from pACTII using UKp68-F and Ukp68-B primers incorporating *Eco*RV and *Xho*I restriction sites. Ligated into complementary site in pGFP3 vector.
VAPA	pACTII	Ampicillin	Venables, unpublished data
VAPA	pGFP3	Ampicillin	PCR amplification from pACTII using VAPA-F and VAPA-B primers incorporating *Eco*RI and *Xho*I restriction sites. Ligated into complementary site in pGFP3 vector.
WHSC2	pACTII	Ampicillin	Venables, unpublished data
WHSC2	pGFP3	Ampicillin	PCR amplification from pACTII using WHSC2-F and WHSC2-B primers incorporating *Eco*RI and *Xho*I restriction sites. Ligated into complementary site in pGFP3 vector.
WHSC2(1-248)	pGADT7	Ampicillin	PCR amplification from pACTII using WHSC2-F and WHSC2(744)B primers incorporating *Eco*RI and *Xho*I restriction sites. Ligated into complementary sites in the pGADT7 vector.
WHSC2(248-317)	pGADT7	Ampicillin	PCR amplification from pACTII using WHSC2(744)F and WHSC2(951)B primers incorporating *Eco*RI and *Xho*I restriction sites. Ligated into complementary sites in the pGADT7 vector.
WHSC2(317-427)	pGADT7	Ampicillin	PCR amplification from pACTII using WHSC2(951)F and WHSC2(1281)B primers incorporating *Eco*RI and *Xho*I restriction sites. Ligated into complementary sites in the pGADT7 vector.
WHSC2(317-528)	pGADT7	Ampicillin	PCR amplification from pACTII using WHSC2(951)F and WHSC2-B primers incorporating *Eco*RI and *Xho*I restriction

			sites. Ligated into complementary sites in the pGADT7 vector.
WHSC2(1-248)	pGBKT7	Kanamycin	PCR amplification from pACTII using WHSC2-F and WHSC2(744)B primers incorporating *Eco*RI and *Xho*I restriction sites. Ligated into complementary sites in the pGBKT7 vector.
WHSC2(248-317)	pGBKT7	Kanamycin	PCR amplification from pACTII using WHSC2(744)F and WHSC2(951)B primers incorporating *Eco*RI and *Xho*I restriction sites. Ligated into complementary sites in the pGBKT7 vector.
WHSC2(317-427)	pGBKT7	Kanamycin	PCR amplification from pACTII using WHSC2(951)F and WHSC2(1281)B primers incorporating *Eco*RI and *Xho*I restriction sites. Ligated into complementary sites in the pGBKT7 vector.
WHSC2(317-528)	pGBKT7	Kanamycin	PCR amplification from pACTII using WHSC2(951)F and WHSC2-B primers incorporating *Eco*RI and *Xho*I restriction sites. Ligated into complementary sites in the pGBKT7 vector.
WHSC2(317-427)	pGEX5X1	Ampicillin	PCR amplification from pACTII using WHSC2(951)F and WHSC2(1281)B primers incorporating *Eco*RI and *Xho*I restriction sites. Ligated into complementary sites in the pGEX5X1 vector.
ZC3H14(374-594)	pGADT7	Ampicillin	PCR amplification from Uk-p68 pACTII clone using UKp68(1122)F and UKp68(1782)R primers incorporating *Nde*I and *Xho*I restriction sites. Ligated into complementary sites in the pGADT7 vector.
ZC3H14(554-736)	pGADT7	Ampicillin	PCR amplification from Uk-p68 pACTII clone using UKp68(1662)F and UKp68B primers incorporating *Nde*I and *Xho*I restriction sites. Ligated into complementary sites in the pGADT7 vector.
ZC3H14(374-490)	pGADT7	Ampicillin	PCR amplification from Uk-p68 pACTII clone using UKp68(1122)F and UKp68(1449)R primers incorporating *Eco*RI and *Xho*I restriction sites. Ligated into complementary sites in the pGADT7 vector.
ZC3H14(483-607)	pGADT7	Ampicillin	PCR amplification from Uk-p68 pACTII clone using UKp68(1449)F and UKp68(1782)R primers incorporating *Eco*RI and *Xho*I restriction sites. Ligated into complementary sites in the pGADT7 vector.
ZC3H11A(546-700)	pGADT7	Ampicillin	PCR amplification from KIAA0663 pACTII clone using KIAA0663(1638)F and KIAA0663(2100)R primers incorporating *Eco*RI and *Xho*I restriction sites. Ligated into complementary sites in the pGADT7 vector.
ZC3H11A(678-810)	pGADT7	Ampicillin	PCR amplification from KIAA0663 pACTII clone using KIAA0663(2034)F and KIAA0663B incorporating *Eco*RI and *Xho*I restriction sites. Ligated into complementary sites in the pGADT7 vector.
ZC3H11A(546-633)	pGADT7	Ampicillin	PCR amplification from KIAA0663 pACTII clone using KIAA0663(1638)F and KIAA0663(1875)R primers incorporating *Eco*RI and *Xho*I restriction sites. Ligated into complementary sites in the pGADT7 vector.
ZC3H11A(625-706)	pGADT7	Ampicillin	PCR amplification from KIAA0663 pACTII clone using KIAA0663(1875)F and KIAA0663(2100)R primers incorporating *Eco*RI and *Xho*I restriction sites. Ligated into complementary sites in the pGADT7 vector

References

Abada, R., T. Dreyfuss-Grossman, Y. Herman-Bachinsky, H. Geva, S. R. Masa and R. Sarid (2008). "SIAH-1 interacts with the Kaposi's sarcoma-associated herpesvirus-encoded ORF45 protein and promotes its ubiquitylation and proteasomal degradation." J Virol 82(5): 2230-2240.

Adams, M. D., M. Dubnick, A. R. Kerlavage, R. Moreno, J. M. Kelley, T. R. Utterback, J. W. Nagle, C. Fields and J. C. Venter (1992). "Sequence identification of 2,375 human brain genes." Nature 355(6361): 632-634.

Ahmed, A. U., R. L. Schmidt, C. H. Park, N. R. Reed, S. E. Hesse, C. F. Thomas, J. R. Molina, C. Deschamps, P. Yang, M. C. Aubry, et al. (2008). "Effect of disrupting seven-in-absentia homolog 2 function on lung cancer cell growth." J Natl Cancer Inst 100(22): 1606-1629.

Aida, M., Y. Chen, K. Nakajima, Y. Yamaguchi, T. Wada and H. Handa (2006). "Transcriptional pausing caused by NELF plays a dual role in regulating immediate-early expression of the *junB* gene." Mol Cell Biol 26(16): 6094-6104.

Aiyar, S. E., J. Sun, A. L. Blair, C. A. Moskaluk, Y. Lu, Q. Ye, Y. Yamaguchi, A. Mukherjee, D. Ren, H. Handa, et al. (2004). "Attenuation of estrogen receptor alpha-mediated transcription through estrogen-stimulated recruitment of a negative elongation factor." Genes Dev 18(17): 2134-2146.

Amson, R. B., M. Nemani, J. P. Roperch, D. Israeli, L. Bougueleret, I. Le Gall, M. Medhioub, G. Linares-Cruz, F. Lethrosne, P. Pasturaud, et al. (1996). "Isolation of 10 differentially expressed cDNAs in p53-induced apoptosis: activation of the vertebrate homologue of the *Drosophila seven in absentia* gene." Proc Natl Acad Sci USA 93(9): 3953-3957.

Andreassen, P. R., F. B. Lacroix, E. Villa-Moruzzi and R. L. Margolis (1998). "Differential subcellular localization of protein phosphatase-1 alpha, gamma, and delta isoforms during both interphase and mitosis in mammalian cells." J Cell Biol 141(5): 1207-1215.

Anitei, M., C. Stange, I. Parshina, T. Baust, A. Schenck, G. Raposo, T. Kirchhausen and B. Hoflack (2010). "Protein complexes containing CYFIP/Sra/PIR121 coordinate Arf1 and Rac1 signalling during clathrin-AP1-coated carrier biogenesis at the TGN." Nat Cell Biol 12(4): 330-340.

Aravind, L. and E. V. Koonin (2000). "The U box is a modified RING finger - a common domain in ubiquitination." Curr Biol 10(4): 132-134.

Ardley, H. C. and P. A. Robinson (2004). "The role of ubiquitin protein ligases in neurodegenerative disease." Neurodegener Dis 1: 71-87.

Avraham, E., R. Szargel, A. Eyal, R. Rott and S. Engelender (2005). "Glycogen synthase kinase 3-beta modulates synphilin-1 ubiquitylation and cellular inclusion formation by SIAH: implications for proteasomal function and Lewy body formation." J Biol Chem 280(52): 42877-42886.

Bailey, R. W., B. Aronow, J. A. K. Harmony and M. D. Griswold (2002). "Heat shock-initiated apoptosis is accelerated and removal of damaged cells is delayed in the testis of clusterin/apoJ knock-out mice." Biol Reprod 66(4): 1042-1053.

Ban, R., H. Matsuzaki, T. Akashi, G. Sakashita, H. Taniguchi, S. Y. Park, H. Tanaka, K. Furukawa and T. Urano (2009). "Mitotic regulation of the stability of microtubule plus-end tracking protein EB3 by ubiquitin ligase SIAH-1 and aurora mitotic kinases." J Biol Chem 284(41): 28367-28381.

Banerjee, S., B. R. P. Kumar and T. K. Kundu (2004). "General transcriptional coactivator PC4 activates p53 function." Mol Cell Biol 24(5): 2052-2062.

Becker, J. and E. A. Craig (1994). "Heat-shock proteins as molecular chaperones." Eur J Biochem 219(1-2): 11-23.

Benyamini, H., H. Leonov, S. Rotem, C. Katz, I. T. Arkin and A. Friedler (2009). "A model for the interaction between NF-kappa-B and ASPP2 suggests an I-kappa-B-like binding mechanism." Proteins 77(3): 602-611.

Berg, J. M., J. L. Tymoczko and L. Stryer (2002). Biochemistry. New York, W.H. Freeman and Company.

Bergamaschi, D., Y. Samuels, B. Jin, S. Duraisingham, T. Crook and X. Lu (2004). "ASPP1 and ASPP2: common activators of p53 family members." Mol Cell Biol 24(3): 1341-1350.

Bergamaschi, D., Y. Samuels, N. J. O'Neil, G. Trigiante, T. Crook, J. K. Hsieh, D. J. O'Connor, S. Zhong, I. Campargue, M. L. Tomlinson, et al. (2003). "iASPP oncoprotein is a key inhibitor of p53 conserved from worm to human." Nat Genet 33(2): 162-167.

Bezy, O., C. Elabd, O. Cochet, R. K. Petersen, K. Kristiansen, C. Dani, G. Ailhaud and E. Amri (2005). "Delta-interacting protein A, a new inhibitory partner of CCAAT/enhancer-binding protein beta, implicated in adipocyte differentiation." J Biol Chem 280(12): 11432-11438.

Boehm, J., Y. He, A. Greiner, L. Staudt and T. Wirth (2001). "Regulation of BOB1/OBF1 stability by SIAH." EMBO J 20: 4153-4162.

Braithwaite, A. W., G. Del Sal and X. Lu (2006). "Some p53-binding proteins that can function as arbiters of life and death." Cell Death Differ 13(6): 984-993.

Bruzzoni-Giovanelli, H., A. Faille, G. Linares-Cruz, M. Nemani, F. Le Deist, A. Germani, D. Chassoux, G. Millot, J. P. Roperch, R. B. Amson, et al. (1999). "SIAH-1 inhibits cell growth by altering the mitotic process." Oncogene 18(50): 7101-7109.

Budnik, A. and D. J. Stephens (2009). "ER exit sites - localization and control of COPII vesicle formation." FEBS Lett 583(23): 3796-3803.

Bursen, A., S. Moritz, A. Gaussmann, S. Moritz, T. Dingermann and R. Marschalek (2004). "Interaction of AF4 wild-type and AF4.MLL fusion protein with SIAH proteins: indication for t(4;11) pathobiology." Oncogene 23(37): 6237-6249.

Calzado, M. A., L. de la Vega, A. Moller, D. D. L. Bowtell and M. L. Schmitz (2009). "An inducible autoregulatory loop between HIPK2 and Siah2 at the apex of the hypoxic response." Nat Cell Biol 11(1): 85-91.

Cao, Y., T. Hamada, T. Matsui, T. Date and K. Iwabuchi (2004). "Hepatitis C virus core protein interacts with p53-binding protein, 53BP2/Bbp/ASPP2, and inhibits p53-mediated apoptosis." Biochem Biophys Res Commun 315(4): 788-795.

Capoano, C. A., R. Wettstein, A. Kun and A. Geisinger (2010). "Spats 1 (Srsp1) is differentially expressed during testis development of the rat." Gene Exp Patterns 10(1): 1-8.

Carrell, D. T., B. R. Emery and S. Hammoud (2007). "Altered protamine expression and diminished spermatogenesis: what is the link?" Hum Reprod Update 13(3): 313-327.

Carthew, R. W., T. P. Neufeld and G. M. Rubin (1994). "Identification of genes that interact with the *sina* gene in *Drosophila* eye development." Proc Natl Acad Sci USA 91(24): 11689-11693.

Carthew, R. W. and G. M. Rubin (1990). "*Seven in absentia*, a gene required for specification of R7 cell fate in the *Drosophila* eye." Cell 63(3): 561-577.

Castle, A. and D. Castle (2005). "Ubiquitously expressed secretory carrier membrane proteins (SCAMPs) 1-4 mark different pathways and exhibit limited constitutive trafficking to and from the cell surface." J Cell Sci 118(16): 3769-3780.

Ceulemans, H. and M. Bollen (2004). "Functional diversity of protein phosphatase-1, a cellular economizer and reset button." Physiol Rev 84(1): 1-39.

Chakrabarti, R., L. Cheng, P. Puri, D. Soler and S. Vijayaraghavan (2007). "Protein phosphatase PP1gamma2 in sperm morphogenesis and epididymal initiation of sperm motility." Asian J Androl 9(4): 445-452.

Chaparian, M. G. and D. R. Evans (1988). "Intracellular location of the multidomain protein CAD in mammalian cells." FASEB J 2(14): 2982-2989.

Chasman, D. I., G. Pare, S. Mora, J. C. Hopewell, G. Peloso, R. Clarke, L. A. Cupples, A. Hamsten, S. Kathiresan, A. Malarstig, et al. (2009). "Forty-three loci associated with plasma lipoprotein size, concentration, and cholesterol content in genome-wide analysis." PLoS Genet 5(11): e1000730.

Chen, D., E. Padiernos, F. Ding, I. S. Lossos and C. D. Lopez (2004). "Apoptosis-stimulating protein of p53-2 (ASPP2/53BP2L) is an E2F target gene." Cell Death Differ 12(4): 358-368.

Chen, Y., W. Liu, L. Naumovski and R. L. Neve (2003). "ASPP2 inhibits APP-BP1-mediated NEDD8 conjugation to cullin-1 and decreases APP-BP1-induced cell proliferation and neuronal apoptosis." J Neurochem 85(3): 801-809.

Choi, D. W., Y. M. Seo, E. A. Kim, K. S. Sung, J. W. Ahn, S. J. Park, S. R. Lee and C. Y. Choi (2008). "Ubiquitination and degradation of homeodomain-interacting protein kinase 2 by WD40 repeat/SOCS box protein WSB-1." J Biol Chem 283(8): 4682-4689.

Ciechanover, A. and K. Iwai (2004). "The ubiquitin system: from basic mechanisms to the patient bed." IUBMB Life 56(4): 193 -201.

Clark, A. M., S. M. Maguire and M. D. Griswold (1997). "Accumulation of clusterin/sulfated glycoprotein-2 in degenerating pachytene spermatocytes of adult rats treated with methoxyacetic acid." Biol Reprod 57(4): 837-846.

Cohen, P. T. W. (2002). "Protein phosphatase 1 - targeted in many directions." J Cell Sci 115(2): 241-256.

Cohen, S. B., W. Ma, V. A. Valova, M. Algie, R. Harfoot, A. G. Woolley, P. J. Robinson and A. W. Braithwaite (2009). "Genotoxic stress-induced nuclear localization of oncoprotein YB-1 in the absence of proteolytic processing." Oncogene 29(3): 403-410.

Conaway, R. C., C. S. Brower and J. W. Conaway (2002). "Emerging roles of ubiquitin in transcription regulation." Science 296(5571): 1254-1258.

Conesa, C. and J. Acker (2010). "Sub1/PC4 a chromatin associated protein with multiple functions in transcription." RNA Biol 7(3): Epub ahead of print.

Confalonieri, S., M. Quarto, G. Goisis, P. Nuciforo, M. Donzelli, G. Jodice, G. Pelosi, G. Viale, S. Pece and P. Di Fiore (2009). "Alterations of ubiquitin ligases in human cancer and their association with the natural history of the tumor." Oncogene 28(33): 2959-2968.

Cooper, S. E., C. M. Murawsky, N. Lowe and A. A. Travers (2008). "Two modes of degradation of the tramtrack transcription factors by Siah homologues." J Biol Chem 283(2): 1076-1083.

Criekinge, W. V. and R. Beyaert (1999). "Yeast two-hybrid: state of the art." Biol Proced Online 4: 1-38.

Cukier, C. D., D. Hollingworth, S. R. Martin, G. Kelly, I. Diaz-Moreno and A. Ramos (2010). "Molecular basis of FIR-mediated c-myc transcriptional control." Nat Struct Mol Biol 17(99): 1058-1064.

Daugaard, M., M. Rohde and M. Jäättelä (2007). "The heat shock protein 70 family: highly homologous proteins with overlapping and distinct functions." FEBS Lett 581(19): 3702-3710.

Dawson, T. M. (2006). "Parkin and defective ubiquitination in Parkinson's disease." J Neural Transm Suppl 70: 209-213.

Della, N. G., D. D. Bowtell and F. Beck (1995). "Expression of Siah-2, a vertebrate homologue of *Drosophila sina*, in germ cells of the mouse ovary and testis." Cell Tissue Res 279(2): 411-419.

Della, N. G., P. V. Senior and D. D. Bowtell (1993). "Isolation and characterisation of murine homologues of the *Drosophila seven in absentia* gene (*sina*)." Development 117(4): 1333-1343.

Denuc, A. and G. Marfany (2010). "SUMO and ubiquitin paths converge." Biochem Soc Trans 38: 34-39.

Deshaies, R. J. and C. A. P. Joazeiro (2009). "RING domain E3 ubiquitin ligases." Annu Rev Biochem 78(1): 399-434.

Deshaies, R. J. and R. Schekman (1987). "A yeast mutant defective at an early stage in import of secretory protein precursors into the endoplasmic reticulum." J Cell Biol 105(2): 633-645.

Deshaies, R. J. and R. Schekman (1989). "SEC62 encodes a putative membrane protein required for protein translocation into the yeast endoplasmic reticulum." J Cell Biol 109(6): 2653-2664.

Desterro, J. M. P., J. Thomson and R. T. Hay (1997). "Ubch9 conjugates SUMO but not ubiquitin." FEBS Lett 417(3): 297-300.

Dickins, R. A., I. J. Frew, C. M. House, M. K. O'Bryan, A. J. Holloway, I. Haviv, N. Traficante, D. M. de Kretser and D. D. L. Bowtell (2002). "The ubiquitin ligase

component Siah1a is required for completion of meiosis I in male mice." Mol Cell Biol 22(7): 2294-2303.

Dower, W. J., J. F. Miller and C. W. Ragsdale (1988). "High efficiency transformation of *E.coli* by high voltage electroporation." Nucleic Acids Res 16: 6127-6145.

D'Souza-Schorey, C. and P. Chavrier (2006). "ARF proteins: roles in membrane traffic and beyond." Nat Rev Mol Cell Biol 7(5): 347-358.

Du, X., Q. Wang, Y. Hirohashi and M. I. Greene (2006). "DIPA, which can localize to the centrosome, associates with p78/MCRS1/MSP58 and acts as a repressor of gene transcription." Exp Mol Pathol 81(3): 184-190.

Dufu, K., M. J. Livingstone, J. Seebacher, S. P. Gygi, S. A. Wilson and R. Reed (2010). "ATP is required for interactions between UAP56 and two conserved mRNA export proteins, Aly and CIP29, to assemble the TREX complex." Genes Dev 24(18): 2043-2053.

Egea, G., F. Lázaro-Diéguez and M. Vilella (2006). "Actin dynamics at the Golgi complex in mammalian cells." Curr Opin Cell Biol 18(2): 168-178.

El-Deiry, W. S., S. E. Kern, J. A. Pietenpol, K. W. Kinzler and B. Vogelstein (1992). "Definition of a consensus binding site for p53." Nat Genet 1(1): 45-49.

Elliott, D. J., K. Oghene, G. Makarov, O. Makarova, T. B. Hargreave, A. C. Chandley, I. C. Eperon and H. J. Cooke (1998). "Dynamic changes in the subnuclear organisation of pre-mRNA splicing proteins and RBM during human germ cell development." J Cell Sci 111(9): 1255-1265.

Enerly, E., J. Larsson and A. Lambertsson (2002). "Reverse genetics in *Drosophila*: from sequence to phenotype using UAS-RNAi transgenic flies." Genesis 34(1-2): 152-155.

Engelender, S. (2008). "Ubiquitination of alpha-synuclein and autophagy in Parkinson's disease." Autophagy 4(3): 372-374.

Enninga, J., A. Levay and B. M. A. Fontoura (2003). "Sec13 shuttles between the nucleus and the cytoplasm and stably interacts with Nup96 at the nuclear pore complex." Mol Cell Biol 23(20): 7271-7284.

Espanel, X. and M. Sudol (2001). "Yes-associated protein and p53-binding protein-2 interact through their WW and SH3 domains." J Biol Chem 276(17): 14514-14523.

Fanelli, M., A. Fantozzi, P. De Luca, S. Caprodossi, S. Matsuzawa, M. A. Lazar, P. G. Pelicci and S. Minucci (2004). "The coiled-coil domain is the structural determinant for mammalian homologues of *Drosophila* sina-mediated degradation of promyelocytic leukemia protein and other tripartite motif proteins by the proteasome." J Biol Chem 279(7): 5374-5379.

Fang, S., J. P. Jensen, R. L. Ludwig, K. H. Vousden and A. M. Weissman (2000). "Mdm2 is a RING finger-dependent ubiquitin protein ligase for itself and p53." J Biol Chem 275(12): 8945-8951.

Fathallah, D. M., D. Cherif, K. Dellagi and M. A. Arnaout (1993). "Molecular cloning of a novel human hsp70 from a B cell line and its assignment to chromosome 5." J Immunol 151(2): 810-813.

Fiucci, G., S. Beaucourt, D. Duflaut, A. Lespagnol, P. Stumptner-Cuvelette, A. Geant, G. Buchwalter, M. Tuynder, L. Susini, J. M. Lassalle, et al. (2004). "*Siah-1b* is a direct transcriptional target of p53: identification of the functional p53 responsive element in the *siah-1b* promoter." Proc Natl Acad Sci USA 101(10): 3510-3515.

Fogal, V., N. N. Kartasheva, G. Trigiante, S. Llanos, D. Yap, K. H. Vousden and X. Lu (2005). "ASPP1 and ASPP2 are new transcriptional targets of E2F." Cell Death Differ 12(4): 369-376.

Fourie, A. M., P. A. Peterson and Y. Yang (2001). "Characterization and regulation of the major histocompatibility complex-encoded proteins Hsp70-Hom and Hsp70-1/2." Cell Stress 6(3): 282-295.

Franck, T., R. Krueger, D. Woitalla, T. Muller, S. Engelender and O. Riess (2006). "Mutation analysis of the s*even in absentia homolog 1* (*SIAH1*) gene in Parkinson's disease." J Neural Transm 113(12): 1903-1908.

Frasor, J., J. M. Danes, C. C. Funk and B. S. Katzenellenbogen (2005). "Estrogen down-regulation of the corepressor N-CoR: mechanism and implications for estrogen derepression of N-CoR-regulated genes." Proc Natl Acad Sci USA 102(37): 13153 - 13157.

Freemont, P. S. (2000). "RING for destruction?" Curr. Biol. 10: 84-87.

Frew, I. J., R. A. Dickins, A. R. Cuddihy, M. Del Rosario, C. Reinhard, M. J. O'Connell and D. D. L. Bowtell (2002). "Normal p53 function in primary cells deficient for *Siah* genes." Mol Cell Biol 22(23): 8155-8164.

Frew, I. J., V. E. Hammond, R. A. Dickins, J. M. W. Quinn, C. R. Walkley, N. A. Sims, R. Schnall, N. G. Della, A. J. Holloway, M. R. Digby, et al. (2003). "Generation and analysis of *Siah2* mutant mice." Mol Cell Biol 23(24): 9150-9161.

Frew, I. J., N. A. Sims, J. M. W. Quinn, C. R. Walkley, L. E. Purton, D. D. L. Bowtell and M. T. Gillespie (2004). "Osteopenia in *Siah1a* mutant mice." J Biol Chem 279(28): 29583-29588.

Fukuba, H., T. Takahashi, H. G. Jin, T. Kohriyama and M. Matsumoto (2008). "Abundance of aspargynyl-hydroxylase FIH is regulated by Siah-1 under normoxic conditions." Neurosci Lett 433(3): 209-214.

Futreal, P. A., Q. Liu, D. Shattuck-Eidens, C. Cochran, K. Harshman, S. Tavtigian, L. M. Bennett, A. Haugen-Strano, J. Swensen and Y. Miki (1994). "*BRCA1* mutations in primary breast and ovarian carcinomas." Science 266(5182): 120-122.

Garcia, A., X. Cayla, J. Guergnon, F. Dessauge, V. Hospital, M. P. Rebollo, A. Fleischer and A. Rebollo (2003). "Serine/threonine protein phosphatases PP1 and PP2A are key players in apoptosis." Biochimie 85(8): 721-726.

Garrido, C., S. Gurbuxani, L. Ravagnan and G. Kroemer (2001). "Heat shock proteins: endogenous modulators of apoptotic cell death." Biochem Biophys Res Commun 286(3): 433-442.

Gaynor, E. C., T. R. Graham and S. D. Emr (1998). "COPI in ER/Golgi and intra-Golgi transport: do yeast COPI mutants point the way?" Biochim Biophys Acta 1404(1-2): 33-51.

Geremia, R., C. Boitani, M. Conti and V. Monesi (1977). "RNA synthesis in spermatocytes and spermatids and preservation of meiotic RNA during spermiogenesis in the mouse." Cell Differ 5: 343-355.

Germani, A., H. Bruzzoni-Giovanelli, A. Fellous, S. Gisselbrecht, N. Varin-Blank and F. Calvo (2000). "SIAH-1 interacts with alpha-tubulin and degrades the kinesin Kid by the proteasome pathway during mitosis." Oncogene 19(52): 5997-6006.

Germani, A., A. Prabel, S. Mourah, M. P. Podgorniak, A. D. Carlo, R. Ehrlich, S. Gisselbrecht, N. Varin-Blank, F. Calvo and H. Bruzzoni-Giovanelli (2003). "SIAH-1 interacts with CtIP and promotes its degradation by the proteasome pathway." Nature 22(55): 8845-8851.

Germani, A., F. Romero, M. Houlard, J. Camonis, S. Gisselbrecht, S. Fischer and N. Varin-Blank (1999). "hSiah2 is a new vav binding protein which inhibits vav-mediated signaling pathways." Mol Cell Biol 19(5): 3798-3807.

Gilchrist, D. A., S. Nechaev, C. Lee, S. K. B. Ghosh, J. B. Collins, L. Li, D. S. Gilmour and K. Adelman (2008). "NELF-mediated stalling of Pol II can enhance gene expression by blocking promoter-proximal nucleosome assembly." Genes Dev 22(14): 1921-1933.

Gorina, S. and N. P. Pavletich (1996). "Structure of the p53 tumor suppressor bound to the ankyrin and SH3 domains of 53BP2." Science 274(5289): 1001-1005.

Griffiths, A. J. F., J. H. Miller, D. T. Suzuki, R. C. Lewontin and W. M. Gelbart (2000). An introduction to genetic analysis. New York, W.H. Freeman.

Grosso, A. R., A. Q. Gomes, N. L. Barbosa-Morais, S. Caldeira, N. P. Thorne, G. Grech, M. von Lindern and M. Carmo-Fonseca (2008). "Tissue-specific splicing factor gene expression signatures." Nucleic Acids Res 36(15): 4823-4832.

Gutierrez, G. J., A. Vogtlin, A. Castro, I. Ferby, G. Salvagiotto, Z. Ronai, T. Lorca and A. R. Nebreda (2006). "Meiotic regulation of the CDK activator RINGO/speedy by ubiquitin-proteasome-mediated processing and degradation." Nat Cell Biol 8(10): 1084-1094.

Haass, N. K., M. A. Kartenbeck and R. E. Leube (1996). "Pantophysin is a ubiquitously expressed synaptophysin homologue and defines constitutive transport vesicles." J Cell Biol 134(3): 731-746.

Habelhah, H., I. J. Frew, A. Laine, P. W. Janes, F. Relaix, D. Sassoon, D. D. Bowtell and Z. Ronai (2002). "Stress-induced decrease in TRAF2 stability is mediated by Siah2." EMBO J 21(21): 5756-5765.

Habelhah, H., A. Laine, H. Erdjument-Bromage, P. Tempst, M. E. Gershwin, D. L. Bowtell and Z. Ronai (2004). "Regulation of 2-oxoglutarate (alpha-ketoglutarate) dehydrogenase stability by the RING finger ubiquitin ligase Siah." J Biol Chem 279(51): 53782-53788.

Hackstein, J. H. P., R. Hochstenbach and P. L. Pearson (2000). "Towards an understanding of the genetics of human male infertility: lessons from flies." Trends Genet 16(12): 565-572.

Hakuno, F., S. Kurihara, R. T. Watson, J. E. Pessin and S. Takahashi (2007). "53BP2S, interacting with insulin receptor substrates, modulates insulin signaling." J Biol Chem 282(52): 37747-37758.

Hara, M. and S. H. Snyder (2006). "Nitric oxide-GAPDH-Siah: a novel cell death cascade." Cell Mol Neurobiol 26(4): 525-536.

Hara, M. R., N. Agrawal, S. F. Kim, M. B. Cascio, M. Fujimuro, Y. Ozeki, M. Takahashi, J. H. Cheah, S. K. Tankou, L. D. Hester, et al. (2005). "S-nitrosylated GAPDH initiates apoptotic cell death by nuclear translocation following Siah1 binding." Nat Cell Biol 7(7): 665-674.

Hartl, F. U. (1996). "Molecular chaperones in cellular protein folding." Nature 381(6583): 571-580.

Hastings, M. L., E. Allemand, D. M. Duelli, M. P. Myers and A. R. Krainer (2007). "Control of pre-mRNA splicing by the general splicing factors PUF60 and U2AF65." PLoS ONE 2(6): e538.

Hatakeyama, S. and K. I. Nakayama (2003). "U-box proteins as a new family of ubiquitin ligases." Biochem Biophys Res Commun 302(4): 635-645.

He, H. T., E. Fokas, A. You, R. Engenhart-Cabillic and H. X. An (2010). "Siah1 proteins enhance radiosensitivity of human breast cancer cells." BMC Cancer 10(1).

He, Z., L. Feng, X. Zhang, Y. Geng, D. A. Parodi, C. Suarez-Quian and M. Dym (2005). "Expression of Col1a1, Col1a2 and procollagen I in germ cells of immature and adult mouse testis." Reproduction 130(3): 333-341.

Helps, N. R., H. M. Barker, S. J. Elledge and P. W. Cohen (1995). "Protein phosphatase 1 interacts with p53BP2, a protein which binds to the tumour suppressor p53." FEBS Lett 377(3): 295-300.

Hershko, A. (2005). "The ubiquitin system for protein degradation and some of its roles in the control of the cell division cycle." Cell Death Differ 12(9): 1191-1197.

Hershko, A. and A. Ciechanover (1998). "The ubiquitin system." Annu Rev Biochem 67(1): 425-479.

Hershko, A., H. Heller, E. Eytan and Y. Reiss (1986). "The protein substrate binding site of the ubiquitin-protein ligase system." J. Biol. Chem. 261(26): 11992-11999.

Hershko, T., M. Chaussepied, M. Oren and D. Ginsberg (2005). "Novel link between E2F and p53: proapoptotic cofactors of p53 are transcriptionally upregulated by E2F." Cell Death Differ 12(4): 377-383.

Hicke, L. (2001). "Protein regulation by monoubiquitin." Nat Rev Mol Cell Biol 2(3): 195-201.

Hochstrasser, M. (2009). "Origin and function of ubiquitin-like proteins." Nature 458(7237): 422-429.

Holloway, A. J., N. G. Della, C. F. Fletcher, D. A. Largespada, N. G. Copeland, N. A. Jenkins and D. D. L. Bowtell (1997). "Chromosomal mapping of five highly conserved murine homologues of the *Drosophila* RING finger gene *seven-in-absentia*." Genomics 41(2): 160-168.

Homer, C., D. A. Knight, L. Hananeia, P. Sheard, J. Risk, A. Lasham, J. A. Royds and A. W. Braithwaite (2005). "Y-box factor YB1 controls p53 apoptotic function." Oncogene 24(56): 8314-8325.

Hoppe, T. (2005). "Multiubiquitylation by E4 enzymes: 'one size' doesn't fit all." Trends Biochem. Sci. 30(4): 183-187.

House, C. M., I. J. Frew, H. L. Huang, G. Wiche, N. Traficante, E. Nice, B. Catimel and D. D. L. Bowtell (2003). "A binding motif for Siah ubiquitin ligase." Proc Natl Acad Sci USA 100(6): 3101-3106.

House, C. M., N. C. Hancock, A. Möller, B. A. Cromer, V. Fedorov, D. D. L. Bowtell, M. W. Parker and G. Polekhina (2006). "Elucidation of the substrate binding site of Siah ubiquitin ligase." Structure 14(4): 695-701.

House, C. M., A. Moller and D. D. L. Bowtell (2009). "Siah proteins: novel drug targets in the Ras and hypoxia pathways." Cancer Res 69(23): 8835-8838.

Hu, G., Y. L. Chung, T. Glover, V. Valentine, A. T. Look and E. R. Fearon (1997a). "Characterization of human homologs of the *Drosophila seven in absentia* (*sina*) gene." Genomics 46(1): 103-111.

Hu, G. and E. Fearon (1999). "Siah-1 N-terminal RING domain is required for proteolysis function, and C-terminal sequences regulate oligomerization and binding to target proteins." Mol Cell Biol 19(1): 724-732.

Hu, G., S. Zhang, M. Vidal, J. L. Baer, T. Xu and E. R. Fearon (1997b). "Mammalian homologs of seven in absentia regulate DCC via the ubiquitin-proteasome pathway." Genes Dev 11(20): 2701-2714.

Hughes, H. and D. J. Stephens (2008). "Assembly, organization, and function of the COPII coat." Histochem Cell Biol 129(2): 129-151.

Iinuma, T., A. Shiga, K. Nakamoto, M. B. O'Brien, M. Aridor, N. Arimitsu, M. Tagaya and K. Tani (2007). "Mammalian Sec16/p250 plays a role in membrane traffic from the endoplasmic reticulum." J Biol Chem 282(24): 17632-17639.

Ikeda, F. and I. Dikic (2008). "Atypical ubiquitin chains: new molecular signals." EMBO Rep 9(6): 536-542.

Isono, K. I., Y. I. Fujimura, J. Shinga, M. Yamaki, J. O-Wang, Y. Takihara, Y. Murahashi, Y. Takada, Y. Mizutani-Koseki and H. Koseki (2005). "Mammalian polyhomeotic homologues Phc2 and Phc1 act in synergy to mediate polycomb repression of *Hox* Genes." Mol Cell Biol 25(15): 6694-6706.

Iwabuchi, K., P. L. Bartel, B. L. Li, R. Marraccino and S. Fields (1994). "Two cellular proteins that bind to wild-type but not mutant p53." Proc Natl Acad Sci USA 91(13): 6098-6102.

Iwabuchi, K., B. Li, H. F. Massa, B. J. Trask, T. Date and S. Fields (1998). "Stimulation of p53-mediated transcriptional activation by the p53-binding proteins, 53BP1 and 53BP2." J Biol Chem 273(40): 26061-26068.

Iwai, A., M. Hijikata, T. Hishiki, O. Isono, T. Chiba and K. Shimotohno (2007). "Coiled-coil domain containing 85B suppresses the beta-catenin activity in a p53-dependent manner." Oncogene 27(11): 1520-1526.

Iwai, A., H. Marusawa, S. Matsuzawa, T. Fukushima, M. Hijikata, J. C. Reed, K. Shimotohno and T. Chiba (2004). "Siah-1L, a novel transcript variant belonging to the human Siah family of proteins, regulates beta-catenin activity in a p53-dependent manner." Oncogene 23(45): 7593 - 7600.

Jackson, P. K., A. G. Eldridge, E. Freed, L. Furstenthal, J. Y. Hsu, B. K. Kaiser and J. D. R. Reimann (2000). "The lore of the RINGs: substrate recognition and catalysis by ubiquitin ligases." Trends Cell Biol. 10(10): 429-439.

Joazeiro, C. A. P. and A. M. Weissman (2000). "RING finger proteins: mediators of ubiquitin ligase activity." Cell 102(5): 549-552.

Johnsen, S. A., M. Subramaniam, D. G. Monroe, R. Janknecht and T. C. Spelsberg (2002). "Modulation of transforming growth factor beta (TGFbeta)/smad transcriptional responses through targeted degradation of TGFbeta-inducible early gene-1 by human seven in absentia homologue." J Biol Chem 277(34): 30754-30759.

Kampa, K. M., J. D. Acoba, D. Chen, J. Gay, H. Lee, K. Beemer, E. Padiernos, N. Boonmark, Z. Zhu, A. C. Fan, et al. (2009a). "Apoptosis-stimulating protein of p53 (ASPP2) heterozygous mice are tumor-prone and have attenuated cellular damage-response thresholds." Proc Natl Acad Sci USA 106(11): 4390-4395.

Kampa, K. M., M. Bonin and C. D. Lopez (2009b). "New insights into the expanding complexity of the tumor suppressor ASPP2." Cell Cycle 8(18): 2871-2876.

Kaneko, Y., T. Kimura, M. Kishishita, Y. Noda and J. Fujita (1997). "Cloning of *apg-2* encoding a novel member of heat shock protein 110 family." Gene 189(1): 19-24.

Karin, M. and Y. Ben-Neriah (2000). "Phosphorylation meets ubiquitination: the control of NF-kappaB activity." Annu Rev Immunol 18(1): 621-663.

Kee, Y. and J. M. Huibregtse (2007). "Regulation of catalytic activities of HECT ubiquitin ligases." Biochem Biophys Res Commun 354(2): 329-333.

Kelly, S. M., S. A. Pabit, C. M. Kitchen, P. Guo, K. A. Marfatia, T. J. Murphy, A. H. Corbett and K. M. Berland (2007). "Recognition of polyadenosine RNA by zinc finger proteins." Proc Natl Acad Sci USA 104(30): 12306-12311.

Kerscher, O., R. Felberbaum and M. Hochstrasser (2006). "Modification of proteins by ubiquitin and ubiquitin-like proteins." Annu Rev Cell Dev Biol 22(1): 159-180.

Kim, C. J., Y. G. Cho, C. H. Park, S. W. Jeong, S. W. Nam, S. Y. Kim, S. H. Lee, N. J. Yoo, J. Y. Lee and W. S. Park (2004a). "Inactivating mutations of the *Siah-1* gene in gastric cancer." Oncogene 23(53): 8591-8596.

Kim, H., W. Jeong, K. Ahn, C. Ahn and S. Kang (2004b). "Siah-1 interacts with the intracellular region of polycystin-1 and affects its stability via the ubiquitin-proteasome pathway." J Am Soc Nephrol 15(8): 2042-2049.

Kim, S. Y., D. W. Choi, E. A. Kim and C. Y. Choi (2009). "Stabilization of HIPK2 by escape from proteasomal degradation mediated by the E3 ubiquitin ligase Siah1." Cancer Lett 279(2): 177-184.

Kitada, T., S. Asakawa, N. Hattori, H. Matsumine, Y. Yamamura, S. Minoshima, M. Yokochi, Y. Mizuno and N. Shimizu (1998). "Mutations in the *parkin* gene cause autosomal recessive juvenile parkinsonism." Nature 392(6676): 605-608.

Koegl, M., T. Hoppe, S. Schlenker, H. D. Ulrich, T. U. Mayer and S. Jentsch (1999). "A novel ubiquitination factor, E4, is involved in multiubiquitin chain assembly." Cell 96(5): 635-644.

Kohno, K., H. Izumi, T. Uchiumi, M. Ashizuka and M. Kuwano (2003). "The pleiotropic functions of the Y-box-binding protein, YB-1." BioEssays 25(7): 691-698.

Koike, K., T. Uchiumi, T. Ohga, S. Toh, M. Wada, K. Kohno and M. Kuwano (1997). "Nuclear translocation of the Y-box binding protein by ultraviolet irradiation." FEBS Lett 417(3): 390-394.

Kramer, O. H., S. Muller, M. Buchwald, S. Reichardt and T. Heinzel (2008). "Mechanism for ubiquitylation of the leukemia fusion proteins AML1-ETO and PML-RAR-alpha." FASEB J 22(5): 1369-1379.

Kresge, N., R. D. Simoni and R. L. Hill (2006). "The discovery of ubiquitin-mediated proteolysis by Aaron Ciechanover, Avram Hershko, and Irwin Rose." J Biol Chem 281(40): 32-36.

Langton, P. F., J. Colombani, B. L. Aerne and N. Tapon (2007). "*Drosophila* ASPP regulates C-terminal Src kinase activity." Dev Cell 13(6): 773-782.

Larkin, M. A., G. Blackshields, N. P. Brown, R. Chenna, P. A. McGettigan, H. McWilliam, F. Valentin, I. M. Wallace, A. Wilm, R. Lopez, et al. (2007). "Clustal W and Clustal X version 2.0." Bioinformatics 23(21): 2947-2948.

Latres, E., D. S. Chiaur and M. Pagano (1999). "The human F box protein beta-Trcp associates with the Cul1/Skp1 complex and regulates the stability of beta-catenin." Oncogene 18(4): 849-854.

Lee, C., X. Li, A. Hechmer, M. Eisen, M. D. Biggin, B. J. Venters, C. Jiang, J. Li, B. F. Pugh and D. S. Gilmour (2008a). "NELF and GAGA factor are linked to promoter-proximal pausing at many genes in *Drosophila*." Mol Cell Biol 28(10): 3290-3300.

Lee, J. T., T. C. Wheeler, L. Li and L. S. Chin (2008b). "Ubiquitination of alpha-synuclein by Siah-1 promotes alpha-synuclein aggregation and apoptotic cell death." Hum Mol Genet 17(6): 906-917.

Lee, M. C. S. and E. A. Miller (2007). "Molecular mechanisms of COPII vesicle formation." Sem Cell Dev Biol 18(4): 424-434.

Lee, M. C. S., E. A. Miller, J. Goldberg, L. Orci and R. Schekman (2004). "Bi-directional protein transport between the ER and Golgi." Annu Rev Cell Dev Biol 20(1): 87-123.

Leskov, K. S., D. Y. Klokov, J. Li, T. J. Kinsella and D. A. Boothman (2003). "Synthesis and functional analyses of nuclear clusterin, a cell death protein." J Biol Chem 278(13): 11590-11600.

Leung, S. W., L. H. Apponi, O. E. Cornejo, C. M. Kitchen, S. R. Valentini, G. K. Pavlath, C. M. Dunham and A. H. Corbett (2009). "Splice variants of the human *ZC3H14* gene generate multiple isoforms of a zinc finger polyadenosine RNA binding protein." Gene 439(1-2): 71-78.

Levkowitz, G., H. Waterman, S. A. Ettenberg, M. Katz, A. Y. Tsygankov, I. Alroy, S. Lavi, K. Iwai, Y. Reiss, A. Ciechanover, et al. (1999). "Ubiquitin ligase activity and tyrosine phosphorylation underlie suppression of growth factor signaling by c-Cbl/Sli-1." Mol. Cell 4(6): 1029-1040.

Li, S., Y. Li, R. W. Carthew and Z. C. Lai (1997). "Photoreceptor cell differentiation requires regulated proteolysis of the transcriptional repressor tramtrack." Cell 90(3): 469-478.

Li, S., C. Xu and R. W. Carthew (2002). "Phyllopod acts as an adaptor protein to link the Sina ubiquitin ligase to the substrate protein tramtrack." Mol Cell Biol 22(19): 6854-6865.

Li, W., M. H. Bengtson, A. Ulbrich, A. Matsuda, V. A. Reddy, A. Orth, S. K. Chanda, S. Batalov and C. A. P. Joazeiro (2008). "Genome-wide and functional annotation of human E3 Ubiquitin ligases identifies MULAN, a mitochondrial E3 that regulates the organelle's dynamics and signaling." PLoS ONE 3(1): e1487.

Li, Y., D. Dinsdale and P. Glynn (2003a). "Protein domains, catalytic activity, and subcellular distribution of neuropathy target esterase in mammalian cells." J Biol Chem 278(10): 8820-8825.

Li, Y., D. Dinsdale and P. Glynn (2003b). "Protein domains, catalytic activity, and subcellular distribution of neuropathy target esterase in mammalian cells." J Biol Chem 278(10): 8820-8825.

Liani, E., A. Eyal, E. Avraham, R. Shemer, R. Szargel, D. Berg, A. Bornemann, O. Riess, C. A. Ross, R. Rott, et al. (2004). "Ubiquitylation of synphilin-1 and alpha-synuclein by

SIAH and its presence in cellular inclusions and Lewy bodies imply a role in Parkinson's disease." Proc Natl Acad Sci USA 101(15): 5500-5505.

Lim, K. L. and G. G. Y. Lim (2010). "K63-linked ubiquitination and neurodegeneration." Neurobiol Dis: Epub ahead of print.

Liu, J., F. Kouzine, Z. Nie, H. J. Chung, Z. Elisha-Feil, A. Weber, K. Zhao and D. Levens (2006). "The FUSE/FBP/FIR/TFIIH system is a molecular machine programming a pulse of c-myc expression." EMBO J 25(10): 2119-2130.

Liu, J., J. Stevens, C. Rote, H. Yost, Y. Hu, K. Neufeld, R. White and N. Matsunami (2001). "Siah-1 mediates a novel beta-catenin degradation pathway linking p53 to the adenomatous polyposis coli protein." Mol Cell 7(5): 927-936.

Liu, Z. J., X. Lu, Y. Zhang, S. Zhong, S. Z. Gu, X. B. Zhang, X. Yang and H. M. Xin (2005). "Downregulated mRNA expression of ASPP and the hypermethylation of the 5'-untranslated region in cancer cell lines retaining wild-type p53." FEBS Lett 579(7): 1587-1590.

Liu, Z. J., Y. Zhang, X. B. Zhang and X. Yang (2004). "Abnormal mRNA expression of ASPP members in leukemia cell lines." Leukemia 18(4): 880.

Lopez, C. D., Y. Ao, L. H. Rohde, T. D. Perez, D. J. O'Connor, X. Lu, J. M. Ford and L. Naumovski (2000). "Proapoptotic p53-interacting protein 53BP2 is induced by UV irradiation but suppressed by p53." Mol Cell Biol 20(21): 8018-8025.

Lorick, K. L., J. P. Jensen, S. Fang, A. M. Ong, S. Hatakeyama and A. M. Weissman (1999). "RING fingers mediate ubiquitin-conjugating enzyme E2-dependent ubiquitination." Proc Natl Acad Sci USA 96(20): 11364-11369.

Lossos, I. S., Y. Natkunam, R. Levy and C. D. Lopez (2002). "Apoptosis stimulating protein of p53 (ASPP2) expression differs in diffuse large B-cell and follicular center lymphoma: correlation with clinical outcome." Leuk Lymphoma 43(12): 2309-2317.

Lu, H., O. Flores, R. Weinmann and D. Reinberg (1991). "The nonphosphorylated form of RNA polymerase II preferentially associates with the preinitiation complex." Proc Natl Acad Sci USA 88(22): 10004-10008.

Luo, J., J. Yang, B. Y. Yu, W. Liu, M. Li and S. M. Zhuang (2010). "Identification of Siah-interacting protein as a potential regulator of apoptosis and curcumin resistance." Oncogene 29(48): 6357-6366.

MacLennan, M. (2007). An investigation into the interaction between the ubiquitin ligase, SIAH1, and the ATF3 transcription factor, MRes in Medical and Molecular Biosciences. UK, Newcastle University.

Maeda, A., T. Yoshida, K. Kusuzaki and T. Sakai (2002). "The characterization of the human *Siah-1* promoter." FEBS Lett 512(1-3): 223-226.

Malecz, N., P. C. McCabe, C. Spaargaren, R. G. Qiu, Y. Chuang and M. Symons (2000). "Synaptojanin 2, a novel Rac1 effector that regulates clathrin-mediated endocytosis." Curr Biol 10(21): 1383-1386.

Mariotti, M., M. Manganini and J. A. M. Maier (2000). "Modulation of *WHSC2* expression in human endothelial cells." FEBS Lett 487(2): 166-170.

Matsuo, K., S. Satoh, H. Okabe, A. Nomura, T. Maeda, Y. Yamaoka and I. Ikai (2003). "SIAH1 inactivation correlates with tumor progression in hepatocellular carcinomas." Genes Chromosom Cancer 36(3): 283-291.

Matsuzawa, S., S. Takayama, B. A. Froesch, J. M. Zapata and J. C. Reed (1998). "p53-inducible human homologue of *Drosophila* seven in absentia (Siah) inhibits cell growth: suppression by BAG-1." EMBO J 17(10): 2736-2747.

Matsuzawa, S. I. and J. C. Reed (2001). "Siah-1, SIP, and Ebi collaborate in a novel pathway for beta-catenin degradation linked to p53 responses." Mol Cell 7(5): 915-926.

Mayer, R. J. (2003). "From neurodegeneration to neurohomeostasis: the role of ubiquitin." Drug News Perspect. 16: 103-108.

McKinney, M. M. and A. Parkinson (1987). "A simple, non-chromatographic procedure to purify immunoglobulins from serum and ascites fluid." J Immunol Methods 92(2): 271-278.

Meek, S. E. M., W. S. Lane and H. Piwnica-Worms (2004). "Comprehensive proteomic analysis of interphase and mitotic 14-3-3-binding proteins." J Biol Chem 279(31): 32046-32054.

Mei, Y., C. Xie, W. Xie, Z. Wu and M. Wu (2007). "Siah-1S, a novel splice variant of Siah-1 (seven in absentia homolog), counteracts Siah-1-mediated downregulation of beta-catenin." Oncogene 26(43): 6319-6331.

Meierhofer, D., X. Wang, L. Huang and P. Kaiser (2008). "Quantitative analysis of global ubiquitination in HeLa cells by mass spectrometry." J Proteome Res 7(10): 4566-4576.

Miki, Y., J. Swensen, D. Shattuck-Eidens, P. A. Futreal, K. Harshman, S. Tavtigian, Q. Liu, C. Cochran, L. M. Bennett and W. Ding (1994). "A strong candidate for the breast and ovarian cancer susceptibility gene *BRCA1*." Science 266(5182): 66-71.

Milner, C. M. and R. D. Campbell (1990). "Structure and expression of the three MHC-linked *HSP70* genes." Immunogenetics 32(4): 242-251.

Moller, A., C. M. House, C. S. F. Wong, D. B. Scanlon, M. C. P. Liu, Z. Ronai and D. D. L. Bowtell (2009). "Inhibition of Siah ubiquitin ligase function." Oncogene 28(2): 289-296.

Monesi, V., R. Geremia, A. D'Agostino and C. Boitani (1978). "Biochemistry of male germ cell differentiation in mammals: RNA synthesis in meiotic and postmeiotic cells." Curr Top Dev Biol 12: 11-36.

Moriyoshi, K., K. Iijima, H. Fujii, H. Ito, Y. Cho and S. Nakanishi (2004). "Seven in absentia homolog 1A mediates ubiquitination and degradation of group 1 metabotropic glutamate receptors." Proc Natl Acad Sci USA 101(23): 8614-8619.

Mukherjee, S., R. Chiu, S. M. Leung and D. Shields (2007). "Fragmentation of the Golgi apparatus: an early apoptotic event independent of the cytoskeleton." Traffic 8(4): 369-378.

Mukhopadhyay, D. and H. Riezman (2007). "Proteasome-independent functions of ubiquitin in endocytosis and signaling." Science 315(5809): 201-205.

Nadeau, R. J., J. L. Toher, X. Yang, D. Kovalenko and R. Friesel (2007). "Regulation of sprouty2 stability by mammalian seven-in-absentia homolog 2." J Cell Biochem 100(1): 151-160.

Nagano, Y., H. Yamashita, T. Takahashi, S. Kishida, T. Nakamura, E. Iseki, N. Hattori, Y. Mizuno, A. Kikuchi and M. Matsumoto (2003). "Siah-1 facilitates ubiquitination and degradation of synphilin-1." J Biol Chem 278(51): 51504-51514.

Nakagawa, H., K. Koyama, Y. Murata, M. Morito, T. Akiyama and Y. Nakamura (2000). "APCL, a central nervous system-specific homologue of adenomatous polyposis coli tumor suppressor, binds to p53-binding protein 2 and translocates it to the perinucleus." Cancer Res 60(1): 101-105.

Nakano, K., C. Takase, T. Sakamoto, S. Nakagawa, J. Inazawa, S. Ohta and S. Matuda (1994). "Isolation, characterization and structural organization of the gene and pseudogene for the dihydrolipoamide succinyltransferase component of the human 2-oxoglutarate dehydrogenase complex." Eur J Biochem 224(1): 179-189.

Nakayama, K., I. J. Frew, M. Hagensen, M. Skals, H. Habelhah, A. Bhoumik, T. Kadoya, H. Erdjument-Bromage, P. Tempst, P. B. Frappell, et al. (2004a). "Siah2 regulates stability of prolyl-hydroxylases, controls HIF1-alpha abundance, and modulates physiological responses to hypoxia." Cell 117(7): 941-952.

Nakayama, K., J. Qi and Z. Ronai (2009). "The ubiquitin ligase Siah2 and the hypoxia response." Mol Cancer Res 7(4): 443-451.

Nakayama, K. and Z. Ronai (2004b). "Siah: new players in the cellular response to hypoxia." Cell Cycle 3(11): 1345-1347.

Narita, T., Y. Yamaguchi, K. Yano, S. Sugimoto, S. Chanarat, T. Wada, D. Kim, J. Hasegawa, M. Omori, N. Inukai, et al. (2003). "Human transcription elongation factor NELF: identification of novel subunits and reconstitution of the functionally active complex." Mol Cell Biol 23(6): 1863-1873.

Naumovski, L. and M. L. Cleary (1996). "The p53-binding protein 53BP2 also interacts with Bc12 and impedes cell cycle progression at G2/M." Mol Cell Biol 16(7): 3884-3892.

Nemani, M., G. Linares-Cruz, H. Bruzzoni-Giovanelli, J. P. Roperch, M. Tuynder, L. Bougueleret, D. Cherif, M. Medhioub, P. Pasturaud, V. Alvaro, et al. (1996). "Activation of the human homologue of the *Drosophila sina* gene in apoptosis and tumor suppression." Proc Natl Acad Sci USA 93(17): 9039-9042.

Newton, K. and D. Vucic (2007). "Ubiquitin ligases in cancer: ushers for degradation." Cancer Invest 25(6): 502-513.

Nishimura, Y., M. Hayashi, H. Inada and T. Tanaka (1999). "Molecular cloning and characterization of mammalian homologues of vesicle-associated membrane protein-associated (VAMP-associated) proteins." Biochem Biophys Res Commun 254(1): 21-26.

Okamoto, T., H. Izumi, T. Imamura, H. Takano, T. Ise, T. Uchiumi, M. Kuwano and K. Kohno (2000). "Direct interaction of p53 with the Y-box binding protein, YB-1: a mechanism for regulation of human gene expression." Oncogene 19(54): 6194-6202.

Okui, M., A. Yamaki, A. Takayanagi, J. Kudoh, N. Shimizu and Y. Shimizu (2005). "Transcription factor single-minded 2 (SIM2) is ubiquitinated by the RING-IBR-RING-type E3 ubiquitin ligases." Exp. Cell Res. 309(1): 220-228.

Oliver, P. L., E. Bitoun, J. Clark, E. L. Jones and K. E. Davies (2004). "Mediation of Af4 protein function in the cerebellum by Siah proteins." Proc Natl Acad Sci USA 101(41): 14901-14906.

Page-McCaw, P. S., K. Amonlirdviman and P. A. Sharp (1999). "PUF60: a novel U2AF65-related splicing activity." RNA 5(12): 1548-1560.

Park, H. S., S. G. Cho, C. K. Kim, H. S. Hwang, K. T. Noh, M. S. Kim, S. H. Huh, M. J. Kim, K. Ryoo, E. K. Kim, et al. (2002). "Heat shock protein Hsp72 is a negative regulator of apoptosis signal-regulating kinase 1." Mol Cell Biol 22(22): 7721-7730.

Park, T. J., H. Hamanaka, T. Ohshima, N. Watanabe, K. Mikoshiba and N. Nukina (2003). "Inhibition of ubiquitin ligase Siah-1A by disabled-1." Biochem Biophys Res Commun 302(4): 671-678.

Patel, S., R. George, F. Autore, F. Fraternali, J. E. Ladbury and P. V. Nikolova (2008). "Molecular interactions of ASPP1 and ASPP2 with the p53 protein family and the apoptotic promoters PUMA and Bax." Nucleic Acids Res 36(16): 5139-5151.

Peretti, D., N. Dahan, E. Shimoni, K. Hirschberg and S. Lev (2008). "Coordinated lipid transfer between the endoplasmic reticulum and the Golgi complex requires the VAP proteins and is essential for Golgi-mediated transport." Mol Biol Cell 19(9): 3871-3884.

Pernas-Alonso, R., F. Morelli, U. di Porzio and C. Perrone-Capano (1999). "Multiplex semi-quantitative reverse transcriptase-polymerase chain reaction of low abundance neuronal mRNAs." Brain Res Prot 4(3): 395-406.

Polakis, P. (2001). "More than one way to skin a catenin." Cell 105(5): 563-566.

Price, D. H. (2008). "Poised polymerases: on your mark...get set...go!" Mol Cell 30(1): 7-10.

Prigge, J. R., S. V. Iverson, A. M. Siders and E. E. Schmidt (2009). "Interactome for auxiliary splicing factor U2AF65 suggests diverse roles." Biochim Biophys Acta 1789(6-8): 487-492.

Print, C. G. and K. L. Loveland (2000). "Germ cell suicide: new insights into apoptosis during spermatogenesis." BioEssays 22(5): 423-430.

Qi, J., K. Nakayama, S. Gaitonde, J. S. Goydos, S. Krajewski, A. Eroshkin, D. Bar-Sagi, D. D. Bowtell and Z. Ronai (2008). "The ubiquitin ligase Siah2 regulates tumorigenesis and metastasis by HIF-dependent and -independent pathways." Proc Natl Acad Sci USA 105(43): 16713-16718.

Relaix, F., X. J. Wei, W. Li, J. Pan, Y. Lin, D. D. Bowtell, D. A. Sassoon and X. Wu (2000). "Pw1/Peg3 is a potential cell death mediator and cooperates with Siah1a in p53-mediated apoptosis." Proc Natl Acad Sci USA 97(5): 2105-2110.

Robinson, R. A., X. Lu, E. Y. Jones and C. Siebold (2008). "Biochemical and structural studies of ASPP proteins reveal differential binding to p53, p63, and p73." Structure 16(2): 259-268.

Roperch, J. P., F. Lethrone, S. Prieur, L. Piouffre, D. Israeli, M. Tuynder, M. Nemani, P. Pasturaud, M. C. Gendron, J. Dausset, et al. (1999). "SIAH-1 promotes apoptosis and tumor suppression through a network involving the regulation of protein folding, unfolding, and trafficking: identification of common effectors with p53 and p21Waf1." Proc Natl Acad Sci USA 96(14): 8070-8073.

Rotin, D. and S. Kumar (2009). "Physiological functions of the HECT family of ubiquitin ligases." Nat Rev Mol Cell Biol 10(6): 398-409.

Rott, R., R. Szargel, J. Haskin, V. Shani, A. Shainskaya, I. Manov, E. Liani, E. Avraham and S. Engelender (2008). "Monoubiquitylation of alpha-synuclein by seven in absentia homolog (SIAH) promotes its aggregation in dopaminergic cells." J Biol Chem 283(6): 3316-3328.

Roy, C. R., S. P. Salcedo and J. P. E. Gorvel (2006). "Pathogen endoplasmic-reticulum interactions: in through the out door." Nat Rev Immunol 6(2): 136-147.

Samuels-Lev, Y., D. J. O'Connor, D. Bergamaschi, G. Trigiante, J. K. Hsieh, S. Zhong, I. Campargue, L. Naumovski, T. Crook and X. Lu (2001). "ASPP proteins specifically stimulate the apoptotic function of p53." Mol Cell 8(4): 781-794.

Santelli, E., M. Leone, C. Li, T. Fukushima, N. E. Preece, A. J. Olson, K. R. Ely, J. C. Reed, M. Pellecchia, R. C. Liddington, et al. (2005). "Structural analysis of Siah1-Siah-interacting protein interactions and insights into the assembly of an E3 ligase multiprotein complex." J Biol Chem 280(40): 34278-34287.

Saunders, A., L. J. Core and J. T. Lis (2006). "Breaking barriers to transcription elongation." Nat Rev Mol Cell Biol 7(8): 557-567.

Scheffner, M., U. Nuber and J. M. Huibregtse (1995). "Protein ubiquitination involving an E1-E2-E3 enzyme ubiquitin thioester cascade." Nature 373(6509): 81-83.

Scheffner, M. and O. Staub (2007). "HECT E3's and human disease." BMC Biochem 8(1): 1-14.

Schmidt, R. L., C. H. Park, A. U. Ahmed, J. H. Gundelach, N. R. Reed, S. Cheng, B. E. Knudsen and A. H. Tang (2007). "Inhibition of RAS-mediated transformation and tumorigenesis by targeting the downstream E3 ubiquitin ligase seven in absentia homologue." Cancer Res 67(24): 11798-11810.

Semenza, G. L. (2007). "Hypoxia-inducible factor 1 (HIF-1) pathway." Sci STKE 2007(407): cm8.

Shannan, B., M. Seifert, D. A. Boothman, W. Tilgen and J. Reichrath (2007). "Clusterin over-expression modulates proapoptotic and antiproliferative effects of 1,25(OH)2D3 in prostate cancer cells *in vitro*." J Steroid Biochem Mol Biol 103(3-5): 721-725.

Shilatifard, A. (2004). "Transcriptional elongation control by RNA polymerase II: a new frontier." Biochim Biophys Acta 1677(1-3): 79-86.

Shima, H., Y. Hatano, Y. S. Chun, T. Sugimura, Z. J. Zhang, E. Y. C. Lee and M. Nagao (1993). "Identification of PP1 catalytic subunit isotypes PP1-gamma1, PP1-delta and PP1-alpha in various rat tissues." Biochem Biophys Res Commun 192(3): 1289-1296.

Shima, Y., T. Shima, T. Chiba, T. Irimura, P. P. Pandolfi and I. Kitabayashi (2008). "PML activates transcription by protecting HIPK2 and p300 from SCF-Fbx3-mediated degradation." Mol Cell Biol 28(23): 7126-7138.

Skehel, P. A., R. Fabian-Fine and E. R. Kandel (2000). "Mouse VAP33 is associated with the endoplasmic reticulum and microtubules." Proc Natl Acad Sci USA 97(3): 1101-1106.

Slee, E. A. and X. Lu (2003). "The ASPP family: deciding between life and death after DNA damage." Toxicol Lett 139(2-3): 81-87.

Somesh, B. P., J. Reid, W. F. Liu, T. M. M. Søgaard, H. Erdjument-Bromage, P. Tempst and J. Q. Svejstrup (2005). "Multiple mechanisms confining RNA polymerase II ubiquitylation to polymerases undergoing transcriptional arrest." Cell 121(6): 913-923.

Somesh, B. P., S. Sigurdsson, H. Saeki, H. Erdjument-Bromage, P. Tempst and J. Q. Svejstrup (2007). "Communication between distant sites in RNA Polymerase II through ubiquitylation factors and the polymerase CTD." Cell 129(1): 57-68.

Someya, A., M. Sata, K. Takeda, G. Pacheco-Rodriguez, V. J. Ferrans, J. Moss and M. Vaughan (2001). "ARF-GEP$_{100}$, a guanine nucleotide-exchange protein for ADP-ribosylation factor 6." Proc Natl Acad Sci USA 98(5): 2413-2418.

Sourisseau, T., C. Desbois, L. Debure, D. D. Bowtell, A. C. Cato, J. Schneikert, E. Moyse and D. Michel (2001). "Alteration of the stability of Bag-1 protein in the control of olfactory neuronal apoptosis." J Cell Sci 114(7): 1409-1416.

Stoss, O., M. Olbrich, A. M. Hartmann, H. Konig, J. Memmott, A. Andreadis and S. Stamm (2001). "The STAR/GSG family protein rSLM-2 regulates the selection of alternative splice sites." J Biol Chem 276(12): 8665-8673.

Sullivan, A. and X. Lu (2007). "ASPP: a new family of oncogenes and tumour suppressor genes." Br J Cancer 96(2): 196-200.

Sun, J., G. Watkins, A. L. Blair, C. Moskaluk, S. Ghosh, W. G. Jiang and R. Li (2008a). "Deregulation of cofactor of BRCA1 expression in breast cancer cells." J Cell Biochem 103(6): 1798-1807.

Sun, L. and Z. J. Chen (2004). "The novel functions of ubiquitination in signaling." Curr Opin Cell Biol 16(2): 119-126.

Sun, W. T., P. C. Hsieh, M. L. Chiang, M. C. Wang and F. F. Wang (2008b). "p53 target DDA3 binds ASPP2 and inhibits its stimulation on p53-mediated BAX activation." Biochem Biophys Res Commun 376(2): 395-398.

Sun, Y. (2006). "E3 ubiquitin ligases as cancer targets and biomarkers." Neoplasia 8: 645-654.

Susini, L., B. J. Passer, N. Amzallag-Elbaz, T. Juven-Gershon, S. Prieur, N. Privat, M. Tuynder, M. C. Gendron, A. Israel, R. Amson, et al. (2001). "Siah-1 binds and regulates the function of Numb." Proc Natl Acad Sci USA 98(26): 15067-15072.

Suzuki, Y., C. Demoliere, D. Kitamura, H. Takeshita, U. Deuschle and T. Watanabe (1997). "HAX-1, a novel intracellular protein, localized on mitochondria, directly associates with HS1, a substrate of Src family tyrosine kinases." J Immunol 158(6): 2736-2744.

Szargel, R., R. Rott, A. Eyal, J. Haskin, V. Shani, L. Balan, H. Wolosker and S. Engelender (2009). "Synphilin-1A inhibits seven in absentia homolog (SIAH) and modulates alpha-synuclein monoubiquitylation and inclusion formation." J Biol Chem 284(17): 11706-11716.

Szczepanowski, M., S. Adam-Klages, M. L. Kruse, M. Pollmann, W. Klapper, R. Parwaresch and H. J. Heidebrecht (2007). "Regulation of repp86 stability by human Siah2." Biochem Biophys Res Commun 362(2): 485-490.

Takahashi, N., S. Kobayashi, S. Kajino, K. Imai, K. Tomoda, S. Shimizu and T. Okamoto (2005). "Inhibition of the 53BP2S-mediated apoptosis by nuclear factor kappaB and Bcl-2 family proteins." Genes Cells 10(8): 803-811.

Tang, A. H., T. P. Neufeld, E. Kwan and G. M. Rubin (1997). "PHYL acts to down-regulate TTK88, a transcriptional repressor of neuronal cell fates, by a SINA-dependent mechanism." Cell 90(3): 459-467.

Tanikawa, J., E. Ichikawa-Iwata, C. Kanei-Ishii and S. Ishii (2001). "Regulation of c-myb activity by tumor suppressor p53." Blood Cell Mol Dis 27(2): 479-482.

Telerman, A. and R. Amson (2009). "The molecular programme of tumour reversion: the steps beyond malignant transformation." Nat Rev Cancer 9(3): 206-216.

Thompson, M., D. Xu and B. Williams (2009). "ATF3 transcription factor and its emerging roles in immunity and cancer." J Mol Med 87(11): 1053-1060.

Thornton, J. K. (2005). Protein-protein interaction screens: an investigation into the interactions of Sam68 and ASPP1 in the testis, PhD thesis. Institute of Human Genetics. UK, University of Newcastle upon Tyne.

Thornton, J. K., C. Dalgleish, J. P. Venables, K. A. Sergeant, I. E. Ehrmann, X. Lu, P. T. K. Saunders and D. J. Elliott (2006). "The tumour-suppressor protein ASPP1 is nuclear in human germ cells and can modulate ratios of CD44 exon V5 spliced isoforms *in vivo*." Oncogene 25(22): 3104-3112.

Tidow, H., A. Andreeva, T. J. Rutherford and A. R. Fersht (2007). "Solution structure of ASPP2 N-terminal domain (N-ASPP2) reveals a ubiquitin-like fold." J Mol Biol 371(4): 948-958.

Tiedt, R., B. A. Bartholdy, G. Matthias, J. W. Newell and P. Matthias (2001). "The RING finger protein Siah-1 regulates the level of the transcriptional coactivator OBF-1." EMBO J 20: 4143-4152.

Tonkin, E., D. M. Hagan, W. Li and T. Strachan (2002). "Identification and characterisation of novel mammalian homologues of *Drosophila* polyhomeotic permits new insights into relationships between members of the polyhomeotic family." Hum Genet 111(4): 435-442.

Trigiante, G. and X. Lu (2006). "ASPPs and cancer." Nat Rev Cancer 6(3): 217-226.

Tuynder, M., L. Susini, S. Prieur, S. Besse, G. Fiucci, R. Amson and A. Telerman (2002). "Biological models and genes of tumor reversion: cellular reprogramming through tpt1/TCTP and SIAH-1." Proc Natl Acad Sci USA 99(23): 14976-14981.

Twomey, E., Y. Li, J. Lei, C. Sodja, M. Ribecco-Lutkiewicz, B. Smith, H. Fang, M. Bani-Yaghoub, I. McKinnell and M. Sikorska (2010). "Regulation of MYPT1 stability by the E3 ubiquitin ligase SIAH2." Exp Cell Res 316(1): 68-77.

Uhlmann-Schiffler, H., S. Kiermayer and H. Stahl (2009). "The DEAD box protein Ddx42p modulates the function of ASPP2, a stimulator of apoptosis." Oncogene 28(20): 2065-2073.

van de Velde, H. J., A. J. Roebroek, N. H. Senden, F. C. Ramaekers and W. J. Van de Ven (1994). "NSP-encoded reticulons, neuroendocrine proteins of a novel gene family associated with membranes of the endoplasmic reticulum." J Cell Sci 107(9): 2403-2416.

van Wijk, S. J. L. and H. T. M. Timmers (2010). "The family of ubiquitin-conjugating enzymes (E2s): deciding between life and death of proteins." FASEB J. 24(4): 981-993.

Varmuza, S., A. Jurisicova, K. Okano, J. Hudson, K. Boekelheide and E. B. Shipp (1999). "Spermiogenesis is impaired in mice bearing a targeted mutation in the *protein phosphatase 1c gamma* gene." Dev Biol 205(1): 98-110.

Varshavsky, A. (2005). "Regulated protein degradation." Trends Biochem. Sci. 30(6): 283-286.

Venables, J. P. (2002). "Alternative splicing in the testes." Curr Opin Genet Dev 12(5): 615-619.

Venables, J. P., C. Dalgliesh, M. P. Paronetto, L. Skitt, J. K. Thornton, P. T. Saunders, C. Sette, K. T. Jones and D. J. Elliott (2004). "SIAH1 targets the alternative splicing factor T-STAR for degradation by the proteasome." Hum Mol Gen 13(14): 1525-1534.

Venables, J. P., C. Vernet, S. L. Chew, D. J. Elliott, R. B. Cowmeadow, J. Wu, H. J. Cooke, K. Artzt and I. C. Eperon (1999). "T-STAR/ETOILE: a novel relative of SAM68

that interacts with an RNA-binding protein implicated in spermatogenesis." Hum Mol Gen 8(6): 959-969.

Vijayaraghavan, S., D. T. Stephens, K. Trautman, G. D. Smith, B. Khatra, E. F. da Cruz e Silva and P. Greengard (1996). "Sperm motility development in the epididymis is associated with decreased glycogen synthase kinase-3 and protein phosphatase 1 activity." Biol Reprod 54(3): 709-718.

Von Rotz, R. C., S. Kins, R. Hipfel, H. Von der Kammer and R. M. Nitsch (2005). "The novel cytosolic RING finger protein dactylidin is up-regulated in brains of patients with Alzheimer's disease." Eur. J. Neurosci. 21(5): 1289-1298.

Wadhwa, R., K. Taira and S. C. Kaul (2002a). "An Hsp70 family chaperone, mortalin/mthsp70/PBP74/Grp75: what, when, and where?" Cell Stress 7(3): 309-316.

Wadhwa, R., S. Takano, M. Robert, A. Yoshida, H. Nomura, R. R. Reddel, Y. Mitsui and S. C. Kaul (1998). "Inactivation of tumor suppressor p53 by mot-2, a hsp70 family member." J Biol Chem 273(45): 29586-29591.

Wadhwa, R., T. Yaguchi, M. K. Hasan, Y. Mitsui, R. R. Reddel and S. C. Kaul (2002b). "Hsp70 family member, mot-2/mthsp70/GRP75, binds to the cytoplasmic sequestration domain of the p53 protein." Exp Cell Res 274(2): 246-253.

Wang, H., L. Wang, H. Erdjument-Bromage, M. Vidal, P. Tempst, R. S. Jones and Y. Zhang (2004). "Role of histone H2A ubiquitination in Polycomb silencing." Nature 431(7010): 873-878.

Watson, P., A. K. Townley, P. Koka, K. J. Palmer and D. J. Stephens (2006). "Sec16 defines endoplasmic reticulum exit sites and is required for secretory cargo export in mammalian cells." Traffic 7(12): 1678-1687.

Welchman, R. L., C. Gordon and R. J. Mayer (2005). "Ubiquitin and ubiquitin-like proteins as multifunctional signals." Nat Rev Mol Cell Biol 6(8): 599-609.

Wen, L., J. Liu, Y. Chen and D. Wu (2010a). "Identification and preliminary functional analysis of alternative splicing of Siah1 in *Xenopus laevis*." Biochem Biophys Res Commun 396(2): 419-424.

Wen, Y. Y., Z. Q. Yang, M. Song, B. L. Li, J. J. Zhu and E. H. Wang (2010b). "SIAH1 induced apoptosis by activation of the JNK pathway and inhibited invasion by inactivation of the ERK pathway in breast cancer cells." Cancer Sci 101(1): 73-79.

Wheeler, T. C., L. S. Chin, Y. Li, F. L. Roudabush and L. Li (2002). "Regulation of synaptophysin degradation by mammalian homologues of seven in absentia." J Biol Chem 277(12): 10273-10282.

Willems, A. R., M. Schwab and M. Tyers (2004). "A hitchhiker's guide to the cullin ubiquitin ligases: SCF and its kin." Biochim Biophys Acta 1695(1-3): 133-170.

Windoffer, R., M. Borchert-Stuhltrager, N. K. Haass, S. Thomas, M. Hergt, C. J. Bulitta and R. E. Leube (1999). "Tissue expression of the vesicle protein pantophysin." Cell Tissue Res 296(3): 499-510.

Winter, M., D. Sombroek, I. Dauth, J. Moehlenbrink, K. Scheuermann, J. Crone and T. Hofmann (2008). "Control of HIPK2 stability by ubiquitin ligase Siah-1 and checkpoint kinases ATM and ATR." Nat Cell Biol 10(7): 812 - 824.

Wright, T. J., J. L. Costa, C. Naranjo, W. P. Francis and M. R. Altherr (1999). "Comparative analysis of a novel gene from the Wolf-Hirschhorn/Pitt-Rogers-Danks syndrome critical region." Genomics 59(2): 203-212.

Wu, B., C. Hunt and R. Morimoto (1985). "Structure and expression of the human gene encoding major heat shock protein HSP70." Mol Cell Biol 5(2): 330-341.

Wu, C. H., C. Lee, R. Fan, M. J. Smith, Y. Yamaguchi, H. Handa and D. S. Gilmour (2005). "Molecular characterization of *Drosophila* NELF." Nucleic Acids Res 33(4): 1269-1279.

Wu, H., Y. Lin, Y. Shi, W. Qian, Z. Tian, Y. Yu and K. Huo (2010). "SIAH-1 interacts with mammalian polyhomeotic homologues HPH2 and affects its stability via the ubiquitin-proteasome pathway." Biochem Biophys Res Commun 397(3): 391-396.

Xu, Z., A. Sproul, W. Wang, N. Kukekov and L. A. Greene (2006). "Siah1 interacts with the scaffold protein POSH to promote JNK activation and apoptosis." J Biol Chem 281(1): 303-312.

Yamaguchi, Y., J. Filipovska, K. Yano, A. Furuya, N. Inukai, T. Narita, T. Wada, S. Sugimoto, M. M. Konarska and H. Handa (2001). "Stimulation of RNA polymerase II elongation by hepatitis delta antigen." Science 293(5527): 124-127.

Yamaguchi, Y., N. Inukai, T. Narita, T. Wada and H. Handa (2002). "Evidence that negative elongation factor represses transcription elongation through binding to a DRB sensitivity-inducing factor/RNA polymerase II complex and RNA." Mol Cell Biol 22(9): 2918-2927.

Yamaguchi, Y., T. Takagi, T. Wada, K. Yano, A. Furuya, S. Sugimoto, J. Hasegawa and H. Handa (1999). "NELF, a multisubunit complex containing RD, cooperates with DSIF to repress RNA polymerase II elongation." Cell 97(1): 41-51.

Yang, C. R., K. S. Leskov, K. Hosley-Eberlein, T. Criswell, J. J. Pink, T. J. Kinsella and D. A. Boothman (2000). "Nuclear clusterin/XIP8, an x-ray-induced Ku70-binding protein that signals cell death." Proc Natl Acad Sci USA 97(11): 5907-5912.

Yang, J. P., M. Hori, N. Takahashi, T. Kawabe, H. Kato and T. Okamoto (1999). "NF-kappaB subunit p65 binds to 53BP2 and inhibits cell death induced by 53BP2." Oncogene 18(37): 5177-5186.

Ye, Q., Y. F. Hu, H. Zhong, A. C. Nye, A. S. Belmont and R. Li (2001). "BRCA1-induced large-scale chromatin unfolding and allele-specific effects of cancer-predisposing mutations." J Cell Biol 155(6): 911-922.

Yeo, G., D. Holste, G. Kreiman and C. Burge (2004). "Variation in alternative splicing across human tissues." Genome Biol 5(10): R74.

Yoon, H., S. Liyanarachchi, F. A. Wright, R. Davuluri, J. C. Lockman, A. de la Chapelle and N. S. Pellegata (2002). "Gene expression profiling of isogenic cells with different TP53 gene dosage reveals numerous genes that are affected by TP53 dosage and identifies CSPG2 as a direct target of p53." Proc Natl Acad Sci USA 99(24): 15632-15637.

Yoshibayashi, H., H. Okabe, S. Satoh, K. Hida, K. Kawashima, S. Hamasu, A. Nomura, S. Hasegawa, I. Ikai and Y. Sakai (2007). "SIAH1 causes growth arrest and apoptosis in hepatoma cells through beta-catenin degradation-dependent and independent mechanisms." Oncol Rep 17: 549-556.

Yun, S., A. Moller, S. K. Chae, W. P. Hong, Y. J. Bae, D. D. L. Bowtell, S. H. Ryu and P. G. Suh (2008). "Siah proteins induce the epidermal growth factor-dependent degradation of phospholipase C epsilon." J Biol Chem 283(2): 1034-1042.

Yung, T. M. C., T. Narita, T. Komori, Y. Yamaguchi and H. Handa (2009). "Cellular dynamics of the negative transcription elongation factor NELF." Exp Cell Res 315(10): 1698-1705.

Zaccheo, O., D. Dinsdale, P. A. Meacock and P. Glynn (2004). "Neuropathy target esterase and its yeast homologue degrade phosphatidylcholine to glycerophosphocholine in living cells." J Biol Chem 279(23): 24024-24033.

Zhang, J., M. G. Guenther, R. W. Carthew and M. A. Lazar (1998). "Proteasomal regulation of nuclear receptor corepressor-mediated repression." Genes Dev 12(12): 1775-1780.

Zhao, H. L., N. Ueki and M. J. Hayman (2010). "The Ski protein negatively regulates Siah2-mediated HDAC3 degradation." Biochem Biophys Res Commun 399(4): 623-628.

Zheng, N., P. Wang, P. D. Jeffrey and N. P. Pavletich (2000). "Structure of a c-Cbl-UbcH7 complex: RING domain function in ubiquitin-protein ligases." Cell 102(4): 533-539.

Zhou, Y., L. Li, Q. Liu, G. Xing, X. Kuai, J. Sun, X. Yin, J. Wang, L. Zhang and F. He (2008). "E3 ubiquitin ligase SIAH1 mediates ubiquitination and degradation of TRB3." Cell Signal 20(5): 942-948.

Zhu, Z., J. Ramos, K. Kampa, S. Adimoolam, M. Sirisawad, Z. Yu, D. Chen, L. Naumovski and C. D. Lopez (2005). "Control of ASPP2/53BP2L protein levels by proteasomal degradation modulates p53 apoptotic function." J Biol Chem 280(41): 34473-34480.